An exploration of aboveground and belowground interactions that shape forest dynamics

by

Joseph Cooper

A thesis submitted in partial fulfillment of the requirements for the degree of

Doctor of Philosophy

in

Forest Biology and Management

Department of Renewable Resources

University of Alberta

Abstract

Growth is limited when trees are restricted in resources or they experience conditions outside of their physiological adaptation, such as extreme cold. However, no tree exists in isolation. A variety of aboveground and belowground species interactions modulate the degree to which trees respond to resource limitation. Specifically, aboveground competitive or facilitative interactions may alter how trees grow, survive, and reproduce. Likewise, belowground interactions with fungi, ectomycorrhizal or otherwise, can alter access to resources and have a variety of beneficial or harmful impacts on tree growth. The overarching focus of my thesis is investigating the interactions that influence how trees experience growth-limitation and how these interactions may change with time. First, to investigate the role of aboveground interactions on forest demography and spatial patterns indicative of competition and facilitation, I compiled existing data and added to a census of a forest plot at the edge of the southern boreal forest. I found a precipitous decline in tree recruitment and a rising mortality rate that had resulted in the loss of 70% of the trees within the last 30 years. However, density-dependent processes of facilitation and competition resulted in a near-equilibrium of the spatial distribution of trees across the stand. Density-dependent competition compounded with repeated drought, defoliator, and bark-beetle disturbances influenced spatial patterns as well as stand demography. My results suggest that density-dependent interactions and resource limitations have shifted the forest onto a novel successional trajectory, which likely will transition to an open-canopy shrubland. Second, to investigate how belowground interactions between trees, mediated by ectomycorrhizal networks, influence the growth of *Pseudotsuga menziesii,* I used dendroecology to assess tree growth responses to network topology. I found that trees with more connections to other trees through the ectomycorrhizal fungal species, *Rhizopogon vinicolor*, had greater growth

and lower interannual variation in growth than trees with fewer connections. Trees that were colonized by more unique genets of the ectomycorrhizal fungus, *Rhizopogon vesiculosus*, had greater growth than trees with fewer connections. My results suggest that ectomycorrhizal networks can transport biologically meaningful resources among adult trees and that interspecific differences exist between fungal species in their association with tree growth. These belowground interactions may have important implications for the mature forest growth. Third, because fungal communities driving belowground interactions can vary in composition, it is important to understand the processes that influence their assembly. Variations in the proportion of stochasticity or determinism could result in different fungal communities with cascading implications for tree growth. Stochastic community assembly emerges from functional equivalence between taxa while determinism arises from environmental filters acting on species. To investigate if stochastic and deterministic processes change for fungal communities on roots, soils, and with tree age, I surveyed four forests of *Pseudotsuga menziesii* across the fringes of its range in western North America. Across 1800 km, these forests vary in precipitation limitation, nutrient availability, and growing season length. I found that the proportion of assembly processes differed between sites but that deterministic pressures selecting for homogenizing communities were largely dominant. Community assembly processes were independent of tree age at all sites. My results suggest that fungal communities assemble with site-specific processes and that changes in environmental factors, such as local climate, may have unequal impacts on fungal community composition across the range of *Pseudotsuga menzies*ii. Finally, to further explore factors affecting the community assembly of belowground fungal communities, I investigated how the identity and age of the at-risk species, *Pinus flexilis* and *Pinus longaeva,* influenced the composition of fungal communities. The root-associated fungal communities were

distinct for *Pinus flexilis* and *Pinus longaeva,* while soil-associated fungal communities were similar. Ectomycorrhizal fungi had the greatest number of sequences and fungal species were largely shared between the two pines. Tree age was associated with the composition of root-associated fungal communities on *Pinus flexilis* and displayed increasing dissimilarity between soil and root communities with tree age. These results suggest distinct but overlapping fungal communities dominated by shared ectomycorrhizal fungi. The potential influence of tree age on root-associated fungal communities suggest that partner selection changes over multiple centuries as trees mature. Cumulatively, my work highlights the influence of aboveground and belowground interactions in shaping forest health, as well as how these interactions are variable across space and time.

Preface

Chapter 1 is an original work by Joseph Cooper and has not been previously published.

Chapter 2 has been published as Birch, J. D., Lutz, J. A., Hogg, E. H., Simard, S. W., Pelletier, R., LaRoi, G. H., & Karst, J. (2019). Decline of an ecotone forest: 50 years of demography in the southern boreal forest. *Ecosphere*, *10*(4), e02698. J. D. Birch was responsible for data collection, statistical analysis, and writing the manuscript. J. Lutz assisted with statistical analysis and writing the manuscript. E. H. Hogg assisted with analysis and writing the manuscript. S. W. Simard was a co-supervisor and provided feedback on the manuscript. R. Pelletier assisted with data digitization and provided manuscript feedback. G. H. LaRoi designed the original experimental plot. J. Karst assisted with the analysis and writing of the manuscript.

Chapter 3 has been published as Birch, J. D., Lutz, J. A., Simard, S. W., Pelletier, R., LaRoi, G. H., & Karst, J. (2019). Density-dependent processes fluctuate over 50 years in an ecotone forest. *Oecologia*, *191*(4), 909-918. J. D. Birch was responsible for data collection, statistical analysis, and writing the manuscript. J. Lutz assisted with the analysis and writing the manuscript. S. W. Simard provided feedback on the manuscript. R. Pelletier assisted with data digitization and provided feedback on the manuscript. G. H. LaRoi established the original experimental plot. J. Karst assisted with the analysis and writing of the manuscript.

Chapter 4 has been published as Birch, J. D., Simard, S. W., Beiler, K., & Karst, J. (2021) Ectomycorrhizal networks and unique fungal genets are associated with greater growth of mature *Pseudotsuga menziesii*. *Journal of Ecology*. doi:10.1111/1365-2745.13507. J. D. Birch was responsible for the experimental design, data collection, statistical analysis, and writing the manuscript. S.W. Simard assisted with writing the manuscript. K. Beiler collected a portion of

the data and provided feedback for the manuscript. J. Karst assisted with the analysis and writing of the manuscript.

Chapter 5 will be submitted for publication as Birch, J. D., Lutz, J. A., & Karst, J. Dancing with Douglas-fir: fungal community assembly processes vary across disparate forests. J. D. Birch was responsible for the data collection, analysis, and writing the manuscript. J. A. Lutz assisted with data collection, analysis, and writing the manuscript. J. Karst assisted with experimental design, analysis, and writing the manuscript.

Chapter 6 will be submitted for publication as Birch, J. D., Lutz, J. A., & Karst, J (2020). Shared fungal communities in ancient *Pinus flexilis* and *Pinus longaeva*. J. D. Birch was responsible for the experimental design, data collection, analysis, and writing the manuscript. J. A. Lutz assisted with data collection, analysis, and writing the manuscript. J. Karst assisted with the experimental design, analysis, and writing the manuscript.

Chapter 7 is an original work by Joseph Cooper and has not been previously published.

Dedication

For all those lost along the way. You are missed.

Acknowledgments

First, I want to acknowledge the guidance and support offered by my primary supervisor, Dr. Justine Karst. I was extremely lucky to join the Karst lab and have her guidance and mentorship over the past several years. It has truly been a life-changing experience and I will forever be grateful that I spent these years in the mentorship of Dr. Karst. I also want to acknowledge the mentorship of Dr. James Lutz who first taught me the ways of forest ecology as a wide-eyed undergraduate and helped prepare me for graduate school. His continued support and mentorship have been invaluable during my frequent forays back to the US. The advice and feedback from Dr. Hogg and Dr. Simard have greatly improved my research and changed the way that I think about forest ecology. I have been extremely lucky to have had such a collection of brilliant and empathetic mentors during my program.

I would not be where I am without the support and influence of my mom, brother, and grandmother. I am grateful for the sacrifices that my mom made throughout my life so that I could have a stable, adventurous upbringing. Her passion and compassion for nature and all life are a continual source of inspiration for my work. My grandmother provided continual support throughout my program and her passion for education helped inspire me to pursue ecology. My brother proved himself to be a more-than-capable fill-in field technician during the various blizzards and mountain-top forays of the past several years. My grandfather provided crucial support throughout my undergraduate program and provided logistical support for my graduate research. My father provided financial support that helped me complete my undergraduate program and enter graduate school. I would not be where I am today without the support from my family.

I am also grateful for all the friendly Canadians who helped make me feel welcome during my times in Canada. The Karst lab were a fantastic group of people that helped make my time in Canada better. I also want to thank Barb and Alley Maheu for being gracious hosts and friends during the last few years of my program.

I am grateful for the work of George LaRoi that established the foundation for my first two data chapters. His passion and dedication for forestry was evident in his work and helped inspire me as an ecologist. Kevin Beiler mapped the *Rhizopogon* EMNs that were crucial for the work of my third data chapter. My fieldwork spanned four years and I was lucky to have a variety of talented and tenacious technicians and volunteers. I would like to specifically thank Marc La Fleche, Paul Metzler, Evan Fellrath, Joshua Wasyliw, Chloe Christenson, Dana Hopfauf, Jerry Shaw, Nico Sasso, Alexia Constantinou, Colten Stephens, Justine Cornwall, Nike Birch, and Joshua Birch for their assistance. This work would not have been possible without logistical assistance from the Western Forest Initiative, Lauche Fraser, Joy Birch, Maria Birch, Duane Loveland, Lee Foote, Raúl Ballesteros, Juan Villalba, Justin DeRose, Joey Petit, Jelveh Tamjidi, managers and staff of Cedar Breaks National Monument, the Logan office of the US Forest Service, and John Prince Research Forest. I received helpful feedback and advice from Jason Hoeksema, Marcel van der Heijden, Justin DeRose, Tucker Furniss, James Loveland, Nicholas Brown, James Franklin, and numerous anonymous reviewers. My research was supported by funding from the Natural Science and Engineering Council of Canada, the Alberta Conservation Association Grants for Biodiversity, and several scholarships offered by the University of Alberta. Looking back at this journey I am humbled by the help that I have received and the adventures (good and bad) along the way. Thank you all!

Table of contents

List of Tables

List of Figures

Glossary of terms and abbreviations

ASV – amplicon sequence variant

BAI – basal area increment (mm^2)

CNDD – conspecific negative density-dependence

DBH – diameter at breast height (measured at 1.35 m in height for chapters 2 and 3; 1.37 m for all other chapters)

Dispersal limitation – A stochastic process where fluctuations in propagule dispersal result in community distributions under a null model.

Drift – A stochastic fluctuation of members in a community causes compositional change.

EMF – ectomycorrhizal fungi

EMN – ectomycorrhizal network

Genet – a genetically unique fungal individual

HNDD – heterospecific negative density-dependence

Homogenizing dispersal – A stochastic process where propagules easily disperse into all communities and drive communities towards a homogenous composition.

Homogenizing selection – A deterministic process where a directional selection pressure moves the community towards a community that is more similar than expected by random chance.

NDD – negative density-dependence

Overdispersion – A community where sequences are less phylogenetically related to one another than would be expected under a stochastic null model.

Priority effects – The process in which the first individual to arrive in an environment preempts subsequent colonization through alteration to the environment or occupation of the habitat

Underdispersion – A community where sequences are more phylogenetically related to one another than would be expected under a stochastic null model.

Variable selection – A deterministic process where multiple directional selection pressures moves the towards several, divergent community compositions best suited for the local selecting pressure.

Chapter 1: Introduction

1.1.1 Background

In recent decades there have been rapid changes in forest demography across western North America (van Mantgem 2009, Worrall et al. 2013). Changing climates have been implicated in increased drought frequency and severity, altered disturbance regimes, and range shifts (Allen et al. 2010, Bentz et al. 2010, Kirchmeier-Young et al. 2018, Liang et al. 2018, Biedermann et al. 2019, Vila-Cabrera et al. 2019). As climate continues to change, we expect warmer and drier climates across much of western North America, which could cause greater growth limitation, particularly in forests or trees at the margins of their physiological tolerance for water limitation. When resource limitation increases, a tree responds by further limiting growth and altering physiological function, even to the point of damage or death (Close et al. 2000, Pallardy 2010). However, interactions between a tree and other organisms within the ecosystem can modulate the severity of resource limitation. For example, density-dependent interactions can vary from positive facilitation, where one tree shades another — reducing drought stress — to competitive interactions for light, water, or other nutrients (Calder and St. Clair 2012, Clair et al. 2013). Similarly, interactions with belowground fungal communities can vary from direct symbiotic or pathogenic to indirect interactions with saprotrophic fungi that influence the cycling of nutrients on which trees depend (Karst et al. 2008; Jactel et al., 2012; Dighton 2007). Importantly, these above and belowground interactions are not static and may change with space, time, or environmental pressures. Because of this, it is important to understand the influence of these interactions as well as how they may change.

1.1.2 Density-dependent interactions

Density-dependent interactions may have long-term implications for forest demography by altering patterns of establishment, growth, disturbance, and mortality events (He and Duncan 2000, Green and Hawkins 2005, Clair et al. 2013). Negative density-dependent interactions can include competition for resources such as light, water, space, or Janzen-Connell effects (Janzen 1970, Connell 1971). Conversely, positive density-dependence can involve ameliorating harmful environmental conditions, beneficial plant-soil feedbacks, or root or bole grafting (Simard and Vyse 2006, Bonanomi et al. 2008, Salomón et al. 2016).

Competitive interactions, particularly between conspecific trees, can have a stronger influence on tree mortality rates than does facilitation (Johnson et al. 2012, Zhang et al. 2015, Chen et al. 2018). Competitive interactions can also influence how trees respond to disturbance and resource limitation (Bottero et al. 2017, Ford et al. 2016). However, facilitative interactions can also strongly influence forest composition and can vary in strength with forest succession. The nature of density-dependent interactions is that they will change in strength and type as trees grow, die, and the spatial structure of the forest changes with time. For example, mature *Populus tremuloides* (aspen) on the Colorado Plateau can facilitate the establishment of seedling *Abies bifolia* (Rocky Mountain subalpine fir), which will eventually outcompete *P. tremuloides* (Calder and St. Clair 2012, Furniss et al. 2017). Altered climatic regimes may shift resource limitations and alter the nature of these density-dependent interactions (Clark et al. 2014, Bachelot et al. 2020). Interactions between pronounced drought and competition are implicated in increased forest mortality across entire landscapes (Young et al. 2017), which could increase in the future. Mortality rates have risen across western North America and both climate and competition are implicated in driving the increase (van Mantgem et al. 2009, Worrall et al. 2013, Zhang et al.

2015). The varied, complex, and important nature of density-dependent interactions underscores the need to understand how these processes shape forest succession and how they vary between stands and due to differing resource limitations.

1.1.3 Belowground interactions: ectomycorrhizal networks and fungal communities

The influence of density-dependence is not confined to aboveground interactions. Many of the most ecological and anthropogenically important tree species in western North America are within the Pinaceae family and form ectomycorrhizal symbioses. Recent work shows widespread aggregation among closely related trees associating with ectomycorrhizal fungi and dispersion among trees associating with arbuscular mycorrhizae (Bennett et al. 2017, Segnitz et al. 2020). Proximity to other trees can influence fungal community composition or lead to the formation of ectomycorrhizal networks (EMN) if an ectomycorrhizal fungus colonizes the roots of two or more different host plants (Teste and Simard 2008). Ectomycorrhizal networks can shepherd resources from one tree to another and can influence density-dependent establishment of seedlings by providing facilitative resource transfer to seedlings that are nearby (Simard et al. 1997; Teste et al. 2009b). Ectomycorrhizal networks have a variety of important benefits for immature trees including improved survival, drought resistance, and growth (Teste et al. 2009a, Booth and Hoeksema 2010. While the presence of EMNs in mature forests has been implicated in the transport of nutrients between mature trees (Simard et al. 2012, Klein et al. 2016), less is known on how EMN influence mature tree growth. The topology of the EMN in mature forests is robust to the loss of a single tree and multiple concurrent networks can exist when different species or individual fungi colonize multiple trees (Beiler et al. 2010, Van Dorp et al. 2020). The stability of EMNs could lead to relatively resilient pathways through which mature trees can interact with one another, potentially facilitating growth and survival of other connected trees.

Overall, EMN have been proven to have important implications for juvenile trees and could serve as mediators of resource transfers between mature trees, potentially offsetting competition for resources. The apparent stability and resilience of EMN could feasibly provide pathways for long-term interactions among mature and juvenile trees.

Beyond EMN, belowground fungal communities can influence tree growth and health (Table 1.1.). Fungal communities have enormous functional diversity spanning symbiotic, opportunistic, endophytic, pathogenic, or saprotrophic guilds, which can moderate resource limitations, health, and nutrient cycling and availability (Frac et al. 2018, Terhonen et al. 2019). The composition of fungal communities can have an important influence on tree growth and health when considering the relative abundance and diversity of beneficial or harmful fungal taxa, such as *Armillaria* spp. (Munkvold et al. 2004, Baumgartner et al. 2011, Pena et al. 2013). Because fungal communities can have a variety of direct and indirect influences on forest growth and health, the composition and assembly of fungal communities can have important implications for forests.

The composition of fungal communities will likely depend on both deterministic niche-based processes as well as stochastic dispersal limitation and community drift, i.e., neutral processes (Dumbrell et al. 2010, Wang et al. 2020). Niche-based processes include biotic interactions and environmental filtering that act on functional differences among species. One deterministic interaction is partner selection, which likely occurs from both plant and fungal perspectives and may vary with the degree of local resource limitations and the availability of other competitive plant or fungal partners (Werner and Kiers 2015, Chagnon et al. 2020). Partner selection and host-specificity could play important roles in shaping the pool of fungal species

within an ecosystem. Because aboveground vegetation can shape belowground fungal communities, there is a potential for fungal communities to change with forest succession, or forest age (Wu et al. 2013, Rudawska et al. 2018). As trees age, they alter their local environment and undergo physiological changes with growth and senescence (Zinke 1962, Tang et al. 2014). The combination of these processes could directly influence fungal community composition by altering selection pressures from the tree and local environment. In turn, changing fungal communities may have feedbacks on forest growth and health and could conceivably contribute to the maintenance of old-growth forests and trees. This is important because large, old trees can have a disproportionate impact on ecosystem services, such as carbon sequestration, and are important components of forest structure (Lutz et al. 2018). Some species, such as *Pinus flexilis* (limber pine) or *Pinus longaeva* (Great Basin bristlecone pine) are capable of living for several millennia and serve as keystone or foundational species across much of their ranges (Brown 1996, Schoettle 2004). In these tree species, the assembly and composition of fungal communities may be especially interesting considering length of time in which trees have influenced their local environment and potentially applied partner selection to fungal communities.

Cumulatively, the suite of aboveground and belowground interactions, mediated by spatial distance or fungi, can alter resource limitations, and have profound impacts on forest growth and health. How these processes change with time, space, and their environment is of key interest when seeking to understand forest growth. Understanding the impact of these processes and how they form will enable us to better understand how trees grow and interact in ecosystems defined by persistent limitation of resources.

1.1.4 Research questions and objectives

My first two data chapters (Chapter 2 and Chapter 3) were conducted to explore how demographic trends and patterns of density dependence have influenced forest health and composition in an ecotone forest from 1967–2017. In my first research chapter (Chapter 2), I investigated 1) how forest demographic rates had changed through succession and with disturbance in a boreal mixed-wood forest. In Chapter 3, I investigated 1) how conceptual models of succession matched observed patterns in a boreal mixed-wood forest, and 2) how legacy and native disturbances influenced density-dependent interactions. In Chapter 4 I leveraged a previously existing EMN topology to investigate how connections to other trees through the EMN may influence mature tree growth. There, I investigated how the number of connections 1) to other trees through ectomycorrhizal networks and 2) unique EMF genets influenced the magnitude and variation of growth in mature *Pseudotsuga*. In my last two data chapters (Chapter 5 and Chapter 6), I explored the role of deterministic processes, host-specificity, tree age, and stochastic processes on the assembly of fungal communities, with a special focus on EMF. In Chapter 5, I investigated 1) whether the relative proportion of selection and stochastic assembly processes varied for fungal communities on roots and soils of *Pseudotsuga*, 2) if the relative proportion of selection and stochastic assembly processes varied for fungal communities across the range of *Pseudotsuga*, and 3) if selection pressures on fungal communities varied with tree age. In Chapter 6, I investigated how 1) fungal community composition differed on roots and soils around the long-lived tree species *Pinus flexilis* (limber pine) and *Pinus longaeva* (Great Basin bristlecone pine), and 2) if advanced tree age was associated with changing fungal community composition.

1.2 REFERENCES

Allen, C. D., A. K. Macalady, H. Chenchouni, D. Bachelet, N. McDowell, M. Vennetier, T. Kitzberger, A. Rigling, D. D. Breshears, E. H. Hogg, P. Gonzalez, R. Fensham, Z. Zhang, J. Castro, N. Demidova, J.-H. Lim, G. Allard, S. W. Running, A. Semerci, and N. Cobb. 2010. A global overview of drought and heat-induced tree mortality reveals emerging climate change risks for forests. *Forest Ecology and Management* 259:660-684.

Bachelot, B., A. M. Alonso-Rodríguez, L. Aldrich-Wolfe, M. A. Cavaleri, S. C. Reed, and T. E. Wood. 2020. Altered climate leads to positive density-dependent feedbacks in a tropical wet forest. *Global Change Biology*. 26:3417-3428

Baumgartner, K., M. P. Coetzee, and D. Hoffmeister. 2011a. Secrets of the subterranean pathosystem of *Armillaria*. *Molecular Plant Pathology* 12:515-534.

Beiler, K. J., D. M. Durall, S. W. Simard, S. A. Maxwell, and A. M. Kretzer. 2010. Architecture of the wood-wide web: *Rhizopogon* spp. genets link multiple Douglas-fir cohorts. *New Phytologist* 185:543-553.

Bennett, J. A., H. Maherali, K. O. Reinhart, Y. Lekberg, M. M. Hart, and J. Klironomos. 2017. Plant-soil feedbacks and mycorrhizal type influence temperate forest population dynamics. *Science* 355:181-184.

Bentz, B. J., J. Régnière, C. J. Fettig, E. M. Hansen, J. L. Hayes, J. A. Hicke, R. G. Kelsey, J. F. Negrón, and S. J. Seybold. 2010. Climate change and bark beetles of the western United States and Canada: direct and indirect effects. *BioScience* 60:602-613.

Biedermann, P. H. W., J. Muller, J. C. Gregoire, A. Gruppe, J. Hagge, A. Hammerbacher, R. W. Hofstetter, D. Kandasamy, M. Kolarik, M. Kostovcik, P. Krokene, A. Salle, D. L. Six, T.

Turrini, D. Vanderpool, M. J. Wingfield, and C. Bassler. 2019. Bark beetle population dynamics in the anthropocene: challenges and solutions. *Trends in Ecology and Evolution* 34:914-924.

Bonanomi, G., M. Rietkerk, S. C. Dekker, and S. Mazzoleni. 2008. Islands of fertility induce co-occurring negative and positive plant-soil feedbacks promoting coexistence. *Plant Ecology* 197:207-218.

Booth, M. G., and J. D. Hoeksema. 2010. Mycorrhizal networks counteract competitive effects of canopy trees on seedling survival. *Ecology* 91:2294-2302.

Bottero, A., A. W. D'Amato, B. J. Palik, J. B. Bradford, S. Fraver, M. A. Battaglia, and L. A. Asherin. 2017. Density-dependent vulnerability of forest ecosystems to drought. *Journal of Applied Ecology* 54:1605-1614.

Brown, P. M. 1996. OLDLIST: a database of maximum tree age. *Tree rings, environment, and humanity. Radiocarbon*, 1996: 727 - 731.

Calder, W. J., and S. B. St. Clair. 2012. Facilitation drives mortality patterns along succession gradients of aspen-conifer forests. *Ecosphere* 3:1-11.

Chagnon, P. L., R. L. Bradley, and J. N. Klironomos. 2020. Mycorrhizal network assembly in a community context: the presence of neighbours matters. *Journal of Ecology* 108:366-377.

Chen, L., L. S. Comita, S. J. Wright, N. G. Swenson, J. K. Zimmerman, X. Mi, Z. Hao, W. Ye, S. P. Hubbell, W. J. Kress, M. Uriarte, J. Thompson, C. J. Nytch, X. Wang, J. Lian, and K. Ma. 2018. Forest tree neighborhoods are structured more by negative conspecific

density dependence than by interactions among closely related species. *Ecography* 41:1114-1123.

Clair, S. B. S., X. Cavard, and Y. Bergeron. 2013. The role of facilitation and competition in the development and resilience of aspen forests. *Forest Ecology and Management* 299:91-99.

Clark, J. S., D. M. Bell, M. C. Kwit, and K. Zhu. 2014. Competition-interaction landscapes for the joint response of forests to climate change. *Global Change Biology* 20:1979-1991.

Close, D. C., C. L. Beadle, P. H. Brown, and G. K. Holz. 2000. Cold-induced photoinhibition affects establishment of *Eucalyptus nitens* (Deane and Maiden) Maiden and *Eucalyptus globulus Labill*. *Trees* 15:32-41.

Connell, J. H. 1971. On the role of natural enemies in preventing competitive exclusion in some marine animals and in rain forest trees. *Dynamics of populations* 298:312.

Das, A. J., N. L. Stephenson, and K. P. Davis. 2016. Why do trees die? Characterizing the drivers of background tree mortality. *Ecology* 97:2616-2627.

Dighton, J. 2007. 16 nutrient cycling by saprotrophic fungi in terrestrial habitats. *Environmental and Microbial Relationships* 4:287.

Dumbrell, A. J., M. Nelson, T. Helgason, C. Dytham, and A. H. Fitter. 2010. Relative roles of niche and neutral processes in structuring a soil microbial community. *The ISME Journal* 4:337-345.

Faeth, S. H., and W. F. Fagan. 2002. Fungal endophytes: common host plant symbionts but uncommon mutualists. *Integrative and Comparative Biology* 42:360-368.

Ford, K. R., I. K. Breckheimer, J. F. Franklin, J. A. Freund, S. J. Kroiss, A. J. Larson, E. J. Theobald, and J. HilleRisLambers. 2017. Competition alters tree growth responses to climate at individual and stand scales. *Canadian Journal of Forest Research* 47:53-62.

Frac, M., S. E. Hannula, M. Belka, and M. Jedryczka. 2018. Fungal biodiversity and their role in soil health. *Frontiers in Microbiology* 9:707.

Furniss, T. J., A. J. Larson, and J. A. Lutz. 2017. Reconciling niches and neutrality in a subalpine temperate forest. *Ecosphere* 8:e01847.

Green, D. S., and C. D. Hawkins. 2005. Competitive interactions in sub-boreal birch–spruce forests differ on opposing slope aspects. *Forest Ecology and Management* 214:1-10.

Hansen, E. M., and E. M. Goheen. 2000. *Phellinus Weirii* and other native root pathogens as determinants of forest structure and process in western North America. *Annual Review of Phytopathology* 38:515-539.

He, F., and R. P. Duncan. 2000. Density-dependent effects on tree survival in an old-growth Douglas fir forest. *Journal of Ecology* 88:676-688.

Jactel, H., J. Petit, M.-L. Desprez-Loustau, S. Delzon, D. Piou, A. Battisti, and J. Koricheva. 2012. Drought effects on damage by forest insects and pathogens: a meta-analysis. *Global Change Biology* 18:267-276.

Janzen, D. H. 1970. Herbivores and the number of tree species in tropical forests. *The American Naturalist* 104:501-528.

Johnson, D. J., W. T. Beaulieu, J. D. Bever, and K. Clay. 2012. Conspecific negative density dependence and forest diversity. *Science* 336:904-907.

Karst, J., L. Marczak, M. D. Jones, and R. Turkington. 2008. The mutualism–parasitism continuum in ectomycorrhizas: a quantitative assessment using meta-analysis. *Ecology* 89:1032-1042.

Kirchmeier-Young, M. C., N. P. Gillett, F. W. Zwiers, A. J. Cannon, and F. S. Anslow. 2018. Attribution of the influence of human-induced climate change on an extreme fire season. *Earth's Future*, 7:2-10

Klein, T., R. T. W. Siegwolf, and C. Körner. 2016. Belowground carbon trade among tall trees in a temperate forest. *Science* 352:342-344.

Liang, Y., M. J. Duveneck, E. J. Gustafson, J. M. Serra-Diaz, and J. R. Thompson. 2018. How disturbance, competition, and dispersal interact to prevent tree range boundaries from keeping pace with climate change. *Global Change Biology* 24:e335-e351.

Lindahl, B. D., and A. Tunlid. 2015. Ectomycorrhizal fungi – potential organic matter decomposers, yet not saprotrophs. *New Phytologist* 205:1443-1447.

Lutz, J. A., T. J. Furniss, D. J. Johnson, S. J. Davies, D. Allen, A. Alonso, K. J. Anderson-Teixeira, A. Andrade, J. Baltzer, K. M. L. Becker, E. M. Blomdahl, N. A. Bourg, S. Bunyavejchewin, D. F. R. P. Burslem, C. A. Cansler, K. Cao, M. Cao, D. Cárdenas, L.-W. Chang, K.-J. Chao, W.-C. Chao, J.-M. Chiang, C. Chu, G. B. Chuyong, K. Clay, R. Condit, S. Cordell, H. S. Dattaraja, A. Duque, C. E. N. Ewango, G. A. Fischer, C. Fletcher, J. A. Freund, C. Giardina, S. J. Germain, G. S. Gilbert, Z. Hao, T. Hart, B. C. H. Hau, F. He, A. Hector, R. W. Howe, C.-F. Hsieh, Y.-H. Hu, S. P. Hubbell, F. M. Inman-Narahari, A. Itoh, D. Janík, A. R. Kassim, D. Kenfack, L. Korte, K. Král, A. J. Larson, Y. Li, Y. Lin, S. Liu, S. Lum, K. Ma, J.-R. Makana, Y. Malhi, S. M. McMahon, W. J.

McShea, H. R. Memiaghe, X. Mi, M. Morecroft, P. M. Musili, J. A. Myers, V. Novotny, A. de Oliveira, P. Ong, D. A. Orwig, R. Ostertag, G. G. Parker, R. Patankar, R. P. Phillips, G. Reynolds, L. Sack, G.-Z. M. Song, S.-H. Su, R. Sukumar, I.-F. Sun, H. S. Suresh, M. E. Swanson, S. Tan, D. W. Thomas, J. Thompson, M. Uriarte, R. Valencia, A. Vicentini, T. Vrška, X. Wang, G. D. Weiblen, A. Wolf, S.-H. Wu, H. Xu, T. Yamakura, S. Yap, and J. K. Zimmerman. 2018. Global importance of large-diameter trees. *Global Ecology and Biogeography* 27:849-864.

Munkvold, L., R. Kjøller, M. Vestberg, S. Rosendahl, and I. Jakobsen. 2004. High functional diversity within species of arbuscular mycorrhizal fungi. *New Phytologist* 164:357-364.

Pallardy, S. G. 2010. Physiology of woody plants. Academic Press.

Pena, R., J. Tejedor, B. Zeller, M. Dannenmann, and A. Polle. 2013. Interspecific temporal and spatial differences in the acquisition of litter-derived nitrogen by ectomycorrhizal fungal assemblages. *New Phytologist* 199:520-528.

Rudawska, M., R. Wilgan, D. Janowski, M. Iwański, and T. Leski. 2018. Shifts in taxonomical and functional structure of ectomycorrhizal fungal community of Scots pine (*Pinus sylvestris L.*) underpinned by partner tree ageing. *Pedobiologia* 71:20-30.

Salomón, R. L., E. Tarroux, and A. DesRochers. 2016. Natural root grafting in *Picea mariana* to cope with spruce budworm outbreaks. *Canadian Journal of Forest Research* 46:1059-1066.

Schoettle, A. 2004. Ecological roles of five-needle pine in Colorado: potential consequences of their loss. *Breeding and genetic resources of five-needle pines: growth, adaptability and pest resistance*. *USDA Forest Service, Rocky Mountain Research Station*:124-135.

Segnitz, R. M., S. E. Russo, S. J. Davies, and K. G. Peay. 2020. Ectomycorrhizal fungi drive positive phylogenetic plant–soil feedbacks in a regionally dominant tropical plant family. *Ecology* 101:e03083.

Simard, S., and A. Vyse. 2006. Trade-offs between competition and facilitation: a case study of vegetation management in the interior cedar–hemlock forests of southern British Columbia. *Canadian Journal of Forest Research* 36:2486-2496.

Simard, S. W., D. A. Perry, M. D. Jones, D. D. Myrold, D. M. Durall, and R. Molina. 1997. Net transfer of carbon between ectomycorrhizal tree species in the field. *Nature* 388:579-582.

Simard, S. W., K. J. Beiler, M. A. Bingham, J. R. Deslippe, L. J. Philip, and F. P. Teste. 2012. Mycorrhizal networks: mechanisms, ecology and modelling. *Fungal Biology Reviews* 26:39-60.

Smith, S. E., and D. J. Read. 2010. Mycorrhizal symbiosis. Academic press.

Tang, J., S. Luyssaert, A. D. Richardson, W. Kutsch, and I. A. Janssens. 2014. Steeper declines in forest photosynthesis than respiration explain age-driven decreases in forest growth. *Proceedings of the National Academy of Sciences* 111:8856-8860.

Terhonen, E., K. Blumenstein, A. Kovalchuk, and F. O. Asiegbu. 2019. Forest tree microbiomes and associated fungal endophytes: functional roles and impact on forest health. *Forests* 10:42.

Teste, F. P., and S. W. Simard. 2008. Mycorrhizal networks and distance from mature trees alter patterns of competition and facilitation in dry Douglas-fir forests. *Oecologia* 158:193-203.

Teste, F. P., S. W. Simard, and D. M. Durall. 2009b. Role of mycorrhizal networks and tree proximity in ectomycorrhizal colonization of planted seedlings. *Fungal Ecology* **2**:21-30.

Teste, F. P., S. W. Simard, D. M. Durall, R. D. Guy, M. D. Jones, and A. L. Schoonmaker. 2009a. Access to mycorrhizal networks and roots of trees: importance for seedling survival and resource transfer. *Ecology* 90:2808-2822.

Van Dorp, C. H., S. W. Simard, and D. M. Durall. 2020. Resilience of *Rhizopogon*-Douglas-fir mycorrhizal networks 25 years after selective logging. *Mycorrhiza* 30:467-474.

van Mantgem, P. J., N. L. Stephenson, J. C. Byrne, L. D. Daniels, J. F. Franklin, P. Z. Fulé, M. E. Harmon, A. J. Larson, J. M. Smith, A. H. Taylor, and T. T. Veblen. 2009. Widespread increase of tree mortality rates in the western United States. *Science* 323:521-524.

Vila-Cabrera, A., A. C. Premoli, and A. S. Jump. 2019. Refining predictions of population decline at species' rear edges. *Global Change Biology* 25:1549-1560.

Wang, P., S. P. Li, X. Yang, J. Zhou, W. Shu, and L. Jiang. 2020. Mechanisms of soil bacterial and fungal community assembly differ among and within islands. *Environmental Microbiology* 22:1559-1571.

Werner, G. D., and E. T. Kiers. 2015. Partner selection in the mycorrhizal mutualism. *New Phytologist* 205:1437-1442.

Worrall, J. J., G. E. Rehfeldt, A. Hamann, E. H. Hogg, S. B. Marchetti, M. Michaelian, and L. K. Gray. 2013. Recent declines of *Populus tremuloides* in North America linked to climate. *Forest Ecology and Management* 299:35-51.

Wu, Y. T., T. Wubet, S. Trogisch, S. Both, T. Scholten, H. Bruelheide, and F. Buscot. 2013. Forest age and pant species composition determine the soil fungal community composition in a Chinese subtropical sorest. *PLoS One* 8:e66829.

Young, D. J., J. T. Stevens, J. M. Earles, J. Moore, A. Ellis, A. L. Jirka, and A. M. Latimer. 2017. Long-term climate and competition explain forest mortality patterns under extreme drought. *Ecology Letters* 20:78-86.

Zhang, J., S. Huang, and F. He. 2015. Half-century evidence from western Canada shows forest dynamics are primarily driven by competition followed by climate. *Proceedings of the National Academy of Science*s 112:4009-4014.

Zinke, P. J. 1962. The pattern of influence of individual forest trees on soil properties. *Ecology* 43:130-133

1.3 TABLES

Table 1.1. A limited overview of fungal functional guilds and the potential avenues in which they influence forest growth and health.

Functional guild	Influence on forest	Source
Endophyte	Production of defense compounds, opportunistic exploitation	Faeth and Fagan 2002, Terhonen et al. 2019
Mycorrhizae	Provide nutrients to plant host; form common mycorrhizal networks; nutrient cycling	Smith and Read 2010, Simard et al. 2012, Lindahl and Tunlid 2015
Pathogen	Direct (*Armillaria*) or indirect factor (various heart-rots) in tree mortality; reduction in tree vigor	Das et al. 2016, Hansen and Goheen 2000
Saprotroph	Nutrient cycling and decomposition of dead organic matter	Dighton 2007

Chapter 2: Decline of an ecotone forest: 50 years of demography in the southern boreal forest [1]

2.1 ABSTRACT

Variation in tree recruitment, mortality, and growth can fundamentally alter forest community composition, structure, and the strength of conspecific and heterospecific interactions. Because tree recruitment and mortality events are generally infrequent, long-time scales are needed to confirm trends in forests. I performed a 50-year demographic and spatial analysis on a forest plot located on the southern edge of the Canadian boreal forest, a region currently experiencing forest die-back in response to direct and indirect effects of recent severe droughts. Here, I show that the last 30 years have seen a collapse in biomass, basal area, growth, and recruitment along with a precipitous rise in mortality across the dominant tree species. However, among decades, the strength and direction of these demographic varied in response with time and disturbance severity. The stand experienced periods of drought in combination with multiple outbreaks of forest tent caterpillar (*Malacosoma disstria*) and spruce beetle (*Dendroctonus rufipennis*), an insect novel to this region. These insect disturbances interacted to strongly increase mortality rates within the stand and decrease stand density. The interaction of endogenous and exogeneous factors may shift forests in this region onto novel successional trajectories with the possibility of changes in regional vegetation type.

[1] A version of this chapter was published as Birch, J. D., J. A. Lutz, E. Hogg, S. W. Simard, R. Pelletier, G. H. LaRoi, and J. Karst. 2019a. Decline of an ecotone forest: 50 years of demography in the southern boreal forest. *Ecosphere* 10:e02698.

2.2 INTRODUCTION

Forests change through mortality, recruitment of new stems, and growth. These processes underlie stand demography and are critical for predicting the responses to future climates (Kobe 1996, Dietze and Moorcroft 2011, Chen and Luo 2015). Tree mortality rates have increased in forests across North America (van Mantgem et al. 2009, Peng et al. 2011) with some regions demonstrating concomitant reductions in growth and recruitment rates (Barber et al. 2000, Chen and Luo 2015, Hogg et al. 2017). Long-term studies are critical for predicting forest responses to future climates and disturbance regimes. Of particular importance is to understand how forests have already responded to altered climate to better predict future forest change.

Portions of the boreal forest have already responded to drought with altered demographic rates, shifts in disturbance regimes, and range shifts of some tree species (Soja et al. 2007, Allen et al. 2010). Widespread increases in tree mortality have been reported, particularly for *Populus tremuloides* Michx. in the aspen parkland ecozone that forms an ecotone between the Great Plains and the boreal forest. In recent decades, *Populus* has experienced drought and insect-induced mortality (Hogg et al. 2002a, Michaelian et al. 2011); however, the decline in tree health is not isolated to *Populus*. *Picea glauca* (Moench) Voss has also experienced drought-induced decline in growth rates across west-central Canada and has projected loss in cover under future climates (Gray and Hamann 2011, Hogg et al. 2017).

Mortality rates have risen across the North American boreal forest in the last half-century, and climatic conditions are implicated as the likely driver (Peng et al. 2011, Worrall et al. 2013). As mortality events have become more frequent, a consistent loss in aboveground biomass has arisen across the western boreal forest (Michaelian et al. 2011, Chen and Luo 2015).

Continued warming and drying of the southern boreal forest could shift the aspen parkland northward (Hogg and Hurdle 1995, Frelich and Reich 2010). The shift from boreal forest to sparse woodland could be rapid and characteristic of a stable state change (Scheffer et al. 2012).

Succession in the western boreal forest is variable but is usually characterized by a transition from *Populus* or *Pinus* to the more shade tolerant *Picea* (Brassard and Chen 2006, Bergeron et al. 2014). However, successional pathways could change with future climates and under novel disturbance regimes. As warming and species-specific die-offs within the southern boreal forest continue, understanding stand dynamics and climate responses is crucial to understanding future forest ecosystem processes (Hogg and Hurdle 1995, Hogg et al. 2002a, Michaelian et al. 2011).

To explore how demographic rates changed in the southern boreal forest ecotone, I conducted a 50-year demographic and tree-ring analysis in a mixed-wood plot situated at the southern edge of the southwestern Canadian boreal forest. Over the past 50 years, this forest has experienced episodic severe drought, defoliation by forest tent caterpillar (*Malacosoma disstria*), and out-breaks of unidentified bark beetles. I compiled and extended the decadal surveys to investigate how demographic rates changed for common tree species and the successional pathway of the forest. This study provides an unparalleled reference on trends in forest demography in the region which subsequent studies can be compared. Importantly, this study will allow us to identify deviations from long-term trends in forest structure and composition.

2.3 METHODS

Site description

The George LaRoi Forest Plot (herein referred to as the "GLR plot") covers 1.4 ha (110 × 130 m) of boreal mixed-wood located at 53.408 N, 113.751 W, near Edmonton, Alberta, Canada. The study area is a mixed forest consisting of *Picea glauca* (Moench) Voss, *Pinus banksiana* Lambert, *Populus tremuloides* Michx, and *Betula papyrifera* Marshall, Arbust. The forest exists in one of the southernmost pockets of *Pinus banksiana* within Alberta. Other tree and shrub species in the study area are *Picea mariana* (Miller) Britton*, Prunus virginiana* Linnaeus, *Prunus pensylvanica* Linnaeus f, *Amelanchier alnifolia* (Nuttall) Nuttall ex M. Roemer, *Corylus cornuta* Marshall, and *Salix* spp. (Appendix 2.1 Image S2.1:S2.3). Shrub cover is sporadic and aggregated within the plot. The forest originated from natural regeneration in 1925. Burn scars on the oldest snags suggest a stand-replacing wildfire in the early 1920s. The plot has a 20–60 m buffer of forest separating the boundary from adjacent ornamental gardens and private forested land. The soil of the plot is a Brunisol and derived from aeolian parent material. The soil texture is a sandy loam graduating to a loamy sand with increasing depth. The local climate is characterized by a mean annual temperature of 2.2° ± 1.1°C (SD), yearly precipitation of 451 ± 78 (SD) mm, and growing season-dominated precipitation of 318 ± 76 (SD) mm (May–September) (Environment and Climate Change Canada 2017). Botanical nomenclature follows Flora of North America (Flora of North America Editorial Committee 1993+).

2.3.1 Stand census and stem mapping

The first forest census and stem mapping of the GLR plot was conducted in 1967 as an ecological celebration of Canada's centennial followed by subsequent censuses in 1977, 1988, 1997, and 2017. The planned 2007 census was not conducted because of insufficient funding. During each census, stems were mapped, and diameter measured to calculate stand density, vital rates (mortality and recruitment), and growth (basal area increment). The diameter of all tree

stems was measured at 1.35 m in height (DBH) to the nearest 0.1 cm. Stems <5.0 cm DBH were measured using calipers and larger trees, using fiberglass DBH tapes. Stems were mapped using mirror compasses and transect tapes. To map the stems, tapes were stretched along 5 × 5 m quadrats along an N–S orientation, and the perpendicular intersection with a stem was located on the transect. Stems were marked as gone if they were missed in all subsequent surveys (1977–1997), or if no snag or stump was visible in the 2017 survey. Stems of *Picea* and *Pinus* were examined for beetle entry-exit holes and beetle galleries indicative bark beetles. Bark beetle galleries on *Picea* were likely created by multiple species of bark beetle while those present on *Pinus* were indicative of *Dendroctonus ponderosae*.

2.3.2 Stand demography

Using census data from across the five decades, I calculated stand and species-level density (stems ha^{-1}), mortality and recruitment rates (annually compounded rate), growth (cm $decade^{-1}$), standing biomass (Mg ha^{-1}), and basal area (m^2 ha^{-1}). Mortality rates were calculated using an exponential curve; $t_2 - i = t_1 e^{x*z}$, where $'t_1'$ is the abundance at time one, $'t_2'$ the abundance at time two, $'i'$ is recruitment, $'x'$ the annual compounded rate of change, and $'z'$ the time in years between time one and two. Recruitment was reported as the total number of stems (alive and recently dead) that grew to 1.35 m in height between censuses. Recruitment annual rates were calculated using an exponential curve; $t_1 + i = t_1 e^{x*z}$, where $'t_1'$ is the abundance at time one, $'i'$ is recruitment, $'x'$ the annual compounded rate of change, and $'z'$ the time in years between time one and two. A stem was classified as recruited if it had not been measured in any previous census and was smaller than 8.0 cm DBH in 2017, due to the 20-year gap. The 8.0 cm cutoff was derived from the maximum decadal growth observed in stems within the plot. Stems above 8.0 cm were assumed to have been overlooked in previous censuses.

Tree biomass estimates were calculated by using allometric equations generated from Canadian-wide data (Ung et al. 2008) and scaled up to the stand by summing all living stems biomass. Summary statistics and graphing of demographic rates were conducted in the statistical program R version 3.5.0 (R Core Team 2018). The distributions of DBH for living and dead stems were non-normal. A Wilcoxon Rank Sum test was used to test for significant differences between living and dead DBH for each species per census.

2.3.3 Increment core and basal area increment

In May 2017, to calculate annual growth, identify insect disturbances, and reconstruct climate responses, increment cores were taken from a representative subsample of each of the four common tree species; *Picea*; n=25, *Populus*; n=18, *Betula*; n=12, and *Pinus*; n=22. Trees were randomly selected from trees ≥ 10 cm DBH to avoid long-term damage to the tree. Sample size was reduced for *Populus* and *Betula* due unidentified rot. Two increment cores were taken per tree with a 4.3 mm increment borer (Haglöf Sweden, Mora, Sweden). Increment cores were mounted and sanded with progressively finer grit sandpaper to 1200 grit. Cores were visually crossdated (Fritts 1976, Stokes and Smiley 1996, Speer 2010) scanned at 1200 DPI using a 630 Pro Photo Scanner (Epson, Long Beach, California, USA), and measured using the program Coorecorder 9.3 (Larsson 2018). Crossdating was verified using the COFECHA program (Holmes 1983) and detrended in the statistical program R, using the dplR 1.6.8 package (Bunn et al. 2017, R Core Team 2018). Cores of *Picea* were assessed from pith to bark for signs of diagnostic traumatic resin ducts (TRD), indicating beetle attack in spruce (DeRose et al. 2017), and cores *of Populus* and *Betula* were visually scanned from pith to bark to identify white discolored rings indicating defoliation events (Hogg et al. 2002b) (Appendix 2.1 Fig. S2.1A, S2.1B). Using raw ring widths, I calculated growth rates ($mm^2\ yr^{-1}$) and standardized ring widths

for each species. Basal area increment (BAI) was calculated using the dplR package (Bunn et al. 2017). Standardized ring widths were calculated by detrending the width measurements with a spline. Each core was individually detrended to remove low frequency variation in raw ring width, including age-related growth trend. Multiple splines were visually assessed for goodness of fit and a Friedman variable span smoother was selected as the most appropriate spline. Standardized tree ring widths were used in chronology assembly and climate analysis.

2.3.4 Climate response analysis

To determine which climate variables influenced tree growth, I conducted a seasonal climate correlation analysis. I used species-specific chronologies and conducted Pearson correlation analysis between each species' chronology and the climate variables of interest using the R package, treeclim 2.0.0 (Zang and Biondi 2015). Specifically, I used the SEASCORR procedure (Meko et al. 2011), which uses Monte Carlo simulations to assess significance of the correlations (Percival and Constantine 2006). The chronology was prewhitened and a biweight robust estimate of the mean was used to minimize the influence of outliers on the chronology (Cook 1985). I chose monthly precipitation, mean maximum temperature, and mean minimum temperature as the climate variables for analysis as these variables were continuous throughout the climatic record and likely to represent conditions limiting tree growth. The analysis covered the years 1961–2017; the earliest and last year of complete climatic data, respectively. Historical weather data (1961–2017) were concatenated from two climate reporting stations 16 km from the center of the plot at the Edmonton International Airport, Alberta, Canada (Environment and Climate Change Canada 2017). I specified September as the end of the growing season and used season lengths of 1, 3, 6, 9, and 12 months. Monthly correlations were generated by aggregating variables over the season lengths provided with seasons shifting in monthly increments to assess

how cumulative months of climatic data correlated with tree-ring growth. Seasons of different lengths assess the cumulative effect of monthly climate variables on tree growth. I generated Pearson correlation coefficients for the primary and secondary climatic variables for each species. The secondary climate variables are correlated with the residuals of ring-width explained by the primary variable. Pearson correlation coefficients were generated for each combination of climate variables as the primary and secondary variable.

2.3.5 Regional forest comparison

To compare the GLR plot dataset with regional plots, I used publicly available Alberta biodiversity monitoring Institute (ABMI) data. I selected ABMI plots within 200 km of the GLR plot and subset 5 × 5 m cells that were surveyed within 2015, 2016, or 2017 and had at least one species in common with the GLR plot (ABMI 2017). I performed a non-metric multidimensional ordination (NMDS) with the subset of ABMI data and an equal number of randomly selected 5 × 5 m cells from the GLR plot based on the basal area of tree species. I used the 'vegdist' function in ecodist 2.0.1 to apply Bray-Curtis dissimilarity prior to ordinating the data using the using the 'metaMDS' function in vegan 2.5–2 packages (Oksanen et al. 2018, Goslee and Urban 2007). To compare growth trends between *Picea* within the GLR plot and regional plots, I compared mean raw ring widths from seven local sites and Alberta-wide sites measured by Hogg et al. (2017) against those at the GLR plot. Growth data from *Picea* collected by Hogg et al. (2017) was truncated to 1967–2015 for the analysis as well as growth records from several sites spanning subsets of the full analysis period 1967–2015.

2.4 RESULTS

2.4.1 Changes to stand density, basal area, and biomass

All species declined in density 1967–2017. Stand density peaked at 2408 stems ha^{-1} in 1967 and declined 76% to a low of 569 stems ha^{-1} in 2017. *Picea* increased 16% in density from 1066 stems ha^{-1} in 1967 to 1245 stems ha^{-1} in 1988 before falling 70% to a low of 376 stems ha^{-1} in 2017 (Fig. 2.1A). *Populus* declined by 89% in density from its peak of 1157 stems ha^{-1} in 1967 to 127 stems ha^{-1} in 2017 (Fig. 2.1B). *Betula* declined by 65% in density from a high of 108 stems ha^{-1} in 1967 to 37 stems ha^{-1} in 2017 (Fig. 2.1C). *Pinus* declined by 61% from a high of 76 stems ha^{-1} in 1967 to 29 stems ha^{-1} in 2017 (Fig. 2.1D). Stand basal area increased from 1967 to 1997; it peaked at 28.2 m^2 ha^{-1} in 1997 before declining 29% to 19.8 m^2 ha^{-1} in 2017. Total stand biomass increased from 64 Mg ha^{-1} 1967 to a high of 120 Mg ha^{-1} in 1997 before declining 25% to 90 Mg ha^{-1} in 2017 (Appendix 2.1 Fig. S2.2A, S2.2B). All species increased in mean DBH through time and, except for *Betula*, had significant differences between living and dead stem DBH at every census point (Appendix 2.1 Fig. S2.3). Annual mean basal area increment fluctuated through time. Specifically, mean basal increment of *Populus* precipitously dropped between 1980–1988, which coincided with defoliation by *Malacosoma disstria*. All species declined in growth in 2002, likely due to the severe drought in that year (Fig. 2.2).

2.4.2 Vital rates

Mortality rates varied by species and showed pronounced changes by decade (Fig. 2.3A). *Picea* mortality rates remained comparatively low 1967–1997, before rising to 5.9% $year^{-1}$ during 1997–2017. *Populus* mortality rates peaked at a rate of 6.8% $year^{-1}$ 1988–1997. *Betula* mortality remained stable through time with the lowest mortality rate of 2.1% $year^{-1}$ occurring

1977–1988. *Pinus* mortality increased from 0.98% year^{-1} in 1967 to 2.3% yr^{-1} in 2017 but remained the lowest rate across all species. Recruitment rates were low throughout the duration of the study and declined with time (Fig. 2.3B). Recruitment rates never exceeded mortality rates except for *Picea* 1967–1988. *Picea* recruitment peaked 1977–1988 at an annual rate of 1.6% year^{-1} before decreasing by 79% to 0.35% year^{-1} 1997 – 2017. *Populus* recruitment declined from a rate of 0.46% year^{-1} in 1967 to 0.13% year^{-1} in 2017. *Betula* recruitment increased from 0.38% year^{-1} from 1967–1977 to 1.7% 1988–1997, before falling to 0.69% year^{-1} 1997–2017. *Pinus* recruitment was absent 1967–1997, before rising to 0.07% year^{-1} 1997–2017.

2.4.3 Stand history of insect attack

I observed bands of traumatic resin ducts (TRDs) in *Picea* (n=14) in 11 of 13 years from 2002–2015. The greatest proportion of TRDs was in 2014 with 42% of trees having a TRD (Appendix 2.1 Fig. S2.10A). I detected white rings in 100% of cored *Populus* (n=18) and *Betula* (n=12). White rings occurred on *Populus* during 1979–1988. Six of the ten years of white rings had over 50% of the trees affected. The greatest proportion of white rings were detected in 1980 where 100% of *Populus* cores displayed white rings. Interestingly, *Betula* exhibited only one white ring, in 1987, where 100% of individuals show a white ring (Appendix 2.1 Fig. S2.10B). Diagnostic galleries indicative of mountain pine beetle (*Dendroctonus ponderosae* Hopkins) and *Ips* spp. were observed in less than 20% of *Pinus* individuals ($n \leq 10$). I did not identify any diagnostic features in *Pinus* rings to identify the years of beetle attack. Galleries of multiple species of unidentified bark beetles were observed on *Picea*.

2.4.4 Climate response of trees

Ring widths of all species were significantly correlated with growing season precipitation and declined in annual growth corresponding with drought. Precipitation and temperature show pronounced variation across years (Appendix 2.1 Fig. S2.4A, S2.5A) and with season (Appendix 2.1 Fig. S2.4B, S2.5B). The highest correlations occurred with precipitation as the primary variable and mean maximum temperature as the secondary variable (Appendix 2.1 Fig. S2.6:S2.9). Of the four species, *Betula* displayed the strongest correlation with precipitation. *Picea* and *Pinus* displayed similar correlations with precipitation but varied in the time of year that was associated with the highest correlation. *Populus* displayed the weakest correlation despite its high sensitivity values (Appendix 2.1 Table S2.2).

As the length of the seasonal window increased, the strength of correlation increased between monthly precipitation and *Picea* ring growth. June precipitation was the strongest positively correlated variable across all seasons. Mean maximum temperature in the previous year's September was significantly negatively correlated for the 1 and 3-month seasons with November significant at the 6-month season (Appendix 2.1 Fig. S2.6). *Picea* growth responded favorably to summer precipitation and negatively to warm fall temperatures of the previous year.

Precipitation was significantly positively correlated with *Populus* growth in the 1, 3, 6, and 9-month seasons. The highest correlation was in the 9-month season in May. The highest overall negative correlation was with mean maximum temperature as a secondary variable in the 6-month season during the previous year's November and December (Appendix 2.1 Fig. S2.7). *Populus* growth favors late spring precipitation and declines with warm wintertime temperatures in the previous year.

The most sensitive species, *Betula*, showed strong positive correlations with precipitation across all season lengths. The highest correlation was with the 9-month season and May and June. Mean maximum temperature was negatively correlated across all seasons and most strongly in the 6-month season during November and December of the previous year (Appendix 2.1 Fig. S2.8). *Betula* growth responded favorably with moderately cool, wet conditions; particularly in May and June. As with *Picea* and *Populus*, warm fall and wintertime temperatures are associated with decreased *Betula* growth.

Interestingly, *Pinus* displayed strong, positive correlations with both precipitation and mean maximum temperature. It is the only species to display a positive correlation with mean maximum temperature. The highest correlation with precipitation occurred in the 12-month season in August of the previous year. Mean maximum temperature was most strongly correlated in the 1-month season in December of the previous year (Appendix 2.1 Fig. S2.9). The low series intercorrelation and complacency of *Pinus banksiana* resulted in the detection of anomalies in the series due to poorly behaving trees (Appendix 2.1 Table S2.2) that did not share the stand-wide growth signal.

2.4.5 Regional forest composition

The GLR plot is statistically similar in composition and raw ring growth to other stands within the region. A NMDS of basal area by species from a random subset of the GLR cells overlapped with ABMI plots within 200 km of the GLR plot (Appendix 2.1 Fig. S2.11) (ABMI 2018). Additionally, I compared *Picea* raw ring growth from the GLR and those measured by Hogg et al. (2017) for 1967–2015 and found that *Picea* ring growth within the GLR is

statistically indistinguishable from provincial growth values in all but two (2003, 2009) of the last 48 years (Appendix 2.1 Fig S2.12).

2.5 DISCUSSION

My findings detail 50 years of succession and eventual decline of an ecotone forest undergoing repeated disturbances. The temporal depth and tracking of individual trees through time at the GLR plot provides unique evidence of change at a forest ecotone. These results highlight dramatic changes in mortality rates, ring growth, and recruitment rates in the last twenty years coinciding with repeated drought and the outbreaks of bark beetles. Cumulatively, the results highlight the deterioration of the original forest cohort and the failure of new cohorts to establish in the fallout of repeated insect disturbance and drought. This has resulted in a new successional trajectory that may become more prevalent in the ecotone with repeated drought and the continued outbreaks of bark beetles and other insects.

2.5.1 Comparison of GLR to regional forests and its departure from historic succession

Mortality rates within the GLR plot have varied over time but display substantial departures from the regional and Canada-wide rates. The 2010 mortality rates for *Picea* are expected to be between 1–2% year^{-1}, and 2–3 % year^{-1} for *Populus* (Peng et al. 2011, Zhang et al. 2015). In comparison, I measured 5.94% year^{-1} for *Picea* and 5.32% year^{-1} for *Populus* 1997–2017 in the GLR plot. Not only are the mortality rates for the GLR elevated above reported values but these mortality rates have also grown at double their Canada-wide species-specific rates. Peng et al. (2011) reported that mortality rates are increasing across the Canadian boreal forest with *Picea* increasing by 3.29% year^{-1} and *Populus* increasing by 2.84% year^{-1}. In comparison, the *Picea* mortality rates in GLR increased by 7.1% year^{-1} with *Populus* rates

increasing by 6.24% year^{-1} 1977–1997 and decreasing by 1.24% year^{-1} 1997–2017. The average increase in mortality rates for the western Canadian boreal forest was 4.7% year^{-1} 1963–2008 (Peng et al. 2011), which is still substantially lower than the rates seen in the GLR plot.

Recruitment rates have largely declined with time for the Canadian boreal forest (Zhang et al. 2015), a trend that I also observed at the GLR plot. The values of recruitment for *Picea* were roughly 20% of expected values in 1977, 50% in 1988, 13% in 1997, and 41% of those expected in 2017 (Zhang et al. 2015). Further, recruitment rates of *Populus* were 41% of expected in 1977, 13% in 1988, 3% in 1997, and 40% of expected in 2017 (Zhang et al. 2015). However, the inequality in rates between GLR and region-wide is underestimated because 66% of *Picea* and 28% of *Populus* recruited 1997–2017 were dead at the time of their measurement. The failure of recruited stems to survive means that the successful recruitment rate for the GLR stand is lower than the 'total' recruitment reported in the results.

Normally one would expect stands in the southern boreal forest to progress from an overstory of shade-intolerant *Populus* and *Betula* to shade-tolerant *Picea*, although considerable variation is possible (Brassard and Chen 2006, Bergeron et al. 2014, Chen and Popadiuk 2002). Current conceptual models of succession for the western boreal forest, and Alberta specifically, lack a shrubless, low density woodland phase or bark beetles as a disturbance agent (Chen and Popadiouk 2002). The extremely low rate of successful recruitment over the previous 30 years means that a new cohort, if one begins, will take decades to structurally replace the rapidly dying overstory. Results from my study suggest that historical successional pathways have been stymied and could be a 'new-normal' for other stands in this ecotone; particularly if the bark beetle species seen in the stand outbreak and encroach into regional stands. The recent,

widespread die-off of *Populus* across the region has been documented (Michaelian et al. 2011) and the defoliation years (1979–1988) within the GLR match years of outbreaks of *M. disstria* across Alberta (Hogg et al. 2002a). Multiple years of defoliation can cause high mortality (Moulinier et al. 2014) and long-term changes in cell fibers with possible negative implications for structure and drought response (Hillabrand et al. 2019). The trees used to reconstruct the history of defoliation in the GLR were the surviving, non-rotten cohort and it is possible that the *Populus* that died before 2017 suffered additional defoliation events or died as a direct result of defoliation. The decline of *Populus* overlaps the continuing drought-related decline of *Picea* growth within the region (Hogg et al. 2017). In addition to being implicated in the depressed *Picea* growth, the extreme 2002 drought was likely associated with the outbreak of bark beetles. Previous research have linked outbreaks of *Dendroctonus rufipennis* to drought (Berg et al. 2006) with warming temperatures hastening generation time (Hansen et al. 2001) and increasing the likelihood of outbreak (Hansen and Bentz 2003). Predictably, the initial beetle outbreak at the GLR plot, in 2002, occurred during the driest year since stand establishment in the 1920s. I speculate that the weakened *Picea* were unable to mount an effective defense against bark beetles, and that this led to the expansion and outbreak within the stand. The combined effects of bark beetles and the severe droughts of recent decades likely stressed *Picea* and resulted in precipitous declines in density, growth, recruitment, and biomass. The confluence of these disturbances seems to have shunted the GLR stand onto a new trajectory. The dramatic changes seen in forest composition and structure could be a preview for stands across the southwestern boreal forest of Canada. Further studies are needed to test the generality of the demographic patterns I observed in the GLR plot.

2.5.2 Seasonal climate analysis

Precipitation was the greatest correlate with tree ring growth for all four of the GLR species. All species were positively correlated with wetter growing seasons and some portion of climate variables in the previous year. This supports the other evidence from the plot showing drought caused declines in growth in all species and the multi-year influence of climate on tree ring growth. *Picea* in my study showed strong correlations with precipitation in contrast with work by Goldblum and Rigg (2005) in Ontario, Canada, who found no correlation with precipitation and *Picea* growth. This discrepancy is possibly due to the local topography of the GLR or regional differences in climate between the southern boreal forest of Alberta and Ontario. The *Populus* in the GLR had high series intercorrelation and tree ring sensitivity but the lowest correlation coefficients of the four tree species. One explanation is that the repeated insect defoliation obscure growth climate relationships (see Hogg et al. 2013). However, Huang et al. (2010) also found that *Populus* in Ontario was the least responsive species to recent warming along the southern boreal ecotone. This suggests that *Populus* may be less responsive to climate than its neighboring species.

Pinus was the only species to respond favorably to increasing temperature. It is likely that *Pinus* is temperature-limited within the stand during non-drought years and that warmer temperatures are associated with increased photosynthesis or a longer growing season. Other studies in the Canadian boreal forest have also seen *Pinus* respond favorably with warmer and wetter growing seasons (Brooks et al. 1998, Huang et al. 2010).

Cumulatively, the seasonal analysis for all tree species shows a favorable growth response to growing season precipitation and a largely negative relationship with warming

temperatures. If future climates bring warmer growing season temperatures, I predict a decline in *Picea, Populus*, and *Betula* ring growth and a potential increase in *Pinus* growth.

2.5.3 Conclusion

I present evidence suggesting that in response to recent drought and warming, a novel successional pathway has developed in at least some stands along the southern edge of the western Canadian boreal forest. A decline in forest vital rates and insect-associated mortality has set the stand on a path towards a state characterized by a continued decline of the original establishing cohort and absent new recruitment. Future droughts could see bark beetles and other insect outbreak in stands in the region. As warming and severe climatic events are expected to continue or increase (Diffenbaugh and Field 2013), I anticipate that the results presented here may become commonplace throughout the southwestern boreal forest, but this hypothesis requires further testing. My study highlights the reality that novel disturbance regimes may become widespread across the region and lead to changes in vegetation type. Further, this study highlights the utility of tree ring analysis when paired with long-term demographic and spatial plots (*sensu* Lutz 2015). The use of tree ring analysis reconstructed the inter-census history of the stand and, paired with the census data, allowed me to identify key events that altered forest density. While my study is novel, several limitations exist. The coarse, decadal interval prevents me from identifying specific years for mortality or recruitment events. Further, the mortality agents I identified may have only been the final agent in a suite of stressors that predisposed the tree to death. Larger, replicated plots with more frequent census intervals would address many of these limitations in future studies and detect change across the region. Other studies (Brassard and Chen 2006, Michaelian et al. 2011, Bergeron et al. 2014, Zhang et al. 2015, Chen and Luo 2015, Gendreau-Berthiaume et al. 2016) have captured broad swathes of demographic and

spatial change within the aspen parkland and boreal forest; however, this study elucidates the long-term development of a forest undergoing succession under the influence of pronounced and, in some cases, novel disturbances. Continued monitoring and establishment of new long-term plots will aid in highlighting continued change and trends within the Canadian boreal forest.

2.6 REFERENCES

ABMI (Alberta Biodiversity Monitoring Institute). 2018. ABMI Trees & Snags (5342138678144103563) database: Rotation 2. Retrieved from http://www.ABMI.ca

Allen, C. D., A. K. Macalady, H. Chenchouni, D. Bachelet, N. McDowell, M. Vennetier, T. Kitzberger, A. Rigling, D. D. Breshears, E. H. (Ted) Hogg, P. Gonzalez, R. Fensham, Z. Zhang, J. Castro, N. Demidova, J.–H. Lim, G. Allard, S. W. Running, A. Semerci, and N. Cobb. 2010. A global overview of drought and heat-induced tree mortality reveals emerging climate change risks for forests. *Forest Ecology and Management* 259:660–684.

Barber, V., G. Patrick, and B. Finney. 2000. Reduced growth of Alaskan white spruce in the twentieth century from temperature-induced drought stress. *Nature* 405:668–673.

Berg, E. E., J. David Henry, C. L. Fastie, A. D. De Volder, and S. M. Matsuoka. 2006. Spruce beetle outbreaks on the Kenai Peninsula, Alaska, and Kluane National Park and Reserve, Yukon Territory: Relationship to summer temperatures and regional differences in disturbance regimes. *Forest Ecology and Management* 227:219–232.

Bergeron, Y., H. Y. H. Chen, N. C. Kenkel, A. L. Leduc, and S. E. Macdonald. 2014. Boreal mixedwood stand dynamics: ecological processes underlying multiple pathways. *The Forestry Chronicle* 90:202–213.

Brassard, B. W., and H. Y. H. Chen. 2006. Stand structural dynamics of North American boreal forests. *Critical Reviews in Plant Sciences* 25:115–137.

Brooks, J. R., L. B. Flanagan, and J. R. Ehleringer. 1998. Responses of boreal conifers to climate fluctuations: indications from tree-ring widths and carbon isotope analyses. *Canadian Journal of Forest Research* 28:524–533.

Bunn, A., M. Korpela, F. Biondi, F. Campelo, P. Mérian, F. Qeadan, and C. Zang. 2017. dplR: dendrochronology program library in R. R package version 1.6.8.

Chen, H. Y. H., and Y. Luo. 2015. Net aboveground biomass declines of four major forest types with forest ageing and climate change in western Canada's boreal forests. *Global Change Biology* 21:3675–3684.

Chen, H. Y., and R. V. Popadiouk. 2002. Dynamics of North American boreal mixedwoods. *Environmental Reviews* 10:137–166.

Cook, E. R. 1985. A time-series analysis approach to tree ring standardization. Dissertation. University of Arizona, Tuscon, Arizona, USA.

DeRose, R. J., M. F. Bekker, and J. N. Long. 2017. Traumatic resin ducts as indicators of bark beetle outbreaks. *Canadian Journal of Forest Research* 47:1168–1174.

Dietze, M. C., and P. R. Moorcroft. 2011. Tree mortality in the eastern and central United States: patterns and drivers. *Global Change Biology* 17:3312–3326.

Diffenbaugh, N. S., and C. B. Field. 2013. Changes in ecologically critical terrestrial climate conditions. *Science* 341:486–492.

Environment and Climate Change Canada. 2017. Historical climate database: — climate stations 3012205 and 3012216 – concatenated, 1961 to 2017. Accessed from http://climate.weather.gc.ca/historical_data/search_historic_data_e.html

Flora of North America Editorial Committee, eds. 1993. Flora of North America North of Mexico. New York and Oxford.

Frelich, L. E., and P. B. Reich. 2010. Will environmental changes reinforce the impact of global warming on the prairie-forest border of central North America? *Frontiers in Ecology and the Environment* 8:371–378.

Fritts, H. C. 1976. Tree rings and climate. Academic Press, London; New York, USA.

Gendreau-Berthiaume, B., S. E. Macdonald, and J. J. Stadt. 2016. Extended density-dependent mortality in mature conifer forests: causes and implications for ecosystem management. *Ecological Applications* 26:1486–1502.

Goldblum, D., and L. S. Rigg. 2005. Tree growth response to climate change at the deciduous-boreal forest ecotone, Ontario, Canada. *Canadian Journal of Forest Research* 35:2709–2718.

Goslee, S. C., and D. L. Urban. 2007. The ecodist package for dissimilarity-based analysis of ecological data. *Journal of Statistical Software* 22:1-19.

Gray, L. K., and A. Hamann. 2011. Strategies for reforestation under uncertain future climates: guidelines for Alberta, Canada. *PLoS One* 6:e22977.

Hansen, E. M., and B. J. Bentz. 2003. Comparison of reproductive capacity among univoltine, semivoltine, and re-emerged parent spruce beetles (*Coleoptera: Scolytidae*). *The Canadian Entomologist* 135:697–712.

Hansen, E. M., B. J. Bentz, and D. L. Turner. 2001. Temperature-based model for predicting univoltine brood proportions in spruce beetle (*Coleoptera: Scolytidae*). *The Canadian Entomologist* 133:827–841.

Hillabrand, R. M., V. J. Lieffers, E. H. Hogg, E. Martínez-Sancho, A. Menzel, and U. G. Hacke. 2019. Functional xylem anatomy of aspen exhibits greater change due to insect defoliation than to drought. *Tree Physiology* 39:45–54.

Hogg, E. H., A. G. Barr, and T. A. Black. 2013. A simple soil moisture index for representing multi-year drought impacts on aspen productivity in the western Canadian interior. *Agricultural and Forest Meteorology* 178:173–182.

Hogg, E. H., J. P. Brandt, and B. Kochtubajda. 2002a. Growth and dieback of aspen forests in northwestern Alberta, Canada, in relation to climate and insects. *Canadian Journal of Forest Research* 32:823–832.

Hogg, E. H., M. Hart, and V. J. Lieffers. 2002b. White tree rings formed in trembling aspen saplings following experimental defoliation. *Canadian Journal of Forest Research* 32:1929–1934.

Hogg, E. H., and P. A. Hurdle. 1995. The aspen parkland in western Canada: a dry-climate analogue for the future boreal forest? *Water, Air, and Soil Pollution* 82:391–400.

Hogg, E. H., M. Michaelian, T. I. Hook, and M. E. Undershultz. 2017. Recent climatic drying leads to age-independent growth reductions of white spruce stands in western Canada. *Global Change Biology* 23:5297–5308.

Holmes, R. L. 1983. Computer-assisted quality control in tree-ring dating and measurement. *Tree-ring bulletin*.

Huang, J., J. C. Tardif, Y. Bergeron, B. Denneler, F. Berninger, and M. P. Girardin. 2010. Radial growth response of four dominant boreal tree species to climate along a latitudinal gradient in the eastern Canadian boreal forest. *Global Change Biology* 16:711–731.

Kobe, R. K. 1996. Intraspecific variation in sapling mortality and growth predicts geographic variation in forest composition. *Ecological Monographs* 66:181–201.

Larsson, L. Å. 2018. Coorecorder. Cybis Elektronick & Data AB, Saltsjobaden, Sweden.

Lutz, J. A. 2015. The evolution of long-term data for forestry: large temperate research plots in an era of global change. *Northwest Science* 89:255-269.

Meko, D. M., R. Touchan, and K. J. Anchukaitis. 2011. Seascorr: A MATLAB program for identifying the seasonal climate signal in an annual tree-ring time series. *Computers & Geosciences* 37:1234–1241.

Michaelian, M., E. H. Hogg, R. J. Hall, and E. Arsenault. 2011. Massive mortality of aspen following severe drought along the southern edge of the Canadian boreal forest: aspen mortality following severe drought. *Global Change Biology* 17:2084–2094.

Moulinier, J., F. Lorenzetti, and Y. Bergeron. 2014. Growth and mortality of trembling aspen (*Populus tremuloides*) in response to artificial defoliation. *Acta Oecologica* 55:104–112.

Oksanen, J., F. G. Blanchet, M. Friendly, R. Kindt, P. Legendre, D. McGlinn, P. R. Minchin, R. B. O'Hara, G. L. Simpson, P. Solymos, M. H. H. Stevens, E. Szoecs, and H. Wagner. 2018. vegan: community ecology package. R package version 2.5–2.

Peng, C., Z. Ma, X. Lei, Q. Zhu, H. Chen, W. Wang, S. Liu, W. Li, X. Fang, and X. Zhou. 2011. A drought-induced pervasive increase in tree mortality across Canada's boreal forests. *Nature Climate Change* 1:467–471.

Percival, D. B., and W. L. B. Constantine. 2006. Exact simulation of gaussian time series from nonparametric spectral estimates with application to bootstrapping. *Statistics and Computing* 16:25–35.

R Core Team. 2018. R: A language and environment for statistical computing. The R Foundation. Version 3.50.

Scheffer, M., M. Hirota, M. Holmgren, E. H. Van Nes, and F. S. Chapin. 2012. Thresholds for boreal biome transitions. *Proceedings of the National Academy of Sciences* 109:21384–21389.

Soja, A. J., N. M. Tchebakova, N. H. French, M. D. Flannigan, H. H. Shugart, B. J. Stocks, A. I. Sukhinin, E. I. Parfenova, F. S. Chapin III, and P. W. Stackhouse Jr. 2007. Climate-induced boreal forest change: predictions versus current observations. *Global and Planetary Change* 56:274–296.

Speer, J. H. 2010. Fundamentals of tree-ring research. University of Arizona Press, Tucson, Arizona, USA.

Stokes, M., and T. Smiley. 1996. An introduction to tree-ring dating. University of Arizona Press, Tuscon, Arizona, USA.

Ung, C.-H., P. Bernier, and X.-J. Guo. 2008. Canadian national biomass equations: new parameter estimates that include British Columbia data. *Canadian Journal of Forest Research* 38:1123–1132.

van Mantgem, P. J., N. L. Stephenson, J. Byrne, L. Daniels, J. F. Franklin, P. Fulé, M. Harmon, A. J. Larson, J. Smith, A. Taylor, and T. Veblen. 2009. Widespread increase of tree mortality rates in the western United States. *Science* 323:521–524.

Worrall, J. J., G. E. Rehfeldt, A. Hamann, E. H. Hogg, S. B. Marchetti, M. Michaelian, and L. K. Gray. 2013. Recent declines of *Populus tremuloides* in North America linked to climate. *Forest Ecology and Management* 299:35–51.

Zang, C., and F. Biondi. 2015. treeclim: an R package for the numerical calibration of proxy-climate relationships. *Ecography* 38:431-436.

Zhang, J., S. Huang, and F. He. 2015. Half-century evidence from western Canada shows forest dynamics are primarily driven by competition followed by climate. *Proceedings of the National Academy of Sciences* 112:4009–4014.

2.7 FIGURES

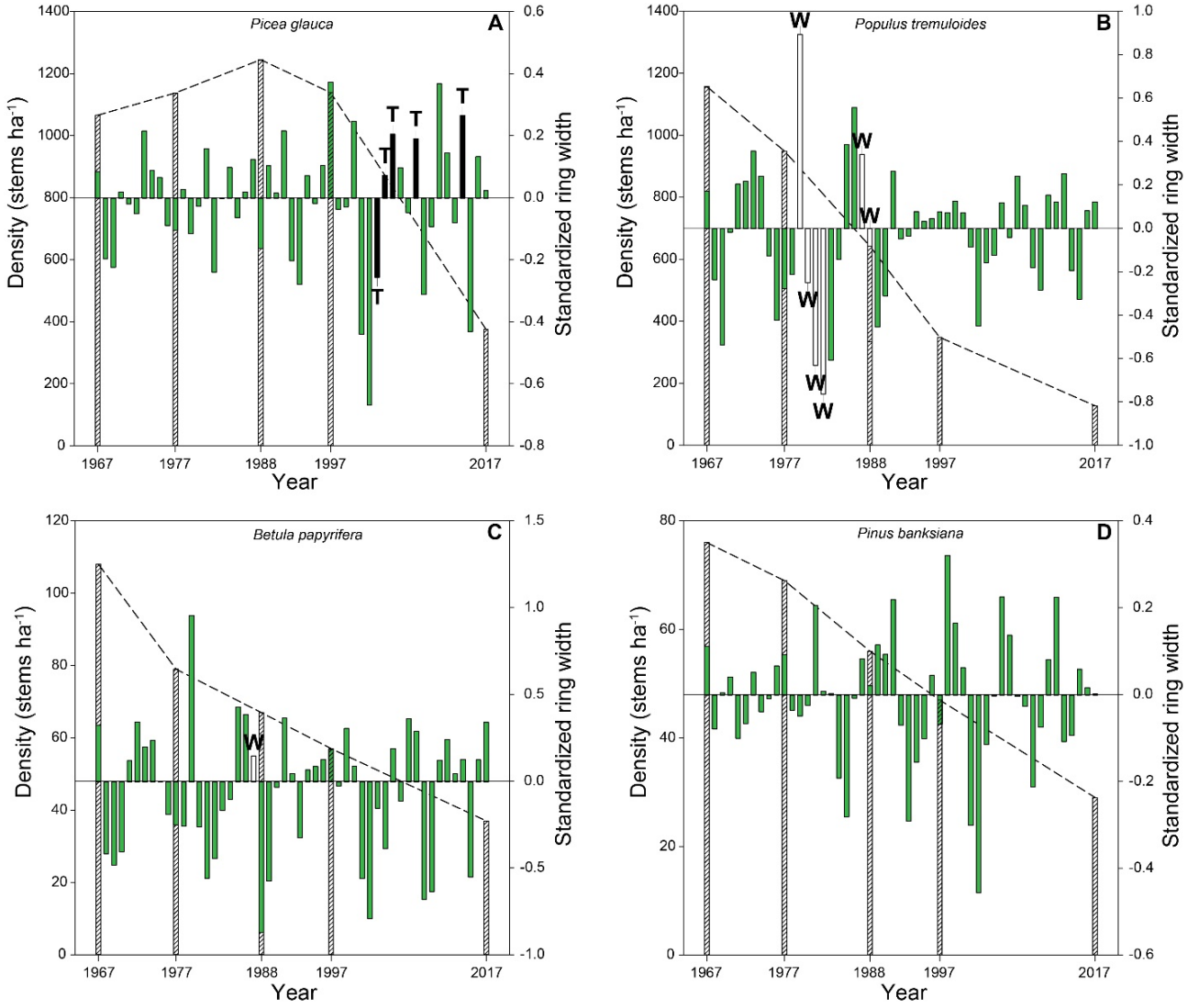

Figure 2.1 Tree density (stems ha^{-1}) (cross-hatched) plotted against standardized ring-widths (green) for the George LaRoi forest plot; Alberta, Canada (1967–2017). Tree species are (A) *Picea glauca*; years with traumatic resin ducts in tree rings on ≥20% of stems are marked with 'T' and colored black, (B) *Populus tremuloides*; years with white tree rings on ≥50% of stems are marked with 'W', colored white, (C) *Betula papyrifera*; years with white tree rings on 100% of stems are marked with 'W', colored light grey, and (D) *Pinus banksiana*. Standardized ring widths > 0 indicate better-than-average growth with ring widths < 0 indicating worse-than-

average growth. For visual clarity, the change in in tree density for each species is marked by the dashed line.

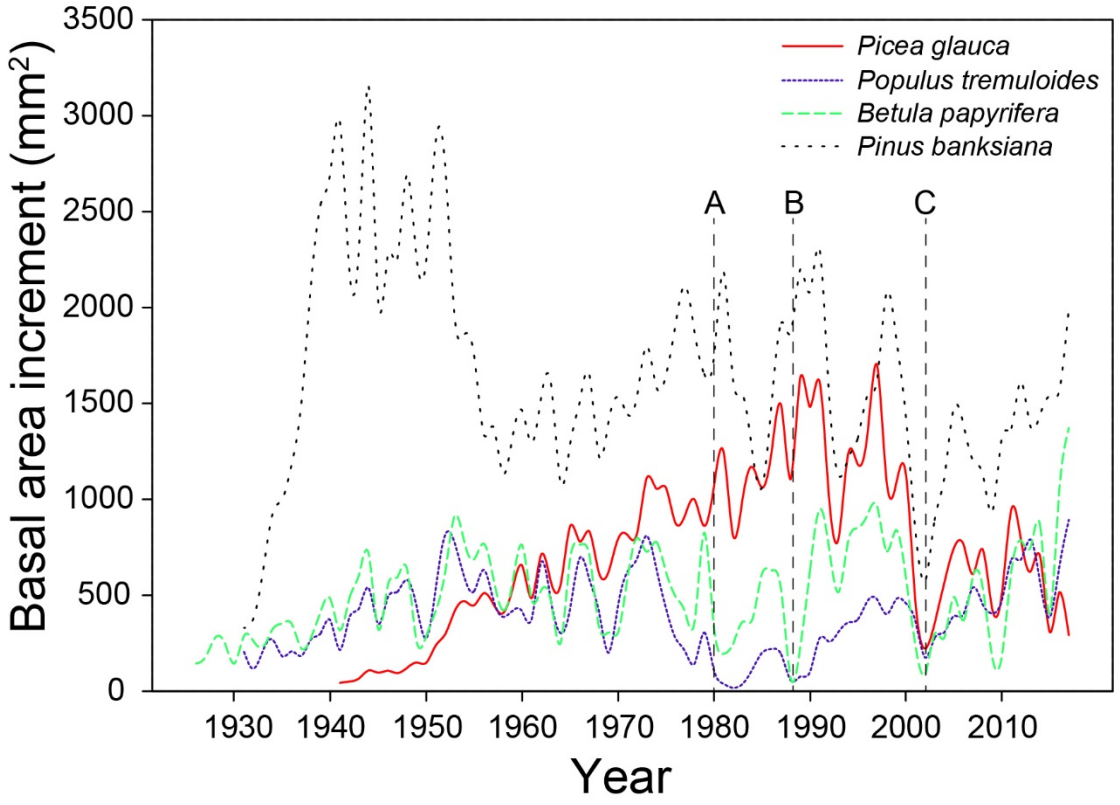

Figure 2.2 Mean annual basal area increments for the four common species at the George LaRoi forest plot; Alberta, Canada. Mean rates were averaged across species (*Picea glauca*; n=22; *Populus tremuloides*; n=10; *Betula papyrifera*; n=10; and *Pinus banksiana*; n=10). Rates fluctuated through time and show a precipitous decrease for *Populus* between 1980 (A) and 1988 (B), which corresponds with defoliation by *Malacosoma disstria*. All species decreased in growth in 2002 (C), likely due to the severe drought in that year.

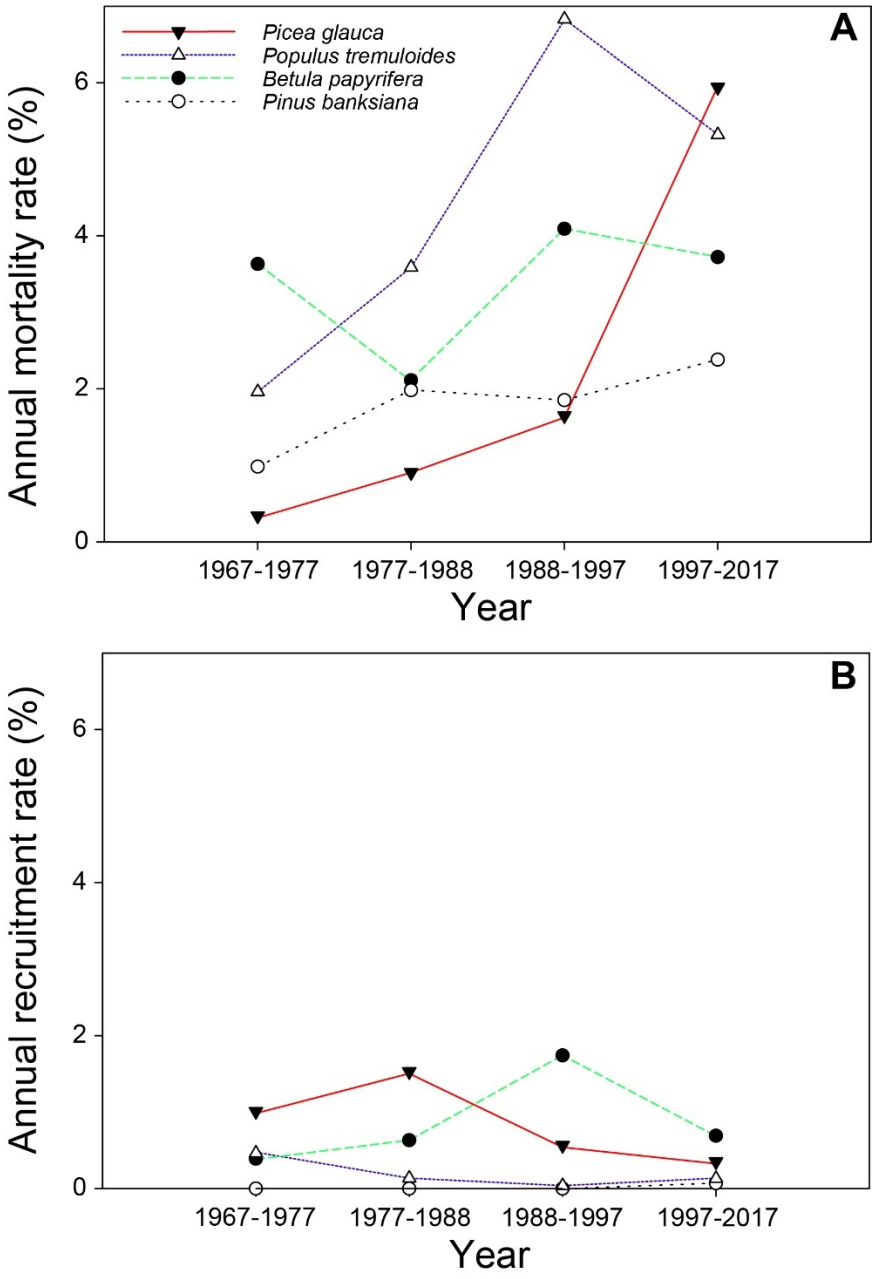

Figure 2.3 Average annual mortality (A), and recruitment (B) rates for the George LaRoi forest plot; Alberta, Canada (1967–2017). Closed triangles identify *Picea glauca*, open triangles identify *Populus tremuloides*, closed circles identify *Betula papyrifera*, and open circles identify *Pinus banksiana*.

Chapter 3: Density-dependent processes fluctuate over 50-years in an ecotone forest [2]

3.1 ABSTRACT

Spatial patterns of trees can inform us of tree recruitment, mortality, and neighbor interactions within forests through time and across disturbances. Specifically, successional trajectories of self-thinning and heterospecific negative density-dependence can be interpreted from the spatial arrangement of forest stems. I conducted a 50-year spatial analysis of a forest undergoing succession at the ecotone of the southwestern Canadian boreal forest. The forest progressed from early to late sere and experienced repeated severe droughts, forest tent caterpillar outbreaks (*Malacosoma disstria*), as well as an outbreak of bark beetles. Cumulatively, the forest lost 70% of stems due to natural succession and a combination of disturbance events. Here, I describe spatial patterns displaying signals of successional self-thinning, responses to disturbance, and changes in patterns of density-dependence across 50 years. Forest succession and disturbance events resulted in fluctuating patterns of density-dependent mortality and recruitment that persisted into late seral stages. The combined effects of conspecific and heterospecific density-dependent effects on mortality and recruitment resulted in near-spatial equilibrium over the study period. However, the strength and direction of these demographic and spatial processes varied in response with time and disturbance severity. The outbreak of forest tent caterpillar, pronounced drought, and bark beetles combined to reduce stand aggregation and promote a spatial equilibrium. Density-dependent processes of competition and facilitation changed in strength and direction with succession of the plot and in

[2] A version of this chapter was published as Birch, J. D., J. A. Lutz, S. W. Simard, R. Pelletier, G. H. LaRoi, and J. Karst. 2019b. Density-dependent processes fluctuate over 50 years in an ecotone forest. *Oecologia* 191:909-918.

combination with disturbance. Together these results reinforce the importance of successional stage and disturbance to spatial patterns.

3.2 INTRODUCTION

Spatial patterns within forests arise from underlying processes that shape the spatial distribution of stems (Cale et al. 1989). Given the longevity of trees, spatial patterns are often the only insight into density-dependent processes such as competition and facilitation in forests (e.g. (Lutz et al. 2014, Després et al. 2017, Furniss et al. 2017). Long-term studies are critical for predicting forest responses to future climates and disturbance regimes, yet few exist, particularly those that track spatial patterns. Spatial patterns of aggregation, dispersion, or randomness can vary through time between species, living and dead stems, and can be used to infer underlying processes shaping forest development (Das et al. 2011, Aakala et al. 2012, Fraver et al. 2014, Gendreau-Berthiaume et al. 2016). For example, density-dependent mortality is expected to result in a forest with stems that are increasingly spatially uniform through time (Kenkel 1988, Moeur 1993). Climate-driven changes in demographic rates can operate within a forest at uneven spatial scales based on density and site characteristics (Greenwood and Weisberg 2008, Horner et al. 2009). Disturbance agents such as insects or climate extremes may differentially impact forests based on stand density and interactions among trees.

As spatial patterns of tree density, age, and size change with time, I expect demographic processes will respond differently to exogeneous influences depending on the neighboring trees (Klos et al. 2009, Linares et al. 2010). Importantly, processes such as intraspecific and interspecific interactions can influence stands even late into succession (Lutz et al. 2014, Zhang et al. 2015). Mortality rates in the western Canadian boreal forest are rising and linked to climate and competition (Worrall et al. 2013, Chen and Luo 2015). Additionally, widespread die-off of *Populus tremuloides* has been linked to climate and defoliation (Hogg et al. 2002a, Michaelian et

al. 2011). The changes in spatial pattern due to disturbance events, such as drought or insect outbreak, can reveal how forest-shaping processes respond to perturbation.

Traditional succession in the western Canadian boreal mixed-wood results in changes in species composition from shade-intolerant early successional species (*Populus, Betula,* or *Pinus* species) to shade-tolerant late seral species, such as *Picea glauca* (Brassard and Chen 2006, Bergeron et al. 2014). In other regions of the boreal mixed-wood, succession can progress to a late-seral stage with dominant northern white cedar (*Thuja occidentalis*) or multiple cohorts of aspen and paper birch (Bergeron et al. 2014). Local abiotic and biotic factors can influence this successional pathway and result in a change in spatial patterns (Turner et al. 1998). Additionally, successional pathways could change with future climates and novel disturbance regimes. Successional models suggest that stands in early and mid-successional stages will exhibit signs of aggregation around favorable microsites (Cornett et al. 1997 and citations therein). Later seral stands exhibit canopy gap-driven recruitment of new cohorts with aggregated, density-dependent recruitment (Fig. 3.1). Point-pattern processes, such as density-dependent mortality, are those underlying forces that shape the spatial arrangement of points (i.e., trees). The point-pattern processes of disturbance agents such as drought or insect-driven mortality should leave a legacy on the forest in the form of altered densities or negative density-dependence.

I sought to examine spatial patterns over 50 years of forest development in the southern ecotone of the Canadian boreal forest through two interrelated questions: 1) How well do spatial patterns support conceptual successional models?, and 2) What legacy do native and novel disturbances have on spatial patterns? In investigating these questions, I sought to understand

inherent forest processes that influence stand arrangement and identify how disturbance agents interact with density-dependent processes that may influence regional forests.

3.3 METHODS

3.3.1 Site description

The George LaRoi forest plot (GLR) is a 1.4 ha (110 × 130 m) forest plot located at 53.408° N, -113.751° W, at the southern ecotone of the Canadian boreal forest and the aspen parkland ecozone. The plot originated from a high-severity fire in the early 1920s with the first cohort of trees establishing in 1925. A 20–60 m buffer of natural forest separates the plot from private forests and ornamental gardens. The soil is a sandy loam Brunisol and derived from aeolian parent material. Mean annual temperature is 2.2 ± 1.1ºC (SD), yearly precipitation of 451 ± 78 mm (SD), and growing season-dominated precipitation of 318 ± 76 mm (SD) (May–September) (Environment and Climate Change Canada 2017).

3.3.2 Stand survey and census

The GLR plot was surveyed in 1967, 1977, 1988, 1997, and 2017. A 2007 census was not conducted due to a lack of funds. Each survey included mapping each stem ≥ 1.35 m tall and recording the diameter at breast height (DBH) and identifying species. Previously, Birch et al. (2019) conducted and detailed a full demographic and tree-ring analysis of the GLR plot. Stems were mapped by stretching transect tapes along 5 × 5 m quadrats along an N-S orientation and the perpendicular intersection with a stem was located on the transect by mirror compass. I marked databased stems as “gone” if they were missed in subsequent surveys (1977–1997), or if no snag or stump was visible in the 2017 survey. Stems that were identified in the 2017 census as having been missed in previous censuses were included in the spatial patterns for previous

censuses. I used the size of missed trees to estimate which census they should have been included within. For example, in 2017 I estimated a 30.0 cm DBH *Betula papyrifera* to have been alive for all previous surveys based on the historic growth rate of *B. papyrifera* at < 2.0 cm per decade. This allowed me to correct spatial patterns from past censuses to account for trees that had been missed by surveyors.

To identify spatial patterns of recruitment and mortality, I conducted the fifth survey and tree census of the GLR plot. The GLR plot is characterized as a boreal mixed-wood, and in 2017, consisted of *Picea glauca* (Moench) Voss (569 stems ha^{-1}; 13.2 m^2 ha^{-1} basal area) and *Populus tremuloides* Michx (127 stems ha^{-1}; 3.6 m^2 ha^{-1}) with smaller numbers of *Betula papyrifera* Marshall, Arbust (37 stems ha^{-1}; 0.5 m^2 ha^{-1}) and *Pinus banksiana* Lambert (29 stems ha^{-1}; 2.3 m^2 ha^{-1}). Botanical nomenclature follows the Flora of North America (Flora of North America Editorial Committee 1993+).

3.3.3 Stand disturbance and decline

I identified three episodic disturbance agents that changed forest structure and composition within the last 50 years. Using tree-ring analysis, I reconstructed the history of drought events, angiosperm defoliation by forest tent caterpillar (*Malacosoma disstria*), and the outbreak of multiple bark beetle species (Birch et al. 2019). Defoliation by *M. disstria* causes distinctly white rings in *P. tremuloides*, while spruce bark beetle (*Dendroctonus rufipennis*) causes bands of traumatic resin ducts in spruce (Hogg et al. 2002b, DeRose et al. 2017). Drought reoccurred throughout the stand's history, most recently in 2001, 2002, 2009, 2014, and 2015. Defoliation by *M. disstria* was present on 100% of *P. tremuloides* during multiple years 1979–

1988 and on *B. papyrifera* in 1987. The bark beetle outbreaks began in 2003 and resulted in continued attacks, most notably in 2014 (Birch et al. 2019) (Appendix 3.1 Fig. S.3.1).

The GLR plot is similar in composition to stands in the southwestern Canadian boreal forest, specifically, in Alberta (hereafter referred to as "regional forests") but has experienced a pronounced decline in density and recruitment, along with rising mortality rates. Previously, I compiled a full description of mortality, recruitment, growth, age, history of insect attack, biomass, basal area, and climate response from the census data (Birch et al. 2019).

3.3.4 Spatial analysis

I characterized the spatial structure of the trees within the GLR plot using the univariate and bivariate inhomogeneous pairwise correlation function (IPCF) (Wiegand and Moloney 2004). The IPCF allowed me to examine patterns of density-dependence and spatial aggregation or dispersion, and compare them against patterns of complete spatial randomness (CSR). The bivariate-IPCF tests marked point patterns and compares spatial patterns of density at increasing distances from a reference point. This is useful because tree stems can be classified (marked) and compared in terms of spatial density. Significant spatial patterns indicate forest-shaping processes such as density-dependent competition or facilitation. I used a quadrat-count with the R package, spatstat version 1.55-1 (Baddeley et al. 2015) to determine that the stem distribution was strongly inhomogeneous.

To test for significance of spatial patterns, I used 2000 Monte Carlo simulations of CSR to create spatial envelopes and used the maximum and minimum envelope values to compare against. Patterns generated by the IPCF that were outside the CSR envelopes were considered significant. For these analyses, I used the plyr package version 1.8.4, spatstat, and ggplot2

version 3.0.0 in the R statistical program to extract the minimum and maximum envelope values for every value *r* and computed the difference between the values (Baddeley et al. 2015, R Core Team 2018, Wickham 2011;2016). To prevent low sample size from interfering with the IPCF analysis, I only analyzed species with stem densities of ≥ 150 stems ha^{-1} in any census. Effectively, this meant I made species comparisons between *P. glauca* and *P. tremuloides* pre-2017 and used an angiosperm category consisting of both *B. papyrifera* and *P. tremuloides* to compensate for low stem numbers of *P. tremuloides* at the 2017 census.

I created multiple categories of marked points based on species, status as alive or dead, diameter, and the presence of beetle attack (Table 3.1). Stems ≥ 4.0 cm DBH were considered mature and stems < 4.0 cm DBH juvenile. I chose the 4.0 cm cutoff based on the average growth rate of < 2.0 cm per decade. These tests allowed me to examine patterns of density-dependence between classes of conspecific and heterospecific stems and analyze how these patterns changed the overall spatial arrangement of stems. For visual clarity I truncated the spatial graphs to a distance of 5.0 m and plotted only significant patterns for each. For a full description of the spatial patterns see Appendix 3.1.

3.4 RESULTS

3.4.1 Species spatial patterns

Pooled species patterns were aggregated at distances of < 5.0 m and largely random between 5.0–25.0 m. This pattern did not change from 1967–1997, but trees became more aggregated at distances < 3.0 m 1997–2017 (Appendix 3.1 Fig. S3.2). *P. glauca* was aggregated 0.0–5.0 m and became more dispersed with time (Appendix 3.1 Fig. S3.3). In comparison, angiosperms were aggregated 0.0–5.0 m and became more aggregated 0.5–1.0 m with time

(Appendix 3.1 Fig. S3.4). Overall the GLR plot was in near equilibrium over the duration of the study (Appendix 3.1 Fig. S3.5).

3.4.2 Density-dependent spatial patterns

The spatial analysis indicated fluctuating patterns of aggregation and density-dependent mortality and recruitment. From these patterns I can infer the underlying forest processes that shaped the GLR plot's development over 50 years. Patterns of negative density-dependence (NDD) between stems captured self-thinning (conspecific NDD) and competition (heterospecific NDD) through time. Overall, patterns of NDD occurred at greater distances with time, but decreased in strength (Fig. 3.2A). Conspecific negative density-dependence (CNDD) differed dramatically between species. *P. glauca* displayed strong CNDD 0.0–5.0 m 1967–2017; however, this pattern weakened 1988–2017 (Fig. 3.2B). Angiosperms displayed CNDD at < 2.0 m in 1967 before displaying a pattern of complete spatial randomness (CSR) 1977–2017 (Fig. 3.2C)). Patterns of heterospecific negative density dependence (HNDD) were present 1967–1997 for all species but had disappeared by 2017. Specifically, *P. glauca* displayed evidence of competition with angiosperms at ≤ 5.0 m 1967–1997 before transitioning to CSR by 2017 (Fig. 3.2D). In comparison, angiosperms displayed CSR 1967–1997 before showing *positive* density-dependence with *P. glauca* at ≤ 1.5 m in 2017 (Fig. 3.2E). Species specific patterns due to either self-thinning or heterospecific competition changed little from 1967–2017 (Appendix 3.1 Fig: S3.6: S3.10).

3.4.3 Spatial patterns of recruitment

Juvenile stems of each species displayed patterns of density-dependence around conspecific and heterospecific mature stems. Juvenile *P. glauca* displayed CSR around mature *P.*

glauca in 1967, were strongly aggregated at < 5.0 m 1977–1997, and slightly aggregated in 2017 (Fig. 3.3A). Surprisingly, juvenile *P. glauca* were more aggregated around mature angiosperms at distances 0.5 m–5.0 m than around mature *P. glauca* (Fig. 3.3C). The juvenile patterns of angiosperms were more variable through time and showed substantial changes by census. Specifically, juvenile angiosperms were strongly aggregated around mature angiosperms at < 5.0 m from 1967–1988, before displaying aggregation at < 1.5 m and dispersion at distances > 2.0 m in 1997, and dispersion at < 5.0 m in 2017 (Fig. 3.3B). In comparison, juvenile angiosperms around mature *P. glauca* displayed CSR in 1967, were aggregated from 1977–1997, and dispersed at < 5.0 m relative to mature angiosperms (Fig. 3.3D).

3.4.4 Spatial patterns of successful bark beetle attack

Picea glauca that died after attack by bark beetles had more clustered neighborhoods of conspecific and heterospecific trees than *P. glauca* that survived attacks. *P. glauca* that died after bark beetle attacks had more living (Appendix 3.1 S3.11A) and dead (Appendix 3.1 S3.11B) *P. glauca* within 1.0–5.0 m than *P. glauca* that survived the attack. Similarly, *P. glauca* that died after bark beetle attacks had denser neighborhoods of living (Appendix 3.1 S3.11C) and dead (Appendix 3.1 S3.11D) angiosperms at < 5.0 m than *P. glauca* that survived the attack.

3.5 DISCUSSION

Spatial patterns through time provide evidence of the GLR plot's path along, and departure from, traditional succession models (Fig. 3.1). I expected that in early succession angiosperms would facilitate juvenile *Picea glauca* and juvenile angiosperms while *P. glauca* would weakly compete with the shade-intolerant angiosperms. As succession progressed, I expected self-thinning to grow stronger and some well-established angiosperms to compete with

smaller *P. glauca* for water and nutrients. Finally, I expected in late succession that angiosperms would experience strong competition from *P. glauca* that had reached the overstory and blocked light from mature angiosperms. However, I found that in the early, aspen-dominant stage that angiosperms facilitated the establishment of juvenile trees of all species, including conspecifics, while also weakly competing with mature *P. glauca* (Fig. 3.4). As the stand progressed to a mid-seral mixed-wood, the angiosperms continued to facilitate juveniles while *P. glauca* began to experience strong self-thinning and moderate conspecific facilitation of juveniles. The transition from mid-seral to late-seral stages was marked by a prolonged outbreak of forest tent caterpillar that likely weakened the angiosperms ability to compete. Finally, in the late-seral-conifer dominant stage, the angiosperms facilitated the establishment of *P. glauca* juveniles but inhibited angiosperm juveniles while also self-thinning. *P. glauca* inhibited juvenile angiosperms but was a strong facilitator of angiosperm adults.

These results detail a forest experiencing classic early and mid-succession pathway before being disrupted by a barrage of native and novel disturbance agents. Despite changes in forest composition and interdecadal density-dependent processes, the GLR plot experienced little overall change in species-specific patterns. Opposing processes driving aggregation and dispersion resulted in a near spatial equilibrium over 50 years (see also Lutz et al. 2014). Natural and novel disturbance regimes influenced the stand though negative density-dependence where mortality and recruitment influenced stand structure and composition.

3.5.1 Endogenous and exogenous influences

The GLR plot followed classic concepts of species-interactions and succession from plot establishment through to 1997 (Fig. 3.1). Significant spatial patterns were largely limited to

distances ≤ 5.0 m but increased in distance with time, likely due to increasing size and neighborhood influence of surviving stems. Self-thinning (CNDD) in *P. glauca* rose with *P. glauca* stem density 1967–1988, when stem density was at its greatest before declining alongside stem density. Likewise, patterns of self-thinning in angiosperms were significant only in 1967 when *P. tremuloides* density was at its highest. Previous studies have reported patterns of increasing uniformity through time within northern forests because of density-dependent self-thinning (Kenkel 1988, Metsaranta and Lieffers 2008, Gendreau-Berthiaume et al. 2016). The GLR plot became more uniform through time but remained aggregated overall in 2017. Despite the aggregation, the plot is now experiencing much lower patterns of density-dependent mortality.

Patterns of recruitment changed repeatedly through time, but recruitment rates have declined steadily to less than half of regional averages (Birch et al. 2019). Interestingly, aggregation of *P. glauca* juveniles around mature angiosperms peaked during the decade of defoliation (1979–1988). This suggests that defoliated angiosperms were better facilitators of *P. glauca* than non-disturbed angiosperms, likely due to their temporarily reduced ability to compete for water and light with juvenile *P. glauca*. *P. glauca* recruitment may be aggregated due to favorable microsites near mature trees, proximity to seed source, and/or higher diversity of mycorrhizal symbionts at proximate distances to mature trees (Teste et al. 2009, Buck and Clair 2014). The pattern of CSR, or dispersion at increased distances around mature trees suggests that large openings in the canopy are less favorable for new *P. glauca* establishment. However, juvenile angiosperms were dispersed away from mature trees of all species and may be preferentially establishing in canopy gaps (Fig. 3.4). Other studies have identified *P. tremuloides* as either a facilitator (Peterson and Squiers 1995, Buck and Clair 2014, Furniss et al. 2017) of

coniferous species or as a competitor (Johnstone 2005; Kenkel et al. 2006) or both (Furniss et al. 2017). In comparison, mature *P. tremuloides* within the plot operates as a facilitator of juvenile *P. glauca* while a competitor of mature *P. glauca*, in keeping with the correlation between competitive intensity and size-symmetry (Weiner and Damgaard 2006). Interestingly, the pattern of negative density-dependence in *P. glauca* around angiosperms offers evidence of angiosperms ability to compete with shade-tolerant mature *P. glauca*, even 70 years after establishment. Remarkably, *P. tremuloides* effectively competed with mature *P. glauca* even as *P. tremuloides* was experiencing defoliation, rising mortality, and a collapse in growth during the 1980s (Birch et al. 2019). The continued senescence, lack of recruitment, and low density of *P. tremuloides* resulted in the faltering of HNDD with *P. glauca* by 2017. Despite this, *P. glauca* growth has declined as *P. tremuloides*-associated HNDD has weakened (Birch et al. 2019). Hogg et al. (2017) reported widespread reductions in *P. glauca* growth due to legacy effects from drought. This provides further evidence that the GLR plot is responding principally to exogeneous influences such as climate rather than endogenous factors such as HNDD with angiosperms.

Picea glauca has become slightly more uniform as density-dependence has weakened but remains aggregated overall. Additionally, the weakening of NDD is uncoupled from overall mortality rates, which have risen steadily through time and at a rate roughly double that of the regional average (Birch et al. 2019). This lends credence to exogeneous factors playing a dominant role in influencing the demographic rates of the GLR plot. Zhang et al. (2015) reported that competition, not climate, was the primary driver of vital rates across the western Canadian boreal forest. The results from the GLR plot suggest that, in contrast, climate and disturbance regimes are the principal factors behind the rapidly rising mortality rates and rampant die-off.

3.5.2 Disturbance and spatial patterns

Increased competition with neighbors may have predisposed *P. glauca* to successful bark beetle attack. This relationship may be heightened in stands with greater stem density. DeRose and Long (2012) reported that *Picea engelmannii* in dense plots suffered higher mortality during late stages of *D. rufipennis* outbreak. This suggests that the density-dependent success of bark beetles in the plot may have strengthened as the outbreak progressed through time. With the beetle outbreaks in 2003, spatial patterns changed, with a marked reduction in CNDD for *P. glauca,* particularly at < 1.0 m. The decline in *P. glauca* CNDD is likely due to the loss of 70% of *P. glauca* such that remaining *P. glauca* are generally too distant from one another for strong CNDD. Greater angiosperm density was associated with a greater chance of *P. glauca* mortality due to bark beetle attack, likely due to heterospecific competition weakening the ability *of P. glauca* to mount a defense against the attacks (Appendix 3.1 Fig S3.11). Additionally, in the last twenty years three major drought events have cooccurred with outbreaks of bark beetles. Drought is also a likely agent of mortality for angiosperms and *P. banksiana,* both of which are sensitive to drought (Birch et al. 2019). Interestingly, my results highlight that the likelihood of *P. glauca* death following bark beetle attack increased with angiosperm density, contrasting with the expectation that shade-tolerant *P. glauca* would experience relatively low levels of competition from angiosperms. In fact, the patterns of HNDD 1997–2017 show that *P. glauca* experienced no detectable NDD from angiosperms. This highlights an intriguing result in that overall pattern of HNDD failed to capture the influence of angiosperms during the beetle outbreaks. These results indicate that during non-outbreak years, *P. glauca* experienced no significant HNDD from angiosperms but experienced HNDD during beetle outbreaks. Angiosperms potentially stressed *P. glauca* by competing for water or other resources and

predisposed stressed *P. glauca* to post-beetle mortality. Combined, these results demonstrate the impact of insect-related disturbance and long-term threats on stand mortality and recruitment rates associated with severe drought.

3.5.3 Conclusion

I found fluctuating patterns of density-dependence across 50 years of forest development. The GLR plot's location at the ecotone of the southern boreal forest and the aspen parkland allows us to infer how regional forests may respond to warming climate and disturbance agents. Despite the long-time span of the study, the small sample size of *P. tremuloides, B. papyrifera*, and *P. banksiana* precluded species-specific spatial analysis and limited the inferences to *P. glauca* and an angiosperm class. Processes in the boreal mixed-wood may not be generalizable to other forest types across the Canadian boreal forest but are certainly indicative of the possibility of great change throughout the 21st century. The establishment of other large, long-term stem-mapped plots (i.e., see Lutz 2015) with sub-decadal resolution across the Canadian boreal forest would address these concerns and allow identification of change across this region. Importantly, tracking stem spatial maps (Appendix 3.1 Fig S3.12:S3.16) over long-time intervals would provide detection of forest processes and their trends. This highlights the importance of creating and regularly surveying long-term monitoring plots. Despite these limitations, my results provide valuable information about forest development and change over the previous half-century. As warming and severe climatic events are expected to continue or increase (Diffenbaugh and Field 2013), I anticipate that the results presented here may become commonplace throughout the southwestern Canadian boreal forest, particularly along the southern ecotone.

3.6 REFERENCES

Aakala, T., S. Fraver, B. J. Palik, and A. W. D'Amato. 2012. Spatially random mortality in old-growth red pine forests of northern Minnesota. *Canadian Journal of Forest Research* 42:899-907.

Baddeley, A., E. Rubak, and R. Turner. 2015. Spatial point patterns: methodology and applications with R. Chapman and Hall/CRC Press.

Bergeron, Y., H. Y. Chen, N. C. Kenkel, A. L. Leduc, and S. E. Macdonald. 2014. Boreal mixedwood stand dynamics: ecological processes underlying multiple pathways. *The Forestry Chronicle* 90:202-213.

Birch, J. D., J. A. Lutz, E. Hogg, S. W. Simard, R. Pelletier, G. H. LaRoi, and J. Karst. 2019. Decline of an ecotone forest: 50 years of demography in the southern boreal forest. *Ecosphere* 10:e02698.

Brassard, B. W., and H. Y. H. Chen. 2006. Stand structural dynamics of North American Boreal Forests. *Critical Reviews in Plant Sciences* 25:115-137.

Buck, J. R., and S. B. S. Clair. 2014. Stand composition, proximity to overstory trees and gradients of soil moisture influence patterns of subalpine fir seedling emergence and survival. *Plant and Soil* 381:61-70.

Cale, W. G., G. M. Henebry, and J. A. Yeakley. 1989. Inferring process from pattern in natural communities. *BioScience* 39:600-605.

Chen, H. Y. H., and Y. Luo. 2015. Net aboveground biomass declines of four major forest types with forest ageing and climate change in western Canada's boreal forests. *Global Change Biology* 21:3675-3684.

Cornett, M. W., P. B. Reich, and K. J. Puettmann. 1997. Canopy feedbacks and microtopography regulate conifer seedling distribution in two Minnesota conifer-deciduous forests. *Ecoscience* 4:353-364.

Das, A., J. Battles, N. L. Stephenson, and P. J. van Mantgem. 2011. The contribution of competition to tree mortality in old-growth coniferous forests. *Forest Ecology and Management* 261:1203-1213.

DeRose, R. J., M. F. Bekker, and J. N. Long. 2017. Traumatic resin ducts as indicators of bark beetle outbreaks. *Canadian Journal of Forest Research* 47:1168-1174.

DeRose, R. J., and J. N. Long. 2012. Factors influencing the spatial and temporal dynamics of Engelmann spruce mortality during a spruce beetle outbreak on the Markagunt Plateau, Utah. *Forest Science* 58:1-14.

Després, T., L. Vítková, R. Bače, V. Čada, P. Janda, M. Mikoláš, J. Schurman, V. Trotsiuk, and M. Svoboda. 2017. Past disturbances and intraspecific competition as drivers of spatial pattern in primary spruce forests. *Ecosphere* 8:e02037.

Diffenbaugh, N. S., and C. B. Field. 2013. Changes in ecologically critical terrestrial climate conditions. *Science* 341:486-492.

Environment and Climate Change Canada (2017) Historical climate data: -- climate stations 3012205 and 3012216 – concatenated, 1961 to 2017. [Data set]. Accessed from https://climate.weather.gc.ca/historical_data/search_historic_data_e.html

Flora of North America Editorial Committee. 1993+. Flora of North America North of Mexico [Online]. Flora of North America Association.

Fraver, S., A. W. D'Amato, J. B. Bradford, B. G. Jonsson, M. Jönsson, and P. A. Esseen. 2014. Tree growth and competition in an old-growth *Picea abies* forest of boreal Sweden: influence of tree spatial patterning. *Journal of Vegetation Science* 25:374-385.

Furniss, T. J., A. J. Larson, and J. A. Lutz. 2017. Reconciling niches and neutrality in a subalpine temperate forest. *Ecosphere* 8:e01847.

Gendreau-Berthiaume, B., S. E. Macdonald, and J. J. Stadt. 2016. Extended density-dependent mortality in mature conifer forests: causes and implications for ecosystem management. *Ecological Applications* 26:1486-1502.

Greenwood, D. L., and P. J. Weisberg. 2008. Density-dependent tree mortality in pinyon-juniper woodlands. *Forest Ecology and Managemen*t 255:2129-2137.

Hogg, E. H., J. P. Brandt, and B. Kochtubajda. 2002a. Growth and dieback of aspen forests in northwestern Alberta, Canada, in relation to climate and insects. *Canadian Journal of Forest Research* 32:823-832.

Hogg, E. H., M. Hart, and V. J. Lieffers. 2002b. White tree rings formed in trembling aspen saplings following experimental defoliation. *Canadian Journal of Forest Research* 32:1929-1934.

Horner, G. J., P. J. Baker, R. Mac Nally, S. C. Cunningham, J. R. Thomson, and F. Hamilton. 2009. Mortality of developing floodplain forests subjected to a drying climate and water extraction. *Global Change Biology* 15:2176-2186.

Johnstone, J. F. 2005. Effects of aspen (*Populus tremuloides*) sucker removal on postfire conifer regeneration in central Alaska. *Canadian Journal of Forest Research* 35:483-486.

Kenkel, N. 1988. Pattern of self-thinning in jack pine: testing the random mortality hypothesis. *Ecology* 69:1017-1024.

Kenkel, N., C. Foster, R. Caners, R. Lastra, and D. Walker. 2006. Spatial and temporal patterns of white spruce recruitment in two boreal mixedwood stands, Duck Mountains, Manitoba. *Project Report.*

Klos, R. J., G. G. Wang, W. L. Bauerle, and J. R. Rieck. 2009. Drought impact on forest growth and mortality in the southeast USA: an analysis using forest health and monitoring data. *Ecological Applications* 19:699-708.

Linares, J. C., J. J. Camarero, and J. A. Carreira. 2010. Competition modulates the adaptation capacity of forests to climatic stress: insights from recent growth decline and death in relict stands of the Mediterranean fir *Abies pinsapo*. *Journal of Ecology* 98:592-603.

Lutz, J. A. 2015. The evolution of long-term data for forestry: large temperate research plots in an era of global change. *Northwest Science* 89:255-269.

Lutz, J. A., A. J. Larson, T. J. Furniss, D. C. Donato, J. A. Freund, M. E. Swanson, K. J. Bible, J. Chen, and J. F. Franklin. 2014. Spatially nonrandom tree mortality and ingrowth maintain equilibrium pattern in an old-growth *Pseudotsuga–Tsuga* forest. *Ecology* 95:2047-2054.

Metsaranta, J. M., and V. J. Lieffers. 2008. A fifty-year reconstruction of annual changes in the spatial distribution of *Pinus banksiana* stands: does pattern fit competition theory? *Plant Ecology* 199:137-152.

Michaelian, M., E. H. Hogg, R. J. Hall, and E. Arsenault. 2011. Massive mortality of aspen following severe drought along the southern edge of the Canadian boreal forest. *Global Change Biology* 17:2084-2094.

Moeur, M. 1993. Characterizing spatial patterns of trees using stem-mapped data. *Forest Science* 39:756-775.

Peterson, C. J., and E. R. Squiers. 1995. Competition and succession in an aspen-white-pine forest. *Journal of Ecology*:449-457.

R Core Team. 2018. R: A language and environment for statistical computing. The R Foundation.

Teste, F. P., S. W. Simard, and D. M. Durall. 2009. Role of mycorrhizal networks and tree proximity in ectomycorrhizal colonization of planted seedlings. *Fungal Ecology* 2:21-30.

Turner, M. G., W. L. Baker, C. J. Peterson, and R. K. Peet. 1998. Factors influencing succession: lessons from large, infrequent natural disturbances. *Ecosystems* 1:511-523.

Weiner, J., and C. Damgaard. 2006. Size-asymmetric competition and size-asymmetric growth in a spatially explicit zone-of-influence model of plant competition. *Ecological Research* 21:707-712.

Wickham, H. 2011. The split-apply-combine strategy for data analysis. *Journal of Statistical Software* 40:1-29.

Wickham, H. 2016. ggplot2: elegant graphics for data analysis. Springer.

Wiegand, T., and K. A. Moloney. 2004. Rings, circles, and null-models for point pattern analysis in ecology. *Oikos* 104:209-229.

Worrall, J. J., G. E. Rehfeldt, A. Hamann, E. H. Hogg, S. B. Marchetti, M. Michaelian, and L. K. Gray. 2013. Recent declines of *Populus tremuloides* in North America linked to climate. *Forest Ecology and Management* 299:35-51.

Zhang, J., S. Huang, and F. He. 2015. Half-century evidence from western Canada shows forest dynamics are primarily driven by competition followed by climate. *Proceedings of the National Academy of Sciences* 112:4009-4014.

3.7 TABLES

Table 3.1 Tests used for the bivariate inhomogeneous pairwise correlation function, the biological interpretation, and corresponding figures plotting the results of each test. Test indicates the result of the inhomogeneous pairwise correlation, 'g(r)', generated by the corresponding function. Appendix 2.1

Test	Function	Interpretation	Figure
$\Delta g(r)$	$g_{t+1}(r) - g_t(r)$	Change in stem density between census periods	Appendix 2.1 Fig. S5A;5B;5C
$g(r)_{NDD}$	$g_{\text{dead, all}}(r) - g_{\text{alive, all}}(r)$	Negative density-dependence	Fig. 2.2A
$g(r)_{CNDD}$	$g_{\text{Species 1: dead, Species 1: all}}(r) - g_{\text{Species 1: alive, Species 1: all}}(r)$	Conspecific negative density-dependence	Fig. 2.2B;2.2C
$g(r)_{HNDD}$	$g_{\text{Species 1: dead, Species 2: all}}(r) - g_{\text{Species 1: alive, Species 2: all}}(r)$	Heterospecific negative density-dependence	Fig. 2.2D;2.2E
$\Delta g(r)_{NDD}$	$g_{\text{alive, alive}}(r) - g_{\text{all, all}}(r)$	Change in stem density due to negative density-dependence	Appendix 2.1 Fig. S2.6

Test	Function	Interpretation	Figure
$\Delta g(r)_{CNDD}$	$g_{\text{Species 1: alive, Species 1: alive}}(r) - g_{\text{Species 1: all, Species 1: all}}(r)$	Change in density due to conspecific negative density-dependence	Appendix 2.1 Fig. S2.7; S2.8
$\Delta g(r)_{HNDD}$	$g_{\text{Species 1: alive, Species 2: alive}}(r) - g_{\text{Species 1: all, Species 2: all}}(r)$	Change in density due to heterospecific negative density-dependence	Appendix 2.1 Fig. S2.9; S2.10
$g(r)_{Cmature}$	$g_{\text{Species 1: juvenile, Species 1: mature}}(r) - g_{\text{Species 1: mature, Species 1: mature}}(r)$	Conspecific influence on recruitment density	Fig. 2.3A;2.3B
$g(r)_{Hrecruit}$	$g_{\text{Species 1: juvenile, Species 2: mature}}(r) - g_{\text{Species 1: mature, Species 2: mature}}(r)$	Heterospecific influence on recruitment density	Fig. 2.3C;2.3D
$g(r)_{Piceaattacked}$	$g_{\text{attacked dead spruce, non-attacked}}(r) - g_{\text{non-attacked alive spruce, non-attacked}}(r)$	Conspecific influence on mortality from beetle-attack	Appendix 2.1 Fig. S2.11A; S2.11B
$g(r)_{Piceaneighbors}$	$g_{\text{attacked dead spruce, non-attacked angiosperm}}(r) - g_{\text{non-attacked alive spruce, non-attacked angiosperm}}(r)$	Heterospecific influence on mortality from beetle-attack	Appendix 2.1 Fig. S2.11C; S2.11D

3.8 FIGURES

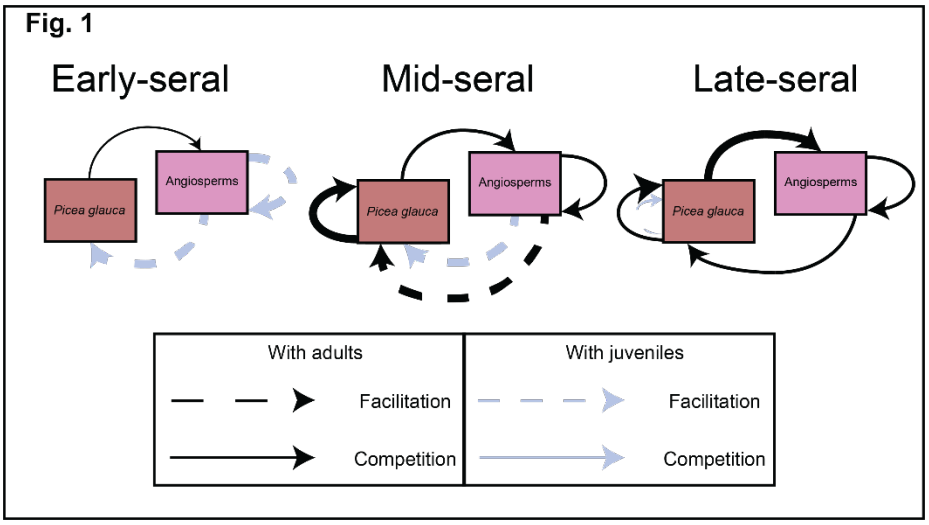

Figure 3.1 A conceptual model of expected successional spatial patterns and density-dependent processes for the George LaRoi forest plot; Alberta, Canada. Dashed arrows represent facilitation. Solid lines represent competition. Line width represents the strength of interaction. Black arrows represent interactions directed at mature trees. Blue arrows represent interactions directed at juvenile trees. Angiosperms represent the paired class of *Populus tremuloides* and *Betula papyrifera*.

Fig. 2

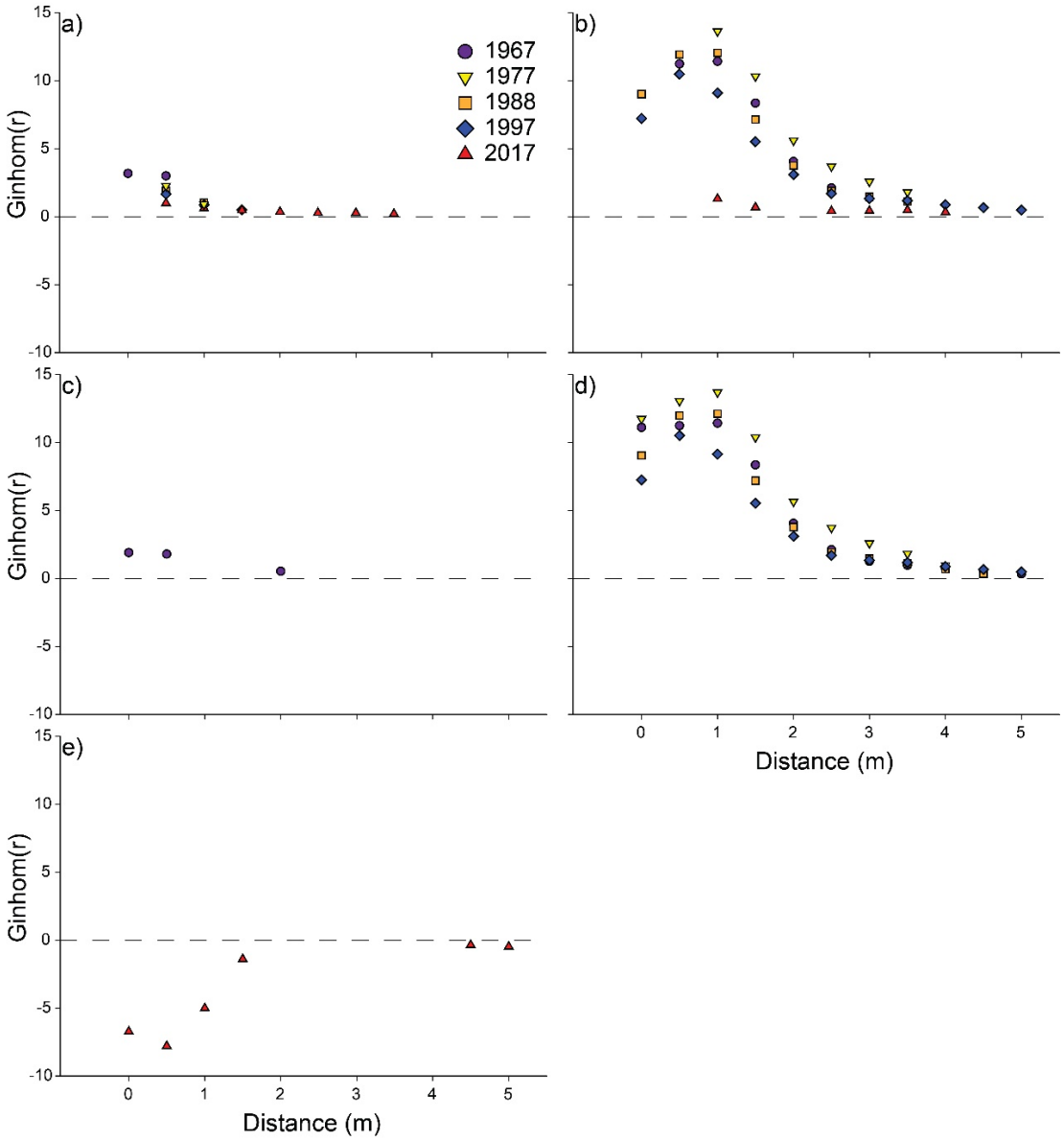

Figure 3.2 Significant conspecific negative density-dependence (CNDD) patterns for *Picea glauca*, *Populus tremuloides*, and *Betula papyrifera* within the George LaRoi forest plot; Alberta, Canada. The y-axis depicts the value of the function Ginhom(r) which is the inhomogeneous pairwise correlation function at the distance 'r'. The x-axis represents distance in meters between the tree-types being compared. Points > 0 (dashed line) represent CNDD. Points < 0 represent positive density-dependence relative to focal stems. Only points that fell outside of

the 2000 Monte Carlo spatial envelopes were plotted for the 1967 (circle), 1977 (downward-triangle), 1988 (square), 1997 (diamond), and 2017 (triangle) censuses. a) Negative density-dependence by decade across all stems. b) CNDD by decade for *P. glauca*. c) CNDD by decade for angiosperms (*P. tremuloides* and *B. papyrifera*). d) Heterospecific negative density-dependence (HNDD) by decade for *P. glauca* around angiosperms. e) HNDD by decade for angiosperms around *P. glauca*.

Fig. 3

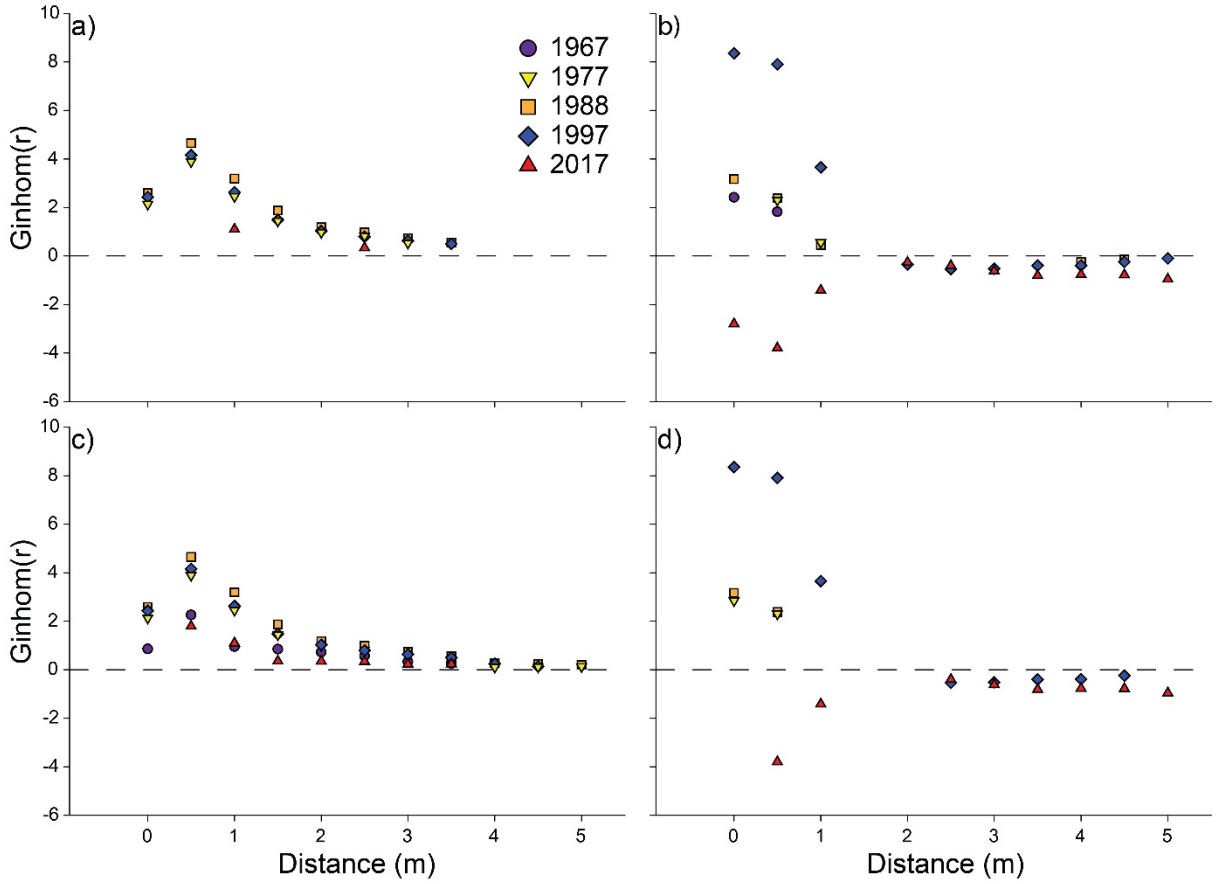

Figure 3.3 Significant spatial patterns of juvenile and mature trees within the George LaRoi forest plot; Alberta, Canada. Points > 0 (dashed line) represent aggregation of stems. The y-axis depicts the value of the function Ginhom(r) which is the inhomogeneous pairwise correlation function at the distance 'r'. The x-axis represents distance in meters between the tree-types being compared. Points < 0 represent dispersion of stems. When the value of g(r)Cmature is greater than zero, I infer juvenile stems are more aggregated around mature stems than are mature stems If g(r)Hrecruit is less than 0, I expect recruitment occurred in canopy gaps. Conversely, if g(r)Hrecruit is greater than 0, I expect mature trees facilitated the establishment of new recruits. a) Juvenile *Picea glauca* relative to mature *P. glauca*, by decade. b) Juvenile angiosperms (*Populus tremuloides* and *Betula papyrifera*) around mature angiosperms by decade. c) Juvenile

P. glauca relative to mature angiosperms by decade. d) Juvenile angiosperms relative to mature *P. glauca* by decade.

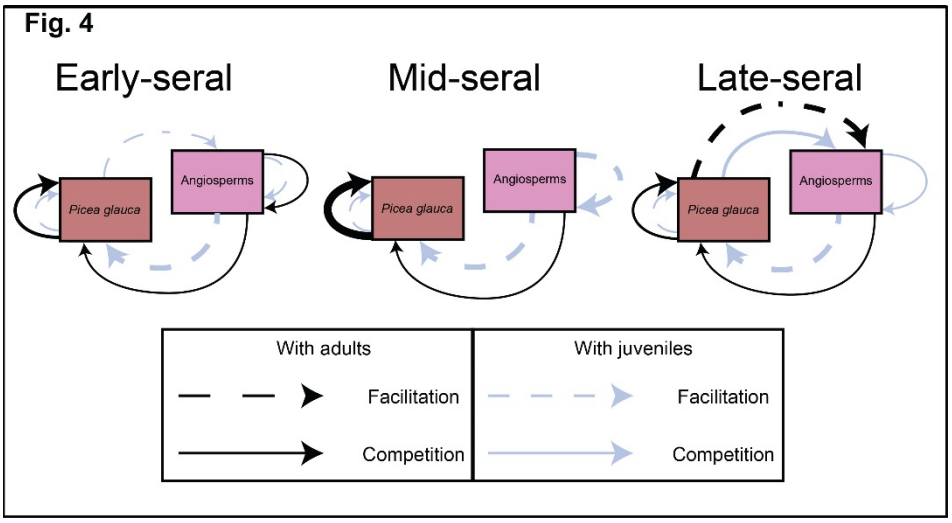

Figure 3.4. A revised, results-based model of succession in the George LaRoi forest plot. Dashed arrows represent facilitation. Solid lines represent competition. Line width represents the strength of interaction. Black arrows represent interactions directed at mature trees. Blue arrows represent interactions directed at juvenile trees. Angiosperms represent the paired class of *Populus tremuloides* and *Betula papyrifera*.

Chapter 4: Beyond seedlings: ectomycorrhizal fungal networks and growth of mature *Pseudotsuga menziesii* [3]

4.1 ABSTRACT

Mycorrhizal networks are conduits for the transfer of resources between hosts. While ectomycorrhizal networks (EMN) are known to influence seedlings, their effect on adult tree growth remains unknown and may have important implications for forest responses to future climates. I used annual basal area increment of trees and previously described *Rhizopogon vesiculosus* and *Rhizopogon vinicolor* EMNs to examine an association between the number of connections between trees through an EMN and the growth of adult interior Douglas-fir. I compared this relationship for the year the networks were mapped, in 2008, with eight years previous and eight years afterward. I also compared the variation in standardized growth (2000–2016) to examine the association between growth variability and EMN variables. Greater growth was positively associated with 1) the number of connections to other trees via a *Rhizopogon vinicolor* EMN, and 2) the number of genets of *Rhizopogon vesiculosis* by which a tree was colonized. Variation of growth (2000–2016) was negatively associated with increasing number of connections to other trees via *Rhizopogon vinicolor*. These findings, for the first time, indicate that EMNs may positively influence the growth of adult trees. The difference in tree growth response between the sister fungal species highlights a novel avenue to identify interspecific differences among and intraspecific differences within mycorrhizal fungal species occurring at different depths in the soil. Our study has important implications when considering the role of EMNs in influencing forest health and mitigating environmental stress.

[3] A version of this chapter was published as Birch, J. D., S. W. Simard, K. J. Beiler, and J. Karst. Beyond seedlings: Ectomycorrhizal fungal networks and growth of mature *Pseudotsuga menziesii*. *Journal of Ecology*.

4.2 INTRODUCTION

When ectomycorrhizal fungal hyphae connect roots of neighboring trees, an ectomycorrhizal network (EMN) is formed. Mycorrhizal networks can transfer carbon, essential nutrients, and water between connected trees and facilitate the sharing of resources from 'source' to 'sink' individuals (Simard et al. 1997, Lerat et al. 2002, Warren et al. 2008, Philip et al. 2010). Ectomycorrhizal fungal symbionts receive an average of 6% of net primary productivity, with higher proportions in nitrogen-limited, conifer-dominated systems (Hobbie 2006, Ouimette et al. 2019, Schiestl-Aalto et al. 2019). In return, ectomycorrhizal fungi provide nutrients and water to their tree-hosts, which can dramatically improve host growth and promote survival (Smith and Read 2010). Carbon allocation and nutrient exchange have important implications for tree growth and survival through feedbacks with water transportation, defense against biotic agents, and carbon starvation (McDowell 2011, Trugman et al. 2018). Networks provide an additional avenue for carbon transport and allocation (Simard et al. 2012) that may influence tree health. However, the costs and benefits of EMN membership may vary with individual tree characteristics, such as tree size or age (Teste et al. 2009).

Large, mature trees may act as 'source' trees in EMNs, with seedlings acting as 'sinks' (Teste and Simard 2008, Booth and Hoeksema 2010). In this source-sink dynamic, seedlings can receive growth-enhancing carbon (Teste et al. 2010) as well as experience lower drought stress (Teste and Simard 2008) and higher survival when connected to an EMN (Booth and Hoeksema 2010). Further, the multiple benefits of EMNs increase with drought stress and promote seedling survival (Bingham and Simard 2011). Interspecific and intraspecific fungal differences within EMNs may also influence the costs and benefits for connected trees (Kiers et al. 2011).

Cumulatively, the benefits of EMNs indicate a potentially potent ameliorator of tree stress. However, how source-sink dynamics operate among a mature, even-sized forest is more difficult to predict. Klein et al. (2016) detected bi-directional carbon transfer without obvious source-sink dynamics. Despite the lack of size-driven source-sink dynamics, the transferred carbon accounted for 40% of fine root carbon among transferring trees (Klein et al. 2016).

Networks can be formed from single or multiple intraspecific fungal genets (Beiler et al. 2010). Each genet potentially provides a discrete network for the transport of resources among trees. One of the few mapped networks to date shows individuals of *Pseudotsuga menziesii* var. *glauca* (interior Douglas-fir) connected together by dense fungal networks formed by multiple genets of two sister fungal species, *Rhizopogon vinicolor* and *Rhizopogon vesiculosus* (Beiler et al. 2010). The EMNs formed by these fungi were characterized by densely-connected 'hub' trees that serve as central nodes, reducing the linkage distance between any two trees (Beiler et al., 2010, 2015). Both *Rhizopogon* species can form hyphae that extend beyond 10 m (Kretzer et al. 2004, Beiler et al. 2010), and are abundant and frequent colonizers of *Pseudotsuga*, (Twieg et al 2007). *Rhizopogon* spp. are likely to be particularly abundant in forests younger than 65 years and will gradually become a smaller portion of the fungal community as the forests mature (Twieg et al., 2007).

The sister fungal species exist at differing depths within the soil profile, likely because of competitive avoidance (Beiler et al., 2012, Mujic et al. 2016). The unique location and topology of these fungal genets could conceivably result in differential abilities to shepherd or steal resources among or from trees. Trees with more connections to other trees could gain access to a wider array of sources from which to receive (or lose) growth-enhancing resources such as

carbon, nitrogen, or water. Trees with connections to more genets may possibly benefit from increased genetic and spatial heterogeneity of their ectomycorrhizal fungal partners. Networking with multiple genets stratified in the soil profile may be an important avenue for trees to access scarce water during droughts.

While much has been learned of EMNs in past experiments, methodological limitations have prevented comprehensive studies of EMNs in mature forests. First, previous studies identifying the benefits of EMNs have focused on seedlings and saplings (Teste et al. 2010, Boothand Hoeksema 2010, Pickles et al. 2017). The significance of EMNs for mature trees remains unknown, and represents an important knowledge gap for predicting forest responses to future climates. Specifically, EMNs may promote forest resilience to recurrent droughts through the transfer of resources within the network. Second, EMNs have been treated as binary; with networked seedlings compared to non-networked controls (Booth 2004, Nara 2006, Bingham and Simard 2011). This approach overlooks the continuous nature of mycorrhizal fungal connections observed in the field, and, importantly, a tree with multiple connections may experience a compound cost/benefit from network membership due to the existence of numerous pathways for the transport of resources. In light of these limitations, I used dendroecological analysis of a mature *Pseudotsuga* forest and leveraged a previously mapped EMNs of sister *Rhizopogon* fungal species (Beiler et al. 2010, 2015) to identify the association between network connectivity and tree growth.

I predicted trees with many connections to other trees via the EMNs would gain a radial-growth advantage over time through the exchange of limiting resources from a wider array of source-trees. Multiple connections within the network should provide extra routes for the

transport of resources as well as ensure security in case a tree is removed from the EMN. I also predicted increasing connections to unique fungal genets would result in greater tree growth due to differential nutrient and water acquisition between genets. Increasing connections with other trees through the EMN would likely result in lower variation of tree growth due to the loss of resources to other sink trees during favorable year and the gain of resources during unfavorable years. Finally, I expected the network to explain progressively less variance in tree growth with increasing time from the year the EMNs was measured, due to changes in the network structure through time.

4.2 METHODS

4.2.1 Study area

The study was in a lower montane forest dominated by *Pseudotsuga menziesii* var. *glauca* (Mayr) Franco (interior Douglas-fir), north of Kamloops, British Columba, Canada (50.853989, -120.522156). The forest has two cohorts of *Pseudotsuga* with younger *Pseudotsuga* in the mid-canopy and understory. The forest was last harvested in 1872 (Global Forest Watch Canada 2008) with the oldest remnant tree dating to 1846. Post-harvest regeneration of the forest occurred naturally. Mean tree age among plots varied from 68 to 113 years old (Table 4.1). Scattered *Pinus ponderosa* (Ponderosa pine) were present within the forest but were killed in several *Dendroctonus* spp. outbreaks from 2005–2008 (Klenner and Arsenault 2009). I did not encounter any living *P. ponderosa* within the study area.

Soils are Brunisols derived from glacial moraine parent material with variable soil texture (Table 4.1). Local climate is characterized by a mean annual temperature of 8.8 ± 9.1ºC (SD), yearly precipitation of 268.5 ± 82.8 mm, and a growing-season temperature of 17.8 ± 3.0ºC

(May–September) with growing-season precipitation of 134.8 ± 21.0 mm (Environment and Climate Change Canada 2017). The trees within the forest are water-limited during the growing season and positively correlate with precipitation during the current growing season (Appendix 4.1 Fig. S4.1).

4.2.2 Characterization of previously sampled ectomycorrhizal networks

Six plots were originally surveyed in 2008 by Beiler et al. (2015) to characterize the EMN associated with *Pseudotsuga*. The plots were placed at varied locations along a hillslope over a half-kilometer distance (Table 4.1). Each plot was at least 150 m away from the nearest plot. In each plot, a 10 × 10 m area was extensively surveyed for EM fungal connections; i.e., mycorrhizal roots were genotyped to individual trees. Fungi colonizing roots were identified as one of two species, *Rhizopogon vinicolor* Smith o*r Rhizopogon vesiculosus* Smith, and genotyped. Roots were sampled beneath the dripline, at four sides of every tree, and with dispersed samples between canopy-cover (Beiler et al., 2015). Trees that were taller than their distance from the plot boundary were also sampled as reference material for roots sampled within the plots. A summary of the methods used and results of the Beiler et al. (2015) survey are available in Appendix 4.2. I assessed only the trees within the core 10 × 10 m plots for the analysis and excluded the surveyed trees outside of the plot boundaries to best capture the network topology (Appendix 4.1 Fig. S4.2). Trees outside of the core 10 × 10 m plots were more likely to have undetected connections with outlying trees.

The previous survey described the topology of the EMN including a map detailing the mycorrhizal fungal connections between trees through each *Rhizopogon* spp. and the identity of the *R. vinicolor* and *R. vesiculosus* genets colonizing each genotyped tree. The average number

of connections across all trees sampled by Beiler et al. (2015) was 16.2 ± 0.68 (SD) with each tree being connected to < 1 (0.64 ± 0.6) *R. vinicolor* genets and 1.0 ± 0.6 *R. vesiculosus* genets. A minority of trees in each plot did not have any connections with genets of one or both *Rhizopogon* species. Within the 10 × 10 m plots, the average number of connections between trees was 20.9 ± 2.1, with each tree connected to 1.1 ± 0.7 *R. vinicolor* genets and 1.5 ± 0.1 *R. vesiculosus* genets (Table 4.1). For a full description of the network topology and features, see the original papers by Beiler et al. (2010, 2015).

4.2.3 Sampling tree growth records and environmental variability

To construct continuous growth records, I sampled increment cores from *Pseudotsuga* within each plot (Table 4.1). In June 2017, I collected two increment cores per tree with a 4.3 mm increment borer (Haglöf Sweden; Mora, Sweden) from all trees ≥ 10 cm diameter at breast height (1.37 m). I selected a ≥ 10 cm DBH cutoff as coring could kill small trees. The unsampled, small trees accounted for 2% of the total tree basal area within the plots. The largest trees originally surveyed by Beiler et al. (2015) are exclusively outside of the core 10 × 10 m plots that I analyzed for this study. Increment cores were sanded with increasingly finer grit sandpaper up to 600 grit. Cores were visually crossdated (Fritts 1976; Stokes and Smiley 1996; Speer 2010), scanned at 1200 DPI (Epson, 630 Pro Photo Scanner), and measured using the software CDendro 9.0 (Larsson 2018). I verified crossdating using the COFECHA program (Holmes 1983) and calculated basal area increment (BAI) and averaged by tree using the R package dplR 1.7.0 (Bunn et al. 2019).

To characterize soil texture and pH as possible covariates of tree growth, I sampled soils adjacent to each cored tree in June 2017, nine years post-EMN measurement. Four soil samples

were collected at the dripline of each tree, separated by 90º, with one additional sample taken adjacent to the bole. Soil samples were collected to a depth of 20 cm using a soil knife (Zenport, Sherwood, Oregon) and pooled by tree. Soil was analyzed by hydrometer for particle size analysis (soil texture) and a pH/EC meter was used for pH (Fisher Scientific, Pittsburgh, Pennsylvania).

4.2.4 Connectivity and growth analysis

To separate fungal species and genet influences on tree growth, I split the EMNs into species-specific categories for *R. vesiculosus* and *R. vinicolor*. Specifically, each tree located in the mapped EMN was characterized by: 1) the number of other trees it was connected to through each *Rhizopogon* sister species' network, and 2) the number of unique genets of a *Rhizopogon* spp. by which it was colonized. I only considered the effect of first-order network connections (tree 1 – genet 1 – tree 2) and excluded n^{th}-order connections (tree 1 – genet 1 – tree 2 – genet 2…) due to the small plot size and lack of replication among n^{th}-order connections.

4.2.5 Statistical analysis

To identify the association between basal area increment and the EMN features, I used a multiple model inference and model averaging approach. Multiple model inference considers multiple competing models and weights them according to the scores of the Akaike information criterion with a correction for small sample size (AICc) (Burnham and Anderson 2002). I created an *a priori* subset of potential explanatory variables and a corresponding candidate set of models. I tested the model for multi-collinearity using the GGally 1.50 package (Schloerke et al. 2020) and found low-to-moderate collinearity between the variables (Fig 4.1). I used the 'geom_smooth' function to graph linear models of each pairwise combination of the dependent

and independent variables (Wickham 2016). I generated models for each hypothesis and ranked the models according to the lowest (best) AICc score and the difference in AICc scores (ΔAICc). Models scoring <7 ΔAICc are generally assumed to be plausible models and become increasingly implausible with increasing ΔAICc (Burnham and Anderson 2002). I generated relative variable importance (RVI) scores, which represent the sum of model weights for all models including the variable of interest. I selected basal area increment (2008) and its variability across 2000–2016 as dependent variables. To calculate variability, I standardized each tree's growth by dividing its annual BAI with the average growth of the previous two years and following two years (Appendix 4.1 Fig S4.3). For the terminal rings, I averaged over the previous two years growth only. I then calculated the standard deviation of the standardized growth. I used the following variables as independent variables: the number of connections to other trees formed by each *Rhizopogon* sister species, the number of genets of each *Rhizopogon* sister species by which a tree was colonized, DBH, age of the tree, as well as soil texture (sand content) and pH. I tested a blocking-by-plot model (AIC = 408.04) against a non-blocked model (AIC = 410.04) and determined that blocking did not significantly improve AIC scores ($p = 0.99$) when soil pH and sand content were included. I used the MuMln 1.43.6 package to test combinations of all variables and used a weighted-average of the top-performing models (ΔAICc < 10) to assemble a global model (Barton, 2019). I used the ggplot2 3.2.1 and ggpubr 0.2.5 packages to graph the model outputs (Kassambara 2020, Wickham 2016).

4.2.6 Model change through time

To test the temporal stability (change in RVI of model variables) of the EMN association with tree ring width, I used multi-model inference for each of the years 2000–2016 and recorded the cumulative RVI value for each year's models. The 2000–2016 window included eight years

before and after the EMN measurement (i.e., the maximum balanced window). I used the basal area increment for each year as the dependent variable and the independent variables were those measured in 2008. I assumed that the independent variables would become increasingly inaccurate as time since measurement increased. For the global models, I report the full coefficient values with shrinkage. The full coefficient values treat variables as having a coefficient and variance of zero in models where they were not present for the purposes of averaging. The full-model averaging is useful in situations where the 'best' model does not have an overwhelming weight (Symonds and Moussalli 2011). All statistical tests were conducted in the program R 3.6.2 (R Core Team 2019) with the R Studio 1.3.1056 interface (R Studio Team 2020). To identify any trends in model performance due to climate I retrieved the annual Hargreaves climatic moisture deficit for 2000–2016 from ClimateNA v5.50 (Wang et al., 2016).

4.3 RESULTS

Basal area increment (BAI) in 2008, the year the EMN was mapped, was significantly, positively correlated with the number of *R. vesiculosus* and *R. vinicolor* genets colonizing a tree, the number of connections to other trees through the *R. vinicolor* network, and DBH (Fig. 4.2). The summed RVI for each variable across all models indicates that the strongest predictors of BAI (2008) were: the tree DBH, number of *R. vesiculosus* genets colonizing the tree, the number of connections to other trees through the *R. vinicolor* network, and the age of the tree (Fig. 4.3a & b). The number of *R. vesiculosus* genets colonizing a tree and *R. vinicolor* connectivity variables were present in the top 10 models (cumulative weight 0.81) (Table 4.2). Of lesser importance were the number of connections through the *R. vesiculosus* network (RVI = 0.65) and the number of colonizing genets of *R. vinicolor* (RVI = 0.45) (Fig 4.3b). In the global model

(2008), tree DBH had a positive association with basal area increment while tree age was negatively associated with BAI (Fig 4.3a). In comparison, the global model indicated a positive association between the number of colonizing *R. vesiculosus* genets, *R. vinicolor* connectivity, and BAI (Fig 4.3b).

The summed RVI for each variable across all models indicates that the variation in tree growth (standard deviation of standardized BAI 2000–2016) was best explained by DBH (RVI = 0.96), the number of connections to other trees through *R. vinicolor* (RVI = 0.95) and sand content (RVI = 0.89). Of lesser importance were the number of connections to other trees through *R. vesiculosus* (RVI = 0.49), the number of *R. vesiculosus* genets colonizing a tree (RVI = 0.27), the soil pH (RVI = 0.22), the number of *R. vinicolor* genets colonizing a tree (RVI = 0.2), and tree age (RVI = 0.18). In the global model only DBH (coefficient = -4.813e-03; p = 0.007), the number of connections to other trees through *R. vinicolor* (coefficient = -5.067e-03; p = 0.012), and sand content (coefficient = -2.4893e-03, p = 0.052) had RVI values above 0.5 and were all negatively correlated with the variation in tree growth.

4.3.1 Model change with time

In the best performing (ΔAICc = 0) non-averaged models from 2000–2016, the number of colonizing *R. vesiculosus* genets occurred in all models from 2000–2014 and the number of *R. vinicolor* connections occurred in all but the 2002 model. Only DBH and tree age were more consistent and appeared in all the top models from 2000–2016 (Fig. 4.3). From 2000–2009, the variable DBH, had the highest RVI before declining slightly until 2013 (Fig. 4.3a). From 2005–2013, the *R. vesiculosus* genet number had an RVI of ≥ 0.99. The RVI of the *R. vinicolor* network connectivity increased with time before peaking 2009–2013. The *Rhizopogon* spp.

variables' RVI declined gradually in 2013, abruptly 2014–2015, and remained low in 2016 (Fig. 4.3b).

The independent variables' coefficient values varied through time in each year's global model (Fig. 4.4). The coefficients for DBH (Fig. 4.4a) and the number of colonizing genets of *R. vesiculosis* (Fig. 4.4b) were the most strongly positive of any of the variables. Similarly, the number of connections through the *R. vinicolor* network was slightly positive while tree age had a slightly negative coefficient. Each year's global model included all the independent variables.

4.4 DISCUSSION

My goal was to determine whether EMNs have a detectable influence on tree radial growth. I identified a positive association between fungal species-specific EMN connectivity and tree growth, lower growth variation with increasing connections through the *R. vinicolor* EMN, and determined trees colonized by more genets of *R. vesiculosus* had greater growth. Importantly, the top 10 models for predicting BAI of Douglas-fir in the year that EMNs were mapped (ΔAICc <3.5, cumulative weight 0.81) included *Rhizopogon* spp. variables (Table 4.2). These results highlight the potential for parsing fungal species-specific influences on mature tree hosts. While my results only identify an association and do not show causation, the novelty of the results and methods highlights an important new avenue for investigating the role of EMNs in mature forests.

4.4.1 A tale of two networks: connectivity and growth

Only one of the two *Rhizopogon* species surveyed, *R. vinicolor*, had a strong, persistent association between tree growth and the number of network connections to other trees. This is

despite the fact that *R. vesiculosus* genets were more prevalent and larger than those of *R. vinicolor* (Kretzer et al. 2004, Beiler et al., 2010, 2012). Though the sister species of *Rhizopogon* are closely related (Kretzer et al. 2003), the difference in the association with connectivity to other trees and annual radial growth was considerable (*R. vesiculosus*, RVI = 0.65; *R. vinicolor* RVI= 0.96). Importantly, the coefficient estimate varied considerably more for *R. vesiculosus* connectivity than it did for *R. vinicolor* connectivity (Fig. 4.2B). Further, the number of connections through the *R. vinicolor* network was associated with lower variation in growth (RVI = 0.95) while the *R. vesiculosus* network did not significantly explain growth variability (RVI = 0.49). My results suggest that EMNs made of *R. vinicolor* have a stronger influence on BAI and its variability than those made of *R. vesiculosus*. Additionally, the high variation in the RVI of *R. vesiculosus* network connectivity suggests that the relationship with BAI is not well defined by the dataset. I expect soil microfauna to disrupt fungal mycelium (Johnson et al. 2005) and that, all else being equal, greater hyphal surface area would be vulnerable to disruption. The smaller, shorter distances formed by *R. vinicolor* may be less prone to disruption than the larger *R. vesiculosus* genets. The connections of *R. vinicolor* are potentially more efficacious in the transfer of carbon or other resources between neighboring trees.

The difference between the sister species may also be attributable to their frequented depths within the soil profile. The tree-derived benefits associated with connecting to multiple intraspecific genets indicates the potential for differential function at the intraspecific level. These results suggest that *R. vesiculosus* genets are not functionally equivalent in the costs and benefits incurred upon their tree-partner. Relatedly, my results indicate interspecific differences between the *Rhizopogon* species. Work by Mujic et al. (2016) shows that differences in depth between the species are likely due to competitive avoidance rather than niche partitioning. The

availability of soil nutrients changes with soil depth (Jobbágy and Jackson 2001) and it is possible that *R. vesiculosus* was able to acquire nutrients or water that were more aggregated at depth or in strata not frequented by *R. vinicolor*. Beiler et al. (2012) reported *R. vinicolor* occurred at 4.95 ± 1.23 cm and *R. vesiculosus* 11.07 ± 4.42 cm depths within the soil profile. Soil depth not only separated these sister species, but also fungal communities in other temperate forests (Toju et al. 2016). There was a significant negative correlation between soil pH and the number of connections through *R. vinicolor* ($r^2 = -0.539$; $p < 0.05$) as well as a non-significant correlation between pH and the number of unique *R. vinicolor* genets ($r^2 = -0.312$; $p = 0.106$) (Fig. 4.1). I speculate that the correlations may be a result of differences in pH with soil depth. Finally, the site is in a region that experiences frequent water limitations during the growing season (Appendix 4.1 Fig. S4.1), and I expect soil moisture to be higher at greater depths within the soil profile. The greater depth of *R. vesiculosus* may provide for greater uptake of soil moisture and subsequent transfer to tree-hosts. The greater tree growth associated with colonization by unique genets of *R. vesiculosus* indicates that niche differentiation may have a substantial influence on the efficacy of ectomycorrhizal fungal species in providing resources to their host.

4.4.2 Who pays the price? The potential sources for EMN-delivered resources

I did not directly measure or identify the transfer of resources along the EMNs and can only speculate that growth-enhancing resources may flow through the EMN from one or more potentially unmeasured sources. Because resource transfer in EMNs are driven by source/sink dynamics (Booth and Hoeksema 2010), I expect that there is a cost for source trees that are highly connected to sink trees. However, the current study design precluded the separation of trees into biologically meaningful size categories. I expect that variation in growth would

increase for source trees that were highly connected and being drained of growth-limiting resources. However, the variation in growth decreased with increasing number of connections through the *R. vinicolor* EMN as well as with DBH. This result suggests that the *R. vinicolor* EMN is either an overall stabilizer of tree growth or does not drain large trees of a detectable amount of growth-limiting resources. Carbon transfer through the EMN is typically < 10% of all photosynthetically derived carbon (Simard et al., 2015), which may indicate that other resources transferred through the networks are partially responsible for the greater tree growth. Multiple source-sink gradients for carbon, water, and nitrogen could exist within the same EMN. Large trees could conceivably act as both a carbon source and water sink through the EMN.

Carbon and other limiting resources could be flowing from the forest outside of the plots and the scattered, large remnant trees that predate the post-logging cohort. Current knowledge of EMNs would suggest that these large trees would be the most likely source trees within each EMN. Unfortunately, these trees had lower resolution of EMN topology and were excluded from the study. Another alternative source of carbon could be the now-deceased *Pinus ponderosa* that existed concurrent with the original EMN mapping in 2008. The *P. ponderosa* died from *Dendroctonus* spp. outbreaks in 2005–2008 (Klenner and Arsenault 2009) and could conceivably have been source trees for carbon and nutrient flux into the EMN. Song et al. (2015) showed an interspecific transfer of carbon and stress signaling enzymes through a shared EMN from defoliated *Pseudotsuga* to *P. ponderosa*. Similarly, the mortally wounded *P. ponderosa* at the sites may have exported resources through a shared EMN.

I expect that all trees will have a limiting growth factor (LGF) per Liebig's Law of the Minimum (Liebig 1840) and that the same LGF need not be shared between all trees within a

stand. Given that mycorrhizal networks can aid in the reallocation of carbon, water, and nitrogen (Egerton-Warburton et al. 2007, He et al. 2009, Teste et al. 2009), I speculate that limiting resources could be transferred via EMN between trees experiencing different LGFs. A tree could lose a non-limiting nutrient to the EMN without incurring a growth loss and still benefit another connected tree. Greater access to a larger pool of trees with different LGFs could provide an avenue for an exchange of limiting resources between trees with LGFs.

4.4.3 The rise and fall of *Rhizopogon* importance

The rise and subsequent fall of the *Rhizopogon* species RVI values could indicate that the topology of network connections changes with time. The map of the EMNs topology were recorded once, in 2008, and is likely increasingly inaccurate with time from 2008. However, the presence of continuous tree-ring records provides an opportunity to indirectly investigate EMN stability through time. Fungal rhizomorphs, such as those produced by *Rhizopogon* spp. can live for an average of 11 months (Treseder et al. 2005) with colonized root tips averaging 1 year (Bledsoe, Allen, and Southworth 2014). Twieg et al. (2007) reported 97% EM fungal colonization of *Pseudotsuga* root tips at a nearby forest in British Columbia. Due to the likelihood of high colonization by *Rhizopogon* and other EM fungal species it is likely that the death of a single rhizomorph or root does not fully sever a tree's connection to a particular fungal genet.

The elevated (RVI > 0.5) values for *R. vesiculosus* genets (2000–2014) and *R. vinicolor* connectivity (2000–2002, 2004–2014) could indicate that EMNs have topology that is stable for multiple growing seasons but changes at decadal timespans. The decline in *Rhizopogon* species RVI values pre-2008 might be best explained by network topology that did not exist by the time

of surveying in 2008. I expect EMNs to fluctuate through time due to fine-root and fungal turnover and the potential for network disturbance. For example, EM fungal communities may shift, and connections severed, due to belowground fungivores (Antunes and Koyama, 2017, Janoušková et al. 2018). Additionally, drought stress could also negatively impact the function and health of the *Rhizopogon* species. Other research has reported that EM fungal communities can shift with drought stress and warming temperatures (Swaty et al. 2004, Cudlín et al. 2007, Li et al. 2015). The plots experienced notable periods of drought in 2003, 2009, and 2015. The sharp decline of RVI values in 2015 are likely due to the severe drought in that year (Fig. 4.3). The proximity of the plots prevented us from testing the interaction of climate and EMN topology. Further research is needed to investigate EMN through time and parse the potential factors influencing topology stability.

4.4.4 Caveats and directions for future research

One alternative explanation of my results is the variables representing EMNs formed by *Rhizopogon* species are serving as proxy variables for the rooting extent and distribution of individual trees. Beiler et al. (2010) reported that older and larger DBH trees were associated with greater EMN connectivity. While my results may be partly attributable to EMN mirroring rooting extent, I would expect tree DBH and age to also be strong predictors of rooting extent (Smith 1964). Unfortunately, the largest trees were outside the core plots established for the Beiler et al., (2015) study and had a low resolution of EMN topology. However, the distribution of tree ages within the plots was similar to that of the surrounding forest (Table 4.1; Appendix 4.1 Table S4.1) and would also be a proxy for rooting extent. The average rate of coarse lateral root growth has been reported at 7.4 cm $year^{-1}$ in British Columbia and higher elsewhere (Richardson 2000). Considering the average age of the trees within the core plots (Table 4.1), it

is likely that even smaller trees have extensive distributions of roots. Oldest trees would conceivably have the greatest rooting extent and consequently have high colonization by fungal genets and growth if the EMN variables were simply a proxy for rooting extent. However, trees in the oldest plots had lower genet colonization and growth compared to those in the younger plots (Table 4.1; Appendix 4.1 Table S4.1). A nearby study of EM fungi in British Columbia found divergent foraging strategies between EM fungi and fine roots (Defrenne et al. 2019). This provides further evidence to suggest that the *Rhizopogon* species variables are poor proxies of rooting distribution. Similarly, the *Rhizopogon* species variables could act as proxies for increasing association with EM fungi and correspondingly higher levels of EM-sourced nutrients. However, Twieg et al. (2007) reported 97% EM colonization of *Pseudotsuga* root tips at a nearby forest in British Columbia. The high rate of colonization suggests that the *Rhizopogon* spp. variables are likely poor proxies for overall EM fungal colonization and that colonization does not vary enough to account for dramatic growth differences.

Another potential route for resource transfer between mature trees is through root grafts (Fraser et al. 2006). Neighboring coarse roots from different trees can graft onto one another and provide numerous potential benefits (Lev-Yadun 2011). While I expect that root grafting occurs throughout the sites, tree age or DBH would likely be the best proxy for root extent and likelihood of grafting with other trees. Finally, root grafts would be long-lasting and unlikely to cause changes in RVI at sub-decadal time scales. I excluded all trees that were < 10 cm DBH from the study which may be one of the most sensitive cohorts to EMN-associated growth modulation. Small trees generally have less connections to other trees through the *R. vinicolor* EMN (Fig. 4.1) and could conceivably have the most growth to gain from resources transferred through the EMN. However, juvenile trees frequently exhibit growth curves that differ markedly

from mature trees (Speer 2010) and many were not capable of being cored. I speculate that small trees likely show a stronger growth benefit from connections through the EMN. Different methods for measuring growth (i.e., annual measurements with calipers or dendrometers) would be needed to include these trees within the study.

Another potential caveat is that I investigated only two ectomycorrhizal fungal species associating with *Pseudotsuga* and have no data on the trove of other fungi that may have detectable influence on their tree hosts. However, *Rhizopogon* spp. are common fungi that account for a substantial portion of the ectomycorrhizal fungal community of *Pseudotsuga*. Specifically, *Rhizopogon* spp. colonized between 50–88% of all trees across the plots (Beiler et al. 2015). Additionally, Twieg et al. (2007) reported that *R. vinicolor*-type fungi were the most abundant colonizers of *Pseudotsuga* roots in separate interior Douglas-fir forests in a nearby region of British Columbia. While other EMNs may exist within the stand, the dual-*Rhizopogon* species likely occupy a substantial portion of the belowground community. Unfortunately, the enormous effort of measuring EMN in non-tuberculate fungal species makes it extremely challenging to identify the full range of networks that exist. Advances in field and laboratory methods are needed to map the full topologies of EMNs across different fungal species.

The topology of the *Rhizopogon* species EMNs are likely underrepresented in the core 10 × 10 m plots and particularly for the fringe trees that were mapped outside of the plots (Beiler et al. 2015). The difference between the average connectivity across all trees (16.2) and those in the exhaustively mapped 10 × 10 plots (20.9) highlights the potential of underreporting connectivity at the fringes of small plots (Beiler et al. 2015). While I restricted the sample size to the core 10 × 10 m plots, it is likely the topology of the EMN is still underrepresented. Larger plot-sizes and

the inclusion of more trees in EMN maps will enable for second and n^{th}-order connection efficacy to be tested. At present, the small sample size results in most trees having identical second-order connectivity. Surveying larger plots within smaller stands would improve the ability to map network topology and understand the influence of network connectivity.

With respect to future research, continued rises in atmospheric CO_2 could interact with EMNs in several ways and in confluence with altered climate. With increased atmospheric CO_2, I expect that much of the range of *Pseudotsuga* will grow warmer and drier with associated climate change (Hamann and Wang 2006). Increases in CO_2 can increase plant growth and EM fungal biomass (Alberton et al. 2005) and ectomycorrhizal trees show a greater biomass increase than do plants associated with arbuscular mycorrhizas (Terrer et al. 2016). Approximately 20% of global tree-ring series show a slight CO_2 fertilization effect during the latter half of the 20^{th} century (Gedalof and Berg 2010). With increased tree biomass and growth rates I might expect an increased flux of carbon to EM fungi and the EMN. However, much of the influence of EMNs will depend on how source trees respond to drier climates. Large trees have an outsized influence as reservoirs of aboveground biomass (Lutz et al. 2018) and frequently serve as network hubs within EMN (Beiler et al. 2015). Globally, large trees have greater relative growth reductions due to drought than do small trees (Bennett et al. 2015). This suggests that drier conditions would lead to large trees providing less carbon to the EMN. However, this may be offset by increasing allocation of resources to root development at the expense of aboveground tissues, as a way of promoting water-uptake (Poorter et al. 2012). The redistribution of water via EMN may become increasingly important under drier conditions. The implications of rising CO_2 concentrations and associated climate change will likely vary substantially with forest community composition, stand structure, tree phenology, resource availability and interactions

therein. More research is needed to disentangle the influence of climate, CO_2, and EMN efficacy in mature forests.

4.4.5 Conclusion

This study provides evidence that EMN connectivity and connections to different individual mycorrhizal fungal genets can positively influence the growth of mature trees. Importantly, the capacity to form EMNs are not limited to *Rhizopogon* spp. or *Pseudotsuga* and my results may be generalizable to other forest systems. However, these results suggest that network efficacy may be highly variable at both the intra- and interspecific fungal species levels and EMNs may not always provide measurable advantages to mature trees. I expect the results to be mirrored in other forests across western North America, particularly where *Rhizopogon* species proliferate (Mujic et al. 2019). More research is needed to better isolate the mechanisms and strength of interactions between EMNs and tree growth. Current dendroecological models for tree growth may benefit from the inclusion of data on belowground symbionts and their relations with neighboring trees. Further, the union of dendroecological tools and the study of ectomycorrhizas provides great utility in examining the impacts of ectomycorrhizal fungal species and networks in mature forests. Future research exploring EM-associated signals within tree rings may provide a fruitful ground for identifying species-specific impacts on tree hosts and changes through time and with climate. My research provides further support for the influence of ectomycorrhizal fungal species and networks on forest health.

4.5 REFERENCES

Alberton, O., T. W. Kuyper, and A. Gorissen. 2005. Taking mycocentrism seriously: mycorrhizal fungal and plant responses to elevated CO2. *New Phytologist* 167:859-868.

Antunes, P., and A. Koyama. 2017. Mycorrhizas as nutrient and energy pumps of soil food webs: multitrophic interactions and feedbacks. Pages 149-173 *Mycorrhizal mediation of soil.* Elsevier.

Barton, K. 2019. MuMIn: Multi-Model Inference. R package.

Beiler, K. J., D. M. Durall, S. W. Simard, S. A. Maxwell, and A. M. Kretzer. 2010. Architecture of the wood-wide web: *Rhizopogon spp*. genets link multiple Douglas-fir cohorts. *New Phytologist* 185:543-553.

Beiler, K. J., S. W. Simard, and D. M. Durall. 2015. Topology of tree–mycorrhizal fungus interaction networks in xeric and mesic Douglas-fir forests. *Journal of Ecology* 103:616-628.

Beiler, K. J., S. W. Simard, V. LeMay, and D. M. Durall. 2012. Vertical partitioning between sister species of *Rhizopogon* fungi on mesic and xeric sites in an interior Douglas-fir forest. *Molecular Ecology* 21:6163-6174.

Bennett, A. C., N. G. McDowell, C. D. Allen, and K. J. Anderson-Teixeira. 2015. Larger trees suffer most during drought in forests worldwide. *Nature Plants* 1:1-5.

Bingham, M. A., and S. W. Simard. 2011. Do mycorrhizal network benefits to survival and growth of interior Douglas-fir seedlings increase with soil moisture stress? *Ecology and Evolution* 1:306-316.

Booth, M. G. 2004. Mycorrhizal networks mediate overstorey-understorey competition in a temperate forest. *Ecology Letters* **7**:538-546.

Booth, M. G., and J. D. Hoeksema. 2010. Mycorrhizal networks counteract competitive effects of canopy trees on seedling survival. *Ecology* 91:2294-2302.

Bunn, A., M. Korpela, F. Biondi, F. Campelo, P. Mérian, F. Qeadan, and C. Zang. 2019. dplR: dendrochronology program library in R. R package version 1.7.0.

Burnham, K. P., and D. R. Anderson. 2002. A practical information-theoretic approach. Model selection and multimodel inference, 2nd ed. Springer, New York 2

Cudlín, P., B. Kieliszewska-Rokicka, M. Rudawska, T. Grebenc, O. Alberton, T. Lehto, M. R. Bakker, I. Børja, B. Konôpka, and T. Leski. 2007. Fine roots and ectomycorrhizas as indicators of environmental change. *Plant Biosystems* 141:406-425.

Defrenne, C. E., T. J. Philpott, S. H. Guichon, W. J. Roach, B. J. Pickles, and S. W. Simard. 2019. Shifts in ectomycorrhizal fungal communities and exploration types relate to the environment and fine-root traits across interior Douglas-fir forests of western Canada. *Frontiers in Plant Science* 10:643.

Egerton-Warburton, L. M., J. I. Querejeta, and M. F. Allen. 2007. Common mycorrhizal networks provide a potential pathway for the transfer of hydraulically lifted water between plants. *Journal of Experimental Botany* 58:1473-1483.

Environment and Climate Change Canada (2017) Historical climate data: -- climate station 1163780– concatenated, 1951 to 2017. [Data set]. Accessed from https://climate.weather.gc.ca/historical_data/search_historic_data_e.html

Fraser, E. C., V. J. Lieffers, and S. M. Landhäusser. 2006. Carbohydrate transfer through root grafts to support shaded trees. *Tree Physiology* 26:1019-1023.

Fritts, H. C. 1976. Tree rings and climate. Academic Press, London; New York, USA.

Gedalof, Z. e., and A. A. Berg. 2010. Tree ring evidence for limited direct CO2 fertilization of forests over the 20th century. *Global Biogeochemical Cycles* 24.

Hamann, A., and T. Wang. 2006. Potential effects of climate change on ecosystem and tree species distribution in British Columbia. *Ecology* 87:2773-2786.

He, X., M. Xu, G. Y. Qiu, and J. Zhou. 2009. Use of 15N stable isotope to quantify nitrogen transfer between mycorrhizal plants. *Journal of Plant Ecology* 2:107-118.

Hobbie, E. A. 2006. Carbon allocation to ectomycorrhizal fungi correlates with belowground allocation in culture studies. *Ecology* 87:563-569.

Holmes, R. L. 1983. Computer-assisted quality control in tree-ring dating and measurement. *Tree Ring Bulletin.*

Janoušková, M., P. Kohout, J. Moradi, P. Doubková, J. Frouz, S. Vosolsobě, and J. Rydlová. 2018. Microarthropods influence the composition of rhizospheric fungal communities by stimulating specific taxa. *Soil Biology and Biochemistry* 122:120-130.

Jobbagy, E. G., and R. B. Jackson. 2001. The distribution of soil nutrients with depth: global patterns and the imprint of plants. *Biogeochemistry* 53:51-77.

Johnson, D., M. Krsek, E. M. Wellington, A. W. Stott, L. Cole, R. D. Bardgett, D. J. Read, and J. R. Leake. 2005. Soil invertebrates disrupt carbon flow through fungal networks. *Science* 309:1047-1047.

Kassambara, A. 2020. ggpubr: 'ggplot2' based publication ready plots.R package version 0.2.5.

Kiers, E. T., M. Duhamel, Y. Beesetty, J. A. Mensah, O. Franken, E. Verbruggen, C. R. Fellbaum, G. A. Kowalchuk, M. M. Hart, and A. Bago. 2011. Reciprocal rewards stabilize cooperation in the mycorrhizal symbiosis. *Science* 333:880-882.

Klein, T., R. T. Siegwolf, and C. Körner. 2016. Belowground carbon trade among tall trees in a temperate forest. *Science* 352:342-344.

Klenner, W., and A. Arsenault. 2009. Ponderosa pine mortality during a severe bark beetle (*Coleoptera: Curculionidae, Scolytinae*) outbreak in southern British Columbia and implications for wildlife habitat management. *Forest Ecology and Management* 258:S5-S14.

Kretzer, A. M., S. Dunham, R. Molina, and J. W. Spatafora. 2004. Microsatellite markers reveal the below ground distribution of genets in two species of *Rhizopogon* forming tuberculate ectomycorrhizas on Douglas fir. *New Phytologist* 161:313-320.

Kretzer, A. M., D. L. Luoma, R. Molina, and J. W. Spatafora. 2003. Taxonomy of the *Rhizopogon vinicolor* species complex based on analysis of ITS sequences and microsatellite loci. *Mycologia* 95:480-487.

Lerat, S., R. Gauci, J. G. Catford, H. Vierheilig, Y. Piché, and L. Lapointe. 2002. 14 C transfer between the spring ephemeral *Erythronium americanum* and sugar maple saplings via arbuscular mycorrhizal fungi in natural stands. *Oecologia* 132:181-187.

Lev-Yadun, S. 2011. Why should trees have natural root grafts? *Tree Physiology* 31:575-578.

Li, Y., D. Sun, D. Li, Z. Xu, C. Zhao, H. Lin, and Q. Liu. 2015. Effects of warming on ectomycorrhizal colonization and nitrogen nutrition of *Picea asperata* seedlings grown in two contrasting forest ecosystems. *Scientific Reports* 5:17546.

Lutz, J. A., T. J. Furniss, D. J. Johnson, S. J. Davies, D. Allen, A. Alonso, K. J. Anderson-Teixeira, A. Andrade, J. Baltzer, K. M. L. Becker, E. M. Blomdahl, N. A. Bourg, S. Bunyavejchewin, D. F. R. P. Burslem, C. A. Cansler, K. Cao, M. Cao, D. Cárdenas, L.-W. Chang, K.-J. Chao, W.-C. Chao, J.-M. Chiang, C. Chu, G. B. Chuyong, K. Clay, R.

Condit, S. Cordell, H. S. Dattaraja, A. Duque, C. E. N. Ewango, G. A. Fischer, C. Fletcher, J. A. Freund, C. Giardina, S. J. Germain, G. S. Gilbert, Z. Hao, T. Hart, B. C. H. Hau, F. He, A. Hector, R. W. Howe, C.-F. Hsieh, Y.-H. Hu, S. P. Hubbell, F. M. Inman-Narahari, A. Itoh, D. Janík, A. R. Kassim, D. Kenfack, L. Korte, K. Král, A. J. Larson, Y. Li, Y. Lin, S. Liu, S. Lum, K. Ma, J.-R. Makana, Y. Malhi, S. M. McMahon, W. J. McShea, H. R. Memiaghe, X. Mi, M. Morecroft, P. M. Musili, J. A. Myers, V. Novotny, A. de Oliveira, P. Ong, D. A. Orwig, R. Ostertag, G. G. Parker, R. Patankar, R. P. Phillips, G. Reynolds, L. Sack, G.-Z. M. Song, S.-H. Su, R. Sukumar, I.-F. Sun, H. S. Suresh, M. E. Swanson, S. Tan, D. W. Thomas, J. Thompson, M. Uriarte, R. Valencia, A. Vicentini, T. Vrška, X. Wang, G. D. Weiblen, A. Wolf, S.-H. Wu, H. Xu, T. Yamakura, S. Yap, and J. K. Zimmerman. 2018. Global importance of large-diameter trees. *Global Ecology and Biogeography* 27:849-864.

McDowell, N. G. 2011. Mechanisms linking drought, hydraulics, carbon metabolism, and vegetation mortality. *Plant Physiology* 155:1051-1059.

Mujic, A. B., D. M. Durall, J. W. Spatafora, and P. G. Kennedy. 2016. Competitive avoidance not edaphic specialization drives vertical niche partitioning among sister species of ectomycorrhizal fungi. *New Phytologist* 209:1174-1183.

Mujic, A. B., B. Huang, M.-J. Chen, P.-H. Wang, D. S. Gernandt, K. Hosaka, and J. W. Spatafora. 2019. Out of western North America: evolution of the *Rhizopogon-Pseudotsuga* symbiosis inferred by genome-scale sequence typing. *Fungal Ecology* 39:12-25.

Nara, K. 2006. Ectomycorrhizal networks and seedling establishment during early primary succession. *New Phytologist* 169:169-178.

Ouimette, A. P., S. V. Ollinger, L. C. Lepine, R. B. Stephens, R. J. Rowe, M. A. Vadeboncoeur, S. J. Tumber-Davila, and E. A. Hobbie. 2019. Accounting for carbon flux to mycorrhizal fungi may resolve discrepancies in forest carbon budgets. *Ecosystems*:1-15.

Philip, L., S. Simard, and M. Jones. 2010. Pathways for below-ground carbon transfer between paper birch and Douglas-fir seedlings. *Plant Ecology & Diversity* 3:221-233.

Pickles, B. J., R. Wilhelm, A. K. Asay, A. S. Hahn, S. W. Simard, and W. W. Mohn. 2017. Transfer of 13C between paired Douglas-fir seedlings reveals plant kinship effects and uptake of exudates by ectomycorrhizas. *New Phytologist* 214:400-411.

Poorter, H., K. J. Niklas, P. B. Reich, J. Oleksyn, P. Poot, and L. Mommer. 2012. Biomass allocation to leaves, stems and roots: meta-analyses of interspecific variation and environmental control. *New Phytologist* 193:30-50.

R Core Team. 2019. R: A language and environment for statistical computing. The R Foundation. Version 3.6.2.

R Studio Team. 2020. RStudio: Integrated Development for R.

Richardson, A. 2000. Coarse root elongation rate estimates for interior Douglas-fir. *Tree Physiology* 20:825-829.

Schiestl-Aalto, P., K. Ryhti, A. Mäkelä, M. Peltoniemi, J. Bäck, and L. Kulmala. 2019. Analysis of the NSC storage dynamics in tree organs reveals the allocation to belowground symbionts in the framework of whole tree carbon balance. *Frontiers in Forests and Global Change* 2.

Schloerke, B., D. Cook, J. Larmarange, F. Briatte, M. Marbach, E. Thoen, A. Elberg, and J. Crowley. 2020. GGally: Extension to 'ggplot2'. R package version 1.5.0.

Simard, S., A. Asay, K. Beiler, M. Bingham, J. Deslippe, X. He, L. Philip, Y. Song, and F. Teste. 2015. Resource transfer between plants through ectomycorrhizal fungal networks. Pages 133-176 *in* T. R. Horton, editor. *Mycorrhizal Networks*. Springer Netherlands, Dordrecht.

Simard, S. W., D. A. Perry, M. D. Jones, D. D. Myrold, D. M. Durall, and R. Molina. 1997. Net transfer of carbon between ectomycorrhizal tree species in the field. *Nature* 388:579-582.

Smith, J. H. G. 1964. Root spread can be estimated from crown width of Douglas-fir, lodgepole pine, and other British Columbia tree species. *The Forestry Chronicle* 40:456-473.

Smith, S. E., and D. J. Read. 2010. Mycorrhizal symbiosis. Academic press.

Song, Y. Y., S. W. Simard, A. Carroll, W. W. Mohn, and R. S. Zeng. 2015. Defoliation of interior Douglas-fir elicits carbon transfer and stress signalling to ponderosa pine neighbors through ectomycorrhizal networks. *Scientific Reports* **5**:8495.

Speer, J. H. 2010. Fundamentals of tree-ring research. University of Arizona Press.

Swaty, R. L., R. J. Deckert, T. G. Whitham, and C. A. Gehring. 2004. Ectomycorrhizal abundance and community composition shifts with drought: predictions from tree rings. *Ecology* 85:1072-1084.

Stokes, M., and T. Smiley. 1996. An introduction to tree-ring dating: Tucson. University of Arizona Press AZ.

Symonds, M. R. E., and A. Moussalli. 2011. A brief guide to model selection, multimodel inference and model averaging in behavioural ecology using Akaike's information criterion. *Behavioral Ecology and Sociobiology* 65:13-21.

Terrer, C., S. Vicca, B. A. Hungate, R. P. Phillips, and I. C. Prentice. 2016. Mycorrhizal association as a primary control of the CO_2 fertilization effect. *Science* 353:72-74.

Teste, F. P., and S. W. Simard. 2008. Mycorrhizal networks and distance from mature trees alter patterns of competition and facilitation in dry Douglas-fir forests. *Oecologia* 158:193-203.

Teste, F. P., S. W. Simard, and D. M. Durall. 2009. Role of mycorrhizal networks and tree proximity in ectomycorrhizal colonization of planted seedlings. *Fungal Ecology* 2:21-30.

Teste, F. P., S. W. Simard, D. M. Durall, R. D. Guy, and S. M. Berch. 2010. Net carbon transfer between *Pseudotsuga menziesii var. glauca* seedlings in the field is influenced by soil disturbance. *Journal of Ecology* 98:429-439.

Treseder, K. K., M. F. Allen, R. W. Ruess, K. S. Pregitzer, and R. L. Hendrick. 2005. Lifespans of fungal rhizomorphs under nitrogen fertilization in a pinyon-juniper woodland. *Plant and Soil* 270:249-255.

Trugman, A. T., M. Detto, M. K. Bartlett, D. Medvigy, W. R. L. Anderegg, C. Schwalm, B. Schaffer, and S. W. Pacala. 2018. Tree carbon allocation explains forest drought-kill and recovery patterns. *Ecology Letters* 21:1552-1560.

Twieg, B. D., D. M. Durall, and S. W. Simard. 2007. Ectomycorrhizal fungal succession in mixed temperate forests. *New Phytologist* 176:437-447.

von Liebig, J. F. 1840. Die organische Chemie in ihrer Anwendung auf Agricultur und Physiologie. F. Vieweg und Sohn.

Wang, T., A. Hamann, D. Spittlehouse, and C. Carroll. 2016. Locally downscaled and spatially customizable climate data for historical and future periods for North America. *PLoS One* 11:e0156720.

Warren, J. M., J. R. Brooks, F. C. Meinzer, and J. L. Eberhart. 2008. Hydraulic redistribution of water from *Pinus ponderosa* trees to seedlings: evidence for an ectomycorrhizal pathway. *New Phytologist* 178:382-394.

4.6 TABLES

Table 4.1 Summary statistics of the six plots in which ectomycorrhizal networks were measured. The plots were originally established by Beiler et al. (2015). Only the trees within the 10 × 10 m plots and ≥ 10.0 cm DBH (diameter at breast height) were used for summary statistics. Standard deviations are provided in parentheses. VEL = the mean number of trees connected via the *Rhizopogon vesiculosus* network; VIL = the mean number of trees connected via the *Rhizopogon vinicolor* network; VEG = the mean number of unique genets of *R. vesiculosus*; and VIG = the mean number of unique genets of *R. vinicolor*.

Plot	Trees sampled	DBH (SD)	Tree age (SD)	Clay/Sand % (SD)	pH (SD)	Mean connections	VEG	VIG	VEL	VIL
1	6	20.3 (1.7)	87 (8.6)	20.9/30.7 (1.7/9.4)	5.8 (0.1)	22.1 (0.1)	1.3 (0.5)	0.0 (0.0)	22.1 (0.4)	0.0 (0.0)
2	5	21.4 (3.4)	102 (3.0)	16.7/42.7 (2.6/8.8)	5.7 (0.3)	11.4 (1.3)	1.2 (0.4)	1.4 (1.1)	9.0 (0.0)	7.4 (4.1)
3	4	36.6 (10.7)	115 (13.2)	18.2/37.2 (1.7/6.6)	5.6 (0.0)	24.75 (0.9)	1.2 (0.5)	2.0 (1.1)	21 (0.0)	13.2 (1.8)
4	5	24.1 (3.3)	64 (3.7)	11.0/48.5 (2.0/10.2)	6.3 (0.1)	18.2 (4.0)	2.2 (0.8)	0.6 (0.5)	18.2 (4.0)	0.6 (0.8)
5	6	21.9 (4.1)	64 (7.3)	12.1/50.7 (1.3/4.0)	5.7 (0.1)	24.5 (0.8)	1.3 (0.5)	1.3 (0.5)	18.5 (0.8)	15.3 (0.5)
6	9	22.5 (9.1)	65 (3.0)	16.5/31.9 (1.8/6.0)	5.4 (0.0)	24.8 (10.5)	1.5 (1.3)	1.6 (1.1)	17.4 (11.2)	13.3 (8.9)

Table 4.2 An abbreviated list (10/40) of the models with the lowest AIC and Δi (ΔAICc) of < 10.0 that were averaged to create a global modela to infer if ectomycorrhizal networks influence radial growth of interior Douglas-fir. Variables are: BAI = basal area increment (2008), AGE = age of tree, DBH = diameter at breast height, pH= the soil pH, SAND = the sand content of the soil around a tree, VEG = the number of unique genets of *Rhizopogon vesiculosus* by which a tree is colonized, VEL = number of connections to other trees via *Rhizopogon vesiculosus*, VIL = number of connections to other trees via *Rhizopogon vinicolor*, and VIG = the number of unique genets of *Rhizopogon vinicolor* by which a tree is colonized.

Models	AICc	Δi	LogLik[b]	Weight	R^2
BAI ~ AGE + DBH + VEG + VEL + VIL	470.553	0.000	-226.203	0.132	0.834
BAI ~ AGE + DBH + VEG + VEL + VIG + VIL	470.556	0.002	-224.509	0.132	0.849
BAI ~ AGE + DBH + SAND + VEG + VEL + VIG + VIL	470.756	0.202	-222.778	0.120	0.864
BAI ~ AGE + DBH +SAND + VEG + VEL +VIL	470.852	0.298	-224.657	0.114	0.848
BAI ~ AGE + DBH +VEG + VIL	470.884	0.330	-227.942	0.112	0.817
BAI ~ AGE + DBH + VEG + VIG + VIL	471.684	1.131	-226.768	0.075	0.829
BAI ~ AGE + DBH + SAND + VEG + VIL	472.794	2.240	-227.323	0.043	0.823
BAI ~ AGE + DBH + pH + VEG + VEL + VIL	473.508	2.955	-225.985	0.030	0.836

Models	AICc	Δi	LogLik[b]	Weight	R^2
BAI ~ AGE + DBH + pH + VEG + VEL +VIG + VIL	473.728	3.174	-224.264	0.027	0.852
BAI ~ AGE + DBH + SAND + VEG + VIG + VIL	473.830	3.277	-226.146	0.025	0.835

[a]Global model: BAI ~ AGE + DBH + PH + SAND + VEG + VEL + VIG + VIL

[b]LogLik: The log-likelihood of the model where larger (more positive) numbers indicate a better statistical fit of the model to the data.

4.7 FIGURES

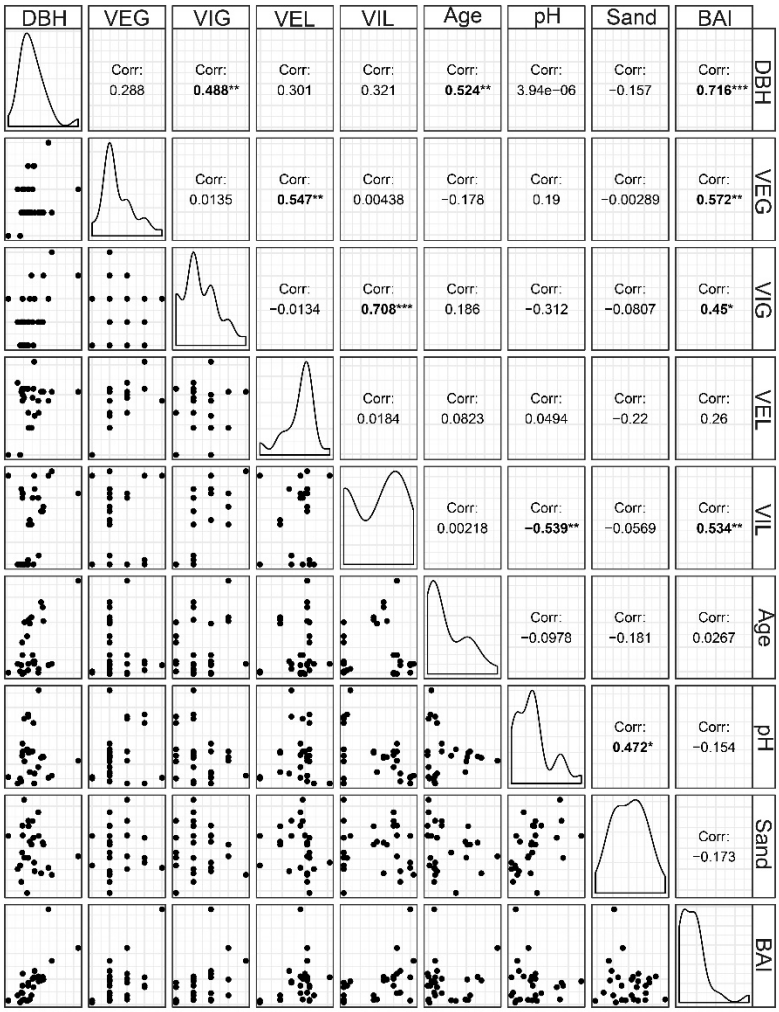

Figure 4.1 Pearson correlation values for each of the variables included in a global model testing the influence of ectomycorrhizal networks on basal area increment. The variables plotted are: DBH = the diameter at breast height of the trees, VEG = the number of *Rhizopogon vesiculosus* genets colonizing a tree, VIG = the number of *Rhizopogon vinicolor* genets colonizing a tree, VEL = the number of connections to other trees through the *R. vesiculosus* network, VIL = the number of connections to other trees through the *R. vinicolor* network, Age = the age of the tree, pH = the pH of the soil, Sand = the sand content of the soil, and BAI = basal area increment.

Significant correlation coefficients are bolded and marked with asterisks ($p < 0.5$; '*'; $p < 0.01$. '**'; $p < 0.001$, '***').

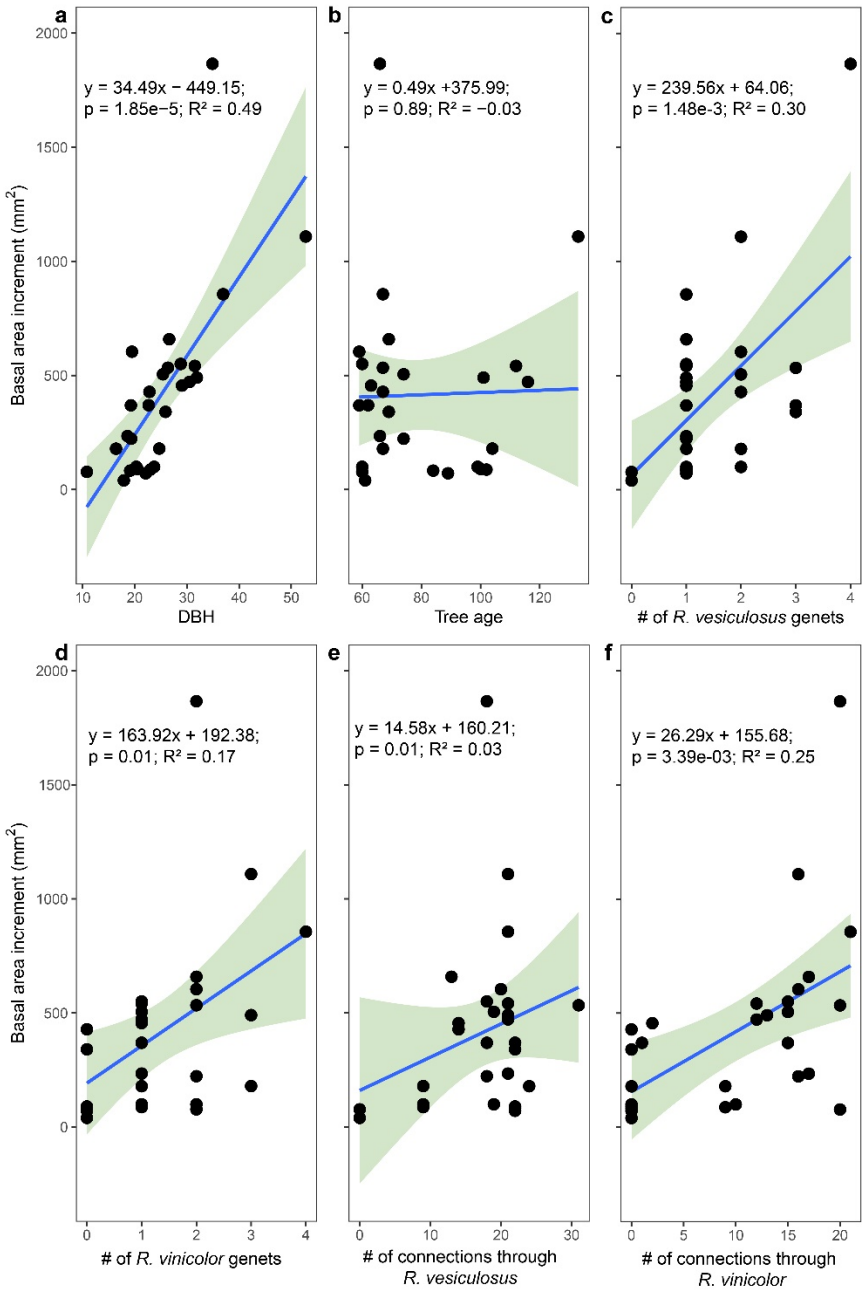

Figure 4.2 The linear relations between basal area increment (BAI) in 2008 and independent variables used in a global model testing the influence of ectomycorrhizal networks on basal area increment. (**a**) The linear relation between BAI and tree DBH (cm). (**b**) The linear relation between BAI and tree age. (**c**) The linear relation between BAI and the number of *Rhizopogon vesiculosus* genets colonizing a tree. (**d**) The linear relation between BAI and the number of

Rhizopogon vinicolor genets colonizing a tree. (**e**) The linear relation between BAI and the number of trees connected to a tree through the *R. vesiculosus* network. (**f**) The linear relation between BAI and the number of trees connected to a tree through the *R. vinicolor* network.

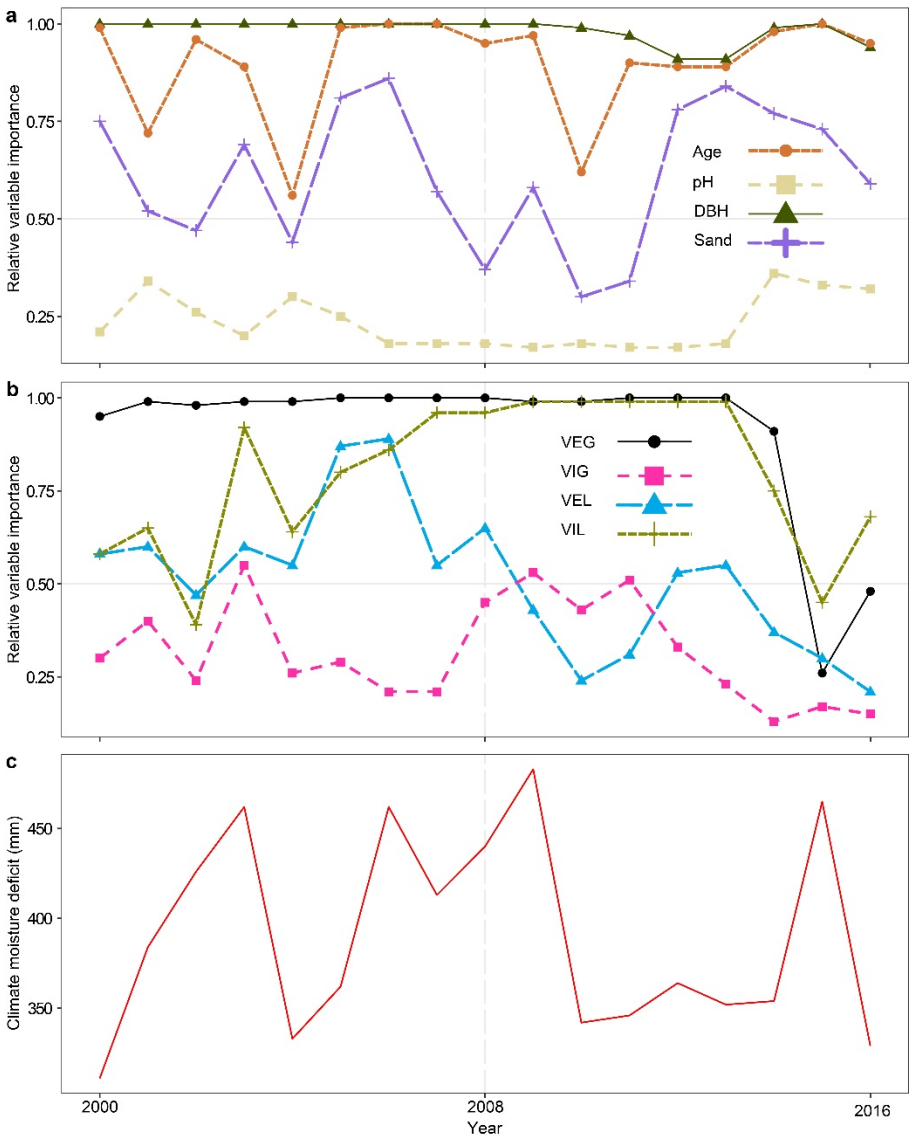

Figure 4.3 The relative variable importance scores (RVI, y-axis) for the variables used in a multi-model average for basal area increment of *Pseudotsuga menziesii* var. *glauca* trees. The x-axis plots the years over which models were generated. The RVI is the sum of the weights for models that contained the variable of interest. A high (low) RVI indicates the variable was present in models that were highly (poorly) weighted. For visual clarity, variables have been split into panel (**a**) and (**b**). (**a**) The RVI scores for DBH (medium-dashed line), Age (solid line), sand content of the soil (mixed-dash line), and soil pH (short-dash line). (**b**) The RVI scores for the

number of unique genets of *Rhizopogon vesiculosus* by which a tree was colonized (VEG, solid line), the number of unique genets of *Rhizopogon vinicolor* by which a tree was colonized (VIG, medium-dashed line), the number of connections to other trees via *R. vesiculosus* (VEL, long-dashed line), and the number of connections to other trees via *R. vinicolor* (VIL, short-dashed line). (**c**) The annual climatic moisture deficit (mm) for 2000–2016.

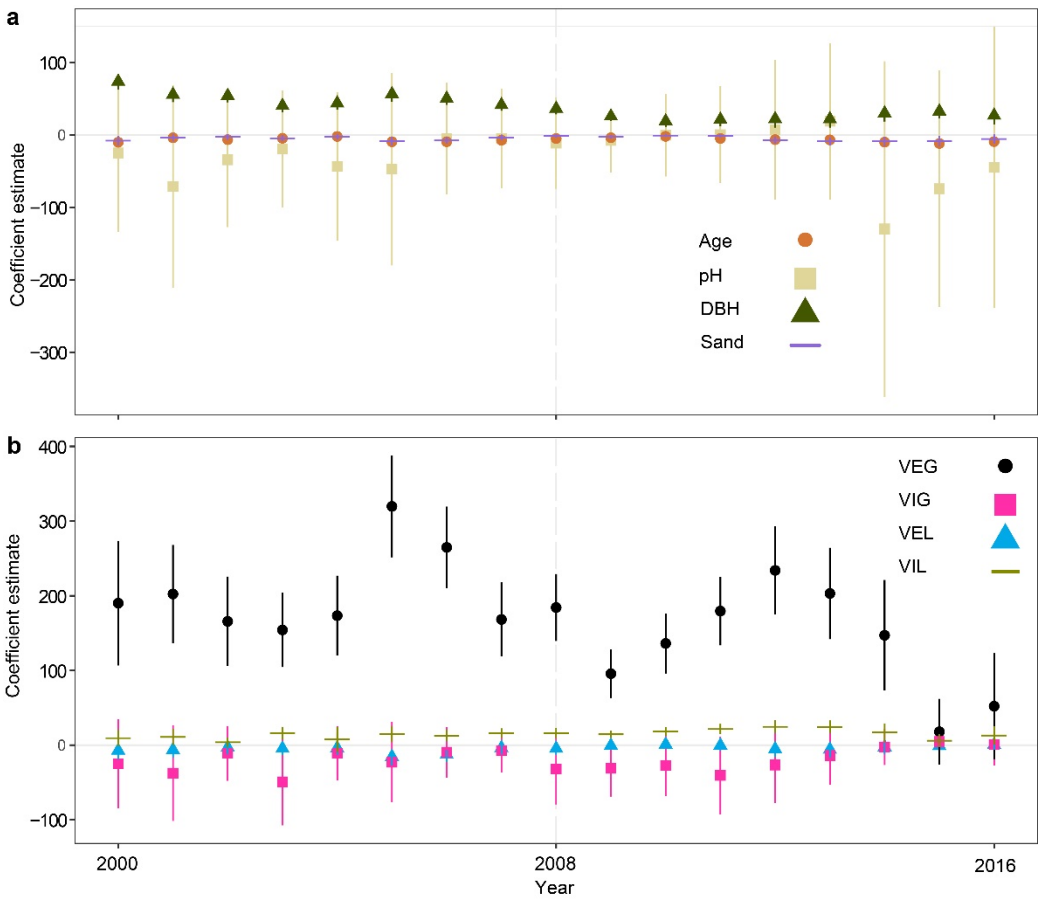

Figure 4.4 The coefficient values (± 1 SE) for the ensemble global model variables. The y-axis plots the coefficient values of each variable. Coefficients represent how much a tree's BAI will change with a unit increase of each dependent variable. The x-axis plots the years over which ensemble global models were generated. The dependent variable for the global models was annual basal area increment of *Pseudotsuga menziesii var. glauca*. Independent variable values were constant from the year they were measured (2008). (**a**) The coefficient value and standard deviations for the independent variables of DBH (triangle), tree age (circle), sand content of the soil (line), and the soil pH (square). (**b**) The coefficient value and standard deviations for the independent variables of the number of unique genets of *Rhizopogon vesiculosus* by which a tree was colonized (VEG, circle), the number of unique genets of *Rhizopogon vinicolor* by which a

tree was colonized (VIG, square), the number of connections to other trees via *R. vesiculosus* (VEL, triangle), and the number of connections to other trees via *R. vinicolor* (VIL, line).

Chapter 5: Dancing with Douglas-fir: fungal community assembly processes vary across disparate forests

5.1 ABSTRACT

Belowground fungal communities can influence the productivity, composition, and health of forests through interactions with plants, soils, plant-soil-feedbacks, and their influence on nutrient cycling. Thus, shifts in fungal community composition could have substantial impacts on forests by altering above and belowground interactions between species and their environments. Fungal community composition is likely shaped by a combination of stochastic and deterministic processes such as priority effects, dispersal-limitation, local climate, and partner preference between trees and the fungi with which they interact. Quantifying the strength of these assembly processes across heterogeneous forests is necessary to test whether assembly processes are generalizable across space and time for belowground fungi. Of the belowground fungi, many form ectomycorrhizas with trees and I predict that these fungi will be largely found within root-associated fungal communities. Due to the influence of partner preference and specificity between trees and their associated fungi, I predicted assembly processes to differ between root and soil-associated fungal communities. Tree age may also influence the assembly processes of fungal communities through altered partner preference owing to tree ontogenesis and senesence. To test if fungal community assembly processes vary between roots versus soils, by site, and with tree age, I surveyed four stands of Douglas-fir forests occurring in relatively disparate environmental conditions across western North America (northern and southern British Columbia, Canada, and northern and southern Utah, USA). I sampled roots and soil around 12 *Pseudotsuga menziesii* at each site and used MiSeq sequencing of fungal environmental rDNA to determine community composition and richness from which I calculated the relative role of deterministic and stochastic processes in shaping fungal communities. I detected 7280 fungal

amplicon sequence variants with 5270 associated with soil, 3887 with roots and 1877 found across both roots and soils. Deterministic processes dominated root and soil fungal communities at all sites except in northern Utah where stochastic processes (i.e., dispersal-limitation and community drift) controlled root-associated communities. Despite the overall dominance of determinism in fungal community assembly, the proportion of assembly processes differed by site. Contrary to my predictions, the proportion of selection pressures did not vary with mature tree age. Taken together, I conclude that deterministic processes, such as local climate and partner preference, between trees and their associated fungi, are likely dominant in most fungal communities associated with *Pseudotsuga menziesii* but that significant differences in the strength of selection exist between sites.

5.2 INTRODUCTION

Deciphering the processes that shape biodiversity is a key question driving ecological research. The processes shaping biodiversity can broadly be categorized into deterministic, selection-based pressures or stochastic birth, death, and dispersal of individuals leading to community drift (HilleRisLambers et al. 2012). Deterministic or 'niche-based' theories posit functional differences among species, where species have an optimal suite of environmental characteristics in which they function and reproduce (Grime 1977, Tilman 1982, Molles 2015). These functional differences emerge from selection pressures from the environment favoring some species over others and as a result, species occurrence can be predicted by environmental conditions. In contrast, neutral theories of community assembly assume some degree of functional equivalence among species at the same trophic level and thus implying that dispersal limitation and stochastic birth, death, and immigration to explain community assembly (Hubbell 2005). Evidence suggests that both niche-based selection and stochastic neutral processes operate in tandem for many communities with varying strength and at different temporal and spatial scales (Leibold and McPeek 2006, Chase 2014).

In microbial communities, such as belowground fungi, a combination of deterministic and stochastic processes has been shown to interweave to influence community assembly (Stegen 2012, Wang et al., 2020). The influence of deterministic and stochastic processes can vary with the environment and time to shape fungal community composition (Li et al., 2020, Wang et al., 2020, Dini-Andreote et al., 2015). These processes can indirectly influence forest growth and health by altering the prevalence and composition of fungal communities. In particular, the prevalence of beneficial or harmful fungi can influence tree growth or health (Swaty et al. 2004, Horton et al. 2013). Niches constructed by species responses to climate, soil

properties or to the composition of aboveground plant communities may underly community composition of belowground fungi by acting as environmental filters of fungal community composition (Dumbrell et al. 2010, Wubet et al. 2012, Glassman et al. 2017b). However, stochastic processes like dispersal limitation or community drift may also play a role in fungal community assembly (Li et al., 2020, Chen et al. 2019). However, these processes may vary between and across systems, making it difficult to predict fungal community assembly in under-studied systems (Wang et al. 2020). Specifically, generalizing assembly processes across large distances, such as a tree's range, may encounter problems with changing environmental features and outliers that break local processes away from expected patterns.

Whether stochastic and deterministic processes are consistent or variable across space have important implications as climate change progresses. Under future climates I might expect that edaphic properties, such as nutrient availability or pH might shift due to changes in temperature and moisture (Rengel 2011, Koyama et al. 2019). These local factors may impose strong filters on belowground fungal communities. If deterministic selection processes have equal strength across a tree's range, I expect that a change in environmental conditions would have a proportionate influence in the assembly of belowground fungal communities across sites (Fig. 5.1A). However, if the strength of selection processes on belowground fungal community assembly vary by site, then the influence of environmental change may be disproportionate across a tree's range and result in varying rates of change in the belowground fungal community (Fig 5.1B). Alternatively, the effects of climate change may not be vary evenly across space with temperature increases are expected to be pronounced at northern latitudes (Pachauri et al., 2014) and have already been implicated in altered forest growth (Williams, Xu, & McDowell 2011). Thus, the uneven impacts of climate change could have further interactions if assembly processes

are site-dependent (Fig. 5.1C). If belowground fungal communities are assembled by predominantly neutral processes, then community changes may be unpredictable in the face of climate change (Fig. 5.1C:D).

Owing to the presence of different fungal functional guilds and the specificity in interactions between fungi and their tree partners, the relative importance of deterministic and stochastic assembly processes in root-associated communities may differ from soil-associated communities. Bi-directional selection pressures could influence fungal composition on roots and surrounding soils and change with the magnitude of resource limitation and with competition among mycorrhizal fungi (Werner and Kiers 2015). Trees can engage in partner preference by favoring certain species of EMF colonizing their roots (Bogar et al. 2019) based on the amount of resources transferred, and inhibit colonization by uncooperative fungi (Hortal et al. 2017) potentially imposing greater selection pressures on EMF relative to other fungi. The influence of partner preference may cause greater deterministic processes in root-associated communities relative to soil-associated communities.

The strength of deterministic and stochastic processes may not only vary across space but also with time and ecological succession. Dini-Andreote et al. (2015) found that the strength of deterministic processes increased with succession for bacterial communities and that changes in soil organic matter altered the balance of deterministic and stochastic processes. Likewise, fungal communities may shift with edaphic variation, rooting density, and stand development (LeDuc et al. 2013, Twieg et al, 2007, Odriozola et al. 2020) which could alter outcome of competition between EMF and reduce the influence of priority effects (Kennedy et al. 2007). Older trees could have altered selection pressures compared to younger trees owing to the time over which selection pressures influence fungal communities or through tree ontogenesis and senescence

altering nutrient requirements (Peri et al. 2006, Bertrand et al. 2011, Tang et al. 2014). Time over which selection pressures occur could also influence fungal communities by causing more pronounced change over time. I expect that the influence of tree age would likely be greatest for root-associated communities that are directly influenced by partner specificity and preference than for surrounding fungal communities in the soil.

In western North America, the tree species *Pseudotsuga menziesii* var. *glauca* (Mayr) Franco (interior Douglas-fir; hereafter *Pseudotsuga*) extends from northern Mexico to central British Columbia, Canada and has critical economic and ecological value across much of its range (Steinberg 2002). Like all Pinaceae, *Pseudotsuga* forms symbiotic associations with ectomycorrhizal fungi (EMF) and is a frequent subject of studies investigating the symbiosis between EMF and their tree-host (Trappe 1977, Twieg et al. 2007, Teste et al. 2009, Defrenne et al. 2019). The extended range of *Pseudotsuga* spans a large variety of elevations, climates, vegetation, and disturbance regimes. In addition to encompassing such wide environmental variation, *Pseudotsuga* also spans early to late seral stages depending on the environment and can persist for over a millennium (Brown 1996). Variation among *Pseudotsuga* populations could interact with warming climates to produce disproportionate growth responses or shifts in the range of *Pseudotsuga* (Hamann and Wang 2006, Chen et al. 2010). Changing growth-limitations or shifts in range could conceivably disrupt the fungal communities associating with *Pseudotsuga* by altering partner selection and the geographic distributions of fungal associates.

Given the wide ecological amplitude of *Pseudotsuga*, I predicted that 1) the strength of deterministic and stochastic processes would differ in forests across the range of this species owing to inherent differences in environmental filters 2), root-associated communities will have greater proportions of deterministic processes than soil-associated communities; and 3) the

influence of deterministic processes on root-associated but not soil-associated fungal communities, would increase with tree age. The belowground assembly of fungal taxa may have important implications for *Pseudotsuga* and understanding the processes that influence community composition will aid predictions of how a changing environment may influence belowground diversity.

5.3 METHODS

5.3.1 Site selection

I chose four sites that had mature populations (> 50 years old) of *Pseudotsuga menziesii* var. *glauca* (Mayr) Franco (interior Douglas-fir; hereafter *Pseudotsuga*), near the margin of the local *Pseudotsuga* habitat, and together represented a wide range of environmental variability (Table 5.1; Appendix 5.1 Table S5.1). These four sites were chosen because they were expected to have climate-induced growth limitation for trees owing to their proximity at the edge of the local *Pseudotsuga* range and thus may be particularly sensitive to warming climates. The sites are: John Prince Research Forest (54.6 N -124.3 W; British Columbia, CA), Kamloops (50.8 N -120.3 W; British Columbia, CA), Wellsville Mountains National Wilderness (41.6 N -112.0 W; Utah, USA), and the Cedar Breaks National Monument (37.6 N -112.8 W; Utah, USA) (Fig 5.1A).

The John Prince and Cedar Breaks sites had heterogenous tree composition with *Pseudotsuga* interspersed with cohorts of predominantly *Abies bifolia* A.Murray bis (Rocky Mountain subalpine fir), *Abies lasiocarpa* (Hooker) Nuttall (subalpine fir), and *Picea engelmannii* Engelm.(Engelmann spruce). The Kamloops and Wellsville sites were largely composed of *Pseudotsuga* with scattered *Pinus flexilis* E. James (limber pine) at the Wellsville

site. Mean tree age varied substantially between and within sites (Table 5.1). Each forest regenerated naturally following harvest (John Prince; 1820s; Kamloops, 1860s), wildfire (Cedar Breaks, 1800s), and drought (Wellsville, intermittent). The trees at each site exhibit a positive growth response to mean monthly precipitation and a negative response to mean maximum temperature during the growing season of the current year (John Prince, Kamloops, and Cedar Breaks) or previous year (Wellsville Mountains) (Appendix 5.1 Fig. S5.1:S5.4).

5.3.2 Belowground sampling

To compare the root-associated and soil-associated fungal communities of *Pseudotsuga,* I sampled paired root and soils around 12 trees at each site (Fig 5.1B). As a precaution against poor quality samples, I sampled several extra trees at each site except Cedar Breaks. I selected trees that appeared visibly healthy and were ≥ 10 cm diameter at breast height (DBH). To minimize spatial autocorrelation of fungal communities, all sampled trees were ≥10 m from other samples. I used a soil knife (Zenport Industries; Sherwood, OR, USA) to sample soil to a depth of 25 cm around each tree. I sampled four locations at the dripline of each tree, separated by 90 degrees and an additional sample adjacent to the bole and pooled the five samples by tree. The soil knife was immersed in a 10% bleach solution and dried between trees to prevent cross-contamination. I froze samples at -20 Cº prior to further processing.

5.3.3 Sample processing

To separate the fine roots from each soil sampled, I thawed each sample prior to sieving roots from soils. To prevent contamination between samples, I bleached and dried the sieves between each sample using a 10% bleach solution. I used progressively finer sieves up to 2.0 mm diameter. I used freshly sterilized forceps to separate fine roots from the sieved soils. I re-froze

the separated roots and soils at -20 Cº prior to freeze-drying. Frozen samples were freeze-dried until they had reached a stable weight.

To estimate soil texture, I used a combination of laser diffraction (John Prince and Kamloops) and hand-texturing (Wellsville and Cedar Breaks) of mineral soil. Difficulties in transporting soil samples across international borders necessitated hand-texturing of the soils originating within the USA. Laser diffraction of Canadian soils was performed by the Natural Resources Analytical Laboratory at the University of Alberta, CA. Due to the differences in precision and accuracy between the methods, I report the soil classifications only as site descriptors (Appendix 5.1 Table S5.2). However, soil texturing conducted by practiced professionals can match laboratory estimates with as much as 66% accuracy (Salley et al., 2018).

5.3.4 Identification of tree age

To identify the age and climatic response of trees, I collected two increment cores per tree with a 4.3 mm increment borer (Haglöf Sweden; Mora, Sweden) close to the root collar. I sanded increment cores with progressively finer sandpaper up to 6-micron grit. I visually cross-dated each core prior to measuring using CDendro (Cybis Elektronik & Data AB; Saltsjöbaden, Sweden) for the cores from British Columbia (0.01 mm resolution) and a Velmex measuring system (Velmex Inc; Bloomfield, NY) for the Utah cores (0.001 mm resolution). I verified cross-dating with the COFECHA program (Holmes 1983) and dplR 1.7.0 (Bunn et al. 2019). I did not estimate tree age for cores that were rotted before pith.

5.3.5 Fungal community sequencing

Prior to DNA extraction, I ground freeze-dried samples to a fine powder using a Tissuelyser 2 (Qiagen; Hilden, Germany). I used MoBio DNeasy PowerSoil Kits (Qiagen;

Hilden, Germany) to extract DNA samples following the manufacturer's instructions. I used a combination of ethanol precipitation and Bovine Serum Albumin (Fisher Scientific; Waltham, MA) to remove PCR inhibitors. The presence of likely PCR inhibitors and poorly performing samples reduced the target sample size from 96 to 86 samples (Appendix 5.1 Table S5.1).

To identify the fungal communities on roots and soil, I used MiSeq sequencing of the ITS2 region of rDNA. I used the primers fITS7 (Ihrmark et al. 2012) and ITS4 (White et al. 1990) to target the ITS2 region. I amplified extracted rDNA through a two-step PCR. I ran the first PCR using 25 µL sample volumes with 2.5 µL DNA template, 7.875 µL water, 12.5 µL Platinum SuperFi PCR MasterMix (Thermo Fisher Scientific, Waltham, MA, USA), 0.125 µL Bovine Serum Albumin, and 1 µL of each of the forward and reverse primers (95ºC for 3 min; 95ºC for 30 secs, 50ºC for 1 min, 72ºC for 30 secs, 35 cycles; and 72ºC for 10 min). The samples were pooled and cleaned using Sera-Mag Select beads (GE Healthcare, Chigaco, IL, USA) and washed in two 80% ethanol washes. I used Illumina Nextera Index primers (Illumina Inc., San Diego, CA, USA) with N7 (N5) for the forward (reverse) reads for the second PCR. For the second PCR, 25 µL volume was used with 5 µL of water, 12.5 µL of Platinum SuperFi PCR MasterMix, 2.5 µL N7xx primers, 2.5 µL N5xx primers, and 2.5 DNA (95ºC for 3 min; 95ºC for 30 secs, 55ºC 30 secs, 72ºC for 30 secs, 72ºC for 5 mins, for 8 cycles).

Following the second PCR the samples were pooled and cleaned using Sera-Mag Select beads (GE Healthcare, Chigaco, IL, USA) and washed in two 80% ethanol washes. ITS2 amplicons were quantified using a dsDNA HS Assay kit on a Qubit fluorometer (Thermo Fisher Scientific, Waltham, MA, USA) and pooled into equimolar concentrations. Sequencing was

conducted at the University of Alberta Molecular Biological Sciences Unit, with an Illumina MiSeq sequencing platform (Illumina Inc., San Diego, CA, USA).

5.3.6 Bioinformatics

I used the dada2 1.12.1 package (Callahan et al. 2016a) to filter and denoise demultiplexed sequences to create amplicon sequence variants (ASVs) that distinguish up to single nucleotide differences between sequences. The precision of ASVs can result in multiple ASVs being assigned the same taxonomic classification and overestimate fungal diversity by 30% (Callahan et al. 2017, Glassman and Martiny 2018). However, using ASVs allows for simple comparisons of sequences across studies and can provide details on intraspecific variation (Edgar 2018).

Filtering and removal of chimeric sequences reduced the number of reads per sample from 45,180 ± 8666 (SD) to 17,819 ± 4,078 (Appendix 5.1 Table 5.3). I assigned taxonomy from the fungal UNITE 8.2 database (Nilsson et al. 2019) with the IDTAXA function in the DECIPHER 2.12.0 package (Wright 2016). The IDTAXA function uses a two-phase process to assign taxonomy to ASVs by learning from a training set and then classifying sequences against a reference database. The IDTAXA compares favorably against other common classification tools and has lower over-classification errors than similar methods (Murali et al. 2018). After assigning taxonomy, I analyzed and visualized the results using the phyloseq 1.28.0, vegan 2.5-6, and the ggplot2 3.2.1 packages (McMurdie and Holmes 2013, Oksanen et al. 2019, Wickham 2016). Statistical analysis and sequence processing were performed in the statistical program R 4.0.2 in the R Studio 1.3.1056 interface (R Core Team 2020, R Studio Team 2020).

I rarefied to 10,000 reads per sample (seed: 4711) to account for uneven sequencing depth using the 'rarefy_even_depth' function in phyloseq 1.28.0 (McMurdie and Holmes 2013). I used the FUNGuild database (Nguyen et al. 2016) to assign functional guilds to taxonomically identified ASVs using a curated database of functional guilds and fungal taxonomy. The FUNGuild database classifies sequences to a single guild, i.e., 'ectomycorrhizal', or multiple potential guilds, 'ectomycorrhizal-wood saprotroph'. Any sequences that are not assigned a functional guild are classified as 'Unknown'. I split the guild assignments into an ectomycorrhizal guild, a saprotrophic guild, a mixed-functional guild including ectomycorrhizal lifestyles, and a catch-all 'other guilds' group for the remaining guilds such as lichenized, orchid mycorrhizal, and pathogenic fungi, among others.

5.3.7 Statistical analysis

To compare fungal community richness between habitats (roots and soils by site), I used the 'estimate_richness' function in phyloseq 1.28.0 (McMurdie and Holmes 2013) to calculate Shannnon's alpha diversity from non-rarefied ASVs. I used pairwise t-tests with a false discovery rate p adjustment to determine planned comparisons of fungal alpha diversity between root and soil at each site and visualized the distributions of fungal diversity in ggplot2 3.2.1 (Wickham 2016). To compare the composition of fungal communities by habitat, I used a Bray-Curtis dissimilarity matrix and used the 'adonis' and 'pairwise.perm.manova' functions to calculate a pairwise permutational analysis of variance (PERMANOVA). PERMANOVA tests can be sensitive to differences in between-group dispersions and I used the 'betadisper' function to test for differences in community dispersion between sites and roots or soils (Oksanen et al. 2019). Roots and soil communities had different dispersions ($p < 0.001$), so I analyzed roots and

soil communities separately for PERMANOVA tests of community composition. Community dispersions were similar across all sites ($p = 0.16$) for communities pooled across roots and soils.

To parse the fungal community assembly processes, I followed the analytical framework pioneered by Stegen et al., (2013), which uses null model testing to separate the assembly processes of microbial communities. This approach assumes that niche similarity is correlated with phylogenetic distance where closely related taxa have similar niches. This method requires a phylogenetic tree to determine the phylogenetic distance between ASVs. To construct a phylogenetic tree from the rarefied sequences, I first aligned sequences using 'AlignSeqs' in DECIPHER 2.13.0 (Wright 2016). I used the 'ModelFinder' function in IQ-TREE 2 1.6.12 to find the tree-creation model with the lowest BIC, which I implemented in R using the phangorn 2.5.5 package (Schliep 2011, Kalyaanamoorthy et al. 2017, Minh et al. 2020). I used a general time-reversable model with gamma rate variation and a maximum likelihood tree as a starting point following the code of Callahan et al. (2016b). I used soil pH and elevation as a surrogate for environmental variation as previous work has found that soil pH strongly influences fungal composition (Dumbrell et al. 2010, Zhang et al. 2016, Glassman et al. 2017b). To test this assumption, I ran a Mantel correlogram on a matrix of estimated ASV environmental optima and a matrix of branch-length phylogenetic distance between each ASV. I calculated the environmental optima of each ASV by estimating the relative abundance weighted average environmental conditions for each ASV. Four samples had missing values for pH (00-0002R, 00-0001, 1000, 1043**)** and were removed from this analysis along with 267 ASVs that were no longer present in the dataset after the removal of the samples. I standardized the optima and used the 'vegdist' function to calculate the pairwise Euclidian distance of each ASVs environmental optima. To calculate the branch-length phylogenetic distance for each ASV, I used the

'cophenetic.phylo' function in ape 5.4 (Paradis and Schliep 2019) and standardized the distances. I used the 'mantel.correlog' function from vegan to run a multivariate Mantel correlogram with 999 permutations and a progressive false-discovery-rate p-adjustment on the matrices of estimated ASV environmental optima and the phylogenetic distances. I found a correlation between environmental optima and phylogenetic distance over relatively short distances, meeting the assumption required for further analysis (Appendix 5.1 Fig. S5.5).

This particular method of null-model testing identifies the pairwise selection processes between any two communities and determines if variable selection, homogenizing selection, community drift, dispersal-limitation, or homogenizing dispersal best explains the assembly of the two communities in relation to one another. Selection is a deterministic process resulting from species interactions with the environment and results in increasingly dissimilar communities (variable selection) in heterogeneous environments or increasingly similar communities in homogenous environments (homogenous selection) (Dini-Andreote et al. 2015). For example, a hypothetical site with patches of low soil pH (<5) and high soil pH (>7) might have variable selection processes owing to soil pH applying selection pressures for two environmental types. In contrast, homogenous selection would arise if a spatially homogenous filter, such as climate, is the predominant selective force in the environment and applies directional selection on all communities. Stochastic fluctuations in community composition can arise from random changes in species abundance (community drift), under-dispersion of species (dispersal-limitation), or hyper-dispersion of species (homogenizing dispersal) (Hubbell 2005, Stegen et al. 2013). I compared the entire fungal communities to one another without separating the communities by functional guild. The high number of ASVs with unknown fungal guilds, mixed guilds, or low confidence means that parsing the communities by functional guild has an

unacceptable amount of error in the estimation of fungal guild membership. Looking across all relevant pairwise comparisons for a sample can provide an estimate for the proportion of the community shaped by each process. I limited pairwise comparisons to roots and soils within each site based on the assumption that fungal inoculum can move from soil to roots and from roots to soil.

I first calculated the β-mean taxon distance (βMNTD) using 'comdistnt' in the picante 1.8.2 (Kembel et al. 2010). The βMNTD is an estimate of phylogenetic change between communities and does not provide information on deterministic or neutral processes. However, by comparing the observed βMNTD to a null distribution of the βMNTD created under stochastic processes, it is possible to calculate the beta-nearest-taxonomic index (βNTI). Values of βNTI > 2.0 indicate variable selection causing phylogenetic overdispersion greater than expected by chance. Likewise, βNTI < -2.0 indicate homogenizing selection causing phylogenetic under dispersion compared with that expected by chance. Non-significant βNTI values (|βNTI| < 2) indicate phylogenetic dispersion expected under stochastic models. I created the βMNTD null model by iterating the data 999 times with phylogenetic tree tips being randomized across each iteration following the code of Stegan et al. (2013). I then calculated the βNTI according to the formula:

$$\beta\text{NTI} = (\beta MNT_{Observed} - \beta MNT_{Null})/\text{sd}(\beta MNT_{Null})$$

Pairwise community comparisons with a (nonsignificant) |BNTI| < 2 can be combined with the modified Bray-Curtis-based Raup-Crick distance metric (RC) to assess the relative strength of homogeneous selection, variable selection, homogenizing dispersal, dispersal limitation, and community drift (Chase et al. 2011, Stegen et al. 2013). Values of RC vary

between 1 and -1 and represent greater than, or less than expected turnover between communities, respectively. Communities that have greater than expected turnover (RC > 0.95) are assumed to operate primarily under dispersal-limitation acting in concert with drift (Stegen et al., 2013). Likewise, communities with lower than expected turnover (RC < -0.95) are assumed to be assembled from high dispersal rates between two non-regional species pools. Finally, non-significant RC values (|RC| <0.95) are expected to exist under community drift. Pairwise community comparisons with a (nonsignificant) |BNTI| < 2 can have a RC value calculated to determine if dispersal-limitation (RC > 0.95), homogenizing dispersal (RC < - 0.95), or community drift (|RC| < 0.95) are the driving force for community assembly (Stegen et al., 2013). These methods were developed and supported by empirical and simulated communities by Stegen et al. (2013, 2015).

To calculate the RC values for each pairwise combination of communities, I calculated a modified Raup-Crick index that utilizes abundance values instead of presence-absence. I used a modified version of the code originally developed by Stegen et al. (2013) that was updated for modern systems by Richter-Heitmann et al., (2020). The calculation involved probabilistically assembling 999 Bray-Curtis dissimilarity null-models for each pairwise comparison between communities at each site. Each ASVs name is randomized across the community with each ASV having a probability of being selected based on its frequency across communities and its abundance. The deviation from the observed and null-model Bray-Curtis distributions are standardized to range from -1 to 1, as a Raup-Crick dissimilarity.

To test if the distributions of βNTI differed between habitats, I used the 'pairwise.perm.t.test' function to run pairwise t-tests with 999 permutations and a false-discovery

rate p-value correction (Hervé 2020). To test if the proportion of assembly processes differed by habitat, I used a Chi-square test using the 'chisq.test' and visualized the residuals using the 'corrplot' function in the corrplot 0.84 package (Wei and Simko 2017). To test if the proportion of selection processes changes with tree age, I created linear regressions for each habitat where the proportion of assembly due to selection was the dependent variable and tree age was the independent variable. Cedar Breaks soils had identical proportions of selection processes across all samples (0.94) and could not be analyzed for age-related changes in assembly processes.

5.4 RESULTS

5.4.1 Difference of assembly processes between habitats and with tree age

Variable selection (βNTI > 2) was not detected in any habitat and mean βNTI values were < -2.0, indicating homogenizing selection was the principle assembly process for each habitat except roots at the Wellsville Mountains (Fig. 5.3). Distributions of βNTI differed significantly between roots and soils, and between sites ($p < 0.05$), except between Cedar Breaks roots and soil, and John Prince roots and soil (Appendix 5.1 Table S5.4) (Fig. 5.3). Homogenizing selection accounted for the largest proportion of assembly processes (> 50%) for root- and soil-associated fungal communities for all habitat-types except for root communities at the Wellsville Mountains (35%) (Fig. 5.3). The proportion of assembly processes varied significantly between habitats (χ^2 (21) = 325.39, $p < 0.001$), largely (52%) driven by the differences in processes at the Wellsville Mountains (Fig. 5.4) (Appendix 5.1 Table S5.5). Contrary to my predictions, the proportion of community assembly due to selection did not vary with tree age ($p > 0.05$) for any habitat (Appendix 5.1 Fig. S6).

The Wellsville Mountains also had the lowest homogenizing selection pressures in soil communities (55%) across all sites (μ = 78%). At this site, the neutral processes of dispersal-limitation and community drift were nearly equal in their average contribution to community assembly with 12% and 13%, respectively. Homogenizing dispersal was only attributed to roots and soils at the Kamloops site where it accounted for < 1% of community assembly.

5.4.2 Fungal composition, diversity, and functional guilds

I found 7280 ASVs across all sites with 3887 ASVs on roots, 5270 ASVs within soil, and 1877 ASVs shared between roots and soils (Appendix 5.1 Table S5.6; Figure S5.7). Soils had greater Shannon's diversity of fungi than roots at all sites except Cedar Breaks where there was no significant difference (Fig. 5.6). Shannon's fungal diversity for root-associated communities showed a slight trend of increasing diversity with latitude where John Prince had higher diversity than Cedar Breaks ($p = 0.01$). Other pairwise comparisons of fungal diversity were marginally significant or non-significant (Appendix 5.1 Table S5.7). Fungal community composition varied among roots ($p < 0.05$) and soils at all sites ($p < 0.01$) (Appendix 5.1 Table S5.8). Ascomycota accounted for 60.1% of sequence reads across all sites (Appendix 5.1 Table S59) while representing 38% of ASV count. In contrast, the Basidiomycota accounted for 18% of sequences and 21% of ASVs. Interestingly, Cedar Breaks had more than double the proportion of Basidiomycota reads at 34.2% compared to an average of 13.4% across the other three sites.

Only 28% of ASVs were assigned a functional guild by the FUNGuild database. The proportion of sequences within each functional guild varied widely between sites and slightly between roots and soils within each site. Averaging across site, the EMF guild was the largest by sequence abundance on roots (16%) and soils (12%) followed by saprotrophs on roots (7%) and in soils (11%) (Appendix 5.1 Table S5.10). The average proportion of EMF sequences was

skewed by Cedar Breaks communities, which had a nearly eight times higher proportion of EMF sequences on roots (44%) and in soils (44%) than did the average across the other three sites (5% for roots; 5% for soils). The higher abundance of EMF sequences at Cedar Breaks may be because it had the lowest proportion of unidentified functional guild sequences (37%) of any of the three sites (60%, John Prince; 68% Kamloops; 77% Wellsville Mountains).

5.5 DISCUSSION

I aimed to discover if the relative strength of determinism and stochastic processes varied for fungal communities between roots and soils, and across tree age along a range of environmental variability encompassed by the range of *Pseudotsuga*. Across all habitats save one, the role of homogenous selection, as inferred from distributions of significant βNTI values, was dominant in shaping fungal communities. Contrary to my initial prediction, mature tree age did not appear to be related to the proportion of deterministic selection processes in fungal community assembly. I found that while the relative roles of determinism and stochastic processes varied across habitats, the northernmost (John Prince) and southernmost (Cedar Breaks) sites had nearly identical assembly processes. Cumulatively, my results highlight that while root- and soil-associated fungal communities occurring near *Pseudotsuga* are largely influenced by homogenous selection, the role of neutral processes still has considerable influence on community assembly.

5.5.1 Why do sites differ? Clues from landscape connectivity, climate, and species composition

Homogenizing selection was the most prevalent assembly process for three of the sites. The overall dominance of homogenizing selection at each site suggests that each site has broad selection pressures that drive fungal community assembly. Site-wide selection pressures could arise from edaphic properties, local climate, or *Pseudotsuga*. Of these, *Pseudotsuga*, and the

local climate, are the two most consistent sources of potential selective pressures. Because soil texture and pH varied within each site along with aspect and elevation (Table 5.1; Appendix 5.1 Table S5.2), edaphic properties are thus unlikely to provide a broad selective pressure within each site. Indeed, variations in local soil properties (pH, organic matter content) have been implicated in *variable* selection for microbial communities (Dini-Andreote et al. 2015). A global meta-analysis indicates that the temperature of the driest annual quarter and precipitation seasonality explained more variation in the geographic distribution of globally abundant fungi than did soil or vegetation (Větrovský et al. 2019). Local climate provides a site-wide filter through which precipitation and temperature alters edaphic properties and the timing and severity of water limitation within each site (Rengel 2011). Despite being widely dispersed across western North America (Fig. 5.1), the *Pseudotsuga* at each site had similar growth correlations to growing season precipitation and temperature, suggesting that drought limitation is a constant limiting factor/process across each of these disparate sites (Appendix 5.1 Fig. S5.1:S5.4). Gehring et al. (2014) found convergent EMF communities on host trees experiencing high drought, parasitism, or herbivory. Similarly, the trees at each of the sites experience precipitation limitation during some or all years. This consistent resource limitation is a strong candidate for the driving force of the homogenizing selection within each site. Changing climate could alter or disrupt this selective pressure by altering the frequency, severity, or seasonality of drought. If precipitation limitation is the primary driver of the inferred homogenizing selection pressures, then uneven changes in climate could cause greater changes at the northern sites (e.g. Fig. 5.1B).

A clear outlier within the dataset is the Wellsville Mountains within northern Utah (Fig. 5.2) where dispersal-limitation and community drift were highly influential on fungal community assembly. One likely contributor for this pattern is that the Wellsville Mountains have a

dispersed tree-island landscape of tightly clustered groupings of *Pseudotsuga* separated by up to several hundred meters of bunchgrass dominated slopes (Appendix 5.1 Image S5.1). In this system, each tree island could represent a refugia for fungi that associate with *Pseudotsuga* instead of graminoid arbuscular mycorrhizal fungi in the broader landscape. Glassman et al., (2017a) found that EMF richness increased with tree island size in an alpine community and decreased with distance from the forest for one of two pine species. Similarly, the islands of *Pseudotsuga* at the Wellsville Mountains may foster strong dispersal-limitation and community drift for their fungal communities owing to the wide grass and rock-lands that separate the pockets of forest. The influence of *Pseudotsuga* on fungal communities would likely be spatially dependent as proximity to mature trees and forest edges can have a substantial effect on EMF composition (Cline et al. 2005, Grove et al. 2019). Community drift is expected to be greater when regional species pools are much greater than local communities (Chase 2003, Chase and Myers 2011). This may be the case at the Wellsville Mountains where the average soil diversity was greater than average root diversity ($p<0.001$) and where drift represented roughly half of stochastic processes. In comparison, other sites had smaller differences in diversity between roots and soils (Fig. 5.6). It is likely that a combination of the dispersed tree-islands and differences in community richness are contributing to the strong stochasticity at the Wellsville Mountains. Interestingly, the *Pseudotsuga* at Cedar Breaks were also separated from one another within a forest dominated by other conifers. However, Cedar Breaks fungal communities were strongly influenced by inferred selection pressures and not through neutral processes. The difference between the isolation of the tree islands at the Wellsville Mountains and the isolated trees at Cedar Breaks may be due to the contiguous nature of the forest at Cedar Breaks, which overwhelmingly consists of ectomycorrhizal trees (Furniss et al. 2017). The continuous forest of

suitable ectomycorrhizal hosts and abundant coarse woody debris could allow for easy dispersal of generalist EMF fungi at Cedar Breaks.

5.5.2 Assembly of root and soil communities

For soil-associated communities at all sites, homogenizing selection accounted for the largest share of community assembly processes. At all sites, the proportion of neutral processes was greater for root-associated communities than for soil-associated communities. These differences suggest that stochastic processes play a slightly stronger role in shaping root-associated communities than they do for soil-associated communities. Goldmann et al. (2016) found an apparent buffering of local abiotic variability for root but not soil-associated fungal communities. This finding suggests that if deterministic processes are driven by environmental variability, such as climate, that they would have a reduced influence on root-associated communities belonging to a single tree species. A reduction in deterministic environmental filtering would lead to a greater role for stochastic assembly processes in fungal community assembly. Community drift may also be more prevalent in root-associated communities due to their lower average diversity relative to the soil-associated fungal communities (Chase 2003, Chase and Myers 2011). Additionally, the ephemeral nature of fine roots could conceivably contribute to stronger stochastic processes than in soil. Temperate fine roots are generally short-lived with most lifespans below a single year and a lucky few living longer than five years (Solly et al., 2018). This brief duration could favor priority effects and slightly disfavor selection processes relative to the somewhat stable soil.

The differences between community composition and in the relative importance of assembly processes in roots and soils could also be partially due to the depth at which they were found. Li et al. (2020) reported that fungal communities in surface soils (0–10 cm) had stronger

selection pressures than did deeper soils (20–40 cm), likely because of different exposure to variation in the environment and easier dispersal in surface soils. The rooting density of *Pseudotsuga* changes with depth and can have concentrated roots within the upper (0–20 cm) profiles (Richardson et al. 2003). I sampled to a depth of 20 cm and homogenized the samples together, potentially disrupting any depth-based signal within my sites. Further, if roots were disproportionately aligned with shallower depths at one or more of my sites, they may have had greater exposure to climatic selection than soils at depth. At least one of the sites, Kamloops, has evidence for fungal niche partitioning with soil depth (Beiler et al. 2012), which further highlights that soil depth may have important, unmeasured influences on the role of assembly processes for roots and soils.

Despite pronounced gradients of mature tree age at each site, individual tree age did not appear to influence the proportion of selection processes for fungi. Importantly, the sites contained predominantly mature or old-growth *Pseudotsuga* and time-related changes in assembly processes may have occurred when the trees or stands were younger. Tree age and, more broadly, successional stage have been implicated in influencing fungal and microbial community composition in other studies (Gao et al. 2015, Hagenbo et al. 2018). However, fungal community composition could conceivably change with time even if assembly processes are largely static. In a laboratory study, Tucker and Fukami (2014) reported that priority effects resulted in exclusion of late-arriving species if temperature were held constant, but that late-arriving species could co-exist when temperature was variable. This suggests that the strength of priority effects and competition among microbial communities will change with the variability of local climatic conditions. Further research is needed to disentangle the role of assembly processes across a broader range of tree ages and across more heterogenous environments.

5.5.3 Fungal richness across the (partial) range of *Pseudotsuga*

Tedersoo et al. (2014) reported that EMF diversity increases with distance from the equator and peaks at ~6000 km coinciding with the extant of *Pinaceae*. Similarly, I found that fungal diversity slightly increased with latitude for root-associated communities and peaked in the northernmost site, John Prince. However, soil diversity did not show the same pattern with the Wellsville Mountains having the highest soil diversity. This result highlights the potential for incongruous patterns of fungal diversity in roots and soils across continental distances.

Across the four sites I found 1022 ASVs that belong in an ectomycorrhizal fungal guild. Trappe (1977) estimated that there could be 2000 EMF that associate with *Pseudotsuga* across its range. Importantly, there were 5169 ASVs that had unidentified fungal guilds and may be EMF. However, ASVs likely overestimate fungal diversity by up to 30% (Glassman and Martiny 2018) and the 1022 ASVs could likely be collapsed if resolving fungal sequences by species identity. Regardless, there are undoubtedly many hundreds, or thousands of EMF taxa that interact directly or indirectly with *Pseudotsuga* across its range. My results suggest that Trappe's estimate of 2000 EMF associates of *Pseudotsuga* may be accurate but that further refinement of taxonomic identification is needed before an accurate estimation can be made. The diversity of EMF associating with *Pseudotsuga* underscores the potential for interspecific differences among the symbionts in their ability to influence *Pseudotsuga* growth and respond to warming climates. More research is needed to improve the taxonomic resolution of the fungal ASVs around *Pseudotsuga* and determine if functional differences among the EMF community can modulate tree growth.

5.5.4 Caveats and directions for future research

The method I chose to analyze the fungal community assembly processes (βNTI and abundance-based Raup-Crick) provides a detailed look at the type and relative proportion of selection, drift, dispersal-limitation, and homogenizing dispersal. However, the method is not without assumptions and potential gaps that could be addressed better with future research. My study detected a phylogenetic signal (Appendix 5.1 Fig S5.5) but I was only able to use the continuous variables of soil pH and elevation to test this assumption. Ideally, I would have had a suite of edaphic properties, nutrient measurements, and local microclimate to test this assumption and identify which variables were driving assembly processes (see Dini-Andreote et al. 2015, Wang et al. 2020). Similarly, a broader range of environmental variables would enable researchers to test if assembly processes change with the magnitude or variation of edaphic properties or with local climate.

Future research of continent-scale trends in fungal assembly or diversity may benefit from excluding sites with dispersed tree-islands, such as the Wellsville Mountains, and having a larger sample size. The stark differences between the Wellsville Mountains and the other sites suggest that forest contiguity may have role in shaping fungal communities. Additional sites located in the intervening distances between northern Utah and southern British Columbia would have enabled a greater discussion of how latitudinal gradients influence fungal composition and diversity.

5.5.5 Conclusion

I found across four disparate sites of *Pseudotsuga* that fungal community assembly processes varied but were consistently dominated by homogenizing selection. This result suggests that these fungal communities follow similar assembly rules across *Pseudotsuga* forests. Mature tree age did not covary with assembly processes, seemingly indicating that old-growth *Pseudotsuga* have fungal communities that operate under the same assembly processes as younger, but still mature trees. The variation in processes across the sites indicate the potential for disjunct changes in fungal community composition if assembly processes vary with climate. Future research should focus on identifying how environmental variation may alter the proportion of assembly processes and if these processes may shift under warmer climates.

5.6 REFERENCES

Beiler, K. J., S. W. Simard, V. LeMay, and D. M. Durall. 2012. Vertical partitioning between sister species of *Rhizopogon* fungi on mesic and xeric sites in an interior Douglas-fir forest. *Molecular Ecology* 21:6163-6174.

Bertrand, R., J.-C. Gégout, and J.-D. Bontemps. 2011. Niches of temperate tree species converge towards nutrient-richer conditions over ontogeny. *Oikos* 120:1479-1488.

Bogar, L., K. Peay, A. Kornfeld, J. Huggins, S. Hortal, I. Anderson, and P. Kennedy. 2019. Plant-mediated partner discrimination in ectomycorrhizal mutualisms. *Mycorrhiza* 29:97-111.

Brown, P. M. 1996. OLDLIST: a database of maximum tree age. *Tree rings, environment, and humanity. Radiocarbon* 1996:727 - 731.

Bunn, A., M. Korpela, F. Biondi, F. Campelo, P. Mérian, F. Qeadan, and C. Zang. 2019. dplR: dendrochronology program library in R. R Package version 1.7.0.

Callahan, B. J., P. J. McMurdie, and S. P. Holmes. 2017. Exact sequence variants should replace operational taxonomic units in marker-gene data analysis. *The ISME Journal* 11:2639-2643.

Callahan, B. J., P. J. McMurdie, M. J. Rosen, A. W. Han, A. J. A. Johnson, and S. P. Holmes. 2016a. DADA2: high-resolution sample inference from Illumina amplicon data. *Nature Methods* 13:581-583.

Callahan, B. J., K. Sankaran, J. A. Fukuyama, P. J. McMurdie, and S. P. Holmes. 2016b. Bioconductor workflow for microbiome data analysis: from raw reads to community analyses. *F1000Research* 5.

Chase, J. M. 2003. Community assembly: when should history matter? Oecologia 136:489-498.

Chase, J. M. 2014. Spatial scale resolves the niche versus neutral theory debate. *Journal of Vegetation Science* 25:319-322.

Chase, J. M., N. J. Kraft, K. G. Smith, M. Vellend, and B. D. Inouye. 2011. Using null models to disentangle variation in community dissimilarity from variation in α-diversity. *Ecosphere* 2:1-11.

Chase, J. M., and J. A. Myers. 2011. Disentangling the importance of ecological niches from stochastic processes across scales. *Philosophical Transactions of the Royal Society B: Biological Sciences* 366:2351-2363.

Chen, L., N. G. Swenson, N. Ji, X. Mi, H. Ren, L. Guo, and K. Ma. 2019. Differential soil fungus accumulation and density dependence of trees in a subtropical forest. *Science* 366:124-128.

Chen, P.-Y., C. Welsh, and A. Hamann. 2010. Geographic variation in growth response of Douglas-fir to interannual climate variability and projected climate change. *Global Change Biology* 16:3374-3385.

Cline, E. T., J. F. Ammirati, and R. L. Edmonds. 2005. Does proximity to mature trees influence ectomycorrhizal fungus communities of Douglas-fir seedlings? *New Phytologist* 166:993-1009.

Defrenne, C. E., T. J. Philpott, S. H. Guichon, W. J. Roach, B. J. Pickles, and S. W. Simard. 2019. Shifts in ectomycorrhizal fungal communities and exploration types relate to the environment and fine-root traits across interior Douglas-fir forests of western Canada. *Frontiers in Plant Science* 10:643.

Dini-Andreote, F., J. C. Stegen, J. D. Van Elsas, and J. F. Salles. 2015. Disentangling mechanisms that mediate the balance between stochastic and deterministic processes in microbial succession. *Proceedings of the National Academy of Sciences* 112:E1326-E1332.

Dumbrell, A. J., M. Nelson, T. Helgason, C. Dytham, and A. H. Fitter. 2010. Relative roles of niche and neutral processes in structuring a soil microbial community. *The ISME Journal* 4:337-345.

Edgar, R. C. 2018. Updating the 97% identity threshold for 16S ribosomal RNA OTUs. *Bioinformatics* 34:2371-2375.

Furniss, T. J., A. J. Larson, and J. A. Lutz. 2017. Reconciling niches and neutrality in a subalpine temperate forest. *Ecosphere* 8:e01847.

Gao, C., Y. Zhang, N. N. Shi, Y. Zheng, L. Chen, T. Wubet, H. Bruelheide, S. Both, F. Buscot, and Q. Ding. 2015. Community assembly of ectomycorrhizal fungi along a subtropical secondary forest succession. *New Phytologist* 205:771-785.

Gehring, C. A., R. C. Mueller, K. E. Haskins, T. K. Rubow, and T. G. Whitham. 2014. Convergence in mycorrhizal fungal communities due to drought, plant competition, parasitism and susceptibility to herbivory: consequences for fungi and host plants. *Frontiers in Microbiology* 5:306.

Glassman, S. I., K. C. Lubetkin, J. A. Chung, and T. D. Bruns. 2017a. The theory of island biogeography applies to ectomycorrhizal fungi in subalpine tree "islands" at a fine scale. *Ecosphere* 8:e01677.

Glassman, S. I., and J. B. Martiny. 2018. Broadscale ecological patterns are robust to use of exact sequence variants versus operational taxonomic units. *MSphere* 3.

Glassman, S. I., I. J. Wang, and T. D. Bruns. 2017b. Environmental filtering by pH and soil nutrients drives community assembly in fungi at fine spatial scales. *Molecular Ecology* 26:6960-6973.

Goldmann, K., K. Schröter, R. Pena, I. Schöning, M. Schrumpf, F. Buscot, A. Polle, and T. Wubet. 2016. Divergent habitat filtering of root and soil fungal communities in temperate beech forests. *Scientific Reports* 6:31439.

Grime, J. P. 1977. Evidence for the existence of three primary strategies in plants and its relevance to ecological and evolutionary theory. *The American Naturalist* 111:1169-1194.

Grove, S., N. P. Saarman, G. S. Gilbert, B. Faircloth, K. A. Haubensak, and I. M. Parker. 2019. Ectomycorrhizas and tree seedling establishment are strongly influenced by forest edge proximity but not soil inoculum. *Ecological Applications* 29:e01867.

Hagenbo, A., J. Kyaschenko, K. E. Clemmensen, B. D. Lindahl, and P. Fransson. 2018. Fungal community shifts underpin declining mycelial production and turnover across a Pinus sylvestris chronosequence. *Journal of Ecology* 106:490-501.

Hamann, A., and T. Wang. 2006. Potential effects of climate change on ecosystem and tree species distribution in British Columbia. *Ecology* 87:2773-2786.

HilleRisLambers, J., P. B. Adler, W. S. Harpole, J. M. Levine, and M. M. Mayfield. 2012. Rethinking community assembly through the lens of coexistence theory. *Annual Review of Ecology, Evolution, and Systematics* 43:227-248.

Holmes, R. L. 1983. Computer-assisted quality control in tree-ring dating and measurement. *Tree Ring Bulletin.*

Hortal, S., K. L. Plett, J. M. Plett, T. Cresswell, M. Johansen, E. Pendall, and I. C. Anderson. 2017. Role of plant–fungal nutrient trading and host control in determining the competitive success of ectomycorrhizal fungi. *The ISME Journal* 11:2666-2676.

Horton, B. M., M. Glen, N. J. Davidson, D. Ratkowsky, D. C. Close, T. J. Wardlaw, and C. Mohammed. 2013. Temperate eucalypt forest decline is linked to altered ectomycorrhizal communities mediated by soil chemistry. *Forest Ecology and Management* 302:329-337.

Hubbell, S. P. 2005. Neutral theory in community ecology and the hypothesis of functional equivalence. *Functional Ecology* 19:166-172.

Ihrmark, K., I. Bödeker, K. Cruz-Martinez, H. Friberg, A. Kubartova, J. Schenck, Y. Strid, J. Stenlid, M. Brandström-Durling, and K. E. Clemmensen. 2012. New primers to amplify the fungal ITS2 region–evaluation by 454-sequencing of artificial and natural communities. *FEMS Microbiology Ecology* 82:666-677.

Kalyaanamoorthy, S., B. Q. Minh, T. K. Wong, A. von Haeseler, and L. S. Jermiin. 2017. ModelFinder: fast model selection for accurate phylogenetic estimates. *Nature Methods* 14:587-589.

Kembel, S. W., P. D. Cowan, M. R. Helmus, W. K. Cornwell, H. Morlon, D. D. Ackerly, S. P. Blomberg, and C. O. Webb. 2010. Picante: R tools for integrating phylogenies and ecology. *Bioinformatics* 26:1463-1464.

Kennedy, P. G., S. Hortal, S. E. Bergemann, and T. D. Bruns. 2007. Competitive interactions among three ectomycorrhizal fungi and their relation to host plant performance. *Journal of Ecology*:1338-1345.

Koyama, A., B. Harlow, and R. D. Evans. 2019. Greater soil carbon and nitrogen in a Mojave Desert ecosystem after 10 years exposure to elevated CO2. *Geoderma* 355:113915.

LeDuc, S. D., E. A. Lilleskov, T. R. Horton, and D. E. Rothstein. 2013. Ectomycorrhizal fungal succession coincides with shifts in organic nitrogen availability and canopy closure in post-wildfire jack pine forests. *Oecologia* 172:257-269.

Leibold, M. A., and M. A. McPeek. 2006. Coexistence of the niche and neutral perspectives in community ecology. *Ecology* 87:1399-1410.

Li, P., W. Li, A. J. Dumbrell, M. Liu, G. Li, M. Wu, C. Jiang, and Z. Li. 2020. Spatial variation in soil fungal communities across paddy fields in subtropical China. *mSystems* 5.

McMurdie, P. J., and S. Holmes. 2013. phyloseq: an R package for reproducible interactive analysis and graphics of microbiome census data. *PLoS One* 8:e61217.

Minh, B. Q., H. A. Schmidt, O. Chernomor, D. Schrempf, M. D. Woodhams, A. Von Haeseler, and R. Lanfear. 2020. IQ-TREE 2: new models and efficient methods for phylogenetic inference in the genomic era. *Molecular Biology and Evolution* 37:1530-1534.

Molles, M. 2015. Ecology: concepts and applications. McGraw-Hill Education.

Murali, A., A. Bhargava, and E. S. Wright. 2018. IDTAXA: a novel approach for accurate taxonomic classification of microbiome sequences. *Microbiome* 6:1-14.

Nguyen, N. H., Z. Song, S. T. Bates, S. Branco, L. Tedersoo, J. Menke, J. S. Schilling, and P. G. Kennedy. 2016. FUNGuild: an open annotation tool for parsing fungal community datasets by ecological guild. *Fungal Ecology* 20:241-248.

Nilsson, R. H., K.-H. Larsson, A. F. S. Taylor, J. Bengtsson-Palme, T. S. Jeppesen, D. Schigel, P. Kennedy, K. Picard, F. O. Glöckner, and L. Tedersoo. 2019. The UNITE database for molecular identification of fungi: handling dark taxa and parallel taxonomic classifications. *Nucleic Acids Research* 47:D259-D264.

Odriozola, I., T. Martinovic, B. D. Bahnmann, D. Ryšánek, T. Mašínová, P. Sedlák, K. Merunková, P. Kohout, M. Tomšovský, and P. Baldrian. 2020. Stand age affects fungal community composition in a Central European temperate forest. *Fungal Ecology* 48:100985.

Oksanen, J., F. G. Blanchet, M. Friendly, R. Kindt, P. Legendre, D. McGlinn, P. R. Minchin, R. B. O'Hara, G. L. Simpson, P. Solymos, M. H. H. Stevens, E. Szoecs, and H. Wagner. 2019. vegan: community ecology package. R package version 2.5-6.

Pachauri, R. K., M. R. Allen, V. R. Barros, J. Broome, W. Cramer, R. Christ, J. A. Church, L. Clarke, Q. Dahe, and P. Dasgupta. 2014. Climate change 2014: synthesis report. Contribution of Working Groups I, II and III to the fifth assessment report of the Intergovernmental Panel on Climate Change. *IPCC*.

Paradis, E., and K. Schliep. 2019. ape 5.0: an environment for modern phylogenetics and evolutionary analyses in R. *Bioinformatics* 35:526-528.

Peri, P. L., V. Gargaglione, and G. M. Pastur. 2006. Dynamics of above- and below-ground biomass and nutrient accumulation in an age sequence of Nothofagus antarctica forest of Southern Patagonia. *Forest Ecology and Management* 233:85-99.

R Core Team. 2020. R: A language and environment for statistical computing. The R Foundation. Version 4.0.2.

Rengel, Z. 2011. Soil pH, soil health and climate change. Pages 69-85. Soil health and climate change. Springer.

Richardson, A. D., C. B. Statland, and T. G. Gregoire. 2003. Root biomass distribution under three cover types in a patchy Pseudotsuga menziesii forest in western Canada. *Annals of Forest Science* 60:469-474.

Richter-Heitmann, T., B. Hofner, F.-S. Krah, J. Sikorski, P. K. Wüst, B. Bunk, S. Huang, K. M. Regan, D. Berner, and R. S. Boeddinghaus. 2020. Stochastic dispersal rather than deterministic selection explains the spatio-temporal distribution of soil bacteria in a temperate grassland. *Frontiers in Microbiology* 11:1391.

R Studio Team. 2020. RStudio: Integrated Development for R. Version 1.3.1056.

Salley, S. W., J. E. Herrick, C. V. Holmes, J. W. Karl, M. R. Levi, S. E. McCord, C. van der Waal, and J. W. Van Zee. 2018. A Comparison of soil texture-by-feel estimates: implications for the citizen soil scientist. *Soil Science Society of America Journal* 82:1526-1537.

Schliep, K. P. 2011. phangorn: phylogenetic analysis in R. Bioinformatics 27:592-593.

Solly, E. F., I. Brunner, H.-S. Helmisaari, C. Herzog, J. Leppälammi-Kujansuu, I. Schöning, M. Schrumpf, F. H. Schweingruber, S. E. Trumbore, and F. Hagedorn. 2018. Unravelling the age of fine roots of temperate and boreal forests. *Nature Communications* 9:1-8.

Stegen, J. C., X. Lin, J. K. Fredrickson, X. Chen, D. W. Kennedy, C. J. Murray, M. L. Rockhold, and A. Konopka. 2013. Quantifying community assembly processes and identifying features that impose them. *The ISME Journal* 7:2069-2079.

Stegen, J. C., X. Lin, J. K. Fredrickson, and A. E. Konopka. 2015. Estimating and mapping ecological processes influencing microbial community assembly. *Frontiers in Microbiology* 6:370.

Stegen, J. C., X. Lin, A. E. Konopka, and J. K. Fredrickson. 2012. Stochastic and deterministic assembly processes in subsurface microbial communities. *The ISME Journal* 6:1653-1664.

Steinberg, P.D. (2002). *Pseudotsuga menziesii* var. *glauca*. In: Fire Effects Information System, [Online]. U.S. Department of Agriculture, Forest Service, Rocky Mountain Research Station, Fire Sciences Laboratory (Producer). Available: https://www.fs.fed.us /database/feis/plants/tree/psemeng/all.html.

Swaty, R. L., R. J. Deckert, T. G. Whitham, and C. A. Gehring. 2004. Ectomycorrhizal abundance and community composition shifts with drought: predictions from tree rings. *Ecology* 85:1072-1084.

Tang, J., S. Luyssaert, A. D. Richardson, W. Kutsch, and I. A. Janssens. 2014. Steeper declines in forest photosynthesis than respiration explain age-driven decreases in forest growth. *Proceedings of the National Academy of Sciences* 111:8856-8860.

Tedersoo, L., M. Bahram, S. Põlme, U. Kõljalg, N. S. Yorou, R. Wijesundera, L. V. Ruiz, A. M. Vasco-Palacios, P. Q. Thu, and A. Suija. 2014. Global diversity and geography of soil fungi. *Science* 346.

Teste, F. P., S. W. Simard, and D. M. Durall. 2009. Role of mycorrhizal networks and tree proximity in ectomycorrhizal colonization of planted seedlings. *Fungal Ecology* 2:21-30.

Tilman, D. 1982. Resource competition and community structure. Princeton University Press, Princeton, New Jersey.

Trappe, J. M. 1977. Selection of fungi for ectomycorrhizal inoculation in nurseries. *Annual Review of Phytopathology* 15:203-222.

Tucker, C. M., and T. Fukami. 2014. Environmental variability counteracts priority effects to facilitate species coexistence: evidence from nectar microbes. *Proceedings of the Royal Society B*: Biological Sciences 281:20132637.

Twieg, B. D., D. M. Durall, and S. W. Simard. 2007. Ectomycorrhizal fungal succession in mixed temperate forests. *New Phytologist* 176:437-447.

Větrovský, T., P. Kohout, M. Kopecký, A. Machac, M. Man, B. D. Bahnmann, V. Brabcová, J. Choi, L. Meszárošová, and Z. R. Human. 2019. A meta-analysis of global fungal distribution reveals climate-driven patterns. *Nature Communications* 10:1-9.

Wang, P., S. P. Li, X. Yang, J. Zhou, W. Shu, and L. Jiang. 2020. Mechanisms of soil bacterial and fungal community assembly differ among and within islands. *Environmental Microbiology* 22:1559-1571.

Wei, T., and V. Simko. 2017. R package "corrplot": Visualization of a Correlation Matrix. R package version 0.84.

Werner, G. D., and E. T. Kiers. 2015. Partner selection in the mycorrhizal mutualism. *New Phytologist* 205:1437-1442.

White, T. J., T. Bruns, S. Lee, and J. Taylor. 1990. Amplification and direct sequencing of fungal ribosomal RNA genes for phylogenetics. *PCR protocols: a guide to methods and applications* 18:315-322.

Wickham, H. 2016. ggplot2: elegant graphics for data analysis. Springer.

Williams, A. P., C. Xu, and N. G. McDowell. 2011. Who is the new sheriff in town regulating boreal forest growth? *Environmental Research Letters* 6:041004.

Wright, E. S. 2016. Using DECIPHER v2. 0 to analyze big biological sequence data in R. *R Journal* 8.

Wubet, T., S. Christ, I. Schöning, S. Boch, M. Gawlich, B. Schnabel, M. Fischer, and F. Buscot. 2012. Differences in soil fungal communities between European beech (*Fagus sylvatica L.*) dominated forests are related to soil and understory vegetation. *PLoS One* 7:e47500.

Zhang, T., N.-F. Wang, H.-Y. Liu, Y.-Q. Zhang, and L.-Y. Yu. 2016. Soil pH is a key determinant of soil fungal community composition in the Ny-Ålesund Region, Svalbard (High Arctic). *Frontiers in Microbiology* 7:227.

5.7 TABLES

Table 5.1 Summary characteristics of the four sites sampled for *Pseudotsuga menziesii* var. *glauca* fungal communities in western North America. The sites are John Prince Research Forest (British Columbia, Canada), Kamloops (British Columbia, Canada), Wellsville Mountains National Wilderness (Utah, USA), and Cedar Breaks National Monument (Utah, USA). Mean values are provided with ± a standard deviation in parentheses. Mean annual precipitation and mean temperature were taken from nearby climate station data over the available data record (Environment and Climate Change Canada 2017; Natural Resources Conservation Service 2020).

Site	Age	DBH (cm)	Elevation (m)	Soil pH	Mean precipitation (mm)	Mean temperature (C°)
John Prince	126	41.6	864	5.0	458	3.1
	(12)	(16.6)	(15)	(0.4)	(100)	(10.4)
Kamloops	104	41.2	1095	5.7	268	8.8
	(35)	(27.6)	(56)	(0.2)	(82)	(9.1)
Wellsville Mountains	338	56.9	2593	7.2	1448	5.6
	(214)	(18.9)	(36)	(0.3)	(103)	(9.5)
Cedar Breaks	169	48.9	3084	7.3	768	3.9
	(75)	(34.2)	(27)	(0.3)	(119)	(7.7)

5.8 FIGURES

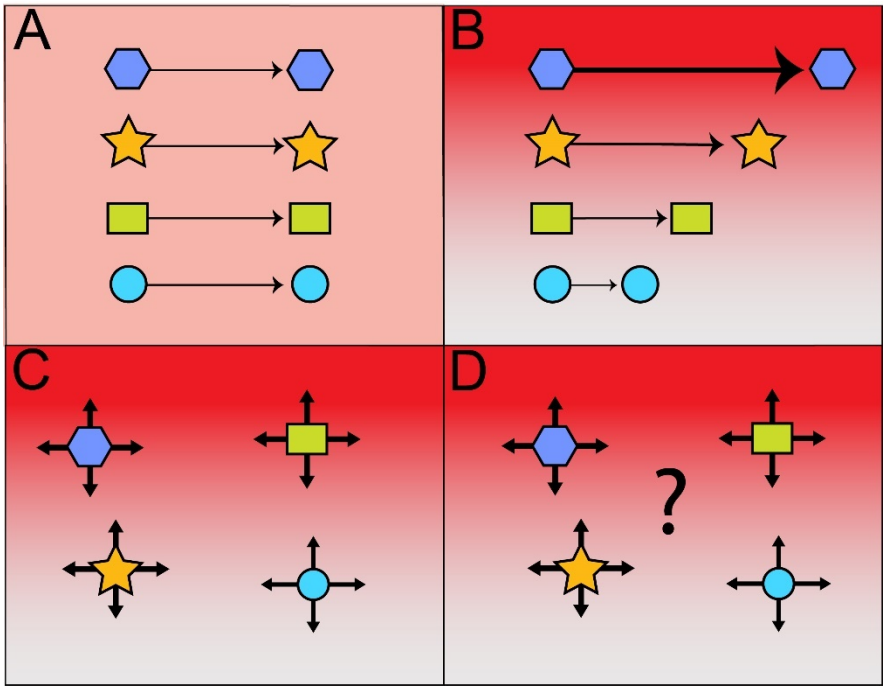

Figure 5.1 A conceptual diagram of how fungal community composition may change under different scenarios of community assembly and with climate change. Symbols represent fungal communities in a multi-dimensional ordination of community similarity. Increasing distance between points represents increasingly dissimilar community composition. Arrows represent change with time. (**A**) Communities are consistently influenced by deterministic processes controlled by local environmental filters. Climate change is equal across space and results in directional, equivalent changes in composition across fungal communities. (**B**) Communities are consistently influenced by deterministic processes controlled by local environmental filters. Climate change is unequal across space and results in directional, uneven changes in composition across fungal communities. (**C**) Communities are influenced by stochastic processes and thus may fluctuate in composition independent of climate change. (**D**) Unequal changes in climate

alter community assembly processes in the proportion of assembly processes and cause unpredictable changes in fungal community composition.

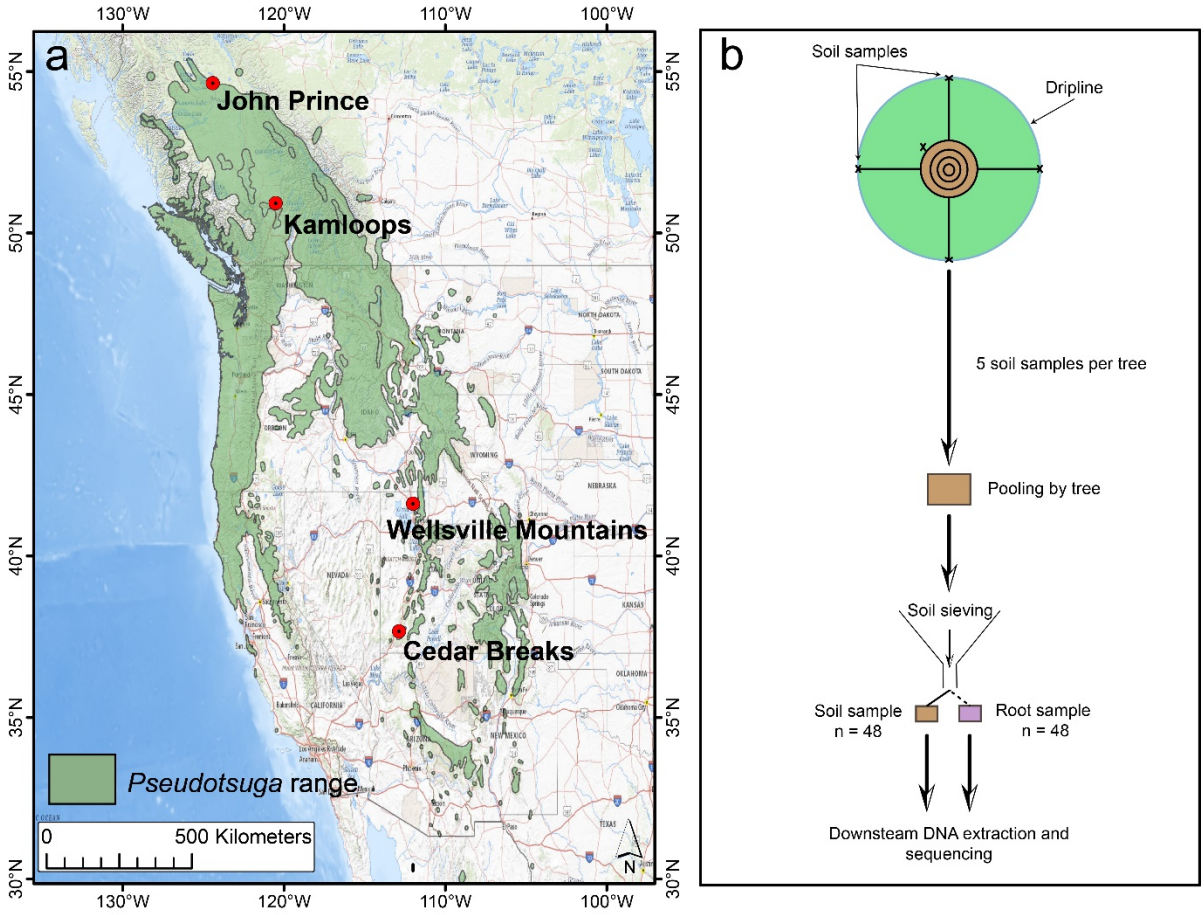

Figure 5.2 The location of sites (a) and a schematic of the methods (b) used to sample roots and soil for fungal communities associated with *Pseudotsuga menziesii* var. *glauca* at John Prince Research Forest (British Columbia, Canada), Kamloops (British Columbia, Canada), Wellsville Mountains National Wilderness (Utah, USA), and Cedar Breaks National Monument (Utah, USA). (**b**) A schematic of the method used when sampling roots and soils around *Pseudotsuga.* At each of the four sites a total of 12 trees were selected for sampling. Soils were sampled at four points at the dripline of each tree and once next to the bole. Samples were pooled by tree prior to sieving. Roots were removed from the soil and separated for separate processing.

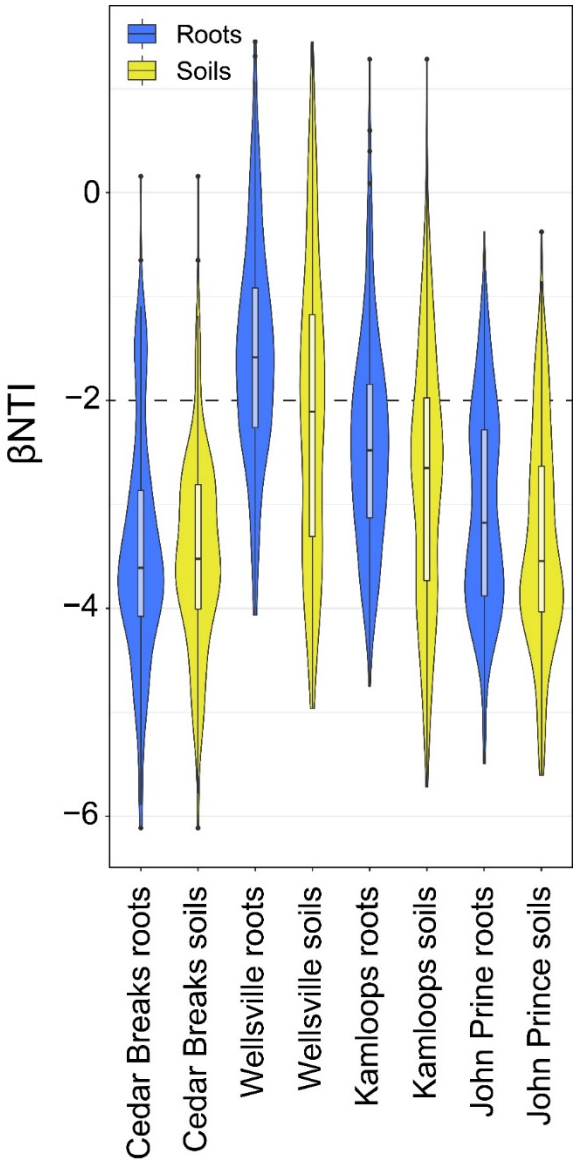

Figure 5.3 he distribution of beta nearest taxonomic index (βNTI) values for fungal communities on roots and soils collected around *Pseudotsuga menziesii* var. *glauca* at John Prince Research Forest (British Columbia, Canada), Kamloops (British Columbia, Canada), Wellsville Mountains National Wilderness (Utah, USA), and Cedar Breaks National Monument (Utah, USA). βNTI values < -2.0 indicate homogenous selection process and phylogenetic turnover less than expected under a null model.

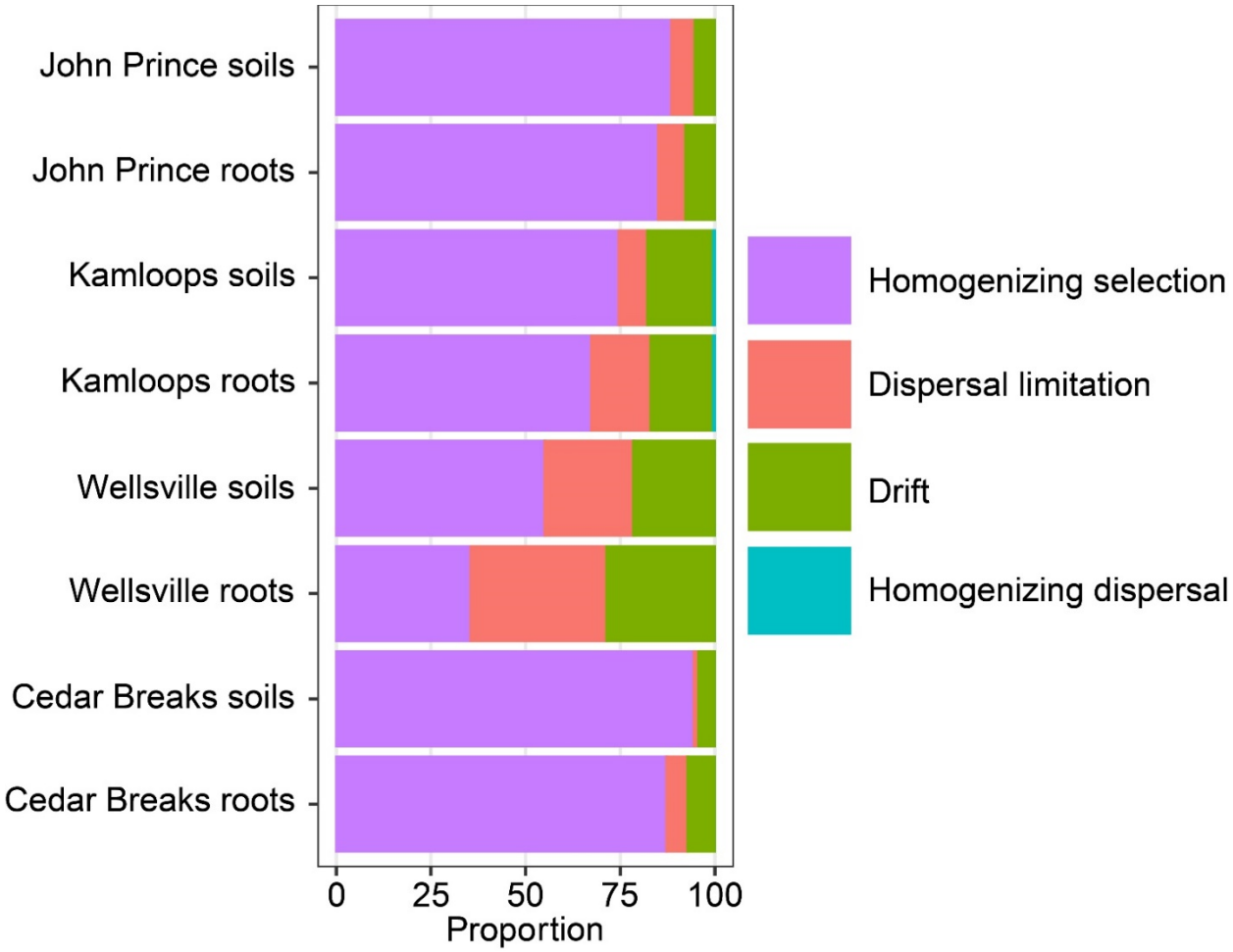

Figure 5.4 The proportion of each assembly process for fungal communities on roots and soils around *Pseudotsuga menziesii* var. *glauca* at John Prince Research Forest (British Columbia, Canada), Kamloops (British Columbia, Canada), Wellsville Mountains National Wilderness (Utah, USA), and Cedar Breaks National Monument (Utah, USA).

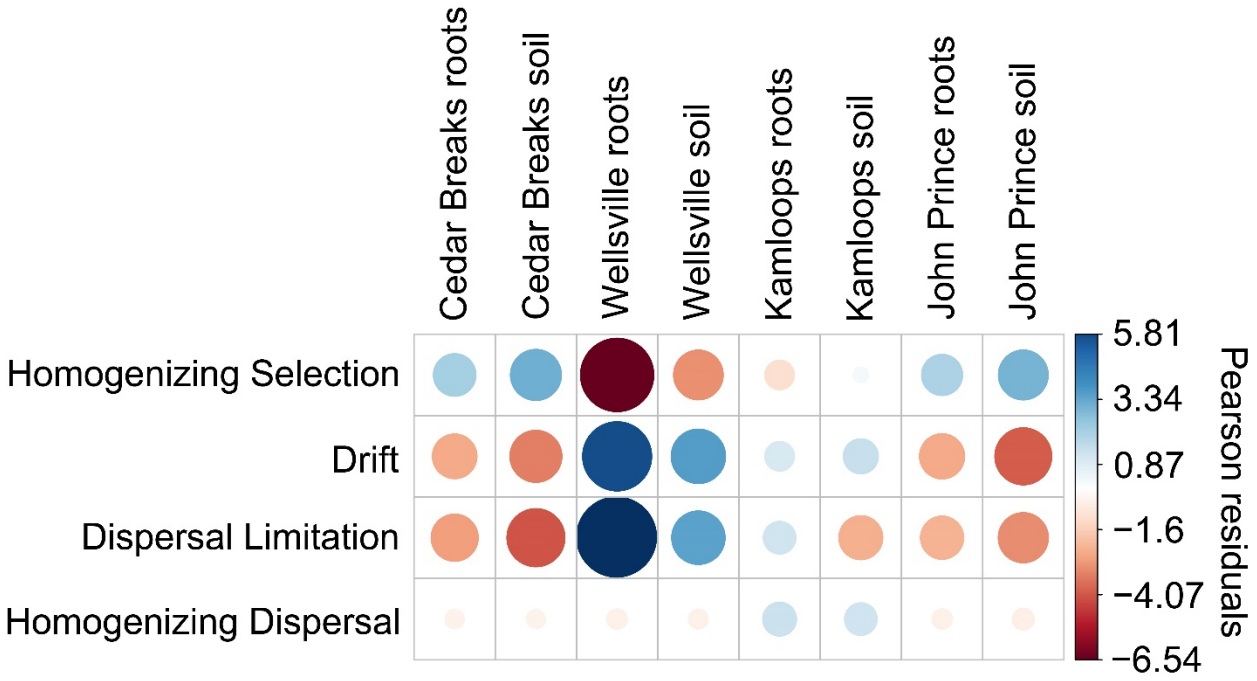

Figure 5.5 The Pearson residuals from a Chi-square analysis testing if the proportion of assembly processes for fungal communities differs between roots and soils collected around *Pseudotsuga menziesii* var. *glauca* at John Prince Research Forest (British Columbia, Canada), Kamloops (British Columbia, Canada), Wellsville Mountains National Wilderness (Utah, USA), and Cedar Breaks National Monument (Utah, USA). The size of the circles indicates the proportion of variation explained while the darkness of the color indicates if the assembly process was positively (blue) or negatively (red) associated with the habitat-type.

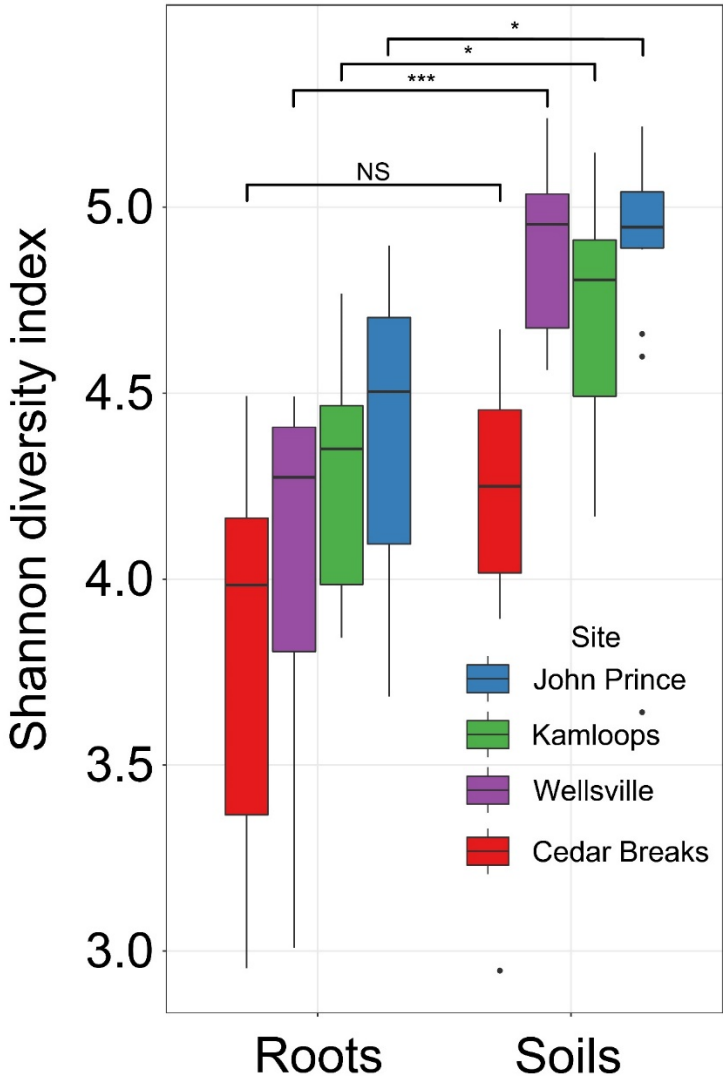

Figure 5.6 The distribution of Shannon's alpha diversity values (y-axis) for fungal ASVs on roots and in soil (x-axis) surrounding *Pseudotsuga menziesii* var. *glauca* at John Prince Research Forest (British Columbia, Canada), Kamloops (British Columbia, Canada), Wellsville Mountains National Wilderness (Utah, USA), and Cedar Breaks National Monument (Utah, USA). Brackets and asterisks indicate significant differences between groups where 'NS' indicates non-significant differences, '*' is $p < 0.05$, '**' is $p < 0.01$, and '***' is $p < 0.001$.

Chapter 6: Shared fungal communities in ancient *Pinus flexilis* and *Pinus longaeva*

6.1 ABSTRACT

The long-lived five-needle pines, *Pinus flexilis* (Limber pine) and *Pinus longaeva* (Great Basin bristlecone pine) can co-occur across their ranges and may form symbiotic partnerships with the same mycorrhizal fungi. The presence of shared symbiotic relationships may mediate belowground facilitation between the two pines and help promote the persistence of these species on the landscape. Through time *P. flexilis* and *P. longaeva* may also assemble unique belowground fungal communities owing to fungal succession and changes in the amount of tree-derived carbon provided to fungi. I used MiSeq sequencing of fungal rDNA to compare fungal community similarity for *P. flexilis* and *P. longaeva* roots and soils in an old-growth forest at the Utah Forest Dynamics Plot, Utah, USA. I cored trees to measure age and analyze how fungal communities change with advanced tree age. I found 720 amplicon sequence variants (ASV) associating with *P. flexilis* roots, 736 with *P. longaeva* roots, and 199 that were shared between the two pines. Root-associated fungal communities were significantly different between *P. flexilis* and *P. longaeva* while soil-communities were similar. Despite the differences between the communities, the most abundant ectomycorrhizal fungi, based on number of sequences, were shared between the two pines. The soil and root-associated fungal community of *P. flexilis* increased in dissimilarity with tree age while fungal alpha diversity was constant. The overlap in common taxa of ectomycorrhizal fungi indicates the potential for belowground interactions between *P. flexilis* and *P. longaeva*. The influence of tree age on fungal community composition indicates that age heterogeneity within old-growth stands may promote fungal diversity.

6.2 INTRODUCTION

Climate change has been linked to a widespread increase in tree mortality across western North America in part due to increased drought and the range expansion of bark beetles (Williams and Liebhold 2002, McDowell et al. 2020). Tree ranges are projected to shift northward or upward in elevation in response to continued climate change (McKenney et al. 2007, Mathys et al. 2017). Under these conditions slow-growing, cold-adapted species in high elevation forests may be particularly sensitive to a warming climate (Serra-Diaz et al. 2015, Trant et al. 2020). Factors that ameliorate stress or facilitate establishment of new individuals may mitigate the stress from a changing climate.

Ectomycorrhizal fungi (EMF) colonize fine tree roots and engage in a symbiotic partnership where tree-derived sugars are exchanged for fungi-sourced nutrients. Partnerships with EMF can benefit trees by improving growth and survival (Smith and Read 2010). Mature trees can act as important sources of EMF inoculum for seedlings by hosting established EMF that can inoculate surrounding trees. For example, *Pseudotsuga menziesii* (Douglas fir) seedlings that established close to mature trees had higher EMF diversity and more similar community composition to the mature tree than did seedlings establishing farther away (Cline et al. 2005, Teste et al. 2009a). Fungal colonization from established EMF communities can have additional benefits for seedlings through the formation of ectomycorrhizal networks (EMN). An EMN can transport nutrients such as carbon, water, or nitrogen between trees along a concentration gradient from ‘source’ to ‘sink’ trees (Egerton-Warburton et al. 2007, Teste et al. 2009b, Philip et al. 2010). The EMN-derived resources can improve seedling drought resistance and survival (Teste and Simard 2008, Booth and Hoeksema 2010). Mature trees can also receive resources

through the EMN, which may be associated with increased growth (Klein et al. 2016). Trees that partner with EMF may facilitate the growth of other EM trees (Bennett et al. 2017, Liang et al. 2020), particularly if they are closely related (Segnitz et al. 2020). These widespread patterns highlight the potential importance of shared EMF communities as mediators of facilitation between conspecific and related, but heterospecific trees (van der Heijden and Horton 2009).

In western North America, the pine species *Pinus flexilis* (limber pine) and *Pinus longaeva* (Great Basin bristlecone pine) are charismatic specialists of montane and sub-alpine ecosystems and can form partnerships with EMF. Both pines can establish on calcareous, exposed sites where other tree species cannot long endure (Tomback and Achuff 2010). Once established these pines can persist for well beyond a millennium, acting as foundation species and providing a variety of irreplaceable ecosystem services by providing habitat, forage, and reducing erosion (Brown 1996, Schoettle 2004, Tomback and Achuff 2010, Tomback et al. 2011). Both pines belong to the "white pine" grouping within *Pinus* but *P. flexilis* is within the *Strobus* section while *P. longaeva* falls within *Parrya* and likely evolved several million years before *P. flexilis* (Schwandt et al. 2010, Eckert and Hall 2006).

In recent decades populations of *P. flexilis* and *P. longaeva* have been threatened by climate change, bark beetle-outbreaks, and the spread of an invasive pathogen, *Cronartium ribicola* (white pine blister rust) (Kinloch Jr. 2003, Schoettle 2004, McKenney et al. 2007, Bockino and Tinker 2012). Changing climate will likely increase the frequency and severity of drought and may prompt range shifts (McKenney et al. 2007). In recent decades both *P. flexilis* and *P. longaeva* have shifted upward in elevation, with *P. flexilis* showing rapid and widespread establishment above previous treeline (Smithers et al. 2018). The danger to *P. flexilis* and *P.*

longaeva is further exacerbated by the range expansion of bark beetles due to climate change (Bentz et al. 2010). *Dendroctonus ponderosae* (mountain pine beetle) has caused widespread mortality among the preferred host, *P. flexilis*, but does not appear to pose as great a threat to *P. longaeva* (Gibson et al. 2008, Gray et al. 2015). Susceptibility to *C. ribicola* varies among the five-needled pines but is frequently lethal to both seedlings and mature trees (Hoff et al. 1980). Fortunately, *P. longaeva* has not had any recorded cases of natural infestation of *C. ribicola* and is likely resistant to infection (Schwandt et al. 2010). In *P. flexilis*, the infestation and spread of *C. ribicola* presents a threat to populations of *P. flexilis* across much of its range (Schwandt et al. 2010). These ongoing disturbances present a persistent and growing threat to the stability of *P. flexilis* and *P. longaeva* stands.

In stands where *P. flexilis* and *P. longaeva* co-occur there is a potential for interspecific belowground interactions mediated by shared fungal communities. Interactions through shared fungal communities may occur along several pathways; 1) mature trees acting as a sources of fungal inoculum that can associate with nearby seedlings; 2) for trees to form an EMN that transports nutrients between trees of any age, and 3) for pathogenic fungi to spread from one host to another. For these interactions to occur there would need to be a substantial overlap in fungal taxa interacting with both *P. flexilis* and *P. longaeva*. The similarity of fungal communities could vary with tree age which could produce pronounced differences between young and older communities given that *P. flexilis* and *P. longaeva* are capable of extraordinary longevity. For example, Glassman et al. (2017a) found that 65-year old alpine tree islands with the closely related *Pinus albicaulis* had a predominantly early seral fungal community despite the presence of mature trees. Neighboring *P. flexilis* and *P. longaeva* can differ by thousands of years in age,

which could enable the existence of neighboring belowground symbiotic communities spanning early to late seral stages.

Previous studies of *P. flexilis* and *P. albicaulis* have used sporocarp surveys to identify associated fungal taxa and identified shared EMF taxa between the two tree species (Cripps and Antibus 2011). Research at the White Mountains of California focusing on *P. longaeva* (Bidartondo et al. 2001) as well as *P. flexilis* (Shemesh et al. 2020) identified a variety of fungal taxa that associate with these trees. However, the studies at the White Mountains used Sanger sequencing which identifies individual fungal taxa and does not have the capacity to fully identify the fungal communities within the soil and around roots. Additionally, these studies focused on sites where the calcareous soil and harsh climate could strongly influence fungal communities in ways that may not be representative of more productive sites. By using MiSeq sequencing of soil and root communities around *P. flexilis* and *P. longaeva* at a closed-canopy, old growth forest in southern Utah, I sought to capture a larger portion of the fungal communities associating with these pines at a site that is productive and diverse relative to sites in previous studies.

As a first step in better understanding the belowground fungal ecology of *P. flexilis* and *P. longaeva* I sought to characterize 1) the fungal communities associating with each pine's roots and soils, 2) identify the extent of shared fungal communities, 3) identify if fungal community composition and richness varied with the age of the associated tree due to the accumulation of fungal taxa, 4) identify any overlap between the fungal sequences in the White Mountains and those from high-elevation, southern Utah.

6.3 METHODS

6.3.1 Site description

The study was in a high-elevation, sub-alpine forest within the Utah Forest Dynamics Plot (UFDP) at Cedar Breaks National Monument, Utah, USA (37.66° N, 112.85°). The UFDP covers 13.64 ha and encompasses 27,845 identified mapped and measured tree stems >1 cm diameter according to the protocols of the Smithsonian ForestGEO network (Anderson-Teixeira et al. 2015, Lutz 2015). Mean elevation is 3087 ± 8.0 (SD) meters with a mean temperature of 3.9 ± 7.7 C^{o} and a mean annual precipitation (winter-dominated) of 768 ± 119 mm. Soil textures within the sampling area are largely categorized as clay to clay loams.

The forest at the UFDP is primarily composed of *Abies bifolia* A. Murray bis (Rocky Mountain subalpine fir), *Populus tremuloides* Michaux (quaking aspen), *Picea pungens* Engelmann (Colorado blue spruce), *Picea engelmannii* var. engelmannii Parry ex Engelmann (Engelmann spruce), *Pinus longaeva* D. K. Bailey (Great Basin bristlecone pine), *Pinus flexilis* E. James (limber pine), with low abundances of *Pseudotsuga menziesii* var. *glauca* (Mayr) Franco (interior Douglas-fir), *Pinus ponderosa* Douglas ex Lawson & C. Lawson (ponderosa pine), *Pinus edulis* Engelmann (pinyon pine), *Abies concolor* (Gordon & Glendinning) Hildebrand (white fir), and *Juniperus scopulorum* Sargent (Rocky Mountain juniper) (Flora of North America Editorial Committee 1993+, Furniss et al. 2017). The UFDP has several hundred *P. longaeva* and *P. flexilis* trees that co-exist in proximity to one another on scales of one to several hundred meters within the same stand (Furniss et al. 2017). The forest has multiple cohorts originating from natural regeneration following patchy high severity fire with the most-

recent fire likely occurring in 1802. The trees sampled within this study had no signs of having been attacked by bark beetles or infected with *C. ribicola*.

6.3.2 Belowground sampling

To determine the fungal associates within the rhizosphere and surrounding soils, I took paired root and soil samples around *P. longaeva* and *P. flexilis*. Permitting restrictions aimed at protecting these charismatic ancient trees limited the number of root samples to 12 *P. longaeva* and 12 *P. flexilis.* I sampled soil and roots over two days in the first week of July 2018. A total of 72 fine root samples, 3 per tree, were taken from both *P. longaeva* and *P. flexilis*. Fine root sampling consisted of tracing roots of *P. longaeva* or *P. flexilis* from the bole to a cluster of fine roots (< 2.0 mm in diameter). I took paired soil samples of approximately 6 cm^3 within 10 cm of each root with a soil knife (Zenport, Sherwood, Oregon) to a depth of 25 cm. I immersed the soil knife in a sanitizing 10% bleach solution between each sample to prevent contamination between samples. Samples were pooled by tree and frozen at -20 C^o for storage prior to processing. I did not measure the distance from the tree where roots were taken, however; the samples were always within 0.5 m of the bole. I sampled exclusively around trees with >10 cm DBH to avoid causing seedling or sapling mortality from root tracing. The sampled trees were chosen to be at least 5.0 m apart from the nearest heterospecific pine bole to avoid autocorrelation of communities and were separated by at most 300 m from the most distant sampled tree (Appendix 6.1 Fig. S6.1).

6.3.3 Identification of tree age

To identify the age of trees within the UFDP I sampled two tree-cores per tree to measure annual growth rings. In July 2018, I collected increment cores with a 4.3 mm increment borer

(Haglöf Sweden; Mora, Sweden) as close to the root collar as possible. I sanded increment cores with progressively finer sandpaper up to 6-micron grit. I visually cross-dated the growth rings prior to measuring using a Velmex measuring system (Velmex Inc; Bloomfield, NY) to a 0.001 mm resolution. I crossdated the cores with the COFECHA program (Holmes 1983) and dplR 1.7.0 (Bunn et al. 2019). I did not estimate the age for trees with partial or rotten cores.

6.3.4 Sample processing

To prepare soil and root samples for DNA extraction, I thawed the samples at room temperature and sieved them through progressively finer sieves up to a final sieve size of 2 mm. I bleached and air-dried sieves between each sample to prevent cross-contamination between samples. I used sterilized forceps to remove fine roots from the soil. Sieved soils and roots were re-frozen at -20 C^o prior to freeze-drying. Root and soil samples were freeze-dried until samples had reached a stable weight. I pulverized freeze-dried samples to a fine powder using the Tissuelyser 2 (Qiagen; Hilden, Germany) prior to DNA extraction. I used MoBio DNeasy PowerSoil Kits (Qiagen; Hilden, Germany) to extract DNA from roots and soils following the manufacturer's instructions. After extraction of fungal DNA, we iteratively amplified and visualized the DNA using gel-electrophoresis and found that a successful amplification of samples occurred only after using a combination of ethanol precipitation (Appendix 6.1), One-Step PCR Inhibitor Removal Kits (Zymo Research; Irvine, CA) and Bovine Serum Albumin (Fisher Scientific; Waltham, MA) to remove likely polymerase chain reaction (PCR) inhibitors.

6.3.5 Fungal community sequencing

To identify the fungal communities on roots and soil I used MiSeq sequencing targeting the ITS2 region of fungal rDNA extracted from soil and roots. I targeted the ITS2 region with the

fITS7 (Ihrmark et al. 2012) and ITS4 (White et al. 1990) primers. I amplified extracted rDNA through a two-step PCR. I ran the first PCR using 25 µL sample volumes with 2.5 µL DNA template, 7.875 µL water, 12.5 µL Platinum SuperFi PCR MasterMix (Thermo Fisher Scientific, Waltham, MA, USA), 0.125 µL Bovine Serum Albumin, and 1 µL of each of the forward and reverse primers (95Cº for 3 min; 95Cº for 30 secs, 50Cº for 1 min, 72Cº for 30 secs, 35 cycles; and 72Cº for 10 min). I used Illumina Nextera Index primers (Illumina Inc., San Diego, CA, USA) with N7 (N5) for the forward (reverse) reads for the second PCR. For the second PCR, 25 µL volume was used with 5 µL of water, 12.5 µL of Platinum SuperFi PCR MasterMix, 2.5 µL N7xx primers, 2.5 µL N5xx primers, and 2.5 DNA (95Cº for 3 min; 95Cº for 30 secs, 55 Cº 30 secs, 72Cº for 30 secs, 72Cº for 5 mins, for 8 cycles).I pooled samples following the second PCR and used Sera-Mag Select beads (GE Healthcare, Chigaco, IL, USA) and two 80% ethanol washes clean the samples. ITS2 amplicons were quantified using a dsDNA HS Assay kit on a Qubit fluorometer (Thermo Fisher Scientific, Waltham, MA, USA) and pooled into equimolar concentrations. Sequencing was conducted at the University of Alberta Molecular Biological Sciences Unit, with an Illumina MiSeq sequencing platform (Illumina Inc., San Diego, CA, USA). My final sample count was 34 due to the loss of low-quality samples.

6.3.6 Bioinformatics

I denoised and quality filtered the demultiplexed sequences in the R package dada2 1.12.1 (Callahan et al. 2016) to create amplicon sequence variants (ASV). Mean amplicon size was 309 ± 38 (SD) base pairs and ranged from 127 – 500 base pairs. The use of ASVs can resolve single nucleotide differences between sequences which can result in multiple unique ASVs being identified to the same taxonomic classification (Callahan et al. 2017) and can overestimate fungal diversity by 30% (Glassman and Martiny 2018). The use of cluster-free

ASVs is a departure from the previously common operational taxonomic units (OTU), which were often clustered together based on a 97% similarity threshold and assigned a taxonomic identity. However, the use of ASVs allows for easy comparisons across studies and can provide information on variation among sequences assigned the same taxonomic identity (Edgar 2018). I filtered sequences to remove those with ambiguous bases and limited the maximum number of expected errors to two per sequence. Following identification and removal of chimeric sequences (Appendix 6.1 Table S6.1), I assigned taxonomy from the UNITE database (Nilsson et al. 2019) with the IDTAXA function in the DECIPHER 2.12.0 package (Wright 2016). The IDTAXA function uses a two-phase process to assign taxonomy to ASVs by learning from a training set and then classifying sequences against a reference database. The IDTAXA compares favorably against other common classification tools and has lower over-classification errors than similar methods (Murali et al. 2018).

After assigning taxonomy, I analyzed and visualized the results using the phyloseq 1.28.0, vegan 2.5-6, and the ggplot2 3.2.1 packages (McMurdie and Holmes 2013; Oksanen et al. 2019; Wickham 2016) within the R Studio 1.3.1056 interface for R 3.6.1 (R Core Team 2019; R Studo Team 2020). I visualized reads with a rank-abundance curve and visually assessed read equality across samples (Appendix 6.1 Fig. S6.2). I rarefied samples to 90% of the minimum read count (13,286 reads) to compensate for uneven sequence depth (Appendix 6.1 Fig. S6.3). Based on the strong linear relationship between ASV frequency and read-abundance ($p < 2.2e\text{-}16$; $R^2 = 0.56$), I used a Bray-Curtis dissimilarity matrix to analyze communities based on read abundance rather than the more conservative Jaccard dissimilarity matrix, which uses presence/absence to assess dissimilarity between communities (Appendix 6.1 Fig. S6.4).

6.3.7 Data analysis

To compare communities between sample types (i.e. roots vs. soils by pine species) I used a permutational analysis of variance (PERMANOVA) with 999 permutations using the 'adonis' function in vegan 2.5-6 (Oksanen et al. 2019). I used a pairwise PERMANOVA with a false-discovery rate p-adjustment (Benjamini and Hochberg 1995), from the RVAideMemoire 0.9-75 package (Hervé, 2020) for pairwise comparisons between sample types. To ordinate the fungal communities, I used a Bray-Curtis dissimilarity matrix and the 'metaMDS' function (Oksanen et al. 2019) to calculate 500 permutations and select the lowest stress ordination for visualization. To test if community variation was different between roots and soils, I used the 'betadisper' function in vegan 2.5-6 to calculate the multivariate dispersion of root and soil communities and used an ANOVA to test for significant differences between the groups (Oksanen et al. 2019). To test if soil nutrients differed between *P. flexilis* and *P. longaeva* I used the vegan 2.5-6 (Oksanen et al. 2019) to run a PERMANOVA and NMDS of interpolated soil nutrient values for each sampled tree (see Appendix 6.1 for methods on nutrient sampling and interpolation).

To test if community composition or richness varied with tree age, I used a combination of PERMANOVA tests and linear regressions with tree age as the independent variable. Several issues prevented me from investigating the influence of tree age on the fungal communities of *P. longaeva*. The *P. longaeva* that I sampled were unevenly distributed across a wide age gradient which lacked adequate sample depth at 'young' (< 200 years) and 'middle' ages (300–800 years) (Appendix 6.1 Fig. S6.5). Additionally, unidentified heartrot prevented the sampling of intact cores of several *P. longaeva* samples and resulted in a low (n = 6) number of dated *P. longaeva* root samples in comparison to the total number of *P. longaeva* root samples (n = 7) used to

calculate richness and fungal community composition by sample type (Appendix 6.1 Table S6.2).

I used separate PERMANOVA tests for the root-associated and soil-associated communities found around *P. flexilis* with tree age as the explanatory variable. To test if dissimilarity between root and soil samples increased with tree age, I calculated the pairwise dissimilarity between all combinations of *P. flexilis* root and soil fungal communities. The pairwise dissimilarity was used as the dependent variable in a linear regression with tree age as the dependent variable. I used a linear model to test if Shannon's alpha diversity index varied with tree age for root and soil-associated communities around *P. flexilis*.

To compare ASVs with archived fungal sequences detected around *P. longaeva* and *P. flexilis* I accessed sequences from GenBank (Sayers et al. 2020) for the Bidartondo et al. (2001) and Shemesh et al. (2020) studies. I used Geneious Prime 2020 1.2 to align the archived sequences against the ASVs and selected only those that overlapped with 100% identity over more than 126 bases (the length of the smallest sequence).

To assign functional guilds to ASVs I used the FUNGuild database (Nguyen et al., 2016). Functional guild classification is based on the taxonomic assignment of the sequence and many ASVs were classed as having an 'Unknown' guild. Additionally, many sequences were assigned to multiple potential guilds, and were classified as 'Mixed EM' if one of the potential guilds was ectomycorrhizal. Similarly, I classified sequences as 'Mixed Non-EM' if none of the potential guilds were ectomycorrhizal.

6.4 RESULTS

6.4.1 Comparison of fungal communities by sample types

Fungal communities differed significantly between the roots of *Pinus flexilis* and *Pinus longaeva*, between roots and soil, but not between the soils surrounding *P. flexilis* and *P. longaeva* (Table 6.1). I identified 720 ASVs from *P. flexilis* roots, 1262 from *P. flexilis* soil, with 285 ASVs in common. Similarly, 736 ASVs were associated with *P. longaeva* roots, 1465 with *P. longaeva* soil, with 338 ASVs in common. There were 199 ASVs shared between the roots of *P. flexilis* and *P. longaeva* while the soils shared 457 ASVs (Appendix 6.1 Table S6.3). There was substantial overlap between the sample types for core ASVs that had at least a 0.1% of total read abundance (Fig. 6.1). A total of 130 core ASVs, representing 51.1% of read abundance, were shared between *P. flexilis* and *P. longaeva* roots and the soil.

Fungal communities were more diverse in soil than on roots, and around *P. longaeva* than *P. flexilis* (Fig. 6.2). Root-associated communities had greater multivariate variance than did soil-associated communities (F_{33}=10.37, p = 0.002) (Appendix 6.2 Table S.4). Both pines had similar abundances of Ascomycota and Basidiomycota on their roots and in adjacent soils (Table 6.2). At the family level, the two pines showed substantial differences in fungal-community abundances. Notably, *P. flexilis* roots and soils had nearly twice as many *Tricholomataceae* than did *P. longaeva* roots and soils. Conversely, *P. longaeva* roots had twice as much *Atheliaceae* and nine times greater *Inocybaceae* than did *P. flexilis* roots. Despite notable differences in the sequence abundance, there was a substantial overlap between fungal community composition on roots and soils, and between *P. flexilis* and *P. longaeva* (Fig. 6.3).

6.4.2 Comparison with sequences from the White Mountains

I identified 10 ASVs from the UFDP that matched against 37 sequences from Shemesh et al. (2020) and two from Bidartondo et al. (2001). The shared sequences were primarily within *Geopora* (21) and *Rhizopogon* (16) genera. The White Mountain sequences had more detailed taxonomic resolution for 15 of the sequences and disagreed with the UFDP taxonomic assignments for four *Rhizopogon* spp. sequences. The matching sequences were largely infrequent at the UFDP with only three of the matching sequences falling within the 100 most abundant ASVs at the UFDP (ASV003, ASV0021, ASV0039). However, two of the most abundant ectomycorrhizal fungal species at the UFDP (*Wilcoxina spp*., ASV003; *Geopora spp*., ASV0021) matched against *Wilcoxina rehmii* (GenBank accession number: AF266708) and *Geopora tolucana* (GenBank accession number: MK842020.1).

6.4.3 Influence of tree age on *P. flexilis* associated fungi

Tree ages ranged from 100–370 years for *P. flexilis* (μ=204 ± 33 SD) and from 230–1340 for *P. longaeva* (μ=879 ± 152 SD). Tree diameter, and presumably the area occupied by tree root systems, showed a strong relationship with tree age (Fig. 6.4). A PERMANOVA indicated that the age of *P. flexilis* was significantly related to the composition of root-associated communities ($F_{(8)} = 1.59$; R^2=0.18; $p = 0.01$) while soil-associated communities showed marginal significance ($F_{(8)} = 1.36$; $R^2 = 0.16$, $p = 0.10$) (Appendix 6.1 Table S6.5). However, linear models did not find that fungal alpha diversity varied with the tree age for either *P. flexilis* roots ($p = 0.50$; $R^2 = -0.06$) or *P. flexilis* soil ($p = 0.42$; $R^2 = -0.03$) (Appendix 6.1 Table S6.6).

Fungal communities on *P. flexilis* roots were increasingly dissimilar with soils with difference in tree age ($Y = 0.0002x + 0.8622$; $F_{(87)} = 9.32$; $p < 0.01$; $R^2 = 0.08$). There was no

significant change in the proportional abundance of fungal guilds with tree age (Appendix 6.1 Fig. S6.6).

6.4.4 Functional guilds of fungal ASVs

Only 28.1% of all ASVs and 44 of the 100 most abundant ASVs, were assigned a functional guild by the FUNGuild database. Fungi capable of forming ectomycorrhizal partnerships accounted for 63.4% of categorized ASVs across all sample types. Saprotrophic fungi accounted for 12.3% of all categorized ASVs while plant pathogens accounted for only 0.4% (Appendix 6.1 Fig. S6.7). A majority of the 20 most read-abundant ASVs for *P. longaeva* roots (55%) and soil (70%) were not assigned a functional guild (Fig. 6.5). In contrast, 80% of the most abundant ASVs for *P. flexilis* roots were assigned functional guilds. The most abundant ASV overall was the probable ectomycorrhizae Tricholomataceae *Tricholoma* spp. (ASV002) which was the 2nd most abundant ASV for *P. flexilis* roots and *P. longaeva* roots and the 7th most abundant ASV in soil. The second most abundant ASV was the EMF Pyronemataceae *Wilcoxina* spp. (ASV001) which was abundant on *P. flexilis* roots (3rd), *P. longaeva* roots (6th), and in soil (3rd) (Table 6.3). The unknown Ascomycota Dothideomycetes (ASV004) was the 3rd most abundant taxa overall and ranked 17th on *P. flexilis* roots, 1st on *P. longaeva* roots, and 9th in soil. Of the 199 ASVs shared between the roots of *P. flexilis* and *P. longaeva*, only 63 ASVs were assigned a functional guild (Appendix 6.1 Table S6.7). Of these, 44% existed solely withing the 'Ectomycorrhizal' guild and with another 32% capable of forming ectomycorrhizal associations.

6.5 DISCUSSION

Given the semi-frequent co-occurrence of *P. longaeva* and *P. flexilis,* I hypothesized that they may have substantial overlap in fungal partners and that the extreme longevity of these

pines may influence fungal community composition. I found that 84% of the root-associated ASVs were specific to *P. flexilis* or *P. longaeva* while accounting for less than 50% of the read abundance. The differences in community composition may be due to the detection of rare ASVs Despite significant differences in community composition the most abundant fungal taxa were shared between both pine species and were often ectomycorrhizal. I found a change in fungal community composition with mature tree age that spanned 100–370 years. Despite a significant change in community composition, I did not observe increased fungal diversity with increasing tree age. This latter result indicates that fungal communities exhibit turnover of fungal ASVs with increasing tree age, even among a mature stand.

6.5.1 Fungal communities and influence of sample type

The difference in the fungal communities on *P. flexilis* and *P. longaeva* roots was likely driven by the presence of many low-abundance ASVs that were pine-species specific. The functional guild of 71.9% of ASVs is unknown. However, the most abundant ASVs across all sample types were largely EMF that were shared between the two pines. This indicates that *P. flexilis* and *P. longaeva* share numerous, abundant fungal symbionts. Many of the most abundant, shared ASVs were ectomycorrhizal taxa such as *Wilcoxina* spp., *Geopora* spp., and *Tricholoma* spp. (Table 6.3). The overlap in shared EMF species indicate that *P. flexilis* and *P. longaeva* could provide sources of beneficial fungal inoculum to nearby trees and form ectomycorrhizal fungal networks. The prevalence of known pathogens (0.4%) was far outweighed by symbiotic fungi (63.4%) that may promote interspecific facilitation between *P. flexilis* and *P. longaeva*. Chen et al. (2019) found that tree species with higher accumulation of pathogenic fungi had greater competition with adjacent conspecific trees, while higher accumulation of EMF was associated with weaker conspecific competition (Chen et al. 2019).

Cumulatively, the high proportion and abundance of EMF would suggest that the EMF at the UFDP play a facilitative role between conspecific trees and could enable heterospecific facilitation. However, these results must be taken with caution as a portion of the unidentified fungi could act as pathogenic fungi.

The comparison of the UFDP sequences with those taken from the White Mountains of California revealed relatively little overlap between the sites, likely due to differences in soil parent material and pH. Glassman et al. (2017b) found that soil characteristics were the primary drivers of fungal community assembly around another white pine, *P. albicaulis*. Only 0.3% of the UFDP sequences matched against those detected around *P. flexilis* or *P. longaeva* in previous studies. I found generally infrequent occurrence of *Rhizopogon* spp. at the UFDP in contrast with ubiquitous *Rhizopogon* spp. found around *P. flexilis* and *P. longaeva* by Shemesh et al. (2020). The genus *Geopora* was abundant across *P. longaeva* and *P. flexilis* within my study and at the White Mountains (Shemesh et al. 2020). The ubiquity of *Geopora* suggests that they are frequent fungal associates of *P. longaeva* and *P. flexilis* in the western USA. More studies are needed across the breadth of the ranges of *P. flexilis* and *P. longaeva* to understand how local environment and host identity interact to influence fungal communities.

6.5.2 Changing fungal communities with tree age

I detected fungal succession on root-associated communities but not soil communities, around mature trees. The increasingly dissimilarity between root and soil communities with tree age suggests a prolonged change in fungal community composition even in an old-growth forest. My study differs from many other fungal chronosequences in three ways, 1) I studied a single, mixed-cohort stand instead of multiple sites, 2) I tested communities of both root- and soil-

associated communities, and, 3) I studied an older age range that consisted of only mature trees. Previous research has found soil-associated fungal communities change with tree age over younger age gradients that span juvenile to mature trees (12–158 years, Hagenbo et al. 2018; 7–87 years, Rudawska et al. 2018; 1–158 years, Kyaschenko et al. 2017). Similarly, root-associated fungal communities also change with tree age (12–50 years, Kolaříková et al. 2017). In contrast, I studied only mature trees (100–370 years) within a single site and did not detect a significant change in soil community composition. However, the soil communities showed marginal significance ($p=0.09$; Appendix 6.1 Table 6.6) and the inclusion of younger trees (<100 years old) and a larger sample size may have clarified an age-related trend like those seen in other studies. The functional implications of a changing fungal community are difficult to isolate in the study. I might expect the function of fungal communities to change with an altered proportion of certain guilds or changes in the exploration type of EMF. In both cases the unresolved taxonomy prevents us from identifying the full communities and implications of fungal succession on the system.

6.5.3 Mechanisms of fungal community change with tree age

Fungal species turnover with tree age could be a result of priority effects and bi-directional selection pressures from fungi and their tree-hosts. Priority effects may initially favor ubiquitous fungi within the soil that can quickly colonize a root tip and prevent other EMF from colonizing (Kennedy et al. 2009). If priority effects were the primary influence on root fungal community composition, I would expect that the most abundant root-associated taxa to have similar abundances in the soil. However, many of the most abundant root-associated fungi were much less frequent in the soil, potentially indicating partner-selection (Table 6.3). Differences in EMF exploration type could also conceivably influence the sequence abundance discrepancy

between roots and soils owing to (Peay et al. 2011; Agerer 2001). Relatedly, I would expect the soil nutrients and pH to strongly influence fungal communities (Glassman et al. 2017b) and could explain some of the differences between the fungal communities of *P. flexilis* and *P. longaeva*. However, the soil nutrients are not significantly different between *P. flexilis* and *P. longaeva* (Appendix 6.1 Fig S6.8; Table S6.8), which suggests that the fungal communities are primarily responding to tree identity and age. Saprotrophic fungi comprised a relatively small component of the categorized ASVs (Appendix 6.1 Fig S6.7) but likely play an important role in the cycling of nutrients within the forest.

Fungi can preferentially provide resources to trees with greater carbon input (Fellbaum et al. 2014) in a value-driven reciprocal transfer that benefits cooperative partners (Kiers et al. 2011). Older trees have a disproportionate decline in photosynthesis relative to respiration (Tang et al. 2014) from 0–450 years which can result in lower net primary productivity. I speculate that a reduction in lower net primary productivity could shift fungal communities towards EMF that are more competitive in low-carbon symbiotic partnerships.

6.5.4 Caveats, implications for management, and areas for future research

The similarity between the soils of both pines indicate a larger species pool located within the soil, likely including a dormant spore bank. Amplifying DNA taken from soil samples opens the possibility of incorporating extracellular ‘relic DNA’ that can inflate abundance and diversity estimates. Relic DNA can cause shifts in fungal composition and abundance away from the living communities within the soil and inflate richness by an average of 12.4% (Carini et al. 2016). My results likely reflect some fungal taxa that are no longer present within the soil.

However, the high content of cations within the soil at the UFDP likely reduces the amount of relic DNA that is present (Carini et al. 2016) (Appendix 6.1 Table S6.9).

Sampling within a single site limits the ability to confidently extrapolate the results across the ranges of *P. flexilis* and *P. longaeva*. However, the difficulty in procuring sampling permits for *P. longaeva* and the lack of accessible sites in which they co-occur in proximity, make multiple sampling locations a difficult hurdle to overcome.

The large number of unidentified ASVs highlights a significant knowledge gap in the identity and ecological function of these fungi. More research is needed to identify trends in colonization, refine taxonomic identities, and determine the ecological function for a majority of the fungal community that I detected. The presence of likely PCR-inhibitors reduced the sample size of successfully aged *P. longaeva* and prevented us from fully testing the original hypotheses. Given the difficulty in extracting and amplifying fungal rDNA from around *P. flexilis* and *P. longaeva*, I would recommend generous sample sizes for future research.

Given that *P. flexilis* and *P. albicaulis* have a shared fungal species-pool (Cripps and Antibus 2011), it is likely that many of the ASVs that were shared between *P. flexilis* and *P. longaeva* may also associate with other at-risk white pines. Inoculation trials could be useful to identify if these fungal communities can improve establishment of planted seedlings and restoration efforts targeting the closely related white pine species. The continued outbreaks of *D. ponderosae* could cause shifts in belowground communities and a decline in EMF abundance and richness around *P. flexilis* like those seen in other systems following *D. ponderosae* outbreak (Pec et al. 2017). Preservation of the unique, age-dependent communities of large, old *P. flexilis*

may require further research to understand what influences the fungi and what role they play in the health of their tree-host.

These results also highlight the importance of large, old *P. flexilis* and *P. longaeva* to ecosystems. In addition to the well-known above-ground importance of large, old trees for conservation (Lindenmayer and Laurence 2017, Lutz et al. 2018) and their precarious state worldwide (Lindenmayer et al. 2012), these results underscore their importance belowground as well. Managers may wish to place even higher priority on preserving large, old individuals due to their association with unique fungal communities.

6.5.5 Conclusion

The diverse, understudied fungal communities of *P. flexilis* and *P. longaeva* may mediate important belowground interactions between these at-risk pines. Age heterogeneity, primarily driven by the presence of large, old trees in old-growth stands may promote fungal diversity on the landscape. My results highlight the need for more research to identify and study the fungal associates of the white pines so that I may better understand their roles in mediating tree health and interspecific interactions.

6.6 REFERENCES

Agerer, R. 2001. Exploration types of ectomycorrhizae. *Mycorrhiza* 11:107-114.

Anderson-Teixeira, K. J., S. J. Davies, A. C. Bennett, E. B. Gonzalez-Akre, H. C. Muller-Landau, S. Joseph Wright, K. Abu Salim, A. M. Almeyda Zambrano, A. Alonso, J. L. Baltzer, Y. Basset, N. A. Bourg, E. N. Broadbent, W. Y. Brockelman, S. Bunyavejchewin, D. F. R. P. Burslem, N. Butt, M. Cao, D. Cardenas, G. B. Chuyong, K. Clay, S. Cordell, H. S. Dattaraja, X. Deng, M. Detto, X. Du, A. Duque, D. L. Erikson, C. E. N. Ewango, G. A. Fischer, C. Fletcher, R. B. Foster, C. P. Giardina, G. S. Gilbert, N. Gunatilleke, S. Gunatilleke, Z. Hao, W. W. Hargrove, T. B. Hart, B. C. H. Hau, F. He, F. M. Hoffman, R. W. Howe, S. P. Hubbell, F. M. Inman-Narahari, P. A. Jansen, M. Jiang, D. J. Johnson, M. Kanzaki, A. R. Kassim, D. Kenfack, S. Kibet, M. F. Kinnaird, L. Korte, K. Kral, J. Kumar, A. J. Larson, Y. Li, X. Li, S. Liu, S. K. Y. Lum, J. A. Lutz, K. Ma, D. M. Maddalena, J.-R. Makana, Y. Malhi, T. Marthews, R. Mat Serudin, S. M. McMahon, W. J. McShea, H. R. Memiaghe, X. Mi, T. Mizuno, M. Morecroft, J. A. Myers, V. Novotny, A. A. de Oliveira, P. S. Ong, D. A. Orwig, R. Ostertag, J. den Ouden, G. G. Parker, R. P. Phillips, L. Sack, M. N. Sainge, W. Sang, K. Sri-ngernyuang, R. Sukumar, I.-F. Sun, W. Sungpalee, H. S. Suresh, S. Tan, S. C. Thomas, D. W. Thomas, J. Thompson, B. L. Turner, M. Uriarte, R. Valencia, M. I. Vallejo, A. Vicentini, T. Vrška, X. Wang, X. Wang, G. Weiblen, A. Wolf, H. Xu, S. Yap, and J. Zimmerman. 2015. CTFS-ForestGEO: a worldwide network monitoring forests in an era of global change. *Global Change Biology* 21:528-549.

Bennett, J. A., H. Maherali, K. O. Reinhart, Y. Lekberg, M. M. Hart, and J. Klironomos. 2017. Plant-soil feedbacks and mycorrhizal type influence temperate forest population dynamics. *Science* 355:181-184.

Bentz, B. J., J. Régnière, C. J. Fettig, E. M. Hansen, J. L. Hayes, J. A. Hicke, R. G. Kelsey, J. F. Negrón, and S. J. Seybold. 2010. Climate change and bark beetles of the western United States and Canada: direct and indirect effects. *BioScience* 60:602-613.

Bidartondo, M., J. Baar, and T. Bruns. 2001. Low ectomycorrhizal inoculum potential and diversity from soils in and near ancient forests of bristlecone pine (*Pinus longaeva*). *Canadian Journal of Botany* 79:293-299.

Bockino, N. K., and D. B. Tinker. 2012. Interactions of white pine blister rust and mountain pine beetle in Whitebark pine ecosystems in the southern Greater Yellowstone Area. *Natural Areas Journal* 32:31-40.

Booth, M. G., and J. D. Hoeksema. 2010. Mycorrhizal networks counteract competitive effects of canopy trees on seedling survival. *Ecology* 91:2294-2302.

Brown, P. M. 1996. OLDLIST: a database of maximum tree age. *Tree rings, environment, and humanity*. *Radiocarbon*, 1996:727 - 731.

Bunn, A., M. Korpela, F. Biondi, F. Campelo, P. Mérian, F. Qeadan, and C. Zang. 2019. dplR: dendrochronology program library in R. R package version 1.7.0.

Callahan, B. J., P. J. McMurdie, and S. P. Holmes. 2017. Exact sequence variants should replace operational taxonomic units in marker-gene data analysis. *The ISME Journal* 11:2639-2643.

Callahan, B. J., P. J. McMurdie, M. J. Rosen, A. W. Han, A. J. A. Johnson, and S. P. Holmes. 2016. DADA2: high-resolution sample inference from Illumina amplicon data. *Nature Methods* 13:581-583.

Carini, P., P. J. Marsden, J. W. Leff, E. E. Morgan, M. S. Strickland, and N. Fierer. 2016. Relic DNA is abundant in soil and obscures estimates of soil microbial diversity. *Nature Microbiology* 2:1-6.

Chen, L., N. G. Swenson, N. Ji, X. Mi, H. Ren, L. Guo, and K. Ma. 2019. Differential soil fungus accumulation and density dependence of trees in a subtropical forest. *Science* 366:124-128.

Cline, E. T., J. F. Ammirati, and R. L. Edmonds. 2005. Does proximity to mature trees influence ectomycorrhizal fungus communities of Douglas-fir seedlings? *New Phytologist* 166:993-1009.

Cripps, C. L., and R. K. Antibus. 2011. Native ectomycorrhizal fungi of limber and whitebark pine: Necessary for forest sustainability? Pages 37-44 in In: Keane, Robert E.; Tomback, Diana F.; Murray, Michael P.; Smith, Cyndi M., eds. The future of high-elevation, five-needle white pines in Western North America: *Proceedings of the High Five Symposium. 28-30 June 2010; Missoula, MT. Proceedings RMRS-P-63. Fort Collins, CO: US Department of Agriculture, Forest Service, Rocky Mountain Research Station*. p. 37-44.

Eckert, A. J., and B. D. Hall. 2006. Phylogeny, historical biogeography, and patterns of diversification for *Pinus* (Pinaceae): Phylogenetic tests of fossil-based hypotheses. *Molecular Phylogenetics and Evolution* 40:166-182.

Edgar, R. C. 2018. Updating the 97% identity threshold for 16S ribosomal RNA OTUs. *Bioinformatics* 34:2371-2375.

Egerton-Warburton, L. M., J. I. Querejeta, and M. F. Allen. 2007. Common mycorrhizal networks provide a potential pathway for the transfer of hydraulically lifted water between plants. *Journal of Experimental Botany* 58:1473-1483.

Fellbaum, C. R., J. A. Mensah, A. J. Cloos, G. E. Strahan, P. E. Pfeffer, E. T. Kiers, and H. Bücking. 2014. Fungal nutrient allocation in common mycorrhizal networks is regulated by the carbon source strength of individual host plants. *New Phytologist* 203:646-656.

Flora of North America Editorial Committee, e. 1993+. Flora of North America North of Mexico [Online]. Flora of North America Association.

Furniss, T. J., A. J. Larson, and J. A. Lutz. 2017. Reconciling niches and neutrality in a subalpine temperate forest. *Ecosphere* 8:e01847.

Gibson, K., K. Skov, S. Kegley, C. Jorgensen, S. Smith, and J. Witcosky. 2008. Mountain pine beetle impacts in high-elevation five-needle pines: current trends and challenges. *US Department of Agriculture Forest Service, Northern Region, Missoula, Montana*. R1-08-020:1-32.

Glassman, S. I., K. C. Lubetkin, J. A. Chung, and T. D. Bruns. 2017a. The theory of island biogeography applies to ectomycorrhizal fungi in subalpine tree “islands” at a fine scale. *Ecosphere* 8:e01677.

Glassman, S. I., and J. B. Martiny. 2018. Broadscale ecological patterns are robust to use of exact sequence variants versus operational taxonomic units. *MSphere* 3.

Glassman, S. I., I. J. Wang, and T. D. Bruns. 2017b. Environmental filtering by pH and soil nutrients drives community assembly in fungi at fine spatial scales. *Molecular Ecology* 26:6960-6973.

Gray, C. A., J. B. Runyon, M. J. Jenkins, and A. D. Giunta. 2015. Mountain pine beetles use volatile cues to locate host limber pine and avoid non-host great basin bristlecone pine. *PLoS One* 10:e0135752.

Hagenbo, A., J. Kyaschenko, K. E. Clemmensen, B. D. Lindahl, and P. Fransson. 2018. Fungal community shifts underpin declining mycelial production and turnover across a *Pinus sylvestris* chronosequence. *Journal of Ecology* 106:490-501.

Hervé, M. 2020. RVAideMemoire: testing and plotting procedures for biostatistics. R package version 0.9-75

Hoff, R., R. T. Bingham, and G. McDonald. 1980. Relative blister rust resistance of white pines. *European Journal of Forest Pathology* 10:307-316.

Holmes, R. L. 1983. Computer-assisted quality control in tree-ring dating and measurement. *Tree Ring Bulletin.*

Ihrmark, K., I. Bödeker, K. Cruz-Martinez, H. Friberg, A. Kubartova, J. Schenck, Y. Strid, J. Stenlid, M. Brandström-Durling, and K. E. Clemmensen. 2012. New primers to amplify the fungal ITS2 region–evaluation by 454-sequencing of artificial and natural communities. *FEMS Microbiology Ecology* 82:666-677.

Kennedy, P. G., K. G. Peay, and T. D. Bruns. 2009. Root tip competition among ectomycorrhizal fungi: are priority effects a rule or an exception? *Ecology* 90:2098-2107.

Kiers, E. T., M. Duhamel, Y. Beesetty, J. A. Mensah, O. Franken, E. Verbruggen, C. R. Fellbaum, G. A. Kowalchuk, M. M. Hart, and A. Bago. 2011. Reciprocal rewards stabilize cooperation in the mycorrhizal symbiosis. *Science* 333:880-882.

Kinloch Jr, B. B. 2003. White pine blister rust in North America: past and prognosis. *Phytopathology* 93:1044-1047.

Klein, T., R. T. Siegwolf, and C. Körner. 2016. Belowground carbon trade among tall trees in a temperate forest. *Science* 352:342-344.

Kolaříková, Z., P. Kohout, C. Krüger, M. Janoušková, L. Mrnka, and J. Rydlová. 2017. Root-associated fungal communities along a primary succession on a mine spoil: Distinct ecological guilds assemble differently. *Soil Biology and Biochemistry* 113:143-152.

Kyaschenko, J., K. E. Clemmensen, A. Hagenbo, E. Karltun, and B. D. Lindahl. 2017. Shift in fungal communities and associated enzyme activities along an age gradient of managed *Pinus sylvestris* stands. *The ISME Journal* 11:863-874.

Liang, M., D. Johnson, D. F. Burslem, S. Yu, M. Fang, J. D. Taylor, A. F. Taylor, T. Helgason, and X. Liu. 2020. Soil fungal networks maintain local dominance of ectomycorrhizal trees. *Nature Communications* 11:1-7.

Lindenmayer, D. B., and W. F. Laurance. 2017. The ecology, distribution, conservation and management of large old trees. *Biological Reviews* 92:1434-1458.

Lindenmayer, D. B., W. F. Laurance, and J. F. Franklin. 2012. Global decline in large old trees. *Science* 338:1305-1306.

Lutz, J. A. 2015. The evolution of long-term data for forestry: large temperate research plots in an era of global change. *Northwest Science* 89:255-269.

Lutz, J. A., T. J. Furniss, D. J. Johnson, S. J. Davies, D. Allen, A. Alonso, K. J. Anderson-Teixeira, A. Andrade, J. Baltzer, and K. M. Becker. 2018. Global importance of large-diameter trees. *Global Ecology and Biogeography* 27:849-864.

Mathys, A. S., N. C. Coops, and R. H. Waring. 2017. An ecoregion assessment of projected tree species vulnerabilities in western North America through the 21st century. *Global Change Biology* 23:920-932.

McDowell, N. G., C. D. Allen, K. Anderson-Teixeira, B. H. Aukema, B. Bond-Lamberty, L. Chini, J. S. Clark, M. Dietze, C. Grossiord, and A. Hanbury-Brown. 2020. Pervasive shifts in forest dynamics in a changing world. *Science* 368.

McKenney, D. W., J. H. Pedlar, K. Lawrence, K. Campbell, and M. F. Hutchinson. 2007. Potential impacts of climate change on the distribution of North American trees. *BioScience* 57:939-948.

McMurdie, P. J., and S. Holmes. 2013. phyloseq: an R package for reproducible interactive analysis and graphics of microbiome census data. *PLoS One* 8:e61217.

Murali, A., A. Bhargava, and E. S. Wright. 2018. IDTAXA: a novel approach for accurate taxonomic classification of microbiome sequences. *Microbiome* 6:1-14.

Nguyen, N. H., Z. Song, S. T. Bates, S. Branco, L. Tedersoo, J. Menke, J. S. Schilling, and P. G. Kennedy. 2016. FUNGuild: an open annotation tool for parsing fungal community datasets by ecological guild. *Fungal Ecology* 20:241-248.

Nilsson, R. H., K.-H. Larsson, A. F. S. Taylor, J. Bengtsson-Palme, T. S. Jeppesen, D. Schigel, P. Kennedy, K. Picard, F. O. Glöckner, and L. Tedersoo. 2019. The UNITE database for molecular identification of fungi: handling dark taxa and parallel taxonomic classifications. *Nucleic Acids Research* 47:D259-D264.

Oksanen, J., F. G. Blanchet, M. Friendly, R. Kindt, P. Legendre, D. McGlinn, P. R. Minchin, R. B. O'Hara, G. L. Simpson, P. Solymos, M. H. H. Stevens, E. Szoecs, and H. Wagner. 2018. vegan: community ecology package. R package version 2.5-6.

Peay, K. G., P. G. Kennedy, and T. D. Bruns. 2011. Rethinking ectomycorrhizal succession: are root density and hyphal exploration types drivers of spatial and temporal zonation? *Fungal Ecology* 4:233-240.

Pec, G. J., J. Karst, D. L. Taylor, P. W. Cigan, N. Erbilgin, J. E. Cooke, S. W. Simard, and J. F. Cahill Jr. 2017. Change in soil fungal community structure driven by a decline in ectomycorrhizal fungi following a mountain pine beetle (*Dendroctonus ponderosae*) outbreak. *New Phytologist* 213:864-873.

Philip, L., S. Simard, and M. Jones. 2010. Pathways for below-ground carbon transfer between paper birch and Douglas-fir seedlings. *Plant Ecology & Diversity* 3:221-233.

R Core Team. 2019. R: A language and environment for statistical computing. The R Foundation. Version 3.6.1

R Studio Team. 2020. RStudio: Integrated Development for R.

Rudawska, M., R. Wilgan, D. Janowski, M. Iwański, and T. Leski. 2018. Shifts in taxonomical and functional structure of ectomycorrhizal fungal community of Scots pine (*Pinus sylvestris L.*) underpinned by partner tree ageing. *Pedobiologia* 71:20-30.

Sayers, E. W., J. Beck, J. R. Brister, E. E. Bolton, K. Canese, D. C. Comeau, K. Funk, A. Ketter, S. Kim, and A. Kimchi. 2020. Database resources of the national center for biotechnology information. *Nucleic Acids Research* **48**:D9.

Schoettle, A. 2004. Ecological roles of five-needle pine in Colorado: potential consequences of their loss. Breeding and genetic resources of five-needle pines: growth, adaptability and pest resistance. *USDA Forest Service, Rocky Mountain Research Station*:124-135.

Schwandt, J. W., I. B. Lockman, J. T. Kliejunas, and J. A. Muir. 2010. Current health issues and management strategies for white pines in the western United States and Canada. *Forest Pathology* 40:226-250.

Segnitz, R. M., S. E. Russo, S. J. Davies, and K. G. Peay. 2020. Ectomycorrhizal fungi drive positive phylogenetic plant–soil feedbacks in a regionally dominant tropical plant family. *Ecology* :e03083.

Serra-Diaz, J. M., R. M. Scheller, A. D. Syphard, and J. Franklin. 2015. Disturbance and climate microrefugia mediate tree range shifts during climate change. *Landscape Ecology* 30:1039-1053.

Shemesh, H., B. E. Boaz, C. I. Millar, and T. D. Bruns. 2020. Symbiotic interactions above treeline of long-lived pines: Mycorrhizal advantage of limber pine (*Pinus flexilis*) over Great Basin bristlecone pine (*Pinus longaeva*) at the seedling stage. *Journal of Ecology* 108:908-916.

Smith, S. E., and D. J. Read. 2010. Mycorrhizal symbiosis. Academic press.

Smithers, B. V., M. P. North, C. I. Millar, and A. M. Latimer. 2018. Leap frog in slow motion: Divergent responses of tree species and life stages to climatic warming in Great Basin subalpine forests. *Global Change Biology* 24:e442-e457.

Tang, J., S. Luyssaert, A. D. Richardson, W. Kutsch, and I. A. Janssens. 2014. Steeper declines in forest photosynthesis than respiration explain age-driven decreases in forest growth. *Proceedings of the National Academy of Sciences* 111:8856-8860.

Teste, F. P., and S. W. Simard. 2008. Mycorrhizal networks and distance from mature trees alter patterns of competition and facilitation in dry Douglas-fir forests. *Oecologia* 158:193-203.

Teste, F. P., S. W. Simard, and D. M. Durall. 2009a. Role of mycorrhizal networks and tree proximity in ectomycorrhizal colonization of planted seedlings. *Fungal Ecology* 2:21-30.

Teste, F. P., S. W. Simard, D. M. Durall, R. D. Guy, M. D. Jones, and A. L. Schoonmaker. 2009b. Access to mycorrhizal networks and roots of trees: importance for seedling survival and resource transfer. *Ecology* 90:2808-2822.

Tomback, D. F., and P. Achuff. 2010. Blister rust and western forest biodiversity: ecology, values and outlook for white pines. *Forest Pathology* 40:186-225.

Tomback, D. F., P. Achuff, A. W. Schoettle, J. W. Schwandt, and R. J. Mastrogiuseppe. 2011. The magnificent high-elevation five-needle white pines: ecological roles and future outlook. Pages 2-28 in In: Keane, Robert E.; Tomback, Diana F.; Murray, Michael P.; Smith, Cyndi M., eds. *The future of high-elevation, five-needle white pines in Western*

North America: Proceedings of the High Five Symposium. 28-30 June 2010; Missoula, MT. Proceedings RMRS-P-63. Fort Collins, CO: US Department of Agriculture, Forest Service, Rocky Mountain Research Station. p. 2-28.

Trant, A., E. Higgs, and B. M. Starzomski. 2020. A century of high elevation ecosystem change in the Canadian Rocky Mountains. *Scientific Reports* 10:1-10.

van der Heijden, M. G. A., and T. R. Horton. 2009. Socialism in soil? The importance of mycorrhizal fungal networks for facilitation in natural ecosystems. *Journal of Ecology* 97:1139-1150.

White, T. J., T. Bruns, S. Lee, and J. Taylor. 1990. Amplification and direct sequencing of fungal ribosomal RNA genes for phylogenetics. *PCR protocols: a guide to methods and applications* 18:315-322.

Wickham, H. 2016. ggplot2: elegant graphics for data analysis. Springer.

Williams, D. W., and A. M. Liebhold. 2002. Climate change and the outbreak ranges of two North American bark beetles. *The Bark Beetles, Fuels, and Fire Bibliography*:34.

Wright, E. S. 2016. Using DECIPHER v2. 0 to analyze big biological sequence data in R. *R Journal 8*.

6.7 TABLES

Table 6.1 The results from a permutational analysis of variance (PERMANOVA) on the fungal communities in soils and on roots of *Pinus flexilis* and *Pinus longaeva* at the Utah Forest Dynamics Plot, Utah, USA. The variable 'Sample type' consists of the unique combinations of tree species by roots or soil. A pairwise PERMANOVA with a false-discovery rate p-adjustment was used for pairwise comparisons between habitat types.

Variable	df	SumsofSq	MeanSqs	F.Model	R^2	Pr(>F)
Sample type	3	1.85	0.61	1.65	0.14	0.001
Residuals	30	11.18	0.37		0.85	
Total	33	13.04			1	

Pairwise-comparison of sample type (P-values)

	P. flexilis roots	*P. flexilis* soils	*P. longaeva* roots
P. flexilis soils	**0.019**		
P. longaeva roots	**0.040**	**0.018**	
P. longaeva soils	**0.006**	0.075	**0.018**

Table 6.2 The proportional abundance (%) of amplicon sequence variants (ASV) from the fungal families that accounted for ≥ 10% of read abundance in one or more sample type categories. Fungal ASVs were sequenced from samples found on root and soils surrounding *Pinus flexilis* and *Pinus longaeva* at the Utah Forest Dynamics Plot, Utah. Values are the percent of the total ASV read abundance by column. The 'NA' category denotes sequences that could not be matched against the reference database and 'unidentified' denotes sequences in which the confidence level for the taxonomic assignment was below the default cutoff.

		Pinus flexilis		*Pinus longaeva*	
		Root	Soil	Root	Soil
Ascomycota	**Family**	53.4	53.7	59.0	52.7
	Cladosporiaceae	3.4	0.0	0.0	0.0
	Gloniaceae	1.8	0.6	0.0	0.2
	Herpotrichiellaceae	0.0	1.8	0.0	0.7
	Melanommataceae	0.6	0.4	1.5	0.5
	NA	19.1	29.9	36.1	33.7
	Pseudeurotiaceae	0.0	1.2	0.1	1.2
	Pyronemataceae	21.1	14.4	15.4	10.1
	unidentified_29	2.7	2.1	2.2	3.2
	unidentified_940	1.9	0.2	0.0	0.0
Basidiomycota		30.4	27.4	26.1	24.2
	Atheliaceae	3.6	1.1	7.6	0.8
	Cantharellales_fam_Incertae_sedis	1.4	0.0	0.0	0.0
	Inocybaceae	0.2	4.8	2.4	6.4
	Lentariaceae	1.2	0.6	0.0	0.7
	NA	1.1	1.3	0.2	2.3
	Rhizopogonaceae	1.7	0.7	0.8	1.0
	Sebacinaceae	1.0	3.6	2.0	0.6
	Thelephoraceae	2.9	4.6	4.8	7.1
	Tricholomataceae	14.7	7.5	7.1	2.3
NA		10.6	16.5	12.2	18.1
Unidentified		5.3	1.4	2.3	2.7

Table 6.3 The 20 most abundant fungal amplicon sequence variants (ASV) for each significant sample type association for roots and soil around *Pinus flexilis* and *Pinus longaeva* from the Utah Forest Dynamics Plot, UT, USA. An 'NA' within the rank columns indicates that the ASV was not found on any sample withing that sample type category. An 'NA" within the taxonomy column indicates that the ASV did not match any known taxa and is unknown at that taxonomic level. Functional guilds were assigned to ASVs based on the taxonomic identity and matched against the FUNGuild database.

ASV	*Pinus flexilis* root	*Pinus longaeva* root	Soil	Taxonomy	Guild
ASV0007	1	69	21	Basidiomycota;Agaricomycetes;Agaricales; Tricholomataceae;Tricholoma;NA	Ectomycorrhizal-Fungal Parasite
ASV0002	2	2	7	Basidiomycota;Agaricomycetes;Agaricales; Tricholomataceae;Tricholoma;NA	Ectomycorrhizal-Fungal Parasite
ASV0001	3	6	3	Ascomycota;Pezizomycetes;Pezizales; Pyronemataceae;Wilcoxina;NA	Ectomycorrhizal

ASV	*Pinus flexilis* root	*Pinus longaeva* root	Soil	Taxonomy	Guild
ASV0005	4	7	13	Basidiomycota;Agaricomycetes;Agaricales; Tricholomataceae;Tricholoma;NA	Ectomycorrhizal-Fungal Parasite
ASV0012	5	95	36	Basidiomycota;Agaricomycetes;Agaricales; Tricholomataceae;Tricholoma;NA	Ectomycorrhizal-Fungal Parasite
ASV0003	6	10	9	Ascomycota;Pezizomycetes;Pezizales; Pyronemataceae;Wilcoxina;NA	Ectomycorrhizal
ASV0031	7	157	221	unidentified;unidentified;unidentified; unidentified;unidentified_1;Fungi_sp	-
ASV0048	8	NA	1462	Ascomycota;Dothideomycetes;Capnodiales; Cladosporiaceae;Cladosporium;NA	Animal Pathogen-Endophyte-Lichen Parasite-

ASV	*Pinus flexilis* root	*Pinus longaeva* root	Soil	Taxonomy	Guild
					Plant Pathogen-Wood Saprotroph
ASV0050	9	NA	1174	Ascomycota;Dothideomycetes;Mytilinidales; Gloniaceae;Cenococcum;NA	Ectomycorrhizal
ASV0016	10	20	71	Ascomycota;Pezizomycetes;Pezizales; Pyronemataceae;Geopora;Geopora_sp	Ectomycorrhizal
ASV0047	11	206	224	unidentified;unidentified;unidentified; unidentified;unidentified_1;Fungi_sp	-
ASV0079	12	NA	NA	Ascomycota;Dothideomycetes;NA; NA;NA;NA	-

ASV	*Pinus flexilis* root	*Pinus longaeva* root	Soil	Taxonomy	Guild
ASV0077	13	NA	NA	Ascomycota;Dothideomycetes;Capnodiales; Cladosporiaceae;Cladosporium;NA	Animal Pathogen-Endophyte-Lichen Parasite-Plant Pathogen-Wood Saprotroph
ASV0032	14	NA	27	Ascomycota;Pezizomycetes;Pezizales; Pyronemataceae;NA;NA	Dung Saprotroph-Ectomycorrhizal-Soil Saprotroph-Wood Saprotroph
ASV0024	15	28	114	Ascomycota;Pezizomycetes;Pezizales; Pyronemataceae;Geopora;Geopora_sp	Ectomycorrhizal

ASV	*Pinus flexilis* root	*Pinus longaeva* root	Soil	Taxonomy	Guild
ASV0015	16	5	46	Ascomycota;Pezizomycetes;Pezizales; Pyronemataceae;Geopora;Geopora_sp	Ectomycorrhizal
ASV0025	17	419	43	Ascomycota;Pezizomycetes;Pezizales; Pyronemataceae;Geopora;Geopora_sp	Ectomycorrhizal
ASV0038	18	NA	34	Ascomycota;Pezizomycetes;Pezizales; Pyronemataceae;NA;NA	Dung Saprotroph-Ectomycorrhizal-Soil Saprotroph-Wood Saprotroph
ASV0043	19	56	110	NA;NA;NA; NA;NA;NA	-

ASV	*Pinus flexilis* root	*Pinus longaeva* root	Soil	Taxonomy	Guild
ASV0044	20	NA	37	Ascomycota;Pezizomycetes;Pezizales; Pyronemataceae;NA;NA	Dung Saprotroph-Ectomycorrhizal-Soil Saprotroph-Wood Saprotroph
ASV0004	83	1	8	Ascomycota;Dothideomycetes;NA; NA;NA;NA	-
ASV0008	111	3	12	Ascomycota;Dothideomycetes;NA; NA;NA;NA	-
ASV0018	204	4	92	Basidiomycota;Agaricomycetes;Atheliales; Atheliaceae;NA;NA	Ectomycorrhizal-Lichen Parasite-Lichenized-Plant Pathogen

ASV	*Pinus flexilis* root	*Pinus longaeva* root	Soil	Taxonomy	Guild
ASV0028	232	8	146	Basidiomycota;Agaricomycetes;Atheliales; Atheliaceae;NA;NA	Ectomycorrhizal-Lichen Parasite-Lichenized-Plant Pathogen
ASV0021	25	9	85	Ascomycota;Pezizomycetes;Pezizales; Pyronemataceae;Geopora;Geopora_sp	Ectomycorrhizal
ASV0022	70	11	64	Ascomycota;NA;NA; NA;NA;NA	-
ASV0020	44	12	39	Ascomycota;Leotiomycetes;NA; NA;NA;NA	-
ASV0073	NA	13	1101	Ascomycota;Leotiomycetes;NA;	-

ASV	*Pinus flexilis* root	*Pinus longaeva* root	Soil	Taxonomy	Guild
				NA;NA;NA	
ASV0052	173	14	84	Ascomycota;Leotiomycetes;Helotiales; NA;NA;NA	-
ASV0042	131	15	103	Ascomycota;NA;NA; NA;NA;NA	-
ASV0093	NA	16	NA	Ascomycota;NA;NA; NA;NA;NA	-
ASV0112	NA	17	NA	Ascomycota;Leotiomycetes;Phacidiales; Phacidiaceae;NA;NA	-
ASV0033	61	18	82	Ascomycota;Leotiomycetes;Helotiales; NA;NA;NA	-

ASV	*Pinus flexilis* root	*Pinus longaeva* root	Soil	Taxonomy	Guild
ASV0082	NA	19	219	Ascomycota;Leotiomycetes;Helotiales; NA;NA;NA	-
ASV0009	42	144	1	Ascomycota;Leotiomycetes;Helotiales; NA;NA;NA	-
ASV0006	133	24	2	Ascomycota;NA;NA; NA;NA;NA	-
ASV0014	68	103	4	NA;NA;NA;NA;NA;NA	-
ASV0011	52	656	5	Ascomycota;Leotiomycetes;Helotiales; NA;NA;NA	-
ASV0010	161	40	6	NA;NA;NA; NA;NA;NA	-

ASV	*Pinus flexilis* root	*Pinus longaeva* root	Soil	Taxonomy	Guild
ASV0023	145	NA	10	Ascomycota;Eurotiomycetes;Chaetothyriales; NA;NA;NA	-
ASV0017	48	30	11	Ascomycota;Leotiomycetes;Helotiales; unidentified_29;unidentified_21;Helotiales_sp	-
ASV0029	219	104	14	Ascomycota;Leotiomycetes;NA; NA;NA;NA	-
ASV0035	243	430	15	Ascomycota;Leotiomycetes;Thelebolales; Pseudeurotiaceae;NA;NA	Plant Saprotroph-Wood Saprotroph
ASV0041	241	202	16	Ascomycota;NA;NA; NA;NA;NA	-

ASV	*Pinus flexilis* root	*Pinus longaeva* root	Soil	Taxonomy	Guild
ASV0027	65	52	17	Ascomycota;Leotiomycetes;Helotiales; unidentified_29;unidentified_21;Helotiales_sp	-
ASV0054	NA	NA	18	Ascomycota;Leotiomycetes;Thelebolales; Pseudeurotiaceae;NA;NA	Plant Saprotroph-Wood Saprotroph
ASV0046	347	125	19	Ascomycota;NA;NA; NA;NA;NA	-
ASV0034	177	81	20	Ascomycota;Leotiomycetes;NA; NA;NA;NA	-

1

6.8 FIGURES

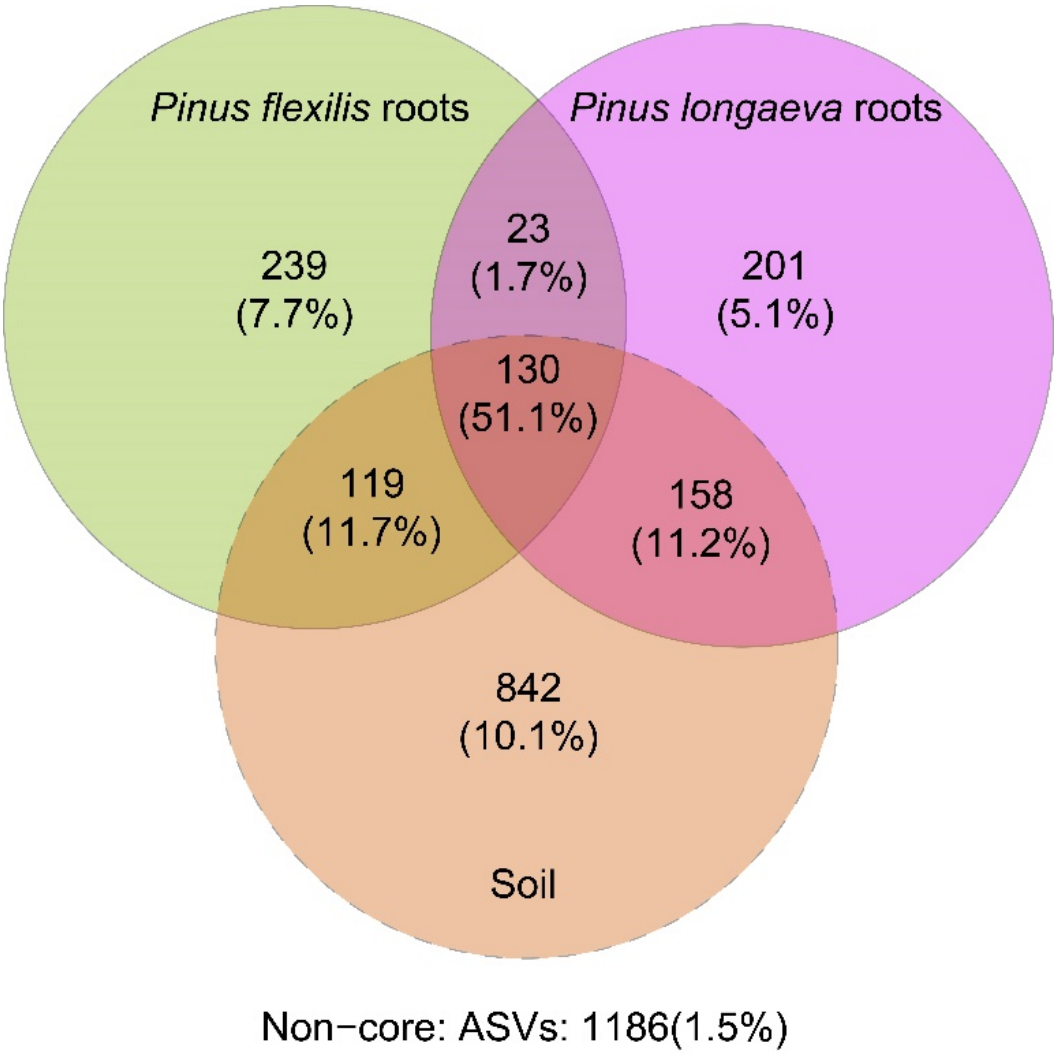

Figure 6.1 The overlap between 'core' fungal amplicon sequence variants (ASV) that were found on roots and in soils around *Pinus flexilis* and *Pinus longaeva* at the Utah Forest Dynamics Plot, Utah, USA. Sequences that represent more than 0.1% of read abundance were considered 'core' taxa. The top number within each section indicates the number of ASVs shared between those categories with the bottom percentage details the mean proportional abundance of sequence reads from the ASVs within that section, by sample.

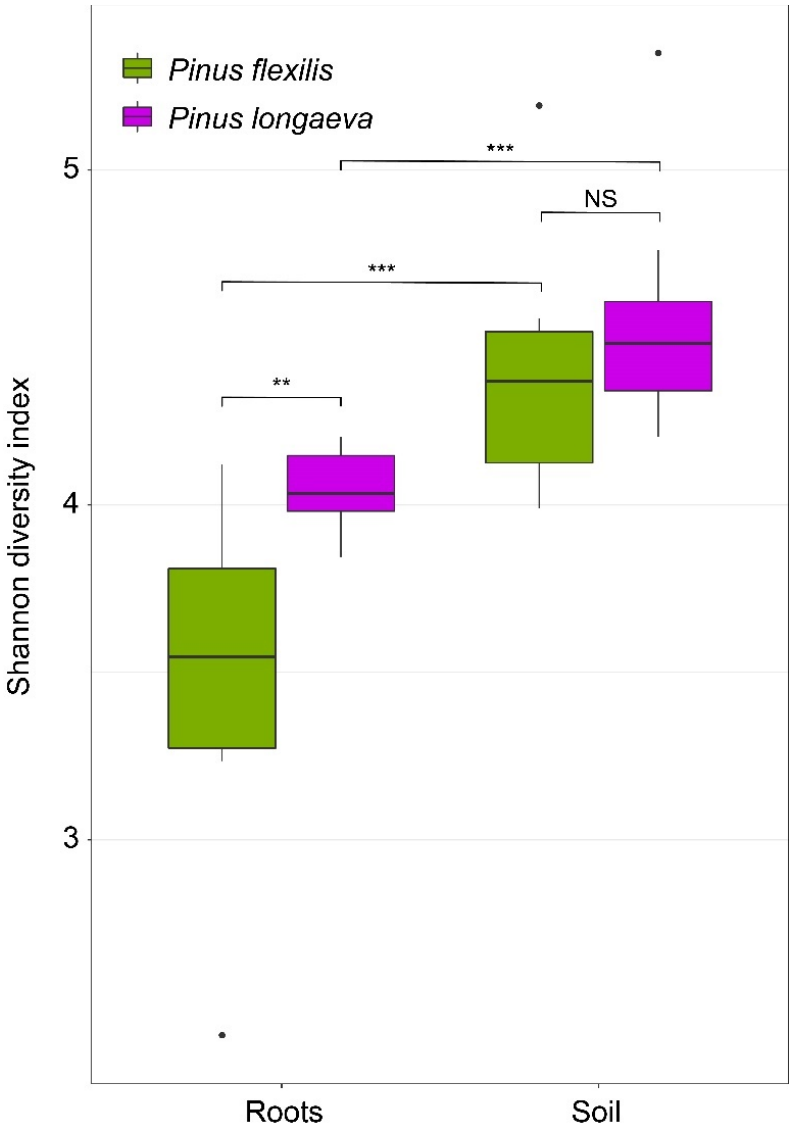

Figure 6.2 Shannon diversity index values for non-rarefied fungal communities associated with root and soil communities around *Pinus flexilis* and *Pinus longaeva* at the Utah Forest Dynamics Plot in Utah, USA. Brackets and asterisks indicate significant differences between groups where 'NS.' indicates non-significant differences, '*' indicates $p < 0.05$, '**' indicates $p < 0.01$, and *** indicates $p < 0.001$.

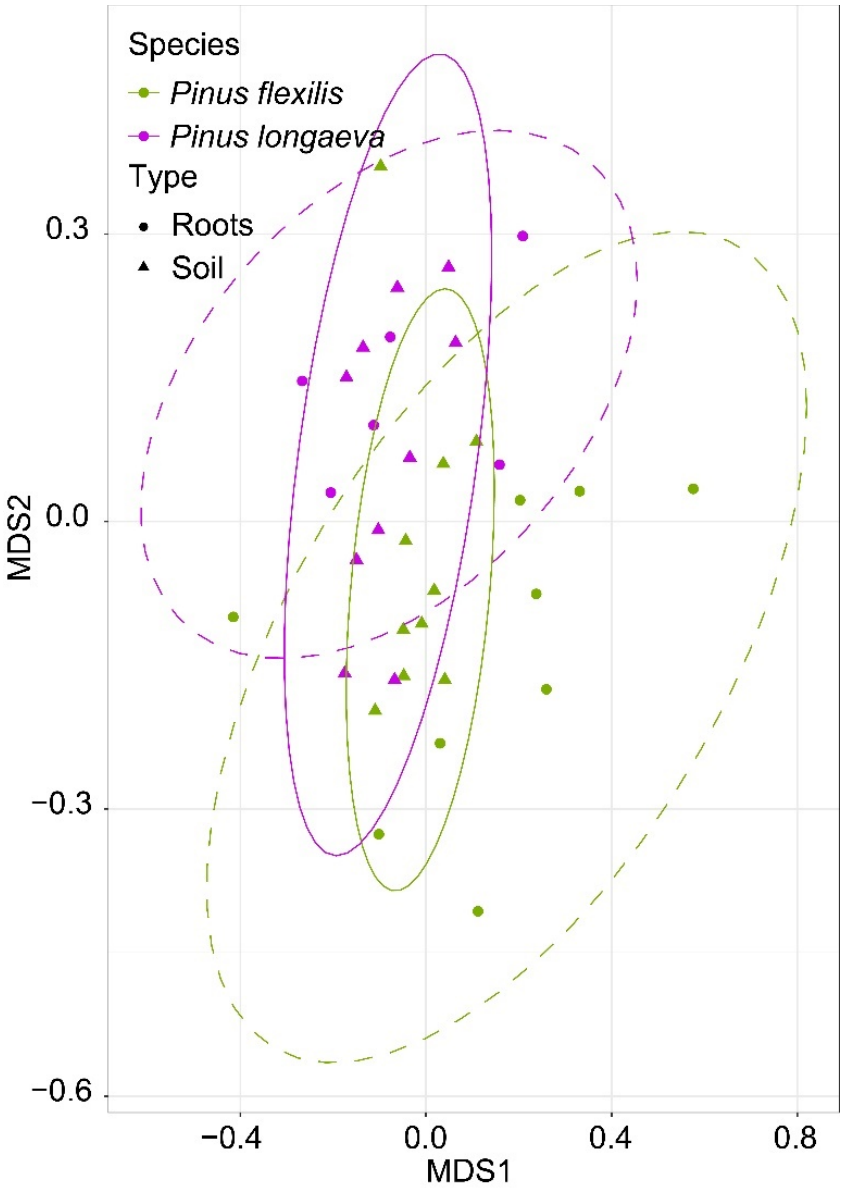

Figure 6.3 A meta non-metric multidimensional scaling (NMDS) of fungal communities from roots (triangles) and soils (circles) around *Pinus flexilis* and *Pinus longaeva* at the Utah Forest Dynamics Plot, Utah, USA. Ellipses are 95% confidence intervals for soil (solid) and roots (dashed). Fungal communities were ordinated using a Bray-Curtis dissimilarity matrix using sequence read number as a proxy for fungal abundance. The lowest stress (0.23) ordination was selected from 500 permutations of the data.

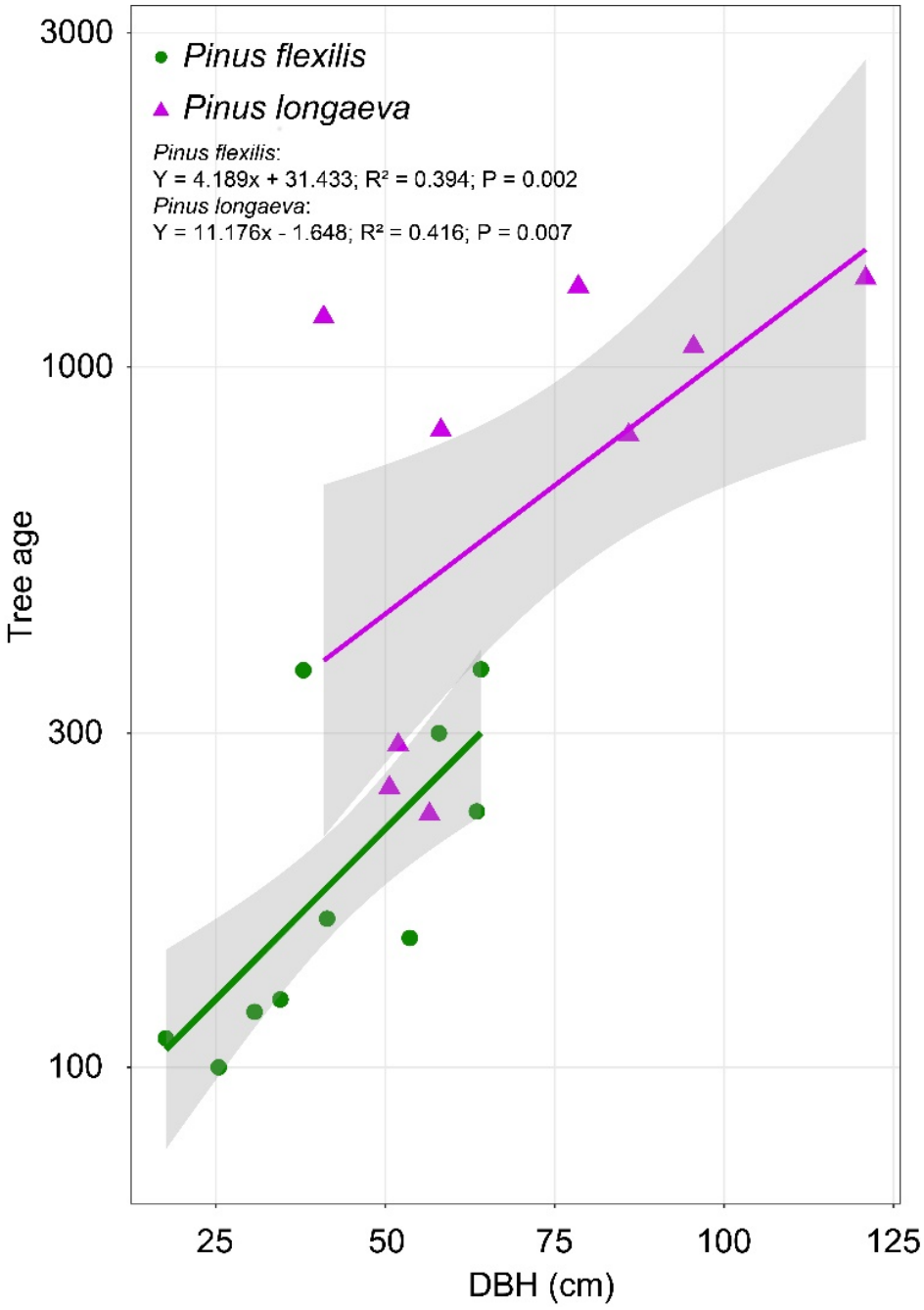

Figure 6.4 The distribution of tree age by diameter at breast height (DBH) for *Pinus flexilis* (circles) and *Pinus longaeva* (triangles) at the Utah Forest Dynamics Plot, Utah, USA. The y-axis is in log-scale. Equations are provided for the species-specific linear models. Shaded 95% confidence intervals are plotted for each linear model.

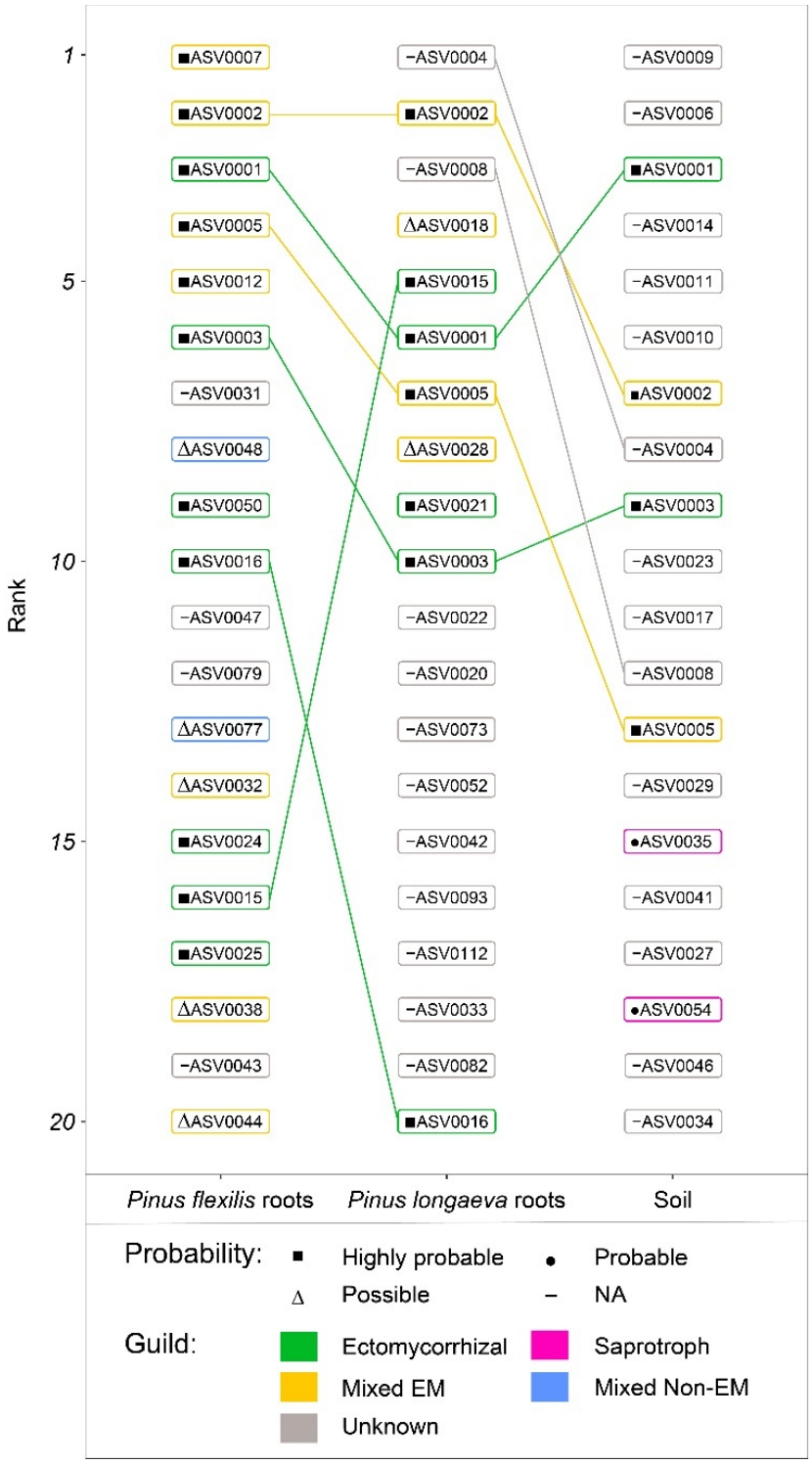

Figure 6.5 The top 20 most read-abundant fungal amplicon sequence variants (ASV) for soils and roots from around *Pinus flexilis* and *Pinus longaeva* at the Utah Forest Dynamics Plot, Utah,

USA. Taxa were assigned functional guilds using the FUNGuild database and assigned a probability of correct guild classification based on the weight of available evidence. Taxa that were not assigned a guild are categorized as ‘Unknown’. Taxa that were assigned to multiple potential guilds are classified as ‘Mixed EM’ if one of the potential guilds included ectomycorrhizal or ‘Mixed Non-EM’ if the guilds were non-mycorrhizal. Lines connect the shared ASVs between sample type categories.

Chapter 7: Conclusion

My research objectives were to identify and characterize some of the interactions that mediate how trees experience resource limitation across time and space. Each chapter focused on a suite of above or belowground interactions that in some way mediate resource limitation within trees. Across the chapters, I explored processes that occurred at the edge of the southern boreal forest of Alberta (Chapter 2 and 3), the montane forests of interior British Columbia (Chapter 3 and 4), and subalpine forests in Utah (Chapter 4 and 5). The main conclusions from each chapter are as follows:

- Chapter 2: Native and novel disturbances interacted to increase forest mortality rates and shift the forest towards a new stable state.
- Chapter 3: Competitive and facilitative interactions fluctuated through time and with disturbance to shift the forest towards a novel successional trajectory.
- Chapter 4: Connections through an ectomycorrhizal network are associated with greater tree growth. Connections to unique fungal genets are associated with greater tree growth.
- Chapter 5: Fungal community assembly processes change across the range of *Pseudotsuga menziesii*. Homogenizing selection is the most prevalent assembly process for fungal communities around *Pseudotsuga.*
- Chapter 6: Distinct fungal communities exist for *Pinus flexilis* and *Pinus longaeva* but are dominated by shared ectomycorrhizal taxa. Fungal community composition on *P. flexilis* roots is correlated with tree age.

Below I will explore the principal results in each chapter and how they relate to one another and influence forest growth-limitation.

7.1.1 Processes underlying a forest in flux: southern boreal forest

My first data chapter (Chapter 2) identified long-term demographic changes occurring through succession and provided evidence for a novel successional trajectory. The combination of pronounced precipitation limitation and novel bark beetle encroachment thrust the forest onto a trajectory for stand dissolution and the potential establishment of a shrubland. My second data chapter (Chapter 3) used the same forest plot to examine how density-dependent interactions through succession matched conceptual models for similar forests, and to identify how density-dependence had been influenced by native and novel disturbance regimes. I found that despite initially matching conceptual frameworks when the forest was young, in late sere, repeated disturbances and precipitation limitation had resulted in unexpected patterns of facilitation and competition. The relative strength of density-dependent competition and facilitation changed with succession and with disturbances, ultimately resulting in a spatial equilibrium.

The demographic rates of growth, recruitment and mortality are indelibly linked to the patterns of density-dependent interactions and disturbances. The growth rates of all tree species in the George La Roi forest plot (GLR) declined during periods of drought, as water became more limiting (Fig. 2.2). Angiosperms (*Populus tremuloides* and *Betula papyrifera*) competed with the shade-tolerant conifer, *P. glauca*, predisposing them to death from bark beetle attack and likely driving the increasing mortality rate of *P. glauca* within the last two decades. As *P. glauca* suffered a loss of 70% of stems, the annual growth of *P. tremuloides* and *B. papyrifera* surpassed that of *P. glauca* for the first time since the 1960s, indicating a likely competitive release. Within the GLR, the most widespread growth-limiting resource is likely water as each

tree species showed a strong, positive climatic growth response to precipitation (Appendix 2.1 Fig. S2.6: S2.9). Tree ring evidence suggests that the first outbreak of bark beetles within the stand occurred in 2002 during a notable drought when *P. glauca* may have been vulnerable to attack (Berg et al. 2006). Throughout the duration of the GLR plot, angiosperms facilitated the establishment of *P. glauca*, likely by shading them and increasing local soil moisture (Buck and Clair 2012). However, the positive density-dependence from angiosperms seemingly fades as *P. glauca* matures and leads to competition for resources and an associated increased risk for death from bark beetles. Bark beetle attacks have continued within the stand since 2002 and will likely persist into the future and risk spreading to neighboring stands. The combination of climate change bringing more frequent, severe drought and insect-disturbances will likely continue to interact with density-dependent interactions to strongly influence growth, mortality, and recruitment rates. Any density-dependent interactions that reduce the availability of growth-limiting precipitation may have increased importance in the future and drive rising mortality rates. Likewise, any positive density-dependent interactions that reduce moisture limitation may be increasingly important. Angiosperm facilitation of juvenile *P. glauca* could serve as an important mechanism for this species local survival under drier conditions. However, the encroachment of bark beetles may disrupt this facilitative relationship in the long-term and prevent the establishment of dominant *P. glauca* overstories.

7.1.2 Identifying how ectomycorrhizal networks influence mature tree growth

The results of Chapter 4 indicate that EMNs can play an important role in providing mature trees with growth-limiting resources. In addition to having greater growth, highly connected trees also had lower variation in growth, potentially indicating some resistance to drought-induced growth decline. Beyond the initial result, there were two additional features of

the study that are particularly notable. First, interspecific differences in *Rhizopogon vinicolor* and *Rhizopogon vesiculosus* networks indicate that these closely related fungi may differ in their ability to transfer growth-limiting resources among trees. Second, intraspecific differences in *Rhizopogon vesiculosus* genets indicate that genets are not equal in the resources each provides to their host tree. Each genet could have different resources available nearby or have different efficacy at acquiring and trading these resources with their tree host. Cumulatively, these results provide insight into the role that EMNs and intraspecific differences in EMF may play in ameliorating growth-limiting resources in mature forests.

7.1.3 Controls on ectomycorrhizal fungal communities across space and time

Chapter 5 continued my goal of understanding the belowground ecology of *Pseudotsuga* and shifted the focus to the mechanisms driving fungal community assembly. I found that while fungal assembly processes differed between sites, deterministic processes were consistently responsible for shaping the fungal communities in soils and around the roots of *Pseudotsuga*. Stochastic processes of dispersal-limitation or community drift were present in all fungal communities but largely acted in a smaller role in fungal community assembly. Tree age was not associated with different assembly processes, which seemingly operate independent of this host property. In Chapter 6, I shifted focal tree species to the at-risk high-elevation pines, *P. flexilis* and *P. longaeva* to identify the composition and overlap of fungal communities between these pines. I found that the communities differed significantly but that many highly abundant EMF taxa occurred on both pines, providing a potential pathway for belowground interactions mediated by EMF between the tree species. Tree age of *P. flexilis* was associated with fungal community composition on roots but not soils, potentially indicating consistent selection

pressures through time or changes in selection pressures with ontogenesis or senescence of *P. flexilis*.

The intraspecific and interspecific differences in *Rhizopogon* species implied from results in Chapter 4 have implications when considering soil fungal diversity and composition. If interspecific differences in even closely related fungi can have substantial influences on the acquisition of growth-limiting resources, then fungal assembly processes may have potent effects for *Pseudotsuga* or other tree species. Homogenizing selection, so common across the range of *Pseudotsuga*, would be expected to reduce interspecific variation in fungal communities by causing phylogenetic under-dispersion relative to stochastic systems (Dini-Andreote et al. 2015). If homogenizing selection is due to local climate then fungal communities may shift in composition to ones less favorable to *Pseudotsuga*. However, if homogenizing selection is due in part to partner selection, then we might expect the homogenizing selection to shift communities towards those fungi best suited to competitively acquire growth-limiting resources.

In Chapter 5 I examined only one focal tree species, *Pseudotsuga*, and thus could not infer any effects from host-specificity in the fungal communities. Chapter 6 had two focal tree species, *P. flexilis* and *P. longaeva*, and I found significantly different fungal communities on roots but not soils around each pine species. Because soil nutrients and pH were similar around these tree species and they co-occurred within close proximity, we can infer that host-specificity and partner selection may drive part of the differences between the root communities of *P. flexilis* and *P. longaeva*. Tree age of *P. flexilis* was significantly associated with both fungal community composition of roots ($R^2 = 0.18$) and root communities were increasingly dissimilar with soil communities with tree age ($R^2 = 0.08$). This result suggests that *P. flexilis* imposes

different selection pressures on root-associated communities than it does on soils. These results contrast with the null results from Chapter 5 where the proportion of selection processes did not change with *Pseudotsuga* age. However, there are multiple differences between the focal tree species, *Pseudotsuga* and *P. flexilis*, as well as their fungal communities that may explain the apparent difference (Appendix 5.1 Table S5.8; Table 6.2). It is possible that inherent differences in the life-histories of *Pseudotsuga* and *P. flexilis* lead to *P. flexilis* applying greater selection pressures to root-associated communities. These selection pressures could directionally shift fungal communities through time, or the selection pressures may change through time as trees age and experience different resource-constraints. This question would be well suited for testing on *P. longaeva,* which does not senesce (Lanner and Connor 2001), and would be more likely to have selection pressures uncoupled from any aging mechanism. However, as discussed in Chapter 6, the sampling design failed to adequately capture a gradient of *P. longaeva* ages and I lost several samples to PCR-inhibitors. Future research could explore this trend along a broader age-range of *P. flexilis* and in *P. longaeva*.

Cumulatively my results suggest that interspecific and intraspecific differences among EMF can influence tree growth and that assembly processes of fungal communities may differ between roots, soils, and forests. Additionally, as trees age there may be an associated change in fungal communities associated with roots. Mature trees may have a growth enhancement from being highly connected to other trees through an EMN and have lower variability in growth through time. However, proximity to other trees may also promote negative density-dependence as trees compete for light, space, or resources. These density-dependent patterns can predispose trees to disturbance events and alter demographic trends unexpectedly through mortality or recruitment events. Any or all these processes can change through time and might be sensitive to

future climate change causing more variable and pronounced water-stress. Changes in EMN relative variable importance coincided with the degree of climatic moisture deficit (Fig. 4.3) possibly indicating that EMN topology or function changes during pronounced drought. Disturbance events such as bark beetle outbreaks or insect defoliation could also alter the nature of belowground interactions. For example, had EMNs existed within the GLR plot, the outbreak of bark beetles and pronounced drought would have severely altered the network topology by killing 70% of *P. glauca*.

7.1.4 Long-term monitoring and tree ring analysis to detect patterns of forest change

Many of the processes that influence forest composition and structure are slow-acting and liable to be missed or misconstrued unless tracked through time. For example, the density-dependent interactions in Chapter 3 fluctuated between competition and facilitation over several decades as the forest composition shifted and disturbances occurred. The use of dendroecology to reconstruct disturbance history and growth rates provided another layer of data to monitor long-term patterns. Repeated measuring of forests through time has an added cost in time, effort, and resources that a single census avoids. When feasible, repeated measurements prove a larger area of inference and enables the detection of temporal variation. Given the long-lived nature of most trees, we can expect that trees will experience a substantial degree of variation within their lifetimes.

Future research of EMN and fungal communities of *Pseudotsuga, P. flexilis*, or *P. longaeva* would benefit from repeated sampling through time and across more sites. The EMNs I studied in Chapter 4 were only measured once, in 2008, and within one forest. I suggest that further mapping and tree ring analysis in different forests would provide invaluable insight into

how EMNs may function across forests. Likewise, my measurements of the fungal communities in Chapters 5 and 6 were snapshots of the fungal communities within a single month. Despite the likely inclusion of relic DNA leftover from deceased fungi, the communities I measured were representative of the fungi present within a very narrow window of time and liable to change with seasonal or interannual variation (Hawkes et al. 2011, Voříšková et al. 2014, Carini et al. 2016). As the results from Chapter 2 and 3 make clear, communities and their interactions can change markedly through forest development and with disturbance. Additional measurements of the EMN and EMF communities would reveal any trends and provide additional insight into the temporal stability of these potentially important communities.

The use of tree ring analysis provides another useful mechanism for reconstructing trends in growth, disturbance history, or climate response in a forest. A unique benefit of tree ring analysis is that it can provide information on growth, disturbance, and climate that predate the historical record and plot establishment. My analysis of the GLR plot would have missed the key disturbances of angiosperm defoliators and bark beetles without the use of tree rings to reconstruct disturbance history. As with repeated measures, tree-ring analysis can be time-intensive and require expertise. However, in each of my chapters the use of dendroecology provided a layer of data that was critical to addressing my research questions as well as providing a detailed description of each forests growth, age structure, disturbance history, and climate response.

7.5 Conclusion

The interactions that influenced resource limitation in forests were variable through time (Chapter 2 and 3) or through fungi (Chapter 4). In turn, fungi were influenced by local conditions

within their forest (Chapter 5) or host-identity and tree age (Chapter 6). Cumulatively, my work suggests the importance of site-dependent processes that may fluctuate through time and in response to climate or disturbance. My work further highlights the utility of tree ring measurements across multiple analyses spanning aboveground and belowground communities that can be used to untangle mechanisms underlying forest dynamics. These findings highlight the highly variable nature of community interactions through time and across space.

7.2 REFERENCES

Buck, J. R., and S. B. S. Clair. 2012. Aspen increase soil moisture, nutrients, organic matter and respiration in Rocky Mountain forest communities. *PLoS One* 7:e52369.

Carini, P., P. J. Marsden, J. W. Leff, E. E. Morgan, M. S. Strickland, and N. Fierer. 2016. Relic DNA is abundant in soil and obscures estimates of soil microbial diversity. *Nature Microbiology* 2:1-6.

Dini-Andreote, F., J. C. Stegen, J. D. Van Elsas, and J. F. Salles. 2015. Disentangling mechanisms that mediate the balance between stochastic and deterministic processes in microbial succession. *Proceedings of the National Academy of Sciences* 112:E1326-E1332.

Hawkes, C. V., S. N. Kivlin, J. D. Rocca, V. Huguet, M. A. Thomsen, and K. B. Suttle. 2011. Fungal community responses to precipitation. *Global Change Biology* 17:1637-1645.

Lanner, R. M., and K. F. Connor. 2001. Does bristlecone pine senesce? *Experimental Gerontology* **36**:675-685.

Voříšková, J., V. Brabcová, T. Cajthaml, and P. Baldrian. 2014. Seasonal dynamics of fungal communities in a temperate oak forest soil. *New Phytologist* 201:269-278.

References

Aakala, T., S. Fraver, B. J. Palik, and A. W. D'Amato. 2012. Spatially random mortality in old-growth red pine forests of northern Minnesota. *Canadian Journal of Forest Research* 42:899–907.

ABMI (Alberta Biodiversity Monitoring Institute). 2018. ABMI Trees & Snags (5342138678144103563) database: Rotation 2. Retrieved from http://www.ABMI.ca

Agerer, R. 2001. Exploration types of ectomycorrhizae. *Mycorrhiza* 11:107-114.

Alberton, O., T. W. Kuyper, and A. Gorissen. 2005. Taking mycocentrism seriously: mycorrhizal fungal and plant responses to elevated CO2. *New Phytologist* 167:859-868.

Allen, C. D., A. K. Macalady, H. Chenchouni, D. Bachelet, N. McDowell, M. Vennetier, T. Kitzberger, A. Rigling, D. D. Breshears, E. H. (Ted) Hogg, P. Gonzalez, R. Fensham, Z. Zhang, J. Castro, N. Demidova, J.–H. Lim, G. Allard, S. W. Running, A. Semerci, and N. Cobb. 2010. A global overview of drought and heat-induced tree mortality reveals emerging climate change risks for forests. *Forest Ecology and Management* 259:660–684.

Anderson-Teixeira, K. J., S. J. Davies, A. C. Bennett, E. B. Gonzalez-Akre, H. C. Muller-Landau, S. Joseph Wright, K. Abu Salim, A. M. Almeyda Zambrano, A. Alonso, J. L. Baltzer, Y. Basset, N. A. Bourg, E. N. Broadbent, W. Y. Brockelman, S. Bunyavejchewin, D. F. R. P. Burslem, N. Butt, M. Cao, D. Cardenas, G. B. Chuyong, K. Clay, S. Cordell, H. S. Dattaraja, X. Deng, M. Detto, X. Du, A. Duque, D. L. Erikson, C. E. N. Ewango, G. A. Fischer, C. Fletcher, R. B. Foster, C. P. Giardina, G. S. Gilbert, N. Gunatilleke, S. Gunatilleke, Z. Hao, W. W. Hargrove, T. B. Hart, B. C. H. Hau, F. He, F. M. Hoffman, R. W. Howe, S. P. Hubbell, F. M. Inman-Narahari, P. A. Jansen, M. Jiang,

D. J. Johnson, M. Kanzaki, A. R. Kassim, D. Kenfack, S. Kibet, M. F. Kinnaird, L. Korte, K. Kral, J. Kumar, A. J. Larson, Y. Li, X. Li, S. Liu, S. K. Y. Lum, J. A. Lutz, K. Ma, D. M. Maddalena, J.-R. Makana, Y. Malhi, T. Marthews, R. Mat Serudin, S. M. McMahon, W. J. McShea, H. R. Memiaghe, X. Mi, T. Mizuno, M. Morecroft, J. A. Myers, V. Novotny, A. A. de Oliveira, P. S. Ong, D. A. Orwig, R. Ostertag, J. den Ouden, G. G. Parker, R. P. Phillips, L. Sack, M. N. Sainge, W. Sang, K. Sri-ngernyuang, R. Sukumar, I.-F. Sun, W. Sungpalee, H. S. Suresh, S. Tan, S. C. Thomas, D. W. Thomas, J. Thompson, B. L. Turner, M. Uriarte, R. Valencia, M. I. Vallejo, A. Vicentini, T. Vrška, X. Wang, X. Wang, G. Weiblen, A. Wolf, H. Xu, S. Yap, and J. Zimmerman. 2015. CTFS-ForestGEO: a worldwide network monitoring forests in an era of global change. *Global Change Biology* 21:528-549.

Antunes, P., and A. Koyama. 2017. Mycorrhizas as nutrient and energy pumps of soil food webs: Multitrophic interactions and feedbacks. Pages 149-173 Mycorrhizal mediation of soil. Elsevier.

Bachelot, B., A. M. Alonso-Rodríguez, L. Aldrich-Wolfe, M. A. Cavaleri, S. C. Reed, and T. E. Wood. 2020. Altered climate leads to positive density-dependent feedbacks in a tropical wet forest. *Global Change Biology*. 26:3417-3428

Baddeley, A., E. Rubak, and R. Turner. 2015. Spatial point patterns: methodology and applications with R. Chapman and Hall/CRC Press.

Baldeck, C. A., K. E. Harms, J. B. Yavitt, R. John, B. L. Turner, R. Valencia, H. Navarrete, S. J. Davies, G. B. Chuyong, and D. Kenfack. 2013. Soil resources and topography shape local tree community structure in tropical forests. *Proceedings of the Royal Society B: Biological Sciences* 280:20122532.

Barber, V., G. Patrick, and B. Finney. 2000. Reduced growth of Alaskan white spruce in the twentieth century from temperature-induced drought stress. *Nature* 405:668–673.

Barton, K. 2019. MuMIn: Multi-Model Inference. R package.

Batagelj, V., and A. Mrvar. 2011. PAJEK: program for analysis and visualization of large networks. Version 2.02.

Baumgartner, K., M. P. Coetzee, and D. Hoffmeister. 2011a. Secrets of the subterranean pathosystem of *Armillaria*. *Molecular Plant Pathology* 12:515-534.

Beiler, K. J., D. M. Durall, S. W. Simard, S. A. Maxwell, and A. M. Kretzer. 2010. Architecture of the wood-wide web: *Rhizopogon* spp. genets link multiple Douglas-fir cohorts. *New Phytologist* 185:543-553.

Beiler, K. J., S. W. Simard, and D. M. Durall. 2015. Topology of tree–mycorrhizal fungus interaction networks in xeric and mesic Douglas-fir forests. *Journal of Ecology* 103:616-628.

Beiler, K. J., S. W. Simard, V. LeMay, and D. M. Durall. 2012. Vertical partitioning between sister species of *Rhizopogon* fungi on mesic and xeric sites in an interior Douglas-fir forest. *Molecular Ecology* 21:6163-6174.

Bennett, A. C., N. G. McDowell, C. D. Allen, and K. J. Anderson-Teixeira. 2015. Larger trees suffer most during drought in forests worldwide. *Nature Plants* 1:1-5.

Bennett, J. A., H. Maherali, K. O. Reinhart, Y. Lekberg, M. M. Hart, and J. Klironomos. 2017. Plant-soil feedbacks and mycorrhizal type influence temperate forest population dynamics. *Science* 355:181-184.

Bentz, B. J., J. Régnière, C. J. Fettig, E. M. Hansen, J. L. Hayes, J. A. Hicke, R. G. Kelsey, J. F. Negrón, and S. J. Seybold. 2010. Climate change and bark beetles of the western United States and Canada: direct and indirect effects. *BioScience* 60:602-613

Berg, E. E., J. David Henry, C. L. Fastie, A. D. De Volder, and S. M. Matsuoka. 2006. Spruce beetle outbreaks on the Kenai Peninsula, Alaska, and Kluane National Park and Reserve, Yukon Territory: relationship to summer temperatures and regional differences in disturbance regimes. *Forest Ecology and Management* 227:219–232.

Bergeron, Y., H. Y. H. Chen, N. C. Kenkel, A. L. Leduc, and S. E. Macdonald. 2014. Boreal mixedwood stand dynamics: ecological processes underlying multiple pathways. *The Forestry Chronicle* 90:202–213.

Bertrand, R., J.-C. Gégout, and J.-D. Bontemps. 2011. Niches of temperate tree species converge towards nutrient-richer conditions over ontogeny. *Oikos* 120:1479-1488.

Bidartondo, M., J. Baar, and T. Bruns. 2001. Low ectomycorrhizal inoculum potential and diversity from soils in and near ancient forests of bristlecone pine (*Pinus longaeva*). *Canadian Journal of Botany* 79:293-299.

Biedermann, P. H. W., J. Muller, J. C. Gregoire, A. Gruppe, J. Hagge, A. Hammerbacher, R. W. Hofstetter, D. Kandasamy, M. Kolarik, M. Kostovcik, P. Krokene, A. Salle, D. L. Six, T. Turrini, D. Vanderpool, M. J. Wingfield, and C. Bassler. 2019. Bark beetle population dynamics in the Anthropocene: challenges and solutions. *Trends in Ecology and Evolution* 34:914-924.

Bingham, M. A., and S. W. Simard. 2011. Do mycorrhizal network benefits to survival and growth of interior Douglas-fir seedlings increase with soil moisture stress? *Ecology and Evolution* **1**:306-316.

Birch, J. D., J. A. Lutz, E. Hogg, S. W. Simard, R. Pelletier, G. H. LaRoi, and J. Karst. 2019. Decline of an ecotone forest: 50 years of demography in the southern boreal forest. *Ecosphere* 10:e02698.

Bockino, N. K., and D. B. Tinker. 2012. Interactions of white pine blister rust and mountain pine beetle in Whitebark pine ecosystems in the southern Greater Yellowstone Area. *Natural Areas Journal* 32:31-40.

Bogar, L., K. Peay, A. Kornfeld, J. Huggins, S. Hortal, I. Anderson, and P. Kennedy. 2019. Plant-mediated partner discrimination in ectomycorrhizal mutualisms. *Mycorrhiza* 29:97-111.

Bonanomi, G., M. Rietkerk, S. C. Dekker, and S. Mazzoleni. 2008. Islands of fertility induce co-occurring negative and positive plant-soil feedbacks promoting coexistence. *Plant Ecology* 197:207-218.

Booth, M. G. 2004. Mycorrhizal networks mediate overstorey-understorey competition in a temperate forest. *Ecology Letters* **7**:538-546.

Booth, M. G., and J. D. Hoeksema. 2010. Mycorrhizal networks counteract competitive effects of canopy trees on seedling survival. *Ecology* 91:2294-2302.

Bottero, A., A. W. D'Amato, B. J. Palik, J. B. Bradford, S. Fraver, M. A. Battaglia, and L. A. Asherin. 2017. Density-dependent vulnerability of forest ecosystems to drought. *Journal of Applied Ecology* 54:1605-1614.

Brassard, B. W., and H. Y. H. Chen. 2006. Stand structural dynamics of North American boreal forests. *Critical Reviews in Plant Sciences* 25:115–137.

Brooks, J. R., L. B. Flanagan, and J. R. Ehleringer. 1998. Responses of boreal conifers to climate fluctuations: indications from tree–ring widths and carbon isotope analyses. *Canadian Journal of Forest Research* 28:524–533.

Brown, P. M. 1996. OLDLIST: a database of maximum tree age. *Tree rings, environment, and humanity. Radiocarbon*, *1996*: 727 - 731.

Buck, J. R., and S. B. S. Clair. 2014. Stand composition, proximity to overstory trees and gradients of soil moisture influence patterns of subalpine fir seedling emergence and survival. *Plant and Soil* 381:61-70.

Bunn, A., M. Korpela, F. Biondi, F. Campelo, P. Mérian, F. Qeadan, and C. Zang. 2017. dplR: dendrochronology program library in R. R package version 1.6.8.

Bunn, A., M. Korpela, F. Biondi, F. Campelo, P. Mérian, F. Qeadan, and C. Zang. 2019. dplR: dendrochronology program library in R. R Package version 1.7.0.

Burnham, K. P., and D. R. Anderson. 2002. A practical information-theoretic approach. Model selection and multimodel inference, 2nd ed. Springer, New York 2.

Calder, W. J., and S. B. St. Clair. 2012. Facilitation drives mortality patterns along succession gradients of aspen-conifer forests. *Ecosphere* 3:1-11.

Cale, W. G., G. M. Henebry, and J. A. Yeakley. 1989. Inferring process from pattern in natural communities. *BioScience* 39:600-605.

Callahan, B. J., P. J. McMurdie, and S. P. Holmes. 2017. Exact sequence variants should replace operational taxonomic units in marker-gene data analysis. *The ISME Journal* 11:2639-2643.

Callahan, B. J., P. J. McMurdie, M. J. Rosen, A. W. Han, A. J. A. Johnson, and S. P. Holmes. 2016a. DADA2: high-resolution sample inference from Illumina amplicon data. *Nature Methods* 13:581-583.

Callahan, B. J., K. Sankaran, J. A. Fukuyama, P. J. McMurdie, and S. P. Holmes. 2016b. Bioconductor workflow for microbiome data analysis: from raw reads to community analyses. *F1000Research* 5.

Carini, P., P. J. Marsden, J. W. Leff, E. E. Morgan, M. S. Strickland, and N. Fierer. 2016. Relic DNA is abundant in soil and obscures estimates of soil microbial diversity. *Nature Microbiology* 2:1-6.

Chagnon, P. L., R. L. Bradley, and J. N. Klironomos. 2020. Mycorrhizal network assembly in a community context: the presence of neighbours matters. *Journal of Ecology* 108:366-377.

Chase, J. M. 2003. Community assembly: when should history matter? Oecologia 136:489-498.

Chase, J. M. 2014. Spatial scale resolves the niche versus neutral theory debate. *Journal of Vegetation Science* 25:319-322.

Chase, J. M., N. J. Kraft, K. G. Smith, M. Vellend, and B. D. Inouye. 2011. Using null models to disentangle variation in community dissimilarity from variation in α-diversity. *Ecosphere* 2:1-11.

Chase, J. M., and J. A. Myers. 2011. Disentangling the importance of ecological niches from stochastic processes across scales. *Philosophical Transactions of the Royal Society B: Biological Sciences* 366:2351-2363.

Chen, L., L. S. Comita, S. J. Wright, N. G. Swenson, J. K. Zimmerman, X. Mi, Z. Hao, W. Ye, S. P. Hubbell, W. J. Kress, M. Uriarte, J. Thompson, C. J. Nytch, X. Wang, J. Lian, and K. Ma. 2018. Forest tree neighborhoods are structured more by negative conspecific density dependence than by interactions among closely related species. *Ecography* 41:1114-1123.

Chen, H. Y. H., and Y. Luo. 2015. Net aboveground biomass declines of four major forest types with forest ageing and climate change in western Canada's boreal forests. *Global Change Biology* 21:3675-3684.

Chen, H. Y., and R. V. Popadiouk. 2002. Dynamics of North American boreal mixedwoods. *Environmental Reviews* 10:137–166.

Chen, L., N. G. Swenson, N. Ji, X. Mi, H. Ren, L. Guo, and K. Ma. 2019. Differential soil fungus accumulation and density dependence of trees in a subtropical forest. *Science* 366:124-128.

Chen, P.-Y., C. Welsh, and A. Hamann. 2010. Geographic variation in growth response of Douglas-fir to interannual climate variability and projected climate change. *Global Change Biology* 16:3374-3385.

Clair, S. B. S., X. Cavard, and Y. Bergeron. 2013. The role of facilitation and competition in the development and resilience of aspen forests. *Forest Ecology and Management* 299:91-99.

Clark, J. S., D. M. Bell, M. C. Kwit, and K. Zhu. 2014. Competition-interaction landscapes for the joint response of forests to climate change. *Global Change Biology* 20:1979-1991.

Cline, E. T., J. F. Ammirati, and R. L. Edmonds. 2005. Does proximity to mature trees influence ectomycorrhizal fungus communities of Douglas-fir seedlings? *New Phytologist* 166:993-1009.

Close, D. C., C. L. Beadle, P. H. Brown, and G. K. Holz. 2000. Cold-induced photoinhibition affects establishment of *Eucalyptus nitens* (Deane and Maiden) Maiden and *Eucalyptus globulus Labill*. *Trees* 15:32-41.

Connell, J. H. 1971. On the role of natural enemies in preventing competitive exclusion in some marine animals and in rain forest trees. *Dynamics of populations* 298:312.

Cook, E. R. 1985. A time-series analysis approach to tree ring standardization. Dissertation. University of Arizona, Tuscon, Arizona, USA.

Cornett, M. W., P. B. Reich, and K. J. Puettmann. 1997. Canopy feedbacks and microtopography regulate conifer seedling distribution in two Minnesota conifer-deciduous forests. *Ecoscience* 4:353-364.

Cripps, C. L., and R. K. Antibus. 2011. Native ectomycorrhizal fungi of limber and whitebark pine: Necessary for forest sustainability? Pages 37-44 in In: Keane, Robert E.; Tomback, Diana F.; Murray, Michael P.; Smith, Cyndi M., eds. The future of high-elevation, five-needle white pines in Western North America: *Proceedings of the High Five Symposium. 28-30 June 2010; Missoula, MT. Proceedings RMRS-P-63. Fort Collins, CO: US Department of Agriculture, Forest Service, Rocky Mountain Research Station*. p. 37-44.

Cudlín, P., B. Kieliszewska-Rokicka, M. Rudawska, T. Grebenc, O. Alberton, T. Lehto, M. R. Bakker, I. Børja, B. Konôpka, and T. Leski. 2007. Fine roots and ectomycorrhizas as indicators of environmental change. *Plant Biosystems* 141:406-425.

Das, A., J. Battles, N. L. Stephenson, and P. J. van Mantgem. 2011. The contribution of competition to tree mortality in old-growth coniferous forests. *Forest Ecology and Management* 261:1203-1213.

Das, A. J., N. L. Stephenson, and K. P. Davis. 2016. Why do trees die? Characterizing the drivers of background tree mortality. *Ecology* 97:2616-2627.

Defrenne, C. E., T. J. Philpott, S. H. Guichon, W. J. Roach, B. J. Pickles, and S. W. Simard. 2019. Shifts in ectomycorrhizal fungal communities and exploration types relate to the environment and fine-root traits across interior Douglas-fir forests of western Canada. *Frontiers in Plant Science* **10**:643.

DeRose, R. J., M. F. Bekker, and J. N. Long. 2017. Traumatic resin ducts as indicators of bark beetle outbreaks. *Canadian Journal of Forest Research* 47:1168-1174.

DeRose, R. J., and J. N. Long. 2012. Factors influencing the spatial and temporal dynamics of Engelmann spruce mortality during a spruce beetle outbreak on the Markagunt Plateau, Utah. *Forest Science* 58:1-14.

Després, T., L. Vítková, R. Bače, V. Čada, P. Janda, M. Mikoláš, J. Schurman, V. Trotsiuk, and M. Svoboda. 2017. Past disturbances and intraspecific competition as drivers of spatial pattern in primary spruce forests. *Ecosphere* 8:e02037.

Dietze, M. C., and P. R. Moorcroft. 2011. Tree mortality in the eastern and central United States: patterns and drivers. *Global Change Biology* 17:3312–3326.

Diffenbaugh, N. S., and C. B. Field. 2013. Changes in ecologically critical terrestrial climate conditions. *Science* 341:486-492.

Dighton, J. 2007. 16 nutrient cycling by saprotrophic fungi in terrestrial habitats. *Environmental and Microbial Relationships* 4:287.

Dini-Andreote, F., J. C. Stegen, J. D. Van Elsas, and J. F. Salles. 2015. Disentangling mechanisms that mediate the balance between stochastic and deterministic processes in microbial succession. *Proceedings of the National Academy of Sciences* 112:E1326-E1332.

Dumbrell, A. J., M. Nelson, T. Helgason, C. Dytham, and A. H. Fitter. 2010. Relative roles of niche and neutral processes in structuring a soil microbial community. *The ISME Journal* 4:337-345.

Eckert, A. J., and B. D. Hall. 2006. Phylogeny, historical biogeography, and patterns of diversification for *Pinus* (Pinaceae): Phylogenetic tests of fossil-based hypotheses. *Molecular Phylogenetics and Evolution* 40:166-182.

Edgar, R. C. 2018. Updating the 97% identity threshold for 16S ribosomal RNA OTUs. *Bioinformatics* 34:2371-2375.

Egerton-Warburton, L. M., J. I. Querejeta, and M. F. Allen. 2007. Common mycorrhizal networks provide a potential pathway for the transfer of hydraulically lifted water between plants. *Journal of Experimental Botany* **58**:1473-1483.

Environment and Climate Change Canada (2017) Historical climate data: -- climate stations 3012205 and 3012216 – concatenated, 1961 to 2017. [Data set]. Accessed from https://climate.weather.gc.ca/historical_data/search_historic_data_e.html

Environment and Climate Change Canada (2017) Historical climate data: -- climate station 1163780– concatenated, 1951 to 2017. [Data set]. Accessed from https://climate.weather.gc.ca/historical_data/search_historic_data_e.html

Environment and Climate Change Canada. (2017). Historical climate data: -- climate station 1163780 and 1092970 – concatenated, 1911 – 2016. [Data set]. Retrieved from https://climate.weather.gc.ca/historical_data/search_historic_data_e.html

Faeth, S. H., and W. F. Fagan. 2002. Fungal endophytes: common host plant symbionts but uncommon mutualists. *Integrative and Comparative Biology* 42:360-368.

Fellbaum, C. R., J. A. Mensah, A. J. Cloos, G. E. Strahan, P. E. Pfeffer, E. T. Kiers, and H. Bücking. 2014. Fungal nutrient allocation in common mycorrhizal networks is regulated by the carbon source strength of individual host plants. *New Phytologist* 203:646-656.

Flora of North America Editorial Committee. 1993+. Flora of North America North of Mexico [Online]. Flora of North America Association.

Ford, K. R., I. K. Breckheimer, J. F. Franklin, J. A. Freund, S. J. Kroiss, A. J. Larson, E. J. Theobald, and J. HilleRisLambers. 2017. Competition alters tree growth responses to climate at individual and stand scales. *Canadian Journal of Forest Research* 47:53-62.

Fox, J., and S. Weisberg. 2018. An R companion to applied regression. Sage publications.

Frac, M., S. E. Hannula, M. Belka, and M. Jedryczka. 2018. Fungal biodiversity and their role in soil health. *Frontiers in Microbiology* 9:707.

Fraser, E. C., V. J. Lieffers, and S. M. Landhäusser. 2006. Carbohydrate transfer through root grafts to support shaded trees. *Tree Physiology* 26:1019-1023.

Fraver, S., A. W. D'Amato, J. B. Bradford, B. G. Jonsson, M. Jönsson, and P. A. Esseen. 2014. Tree growth and competition in an old-growth *Picea abies* forest of boreal Sweden: influence of tree spatial patterning. *Journal of Vegetation Science* 25:374-385.

Frelich, L. E., and P. B. Reich. 2010. Will environmental changes reinforce the impact of global warming on the prairie–forest border of central North America? *Frontiers in Ecology and the Environment* 8:371–378.

Fritts, H. C. 1976. Tree rings and climate. Academic Press, London; New York, USA.

Furniss, T. J., A. J. Larson, and J. A. Lutz. 2017. Reconciling niches and neutrality in a subalpine temperate forest. *Ecosphere* 8:e01847.

Gedalof, Z. e., and A. A. Berg. 2010. Tree ring evidence for limited direct CO2 fertilization of forests over the 20th century. *Global Biogeochemical Cycles* 24.

Gao, C., Y. Zhang, N. N. Shi, Y. Zheng, L. Chen, T. Wubet, H. Bruelheide, S. Both, F. Buscot, and Q. Ding. 2015. Community assembly of ectomycorrhizal fungi along a subtropical secondary forest succession. *New Phytologist* 205:771-785.

Gendreau-Berthiaume, B., S. E. Macdonald, and J. J. Stadt. 2016. Extended density-dependent mortality in mature conifer forests: causes and implications for ecosystem management. *Ecological Applications* 26:1486-1502.

Gehring, C. A., R. C. Mueller, K. E. Haskins, T. K. Rubow, and T. G. Whitham. 2014. Convergence in mycorrhizal fungal communities due to drought, plant competition, parasitism and susceptibility to herbivory: consequences for fungi and host plants. *Frontiers in Microbiology* 5:306.

Gibson, K., K. Skov, S. Kegley, C. Jorgensen, S. Smith, and J. Witcosky. 2008. Mountain pine beetle impacts in high-elevation five-needle pines: current trends and challenges. *US Department of Agriculture Forest Service, Northern Region, Missoula, Montana*. R1-08-020:1-32.

Glassman, S. I., K. C. Lubetkin, J. A. Chung, and T. D. Bruns. 2017a. The theory of island biogeography applies to ectomycorrhizal fungi in subalpine tree "islands" at a fine scale. *Ecosphere* 8:e01677.

Glassman, S. I., and J. B. Martiny. 2018. Broadscale ecological patterns are robust to use of exact sequence variants versus operational taxonomic units. *MSphere* 3.

Glassman, S. I., I. J. Wang, and T. D. Bruns. 2017b. Environmental filtering by pH and soil nutrients drives community assembly in fungi at fine spatial scales. *Molecular Ecology* 26:6960-6973.

Goldblum, D., and L. S. Rigg. 2005. Tree growth response to climate change at the deciduous–boreal forest ecotone, Ontario, Canada. *Canadian Journal of Forest Research* 35:2709–2718.

Goldmann, K., K. Schröter, R. Pena, I. Schöning, M. Schrumpf, F. Buscot, A. Polle, and T. Wubet. 2016. Divergent habitat filtering of root and soil fungal communities in temperate beech forests. *Scientific Reports* 6:31439.

Goslee, S. C., and D. L. Urban. 2007. The ecodist package for dissimilarity-based analysis of ecological data. *Journal of Statistical Software* 22:1-19.

Gray, L. K., and A. Hamann. 2011. Strategies for reforestation under uncertain future climates: guidelines for Alberta, Canada. *PLoS One* 6:e22977.

Gray, C. A., J. B. Runyon, M. J. Jenkins, and A. D. Giunta. 2015. Mountain pine beetles use volatile cues to locate host limber pine and avoid non-host great basin bristlecone pine. *PLoS One* 10:e0135752.

Green, D. S., and C. D. Hawkins. 2005. Competitive interactions in sub-boreal birch–spruce forests differ on opposing slope aspects. *Forest Ecology and Management* 214:1-10.

Greenwood, D. L., and P. J. Weisberg. 2008. Density-dependent tree mortality in pinyon-juniper woodlands. *Forest Ecology and Managemen*t 255:2129-2137.

Grime, J. P. 1977. Evidence for the existence of three primary strategies in plants and its relevance to ecological and evolutionary theory. *The American Naturalist* 111:1169-1194.

Grove, S., N. P. Saarman, G. S. Gilbert, B. Faircloth, K. A. Haubensak, and I. M. Parker. 2019. Ectomycorrhizas and tree seedling establishment are strongly influenced by forest edge proximity but not soil inoculum. *Ecological Applications* 29:e01867.

Hagenbo, A., J. Kyaschenko, K. E. Clemmensen, B. D. Lindahl, and P. Fransson. 2018. Fungal community shifts underpin declining mycelial production and turnover across a *Pinus sylvestris* chronosequence. *Journal of Ecology* 106:490-501.

Hamann, A., and T. Wang. 2006. Potential effects of climate change on ecosystem and tree species distribution in British Columbia. *Ecology* 87:2773-2786.

Hansen, E. M., and B. J. Bentz. 2003. Comparison of reproductive capacity among univoltine, semivoltine, and re-emerged parent spruce beetles (*Coleoptera: Scolytidae*). *The Canadian Entomologist* 135:697–712.

Hansen, E. M., B. J. Bentz, and D. L. Turner. 2001. Temperature-based model for predicting univoltine brood proportions in spruce beetle (*Coleoptera: Scolytidae*). *The Canadian Entomologist* 133:827–841.

Hervé, M. 2020. RVAideMemoire: testing and plotting procedures for biostatistics. R package version 0.9-75

Hillabrand, R. M., V. J. Lieffers, E. H. Hogg, E. Martínez-Sancho, A. Menzel, and U. G. Hacke. 2019. Functional xylem anatomy of aspen exhibits greater change due to insect defoliation than to drought. *Tree Physiology* 39:45–54.

He, F., and R. P. Duncan. 2000. Density-dependent effects on tree survival in an old-growth Douglas fir forest. *Journal of Ecology* 88:676-688.

HilleRisLambers, J., P. B. Adler, W. S. Harpole, J. M. Levine, and M. M. Mayfield. 2012. Rethinking community assembly through the lens of coexistence theory. *Annual Review of Ecology, Evolution, and Systematics* 43:227-248.

Hobbie, E. A. 2006. Carbon allocation to ectomycorrhizal fungi correlates with belowground allocation in culture studies. *Ecology* 87:563-569.

Hoff, R., R. T. Bingham, and G. McDonald. 1980. Relative blister rust resistance of white pines. *European Journal of Forest Pathology* 10:307-316.

Hogg, E. H., A. G. Barr, and T. A. Black. 2013. A simple soil moisture index for representing multi-year drought impacts on aspen productivity in the western Canadian interior. *Agricultural and Forest Meteorology* 178:173–182.

Hogg, E. H., J. P. Brandt, and B. Kochtubajda. 2002a. Growth and dieback of aspen forests in northwestern Alberta, Canada, in relation to climate and insects. *Canadian Journal of Forest Research* 32:823-832.

Hogg, E. H., M. Hart, and V. J. Lieffers. 2002b. White tree rings formed in trembling aspen saplings following experimental defoliation. *Canadian Journal of Forest Research* 32:1929-1934.

Hogg, E. H., and P. A. Hurdle. 1995. The aspen parkland in western Canada: a dry-climate analogue for the future boreal forest? *Water, Air, and Soil Pollution* 82:391–400.

Hogg, E. H., M. Michaelian, T. I. Hook, and M. E. Undershultz. 2017. Recent climatic drying leads to age-independent growth reductions of white spruce stands in western Canada. *Global Change Biology* 23:5297–5308.

Holmes, R. L. 1983. Computer-assisted quality control in tree-ring dating and measurement. *Tree-ring bulletin*.

Horner, G. J., P. J. Baker, R. Mac Nally, S. C. Cunningham, J. R. Thomson, and F. Hamilton. 2009. Mortality of developing floodplain forests subjected to a drying climate and water extraction. *Global Change Biology* 15:2176-2186.

Hortal, S., K. L. Plett, J. M. Plett, T. Cresswell, M. Johansen, E. Pendall, and I. C. Anderson. 2017. Role of plant–fungal nutrient trading and host control in determining the competitive success of ectomycorrhizal fungi. *The ISME Journal* 11:2666-2676.

Horton, B. M., M. Glen, N. J. Davidson, D. Ratkowsky, D. C. Close, T. J. Wardlaw, and C. Mohammed. 2013. Temperate eucalypt forest decline is linked to altered ectomycorrhizal communities mediated by soil chemistry. *Forest Ecology and Management* 302:329-337.

Hubbell, S. P. 2005. Neutral theory in community ecology and the hypothesis of functional equivalence. *Functional Ecology* 19:166-172.

Huang, J., J. C. Tardif, Y. Bergeron, B. Denneler, F. Berninger, and M. P. Girardin. 2010. Radial growth response of four dominant boreal tree species to climate along a latitudinal gradient in the eastern Canadian boreal forest. *Global Change Biology* 16:711–731.

Ihrmark, K., I. Bödeker, K. Cruz-Martinez, H. Friberg, A. Kubartova, J. Schenck, Y. Strid, J. Stenlid, M. Brandström-Durling, and K. E. Clemmensen. 2012. New primers to amplify the fungal ITS2 region–evaluation by 454-sequencing of artificial and natural communities. *FEMS Microbiology Ecology* 82:666-677.

Janoušková, M., P. Kohout, J. Moradi, P. Doubková, J. Frouz, S. Vosolsobě, and J. Rydlová. 2018. Microarthropods influence the composition of rhizospheric fungal communities by stimulating specific taxa. *Soil Biology and Biochemistry* 122:120-130.

Jactel, H., J. Petit, M.-L. Desprez-Loustau, S. Delzon, D. Piou, A. Battisti, and J. Koricheva. 2012. Drought effects on damage by forest insects and pathogens: a meta-analysis. *Global Change Biology* 18:267-276.

Janzen, D. H. 1970. Herbivores and the number of tree species in tropical forests. *The American Naturalist* 104:501-528.

Jobbagy, E. G., and R. B. Jackson. 2001. The distribution of soil nutrients with depth: global patterns and the imprint of plants. *Biogeochemistry* **53**:51-77.

Johnstone, J. F. 2005. Effects of aspen (*Populus tremuloides*) sucker removal on postfire conifer regeneration in central Alaska. *Canadian Journal of Forest Research* 35:483-486.

Johnson, D. J., W. T. Beaulieu, J. D. Bever, and K. Clay. 2012. Conspecific negative density dependence and forest diversity. *Science* 336:904-907.

Kalyaanamoorthy, S., B. Q. Minh, T. K. Wong, A. von Haeseler, and L. S. Jermiin. 2017. ModelFinder: fast model selection for accurate phylogenetic estimates. *Nature Methods* 14:587-589.

Karst, J., L. Marczak, M. D. Jones, and R. Turkington. 2008. The mutualism–parasitism continuum in ectomycorrhizas: a quantitative assessment using meta-analysis. *Ecology* 89:1032-1042.

Kassambara, A. 2020. ggpubr: 'ggplot2' based publication ready plots. R package version 0.2.5.

Kembel, S. W., P. D. Cowan, M. R. Helmus, W. K. Cornwell, H. Morlon, D. D. Ackerly, S. P. Blomberg, and C. O. Webb. 2010. Picante: R tools for integrating phylogenies and ecology. *Bioinformatics* 26:1463-1464.

Kenkel, N. 1988. Pattern of self-thinning in jack pine: testing the random mortality hypothesis. *Ecology* 69:1017-1024.

Kenkel, N., C. Foster, R. Caners, R. Lastra, and D. Walker. 2006. Spatial and temporal patterns of white spruce recruitment in two boreal mixedwood stands, Duck Mountains, Manitoba. *Project Report.*

Kennedy, P. G., S. Hortal, S. E. Bergemann, and T. D. Bruns. 2007. Competitive interactions among three ectomycorrhizal fungi and their relation to host plant performance. *Journal of Ecology*:1338-1345.

Kennedy, P. G., K. G. Peay, and T. D. Bruns. 2009. Root tip competition among ectomycorrhizal fungi: are priority effects a rule or an exception? *Ecology* 90:2098-2107.

Kiers, E. T., M. Duhamel, Y. Beesetty, J. A. Mensah, O. Franken, E. Verbruggen, C. R. Fellbaum, G. A. Kowalchuk, M. M. Hart, and A. Bago. 2011. Reciprocal rewards stabilize cooperation in the mycorrhizal symbiosis. *Science* 333:880-882.

Kinloch Jr, B. B. 2003. White pine blister rust in North America: past and prognosis. *Phytopathology* 93:1044-1047.

Kirchmeier-Young, M. C., N. P. Gillett, F. W. Zwiers, A. J. Cannon, and F. S. Anslow. 2018. Attribution of the influence of human-induced climate change on an extreme fire season. *Earth's Future*, 7:2-10

Klein, T., R. T. W. Siegwolf, and C. Körner. 2016. Belowground carbon trade among tall trees in a temperate forest. *Science* 352:342-344.

Klenner, W., and A. Arsenault. 2009. Ponderosa pine mortality during a severe bark beetle (*Coleoptera: Curculionidae, Scolytinae*) outbreak in southern British Columbia and implications for wildlife habitat management. *Forest Ecology and Management* 258:S5-S14.

Klos, R. J., G. G. Wang, W. L. Bauerle, and J. R. Rieck. 2009. Drought impact on forest growth and mortality in the southeast USA: an analysis using forest health and monitoring data. *Ecological Applications* 19:699-708.

Kobe, R. K. 1996. Intraspecific variation in sapling mortality and growth predicts geographic variation in forest composition. *Ecological Monographs* 66:181–201.

Kolaříková, Z., P. Kohout, C. Krüger, M. Janoušková, L. Mrnka, and J. Rydlová. 2017. Root-associated fungal communities along a primary succession on a mine spoil: distinct ecological guilds assemble differently. *Soil Biology and Biochemistry* 113:143-152.

Koyama, A., B. Harlow, and R. D. Evans. 2019. Greater soil carbon and nitrogen in a Mojave Desert ecosystem after 10 years exposure to elevated CO2. *Geoderma* 355:113915.

Kretzer, A. M., S. Dunham, R. Molina, and J. W. Spatafora. 2004. Microsatellite markers reveal the below ground distribution of genets in two species of *Rhizopogon* forming tuberculate ectomycorrhizas on Douglas fir. *New Phytologist* 161:313-320.

Kretzer, A. M., D. L. Luoma, R. Molina, and J. W. Spatafora. 2003. Taxonomy of the *Rhizopogon vinicolor* species complex based on analysis of ITS sequences and microsatellite loci. *Mycologia* 95:480-487.

Kyaschenko, J., K. E. Clemmensen, A. Hagenbo, E. Karltun, and B. D. Lindahl. 2017. Shift in fungal communities and associated enzyme activities along an age gradient of managed *Pinus sylvestris* stands. *The ISME Journal* 11:863-874.

Larsson, L. Å. 2018. Coorecorder. Cybis Elektronick & Data AB, Saltsjobaden, Sweden.

LeDuc, S. D., E. A. Lilleskov, T. R. Horton, and D. E. Rothstein. 2013. Ectomycorrhizal fungal succession coincides with shifts in organic nitrogen availability and canopy closure in post-wildfire jack pine forests. *Oecologia* 172:257-269.

Liang, M., D. Johnson, D. F. Burslem, S. Yu, M. Fang, J. D. Taylor, A. F. Taylor, T. Helgason, and X. Liu. 2020. Soil fungal networks maintain local dominance of ectomycorrhizal trees. *Nature Communications* 11:1-7.

Lindahl, B. D., and A. Tunlid. 2015. Ectomycorrhizal fungi – potential organic matter decomposers, yet not saprotrophs. *New Phytologist* 205:1443-1447.

Leibold, M. A., and M. A. McPeek. 2006. Coexistence of the niche and neutral perspectives in community ecology. *Ecology* 87:1399-1410.

Lindenmayer, D. B., and W. F. Laurance. 2017. The ecology, distribution, conservation and management of large old trees. *Biological Reviews* 92:1434-1458.

Lindenmayer, D. B., W. F. Laurance, and J. F. Franklin. 2012. Global decline in large old trees. *Science* 338:1305-1306.

Li, P., W. Li, A. J. Dumbrell, M. Liu, G. Li, M. Wu, C. Jiang, and Z. Li. 2020. Spatial variation in soil fungal communities across paddy fields in subtropical China. *mSystems* 5.

Lerat, S., R. Gauci, J. G. Catford, H. Vierheilig, Y. Piché, and L. Lapointe. 2002. 14 C transfer between the spring ephemeral *Erythronium americanum* and sugar maple saplings via arbuscular mycorrhizal fungi in natural stands. *Oecologia* 132:181-187.

Lev-Yadun, S. 2011. Why should trees have natural root grafts? *Tree Physiology* 31:575-578.

Li, Y., D. Sun, D. Li, Z. Xu, C. Zhao, H. Lin, and Q. Liu. 2015. Effects of warming on ectomycorrhizal colonization and nitrogen nutrition of *Picea asperata* seedlings grown in two contrasting forest ecosystems. *Scientific Reports* 5:17546.

Liang, Y., M. J. Duveneck, E. J. Gustafson, J. M. Serra-Diaz, and J. R. Thompson. 2018. How disturbance, competition, and dispersal interact to prevent tree range boundaries from keeping pace with climate change. *Global Change Biology* 24:e335-e351.

Linares, J. C., J. J. Camarero, and J. A. Carreira. 2010. Competition modulates the adaptation capacity of forests to climatic stress: insights from recent growth decline and death in relict stands of the Mediterranean fir *Abies pinsapo*. *Journal of Ecology* 98:592-603.

Lutz, J. A. 2015. The evolution of long-term data for forestry: large temperate research plots in an era of global change. *Northwest Science* 89:255-269.

Lutz, J. A., T. J. Furniss, D. J. Johnson, S. J. Davies, D. Allen, A. Alonso, K. J. Anderson-Teixeira, A. Andrade, J. Baltzer, K. M. L. Becker, E. M. Blomdahl, N. A. Bourg, S. Bunyavejchewin, D. F. R. P. Burslem, C. A. Cansler, K. Cao, M. Cao, D. Cárdenas, L.-W. Chang, K.-J. Chao, W.-C. Chao, J.-M. Chiang, C. Chu, G. B. Chuyong, K. Clay, R. Condit, S. Cordell, H. S. Dattaraja, A. Duque, C. E. N. Ewango, G. A. Fischer, C. Fletcher, J. A. Freund, C. Giardina, S. J. Germain, G. S. Gilbert, Z. Hao, T. Hart, B. C. H. Hau, F. He, A. Hector, R. W. Howe, C.-F. Hsieh, Y.-H. Hu, S. P. Hubbell, F. M. Inman-Narahari, A. Itoh, D. Janík, A. R. Kassim, D. Kenfack, L. Korte, K. Král, A. J. Larson, Y. Li, Y. Lin, S. Liu, S. Lum, K. Ma, J.-R. Makana, Y. Malhi, S. M. McMahon, W. J. McShea, H. R. Memiaghe, X. Mi, M. Morecroft, P. M. Musili, J. A. Myers, V. Novotny, A. de Oliveira, P. Ong, D. A. Orwig, R. Ostertag, G. G. Parker, R. Patankar, R. P. Phillips, G. Reynolds, L. Sack, G.-Z. M. Song, S.-H. Su, R. Sukumar, I.-F. Sun, H. S.

Suresh, M. E. Swanson, S. Tan, D. W. Thomas, J. Thompson, M. Uriarte, R. Valencia, A. Vicentini, T. Vrška, X. Wang, G. D. Weiblen, A. Wolf, S.-H. Wu, H. Xu, T. Yamakura, S. Yap, and J. K. Zimmerman. 2018. Global importance of large-diameter trees. *Global Ecology and Biogeography* 27:849-864.

Lutz, J. A., A. J. Larson, T. J. Furniss, D. C. Donato, J. A. Freund, M. E. Swanson, K. J. Bible, J. Chen, and J. F. Franklin. 2014. Spatially nonrandom tree mortality and ingrowth maintain equilibrium pattern in an old-growth *Pseudotsuga–Tsuga* forest. *Ecology* 95:2047-2054.

Mathys, A. S., N. C. Coops, and R. H. Waring. 2017. An ecoregion assessment of projected tree species vulnerabilities in western North America through the 21st century. *Global Change Biology* 23:920-932.

McDowell, N. G. 2011. Mechanisms linking drought, hydraulics, carbon metabolism, and vegetation mortality. *Plant Physiology* 155:1051-1059.

McKenney, D. W., J. H. Pedlar, K. Lawrence, K. Campbell, and M. F. Hutchinson. 2007. Potential impacts of climate change on the distribution of North American trees. *BioScience* 57:939-948.

McMurdie, P. J., and S. Holmes. 2013. phyloseq: an R package for reproducible interactive analysis and graphics of microbiome census data. *PLoS One* 8:e61217.

Meko, D. M., R. Touchan, and K. J. Anchukaitis. 2011. Seascorr: A MATLAB program for identifying the seasonal climate signal in an annual tree-ring time series. *Computers & Geosciences* **37**:1234-1241.

Metsaranta, J. M., and V. J. Lieffers. 2008. A fifty-year reconstruction of annual changes in the spatial distribution of *Pinus banksiana* stands: does pattern fit competition theory? Plant Ecology 199:137-152.

Michaelian, M., E. H. Hogg, R. J. Hall, and E. Arsenault. 2011. Massive mortality of aspen following severe drought along the southern edge of the Canadian boreal forest. *Global Change Biology* 17:2084-2094.

Minh, B. Q., H. A. Schmidt, O. Chernomor, D. Schrempf, M. D. Woodhams, A. Von Haeseler, and R. Lanfear. 2020. IQ-TREE 2: new models and efficient methods for phylogenetic inference in the genomic era. *Molecular Biology and Evolution* 37:1530-1534.

Moeur, M. 1993. Characterizing spatial patterns of trees using stem-mapped data. *Forest Science* 39:756-775.

Molles, M. 2015. Ecology: concepts and applications. McGraw-Hill Education.

Moulinier, J., F. Lorenzetti, and Y. Bergeron. 2014. Growth and mortality of trembling aspen (*Populus tremuloides*) in response to artificial defoliation. *Acta Oecologica* 55:104–112.

Murali, A., A. Bhargava, and E. S. Wright. 2018. IDTAXA: a novel approach for accurate taxonomic classification of microbiome sequences. *Microbiome* 6:1-14.

Mujic, A. B., D. M. Durall, J. W. Spatafora, and P. G. Kennedy. 2016. Competitive avoidance not edaphic specialization drives vertical niche partitioning among sister species of ectomycorrhizal fungi. *New Phytologist* 209:1174-1183.

Mujic, A. B., B. Huang, M.-J. Chen, P.-H. Wang, D. S. Gernandt, K. Hosaka, and J. W. Spatafora. 2019. Out of western North America: Evolution of the *Rhizopogon*-

Pseudotsuga symbiosis inferred by genome-scale sequence typing. *Fungal Ecology* 39:12-25.

Munkvold, L., R. Kjøller, M. Vestberg, S. Rosendahl, and I. Jakobsen. 2004. High functional diversity within species of arbuscular mycorrhizal fungi. *New Phytologist* 164:357-364.

Nara, K. 2006. Ectomycorrhizal networks and seedling establishment during early primary succession. *New Phytologist* 169:169-178.

Natural Climatic Data Center. (2020). State divisional data. U.S. Department of Commerce. [Data set]. Accessed on Sept 25, 2020 from https://www7.ncdc.noaa.gov/CDO/CDODivisionalSelect.jsp#

Natural Resources Conservation Service. (2020). Utah SNOTEL climate records: -- climate station 332 and 1154. [Data set]. US Department of Agriculture.

Nguyen, N. H., Z. Song, S. T. Bates, S. Branco, L. Tedersoo, J. Menke, J. S. Schilling, and P. G. Kennedy. 2016. FUNGuild: an open annotation tool for parsing fungal community datasets by ecological guild. *Fungal Ecology* 20:241-248.

Nilsson, R. H., K.-H. Larsson, A. F. S. Taylor, J. Bengtsson-Palme, T. S. Jeppesen, D. Schigel, P. Kennedy, K. Picard, F. O. Glöckner, and L. Tedersoo. 2019. The UNITE database for molecular identification of fungi: handling dark taxa and parallel taxonomic classifications. *Nucleic Acids Research* 47:D259-D264.

Odriozola, I., T. Martinovic, B. D. Bahnmann, D. Ryšánek, T. Mašínová, P. Sedlák, K. Merunková, P. Kohout, M. Tomšovský, and P. Baldrian. 2020. Stand age affects fungal community composition in a Central European temperate forest. *Fungal Ecology* 48:100985.

Oksanen, J., F. G. Blanchet, M. Friendly, R. Kindt, P. Legendre, D. McGlinn, P. R. Minchin, R. B. O'Hara, G. L. Simpson, P. Solymos, M. H. H. Stevens, E. Szoecs, and H. Wagner. 2018. vegan: community ecology package. R package version 2.5–2.

Ouimette, A. P., S. V. Ollinger, L. C. Lepine, R. B. Stephens, R. J. Rowe, M. A. Vadeboncoeur, S. J. Tumber-Davila, and E. A. Hobbie. 2019. Accounting for carbon flux to mycorrhizal fungi may resolve discrepancies in forest carbon budgets. *Ecosystems*:1-15.

Pachauri, R. K., M. R. Allen, V. R. Barros, J. Broome, W. Cramer, R. Christ, J. A. Church, L. Clarke, Q. Dahe, and P. Dasgupta. 2014. Climate change 2014: synthesis report. Contribution of Working Groups I, II and III to the fifth assessment report of the Intergovernmental Panel on Climate Change. *IPCC*.

Pallardy, S. G. 2010. Physiology of woody plants. Academic Press.

Paradis, E., and K. Schliep. 2019. ape 5.0: an environment for modern phylogenetics and evolutionary analyses in R. *Bioinformatics* 35:526-528.

Peay, K. G., P. G. Kennedy, and T. D. Bruns. 2011. Rethinking ectomycorrhizal succession: are root density and hyphal exploration types drivers of spatial and temporal zonation? *Fungal Ecology* 4:233-240.

Pebesma, E. J. 2004. Multivariable geostatistics in S: the gstat package. *Computers & Geosciences* **30**:683-691.

Pec, G. J., J. Karst, D. L. Taylor, P. W. Cigan, N. Erbilgin, J. E. Cooke, S. W. Simard, and J. F. Cahill Jr. 2017. Change in soil fungal community structure driven by a decline in ectomycorrhizal fungi following a mountain pine beetle (*Dendroctonus ponderosae*) outbreak. *New Phytologist* 213:864-873.

Peri, P. L., V. Gargaglione, and G. M. Pastur. 2006. Dynamics of above- and below-ground biomass and nutrient accumulation in an age sequence of *Nothofagus antarctica* forest of southern Patagonia. *Forest Ecology and Management* 233:85-99.

Pena, R., J. Tejedor, B. Zeller, M. Dannenmann, and A. Polle. 2013. Interspecific temporal and spatial differences in the acquisition of litter-derived nitrogen by ectomycorrhizal fungal assemblages. *New Phytologist* 199:520-528.

Peng, C., Z. Ma, X. Lei, Q. Zhu, H. Chen, W. Wang, S. Liu, W. Li, X. Fang, and X. Zhou. 2011. A drought-induced pervasive increase in tree mortality across Canada's boreal forests. *Nature Climate Change* 1:467–471.

Percival, D. B., and W. L. B. Constantine. 2006. Exact simulation of gaussian time series from nonparametric spectral estimates with application to bootstrapping. *Statistics and Computing* 16:25–35.

Peterson, C. J., and E. R. Squiers. 1995. Competition and succession in an aspen-white-pine forest. *Journal of Ecology*:449-457.

Philip, L., S. Simard, and M. Jones. 2010. Pathways for below-ground carbon transfer between paper birch and Douglas-fir seedlings. *Plant Ecology & Diversity* 3:221-233.

Pickles, B. J., R. Wilhelm, A. K. Asay, A. S. Hahn, S. W. Simard, and W. W. Mohn. 2017. Transfer of 13C between paired Douglas-fir seedlings reveals plant kinship effects and uptake of exudates by ectomycorrhizas. *New Phytologist* 214:400-411.

Poorter, H., K. J. Niklas, P. B. Reich, J. Oleksyn, P. Poot, and L. Mommer. 2012. Biomass allocation to leaves, stems and roots: meta-analyses of interspecific variation and environmental control. *New Phytologist* 193:30-50.

R Core Team. 2018. R: A language and environment for statistical computing. The R Foundation. Version 3.50.

R Core Team. 2019. R: A language and environment for statistical computing. The R Foundation. Version 3.6.1

R Core Team. 2019. R: A language and environment for statistical computing. The R Foundation. Version 3.6.2.

R Core Team. 2020. R: A language and environment for statistical computing. The R Foundation. Version 4.0.2.

Rengel, Z. 2011. Soil pH, soil health and climate change. *Soil health and climate change*. Springer.

Richardson, A. 2000. Coarse root elongation rate estimates for interior Douglas-fir. *Tree Physiology* 20:825-829.

Richardson, A. D., C. B. Statland, and T. G. Gregoire. 2003. Root biomass distribution under three cover types in a patchy *Pseudotsuga menziesii* forest in western Canada. *Annals of Forest Science* 60:469-474.

Richter-Heitmann, T., B. Hofner, F.-S. Krah, J. Sikorski, P. K. Wüst, B. Bunk, S. Huang, K. M. Regan, D. Berner, and R. S. Boeddinghaus. 2020. Stochastic dispersal rather than deterministic selection explains the spatio-temporal distribution of soil bacteria in a temperate grassland. *Frontiers in Microbiology* 11:1391.

R Studio Team. 2020. RStudio: Integrated Development for R. Version 1.3.1056.

Rudawska, M., R. Wilgan, D. Janowski, M. Iwański, and T. Leski. 2018. Shifts in taxonomical and functional structure of ectomycorrhizal fungal community of Scots pine (*Pinus sylvestris L.*) underpinned by partner tree ageing. *Pedobiologia* 71:20-30.

Salley, S. W., J. E. Herrick, C. V. Holmes, J. W. Karl, M. R. Levi, S. E. McCord, C. van der Waal, and J. W. Van Zee. 2018. A comparison of soil texture-by-feel estimates: implications for the citizen soil scientist. *Soil Science Society of America Journal* 82:1526-1537.

Salomón, R. L., E. Tarroux, and A. DesRochers. 2016. Natural root grafting in *Picea mariana* to cope with spruce budworm outbreaks. *Canadian Journal of Forest Research* 46:1059-1066.

Sayers, E. W., J. Beck, J. R. Brister, E. E. Bolton, K. Canese, D. C. Comeau, K. Funk, A. Ketter, S. Kim, and A. Kimchi. 2020. Database resources of the national center for biotechnology information. *Nucleic Acids Research* **48**:D9.

Scheffer, M., M. Hirota, M. Holmgren, E. H. Van Nes, and F. S. Chapin. 2012. Thresholds for boreal biome transitions. *Proceedings of the National Academy of Sciences* 109:21384–21389.

Schiestl-Aalto, P., K. Ryhti, A. Mäkelä, M. Peltoniemi, J. Bäck, and L. Kulmala. 2019. Analysis of the NSC storage dynamics in tree organs reveals the allocation to belowground symbionts in the framework of whole tree carbon balance. *Frontiers in Forests and Global Change* 2.

Schliep, K. P. 2011. phangorn: phylogenetic analysis in R. *Bioinformatics* 27:592-593.

Schloerke, B., D. Cook, J. Larmarange, F. Briatte, M. Marbach, E. Thoen, A. Elberg, and J. Crowley. 2020. GGally: extension to 'ggplot2'. R package version 1.5.0.

Schoettle, A. 2004. Ecological roles of five-needle pine in Colorado: potential consequences of their loss. *Breeding and genetic resources of five-needle pines: growth, adaptability and pest resistance*. *USDA Forest Service, Rocky Mountain Research Station*:124-135.

Schwandt, J. W., I. B. Lockman, J. T. Kliejunas, and J. A. Muir. 2010. Current health issues and management strategies for white pines in the western United States and Canada. *Forest Pathology* 40:226-250.

Segnitz, R. M., S. E. Russo, S. J. Davies, and K. G. Peay. 2020. Ectomycorrhizal fungi drive positive phylogenetic plant–soil feedbacks in a regionally dominant tropical plant family. *Ecology* 101:e03083.

Serra-Diaz, J. M., R. M. Scheller, A. D. Syphard, and J. Franklin. 2015. Disturbance and climate microrefugia mediate tree range shifts during climate change. *Landscape Ecology* 30:1039-1053.

Simard, S., A. Asay, K. Beiler, M. Bingham, J. Deslippe, X. He, L. Philip, Y. Song, and F. Teste. 2015. Resource transfer between plants through ectomycorrhizal fungal networks. Pages 133-176 *in* T. R. Horton, editor. *Mycorrhizal Networks*. Springer Netherlands, Dordrecht.

Simard, S., and A. Vyse. 2006. Trade-offs between competition and facilitation: a case study of vegetation management in the interior cedar–hemlock forests of southern British Columbia. *Canadian Journal of Forest Research* 36:2486-2496.

Simard, S. W., D. A. Perry, M. D. Jones, D. D. Myrold, D. M. Durall, and R. Molina. 1997. Net transfer of carbon between ectomycorrhizal tree species in the field. *Nature* 388:579-582.

Shemesh, H., B. E. Boaz, C. I. Millar, and T. D. Bruns. 2020. Symbiotic interactions above treeline of long-lived pines: mycorrhizal advantage of limber pine (*Pinus flexilis*) over Great Basin bristlecone pine (*Pinus longaeva*) at the seedling stage. *Journal of Ecology* 108:908-916.

Smith, J. H. G. 1964. Root spread can be estimated from crown width of Douglas Fir, lodgepole pine, and other British Columbia tree species. *The Forestry Chronicle* 40:456-473.

Smith, S. E., and D. J. Read. 2010. Mycorrhizal symbiosis. Academic press.

Smithers, B. V., M. P. North, C. I. Millar, and A. M. Latimer. 2018. Leap frog in slow motion: divergent responses of tree species and life stages to climatic warming in Great Basin subalpine forests. *Global Change Biology* 24:e442-e457.

Solly, E. F., I. Brunner, H.-S. Helmisaari, C. Herzog, J. Leppälammi-Kujansuu, I. Schöning, M. Schrumpf, F. H. Schweingruber, S. E. Trumbore, and F. Hagedorn. 2018. Unravelling the age of fine roots of temperate and boreal forests. *Nature Communications* 9:1-8.

Soja, A. J., N. M. Tchebakova, N. H. French, M. D. Flannigan, H. H. Shugart, B. J. Stocks, A. I. Sukhinin, E. I. Parfenova, F. S. Chapin III, and P. W. Stackhouse Jr. 2007. Climate-induced boreal forest change: predictions versus current observations. *Global and Planetary Change* 56:274–296.

Song, Y. Y., S. W. Simard, A. Carroll, W. W. Mohn, and R. S. Zeng. 2015. Defoliation of interior Douglas-fir elicits carbon transfer and stress signalling to ponderosa pine neighbors through ectomycorrhizal networks. *Scientific Reports* 5:8495.

Speer, J. H. 2010. Fundamentals of tree-ring research. University of Arizona Press, Tucson, Arizona, USA.

Stegen, J. C., X. Lin, J. K. Fredrickson, X. Chen, D. W. Kennedy, C. J. Murray, M. L. Rockhold, and A. Konopka. 2013. Quantifying community assembly processes and identifying features that impose them. *The ISME Journal* 7:2069-2079.

Stegen, J. C., X. Lin, J. K. Fredrickson, and A. E. Konopka. 2015. Estimating and mapping ecological processes influencing microbial community assembly. *Frontiers in Microbiology* 6:370.

Stegen, J. C., X. Lin, A. E. Konopka, and J. K. Fredrickson. 2012. Stochastic and deterministic assembly processes in subsurface microbial communities. *The ISME Journal* 6:1653-1664.

Steinberg, P.D. (2002). *Pseudotsuga menziesii* var. *glauca*. In: Fire Effects Information System, [Online]. U.S. Department of Agriculture, Forest Service, Rocky Mountain Research Station, Fire Sciences Laboratory (Producer). Available: https://www.fs.fed.us /database/feis/plants/tree/psemeng/all.html

Stokes, M., and T. Smiley. 1996. An introduction to tree-ring dating. University of Arizona Press, Tuscon, Arizona, USA.

Swaty, R. L., R. J. Deckert, T. G. Whitham, and C. A. Gehring. 2004. Ectomycorrhizal abundance and community composition shifts with drought: predictions from tree rings. *Ecology* 85:1072-1084.

Symonds, M. R. E., and A. Moussalli. 2011. A brief guide to model selection, multimodel inference and model averaging in behavioural ecology using Akaike's information criterion. *Behavioral Ecology and Sociobiology* 65:13-21.

Tang, J., S. Luyssaert, A. D. Richardson, W. Kutsch, and I. A. Janssens. 2014. Steeper declines in forest photosynthesis than respiration explain age-driven decreases in forest growth. *Proceedings of the National Academy of Sciences* 111:8856-8860.

Tedersoo, L., M. Bahram, S. Põlme, U. Kõljalg, N. S. Yorou, R. Wijesundera, L. V. Ruiz, A. M. Vasco-Palacios, P. Q. Thu, and A. Suija. 2014. Global diversity and geography of soil fungi. *Science* 346.

Terhonen, E., K. Blumenstein, A. Kovalchuk, and F. O. Asiegbu. 2019. Forest tree microbiomes and associated fungal endophytes: functional roles and impact on forest health. *Forests* 10:42.

Teste, F. P., and S. W. Simard. 2008. Mycorrhizal networks and distance from mature trees alter patterns of competition and facilitation in dry Douglas-fir forests. *Oecologia* 158:193-203.

Teste, F. P., S. W. Simard, and D. M. Durall. 2009. Role of mycorrhizal networks and tree proximity in ectomycorrhizal colonization of planted seedlings. *Fungal Ecology* 2:21-30.

Teste, F. P., S. W. Simard, D. M. Durall, R. D. Guy, and S. M. Berch. 2010. Net carbon transfer between *Pseudotsuga menziesii var. glauca* seedlings in the field is influenced by soil disturbance. *Journal of Ecology* 98:429-439.

Teste, F. P., S. W. Simard, D. M. Durall, R. D. Guy, M. D. Jones, and A. L. Schoonmaker. 2009. Access to mycorrhizal networks and roots of trees: importance for seedling survival and resource transfer. *Ecology* 90:2808-2822.

Terrer, C., S. Vicca, B. A. Hungate, R. P. Phillips, and I. C. Prentice. 2016. Mycorrhizal association as a primary control of the CO_2 fertilization effect. *Science* 353:72-74.

Tilman, D. 1982. Resource competition and community structure. Princeton University Press, Princeton, New Jersey.

Tomback, D. F., and P. Achuff. 2010. Blister rust and western forest biodiversity: ecology, values and outlook for white pines. *Forest Pathology* 40:186-225.

Tomback, D. F., P. Achuff, A. W. Schoettle, J. W. Schwandt, and R. J. Mastrogiuseppe. 2011. The magnificent high-elevation five-needle white pines: ecological roles and future outlook. Pages 2-28 in In: Keane, Robert E.; Tomback, Diana F.; Murray, Michael P.; Smith, Cyndi M., eds. *The future of high-elevation, five-needle white pines in Western North America: Proceedings of the High Five Symposium. 28-30 June 2010; Missoula, MT. Proceedings RMRS-P-63. Fort Collins, CO: US Department of Agriculture, Forest Service, Rocky Mountain Research Station.* p. 2-28.

Trant, A., E. Higgs, and B. M. Starzomski. 2020. A century of high elevation ecosystem change in the Canadian Rocky Mountains. *Scientific Reports* 10:1-10.

Trappe, J. M. 1977. Selection of fungi for ectomycorrhizal inoculation in nurseries. *Annual Review of Phytopathology* 15:203-222.

Treseder, K. K., M. F. Allen, R. W. Ruess, K. S. Pregitzer, and R. L. Hendrick. 2005. Lifespans of fungal rhizomorphs under nitrogen fertilization in a pinyon-juniper woodland. *Plant and Soil* 270:249-255.

Trugman, A. T., M. Detto, M. K. Bartlett, D. Medvigy, W. R. L. Anderegg, C. Schwalm, B. Schaffer, and S. W. Pacala. 2018. Tree carbon allocation explains forest drought-kill and recovery patterns. *Ecology Letters* 21:1552-1560.

Twieg, B. D., D. M. Durall, and S. W. Simard. 2007. Ectomycorrhizal fungal succession in mixed temperate forests. *New Phytologist* 176:437-447.

Tucker, C. M., and T. Fukami. 2014. Environmental variability counteracts priority effects to facilitate species coexistence: evidence from nectar microbes. *Proceedings of the Royal Society B*: Biological Sciences 281:20132637.

Turner, M. G., W. L. Baker, C. J. Peterson, and R. K. Peet. 1998. Factors influencing succession: lessons from large, infrequent natural disturbances. *Ecosystems* 1:511-523.

Ung, C.-H., P. Bernier, and X.-J. Guo. 2008. Canadian national biomass equations: new parameter estimates that include British Columbia data. *Canadian Journal of Forest Research* 38:1123–1132.

van der Heijden, M. G. A., and T. R. Horton. 2009. Socialism in soil? The importance of mycorrhizal fungal networks for facilitation in natural ecosystems. *Journal of Ecology* 97:1139-1150.

Van Dorp, C. H., S. W. Simard, and D. M. Durall. 2020. Resilience of *Rhizopogon*-Douglas-fir mycorrhizal networks 25 years after selective logging. *Mycorrhiza* 30:467-474.

van Mantgem, P. J., N. L. Stephenson, J. C. Byrne, L. D. Daniels, J. F. Franklin, P. Z. Fulé, M. E. Harmon, A. J. Larson, J. M. Smith, A. H. Taylor, and T. T. Veblen. 2009. Widespread increase of tree mortality rates in the western United States. *Science* 323:521-524.

Větrovský, T., P. Kohout, M. Kopecký, A. Machac, M. Man, B. D. Bahnmann, V. Brabcová, J. Choi, L. Meszárošová, and Z. R. Human. 2019. A meta-analysis of global fungal distribution reveals climate-driven patterns. *Nature Communications* 10:1-9.

Vila-Cabrera, A., A. C. Premoli, and A. S. Jump. 2019. Refining predictions of population decline at species' rear edges. *Global Change Biology* 25:1549-1560.

von Liebig, J. F. 1840. Die organische Chemie in ihrer Anwendung auf Agricultur und Physiologie. F. Vieweg und Sohn.

Wang, T., A. Hamann, D. Spittlehouse, and C. Carroll. 2016. Locally downscaled and spatially customizable climate data for historical and future periods for North America. *PLoS One* 11:e0156720.

Wang, P., S. P. Li, X. Yang, J. Zhou, W. Shu, and L. Jiang. 2020. Mechanisms of soil bacterial and fungal community assembly differ among and within islands. *Environmental Microbiology* 22:1559-1571.

Warren, J. M., J. R. Brooks, F. C. Meinzer, and J. L. Eberhart. 2008. Hydraulic redistribution of water from *Pinus ponderosa* trees to seedlings: evidence for an ectomycorrhizal pathway. *New Phytologist* 178:382-394.

Weiner, J., and C. Damgaard. 2006. Size-asymmetric competition and size-asymmetric growth in a spatially explicit zone-of-influence model of plant competition. *Ecological Research* 21:707-712.

Wei, T., and V. Simko. 2017. R package "corrplot": visualization of a correlation matrix. R package version 0.84.

Werner, G. D., and E. T. Kiers. 2015. Partner selection in the mycorrhizal mutualism. *New Phytologist* 205:1437-1442.

White, T. J., T. Bruns, S. Lee, and J. Taylor. 1990. Amplification and direct sequencing of fungal ribosomal RNA genes for phylogenetics. *PCR protocols: a guide to methods and applications* 18:315-322.

Wickham, H. 2011. The split-apply-combine strategy for data analysis. *Journal of Statistical Software* 40:1-29.

Wickham, H. 2016. ggplot2: elegant graphics for data analysis. Springer.

Wiegand, T., and K. A. Moloney. 2004. Rings, circles, and null-models for point pattern analysis in ecology. *Oikos* 104:209-229.

Williams, A. P., C. Xu, and N. G. McDowell. 2011. Who is the new sheriff in town regulating boreal forest growth? *Environmental Research Letters* 6:041004.

Worrall, J. J., G. E. Rehfeldt, A. Hamann, E. H. Hogg, S. B. Marchetti, M. Michaelian, and L. K. Gray. 2013. Recent declines of *Populus tremuloides* in North America linked to climate. *Forest Ecology and Management* 299:35-51.

Wright, E. S. 2016. Using DECIPHER v2. 0 to analyze big biological sequence data in R. *R Journal* 8.

Wu, Y. T., T. Wubet, S. Trogisch, S. Both, T. Scholten, H. Bruelheide, and F. Buscot. 2013. Forest age and plant species composition determine the soil fungal community composition in a Chinese subtropical forest. *PLoS One* 8:e66829.

Wubet, T., S. Christ, I. Schöning, S. Boch, M. Gawlich, B. Schnabel, M. Fischer, and F. Buscot. 2012. Differences in soil fungal communities between European beech (*Fagus sylvatica L.*) dominated forests are related to soil and understory vegetation. *PLoS One* 7:e47500.

Young, D. J., J. T. Stevens, J. M. Earles, J. Moore, A. Ellis, A. L. Jirka, and A. M. Latimer. 2017. Long-term climate and competition explain forest mortality patterns under extreme drought. *Ecology Letters* 20:78-86.

Zang, C., and F. Biondi. 2015. treeclim: an R package for the numerical calibration of proxy-climate relationships. *Ecography* 38:431-436.

Zhang, J., S. Huang, and F. He. 2015. Half-century evidence from western Canada shows forest dynamics are primarily driven by competition followed by climate. *Proceedings of the National Academy of Science*s 112:4009-4014.

Zhang, T., N.-F. Wang, H.-Y. Liu, Y.-Q. Zhang, and L.-Y. Yu. 2016. Soil pH is a key determinant of soil fungal community composition in the Ny-Ålesund Region, Svalbard (high Arctic). *Frontiers in Microbiology* 7:227.

Zinke, P. J. 1962. The pattern of influence of individual forest trees on soil properties. *Ecology* 43:130-133.

Appendices

Appendix 2.1

TABLES

Table S2.1 The number of trees sampled for increment cores within the George LaRoi forest plot; Alberta, Canada. Two cores were taken per tree to allow for crossdating between cores from the same tree.

Species	Number of trees sampled	Number of core samples	% of remaining population sampled
Picea glauca	25	50	4%
Populus tremuloides	18	36	10%
Betula papyrifera	12	24	23%
Pinus banksiana	22	44	53%

Table S2.2 COFECHA statistics for the tree cores used for climate analysis of trees in the George LaRoi forest plot; Alberta, Canada. The complacency of *Pinus banksiana* resulted in several anomalous segments from poorly responsive trees.

	Picea glauca	*Populus tremuloides*	*Betula papyrifera*	*Pinus banksiana*
Number of dated series	42	27	18	21
Master series range	1925–2017 (92 years)	1930–2017 (87 years)	1925–2017 (92 years)	1930–2017 (87 years)
Total rings in all series	2471	2019	1468	1201
Total dated rings checked	2456	2018	1468	1199
Series intercorrelation	0.666	0.639	0.772	0.534
Average mean sensitivity	0.304	0.421	0.47	0.225
Segments, possible problems	0	0	0	3
Mean length of series	58.8	74.8	81.6	57.2

Table S2.3 Annually compounded rates of mortality (Mort.) and recruitment (Recr.) for each census interval of the George LaRoi forest plot; Alberta, Canada. Years refer to 1967, 1977, 1988, 1997, and 2017.

	Picea glauca		*Populus tremuloides*		*Betula papyrifera*		*Pinus banksiana*	
Year	Mort.	Recr.	Mort.	Recr.	Mort.	Recr.	Mort.	Recr.
67–77	0.34	1.01	1.96	0.46	3.63	0.38	0.98	0.00
77–88	0.99	1.69	3.95	0.14	2.32	0.61	2.18	0.00
88–97	1.48	0.50	6.15	0.03	3.68	1.57	1.67	0.00
97–17	5.94	0.35	5.32	0.13	3.72	0.69	2.38	0.07

Table S2.4 Averaged diameter at breast height (DBH; cm) of stems by species for the George LaRoi Forest Plot; Alberta, Canada. Note that the last row of measurements in the "2017" row are separated from the row above by a 20-year census gap.

	Picea glauca		*Populus tremuloides*		*Betula papyrifera*		*Pinus banksiana*	
Year	Alive	Dead	Alive	Dead	Alive	Dead	Alive	Dead
1967	6.0	1.4	8.9	1.9	5.7	1.5	13.8	3.5
1977	7.9	2.3	11.5	3.5	7.0	4.0	17.5	5.5
1988	9.1	2.5	13.2	6.6	7.9	3.9	24.2	5.5
1997	10.9	3.7	14.6	8.8	8.4	4.0	26.7	14.6
2017	18.3	7.8	17.9	12.9	11.2	10.5	31.0	23.7

Table S2.5 Biomass (Mg ha^{-1}) for all living stems in the George LaRoi forest plot; Alberta, Canada. Biomass was calculated using Canada-wide allometric equations (Ung et al. 2008) and summed by species for all living individuals.

Year	*Picea glauca*	*Populus tremuloides*	*Betula papyrifera*	*Pinus banksiana*	Total
1967	18.26	33.19	1.98	11.10	64.54
1977	33.30	45.22	2.63	13.23	94.37
1988	54.95	39.57	2.90	18.97	116.40
1997	74.56	26.52	3.28	15.70	120.05
2017	58.24	16.23	3.22	12.45	90.13

FIGURES

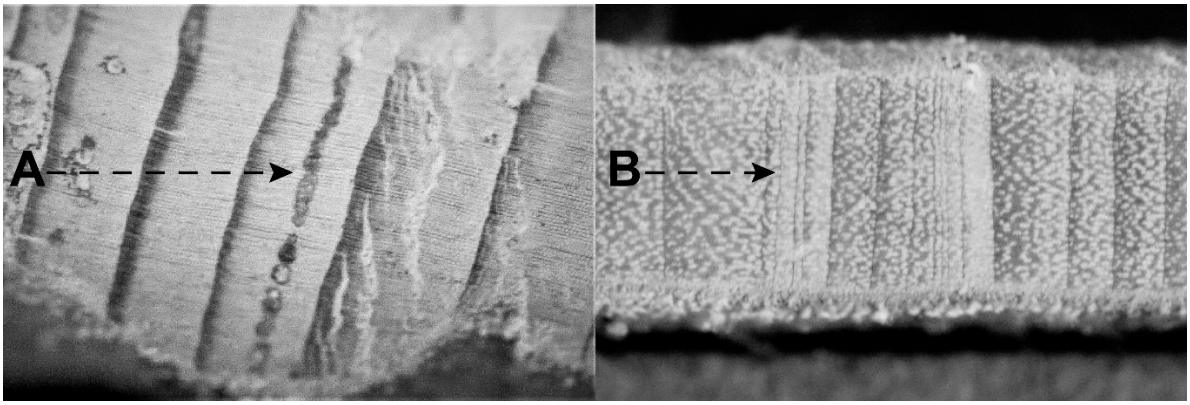

Figure S2.1 Examples of characteristic tree-ring features used to reconstruct insect disturbance events at the George LaRoi forest plot; Alberta, Canada. (**A**) *Picea glauca* rings with a diagnostic traumatic resin duct (TRD) marked with an arrow. The formation of a TRD is indicative of bark beetle attack and corroborated with gallery presence on the tree bole. (**B**) *Populus tremuloides* rings with one of two series of diagnostic white rings marked with an arrow. White rings are indicative of severe defoliation.

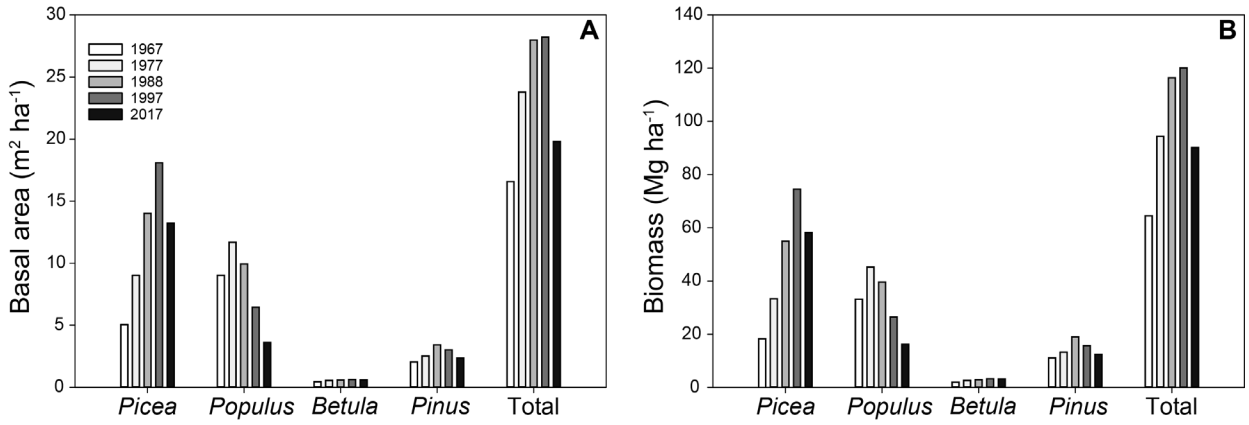

Figure S2.2 Total stand basal area (**A**), and biomass (**B**) of living standing stems for the George LaRoi forest plot; Alberta, Canada (1967–2017). Species listed are *Picea glauca, Populus tremuloides, Betula papyrifera*, and *Pinus banksiana*.

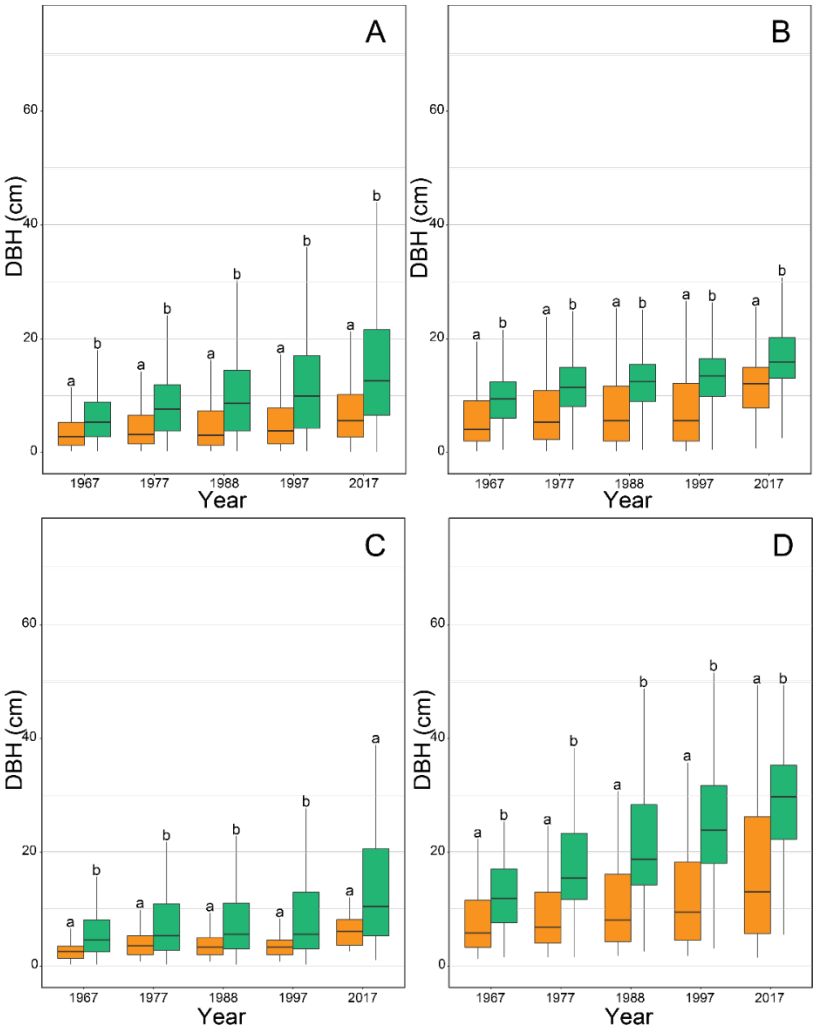

Figure S2.3 Diameter at breast height (DBH) for each of the four tree species (**A**: *Picea glauca*; **B**: *Populus tremuloides*; **C**: *Betula papyrifera*; **D**: *Pinus banksiana*) at the George LaRoi forest plot; Alberta, Canada. Boxplots of DBH are plotted by dead stems (orange) and living (green) for each census period. Significant mean differences in DBH between living and dead stems were assessed using a Wilcoxon Rank-Sum test. Mean differences between living and dead stems were significantly different for all species at each census point except for *B. papyrifera* in 2017.

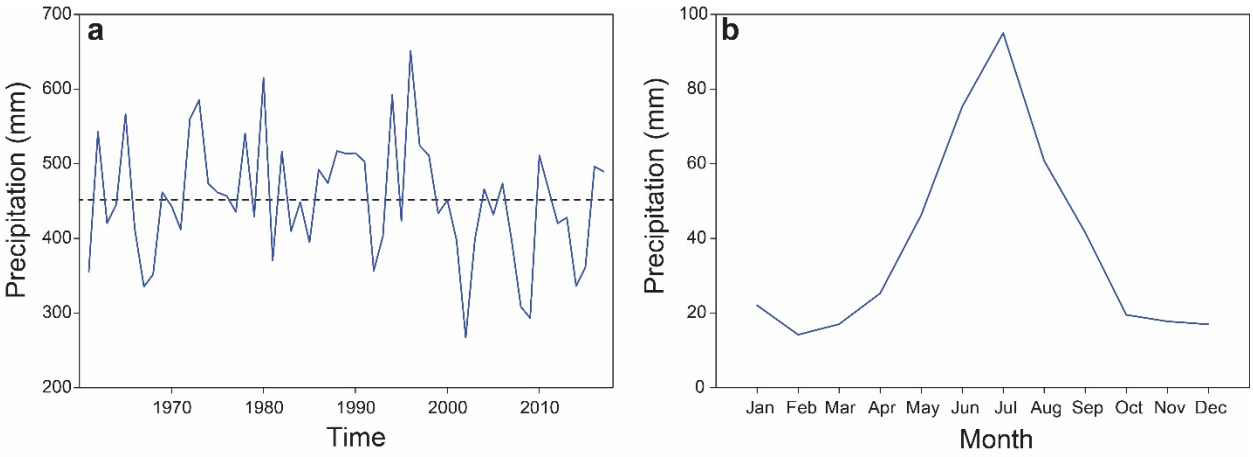

Figure S2.4 Precipitation in mm (y-axis) plotted against time (x-axis) for the George LaRoi forest plot; Alberta, Canada. (**A**) Annual precipitation (blue solid line), and mean precipitation (black dashed line) plotted against time. (**B**) Monthly mean precipitation (blue solid line) plotted by month.

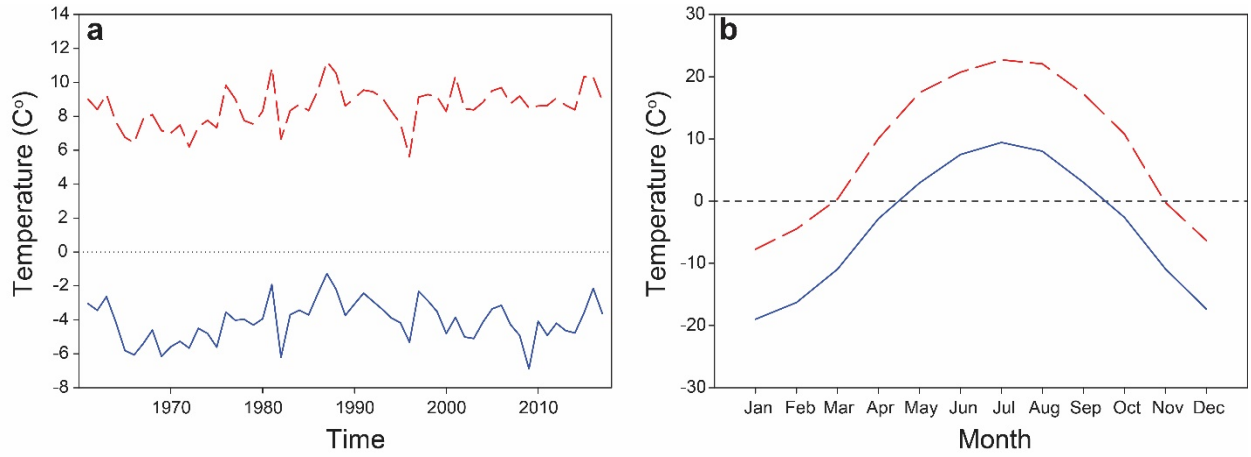

Figure S2.5 Mean temperature maximum (red long-dashed line) and mean minimum temperature (blue solid line) for the George LaRoi forest plot; Alberta, Canada. Freezing point is marked with a short-dashed line for visual clarity. **(A)** Mean annual temperature extremes plotted against time. Time coverage is 1961–2017. **(B)** Mean monthly temperature extremes plotted by month.

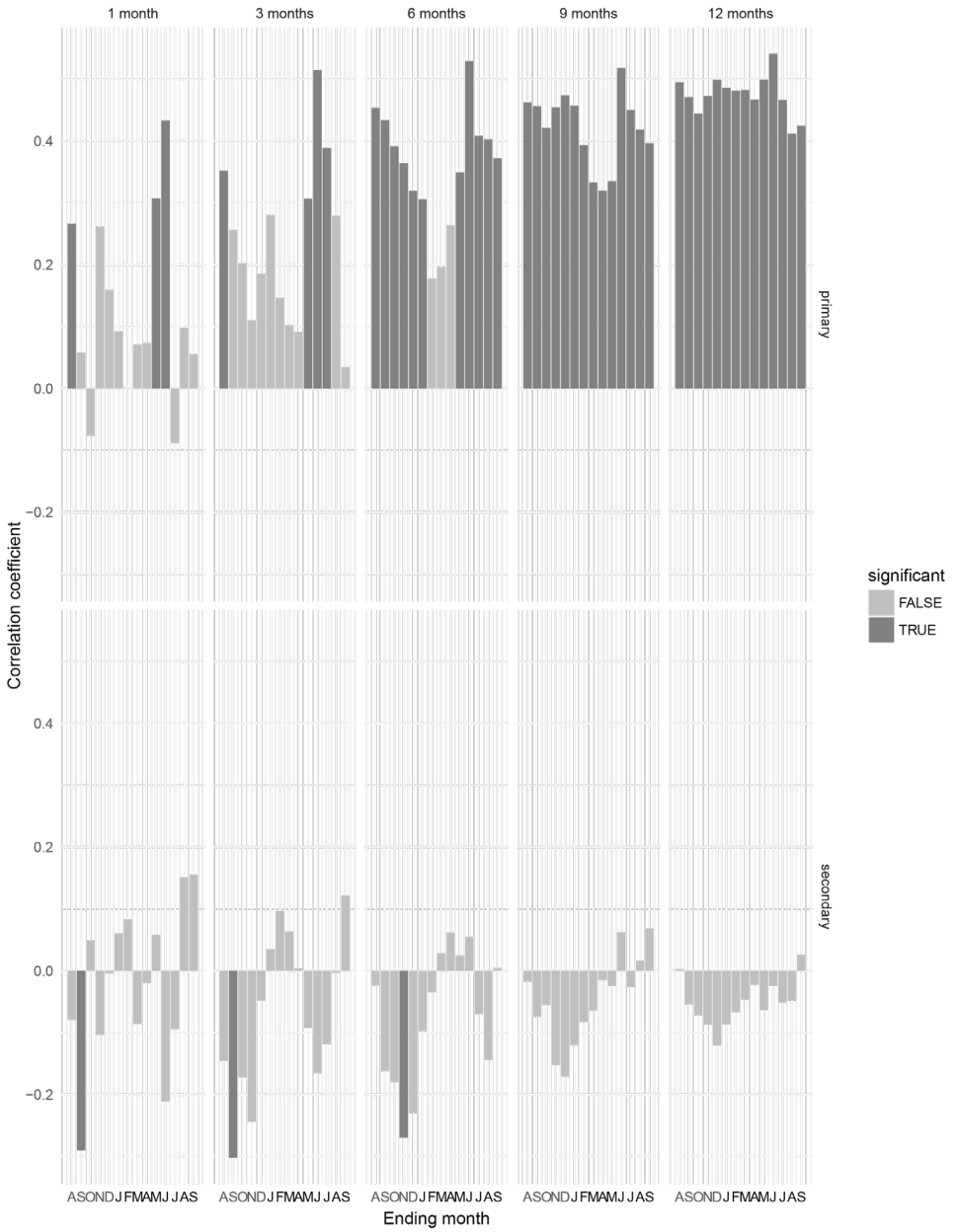

Figure S2.6 Pearson correlation coefficients between primary (precipitation), secondary (mean maximum temperature), and *Picea glauca* ring width at the George LaRoi forest plot; Alberta, Canada. Correlation strength is plotted on the y-axis with time, in months, on the x-axis. Months in the current year are bolded. Data is grouped by length of growing season: 1, 3, 6, 9 and 12 months. Significant correlations are colored dark grey.

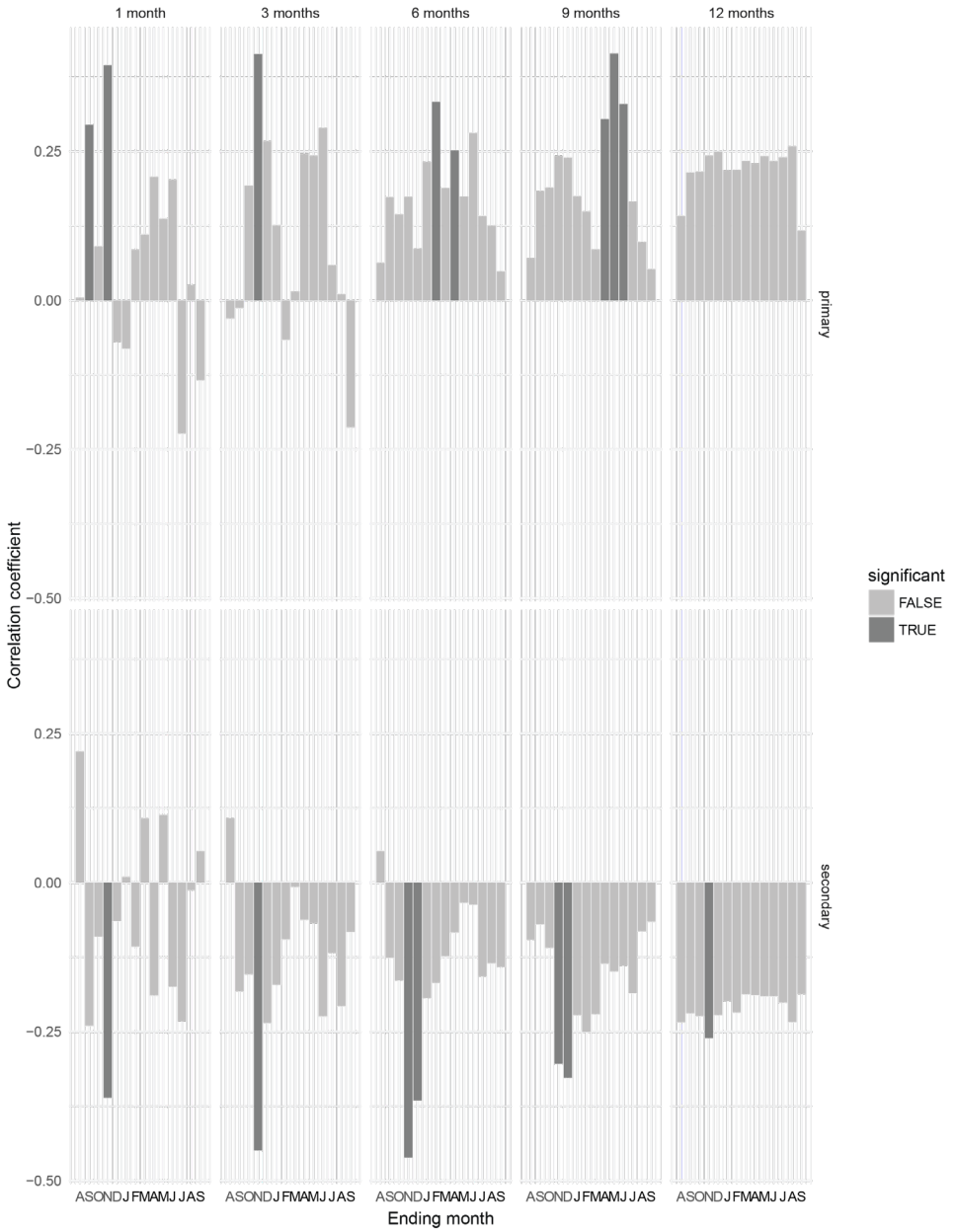

Figure S2.7 Pearson correlation coefficients between primary (precipitation), secondary (mean maximum temperature), and *Populus tremuloides* ring width at the George LaRoi forest plot; Alberta, Canada. Correlation strength is plotted on the y-axis with time, in months, on the x-axis. Months in the current year are bolded. Significant correlations are colored dark grey.

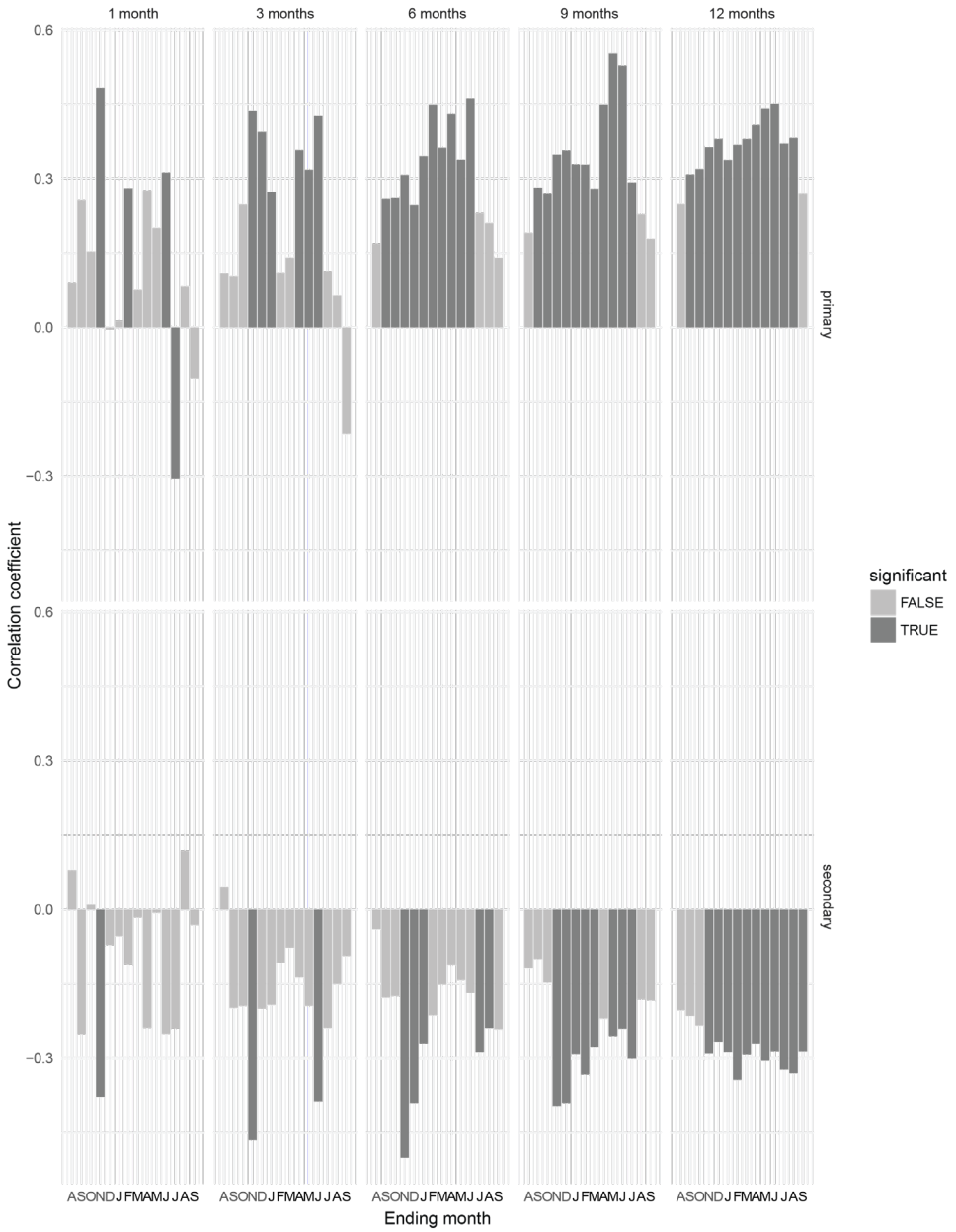

Figure S2.8 Pearson correlation coefficients between primary (precipitation), secondary (mean maximum temperature), and *Betula papyrifera* ring width at the George LaRoi forest plot; Alberta, Canada. Correlation strength is plotted on the y-axis with time, in months, on the x-axis. Months in the current year are bolded. Significant correlations are colored dark grey.

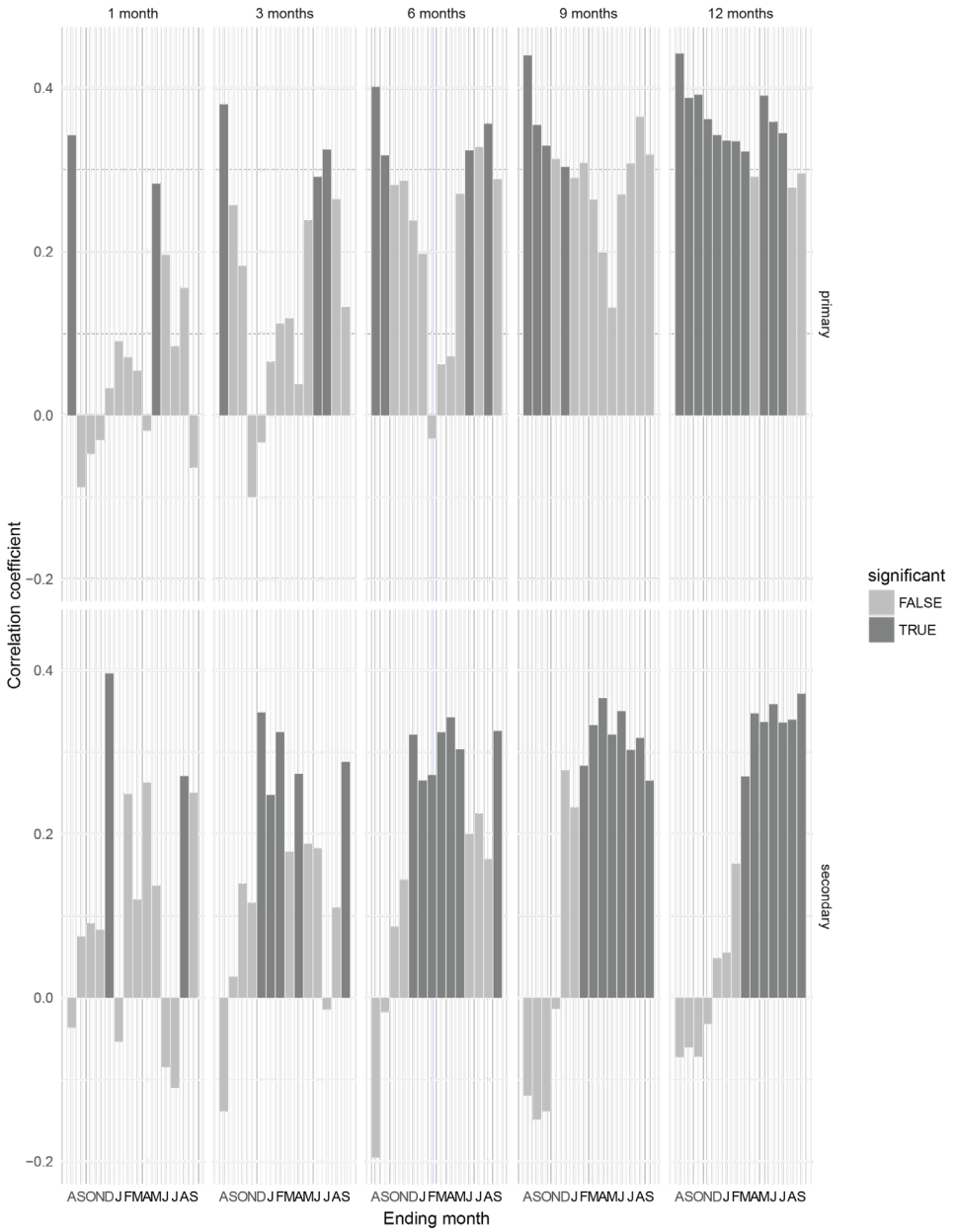

Figure S2.9 Pearson correlation coefficients between primary (precipitation), secondary (mean maximum temperature), and *Pinus banksiana* ring width at the George LaRoi forest plot; Alberta, Canada. Correlation strength is plotted on the y-axis with time, in months, on the x-axis. Months in the current year are bolded. Significant correlations are colored dark grey.

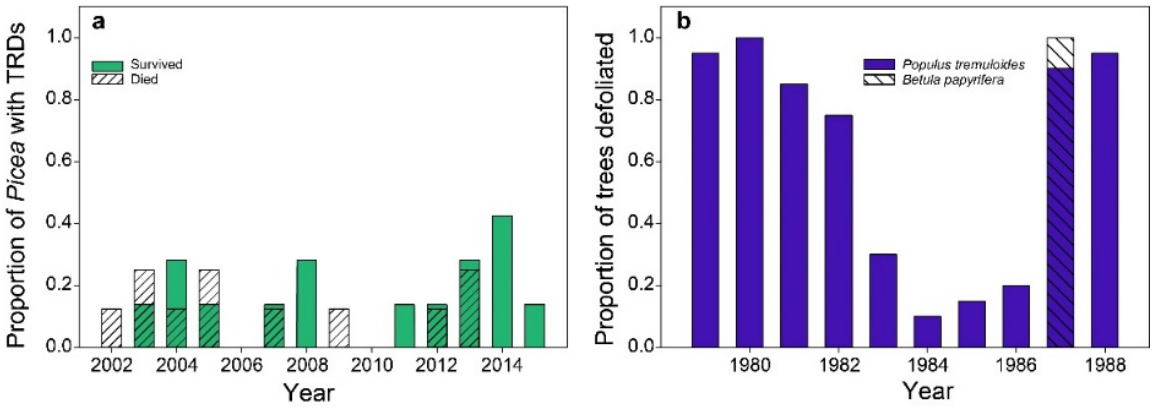

Figure S2.10 Proportion of tree-cores with diagnostic features of insect attack at the George LaRoi forest plot; Alberta, Canada. All years with diagnostic features on more than one tree-core are plotted. (**a**) The proportion of *Picea glauca* with a record of traumatic resin ducts (TRD). Trees alive in 2017 (n= 7) with TRD are plotted in green. Trees that were standing-dead (n=7) in 2017 are plotted as dashed bars. The greatest proportion of TRDs was found at 42% of tree-cores in 2014. The earliest TRD was detected in 2002; the latest in 2015. (**b**) The proportion of *Populus tremuloides* (n=20; filled bars) and *Betula papyrifera* (n=10; hatched bars) with white-colored rings, which are a sign of severe leaf defoliation.

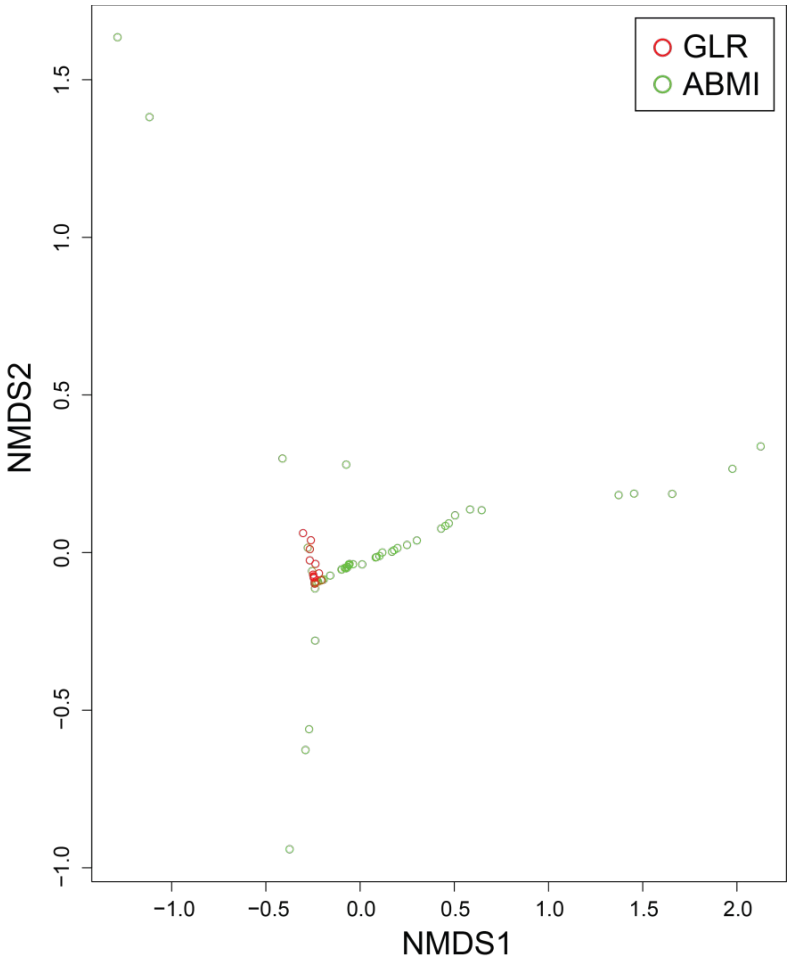

Figure S2.11 Non-metric multidimensional ordination (NMDS) of basal area, by species for the George LaRoi forest plot (red circles) (GLR) and Alberta Biodiversity Monitoring Institute (ABMI) tree plots 2015–2017 (green circles) (ABMI 2018); Alberta, Canada. The GLR points represent 5 × 5 m cells randomly selected from the 2017 census cells of the GLR. The ABMI plots are 5 × 5 m cells within 200 km of the GLR site that have at least one species in common with the GLR plot.

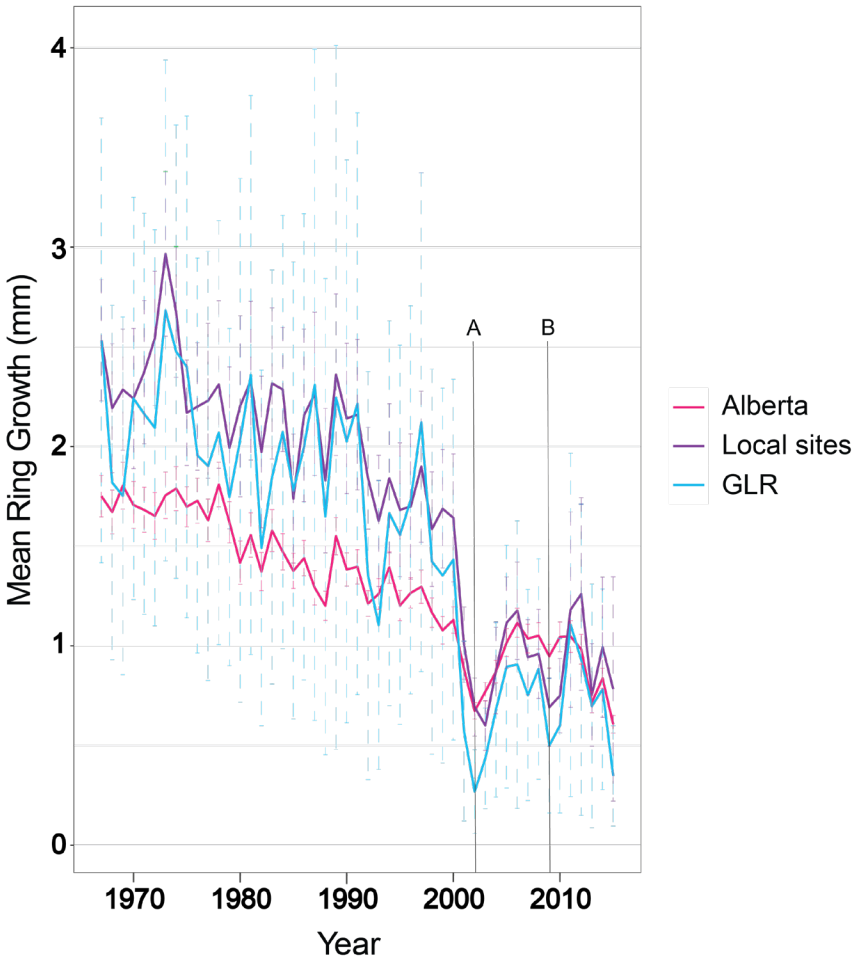

Figure S2.12 A comparison of mean raw ring growth from *Picea glauca* at the George LaRoi forest plot (blue)(GLR) and from the averaged STO1, STO2, STO3, MIL1, MIL2, MIL3, COY sites (purple) with confidence intervals (faded bars), and *Picea* across Alberta (pink) (Hogg et al. 2017). The "A" denotes 2003, the first year for which the GLR series are statistically different. The "B" denotes 2009, the second year for which the GLR series are statistically different than the Alberta series.

Image S2.1 A typical view within the George LaRoi forest plot; AB, Canada. Understory consists of short forbs with sporadic *Prunus virginiana* (western chokecherry).

Image S2.2 Windthrow one month after the 2017 census in the George LaRoi forest plot; AB, Canada.

Image S2.3 A view of the overstory and a medium-sized canopy gap in the George LaRoi forest plot; AB, Canada.

References

ABMI (Alberta Biodiversity Monitoring Institute). 2018. ABMI Trees & Snags (5342138678144103563) database: Rotation 2. Retrieved from http://www.ABMI.ca

Hogg, E. H., M. Michaelian, T. I. Hook, and M. E. Undershultz. 2017. Recent climatic drying leads to age-independent growth reductions of white spruce stands in western Canada. *Global Change Biology* 23:5297-5308.

Ung, C.-H., P. Bernier, and X.-J. Guo. 2008. Canadian national biomass equations: new parameter estimates that include British Columbia data. *Canadian Journal of Forest Research* 38:1123-1132.

Appendix 3.1

FIGURES

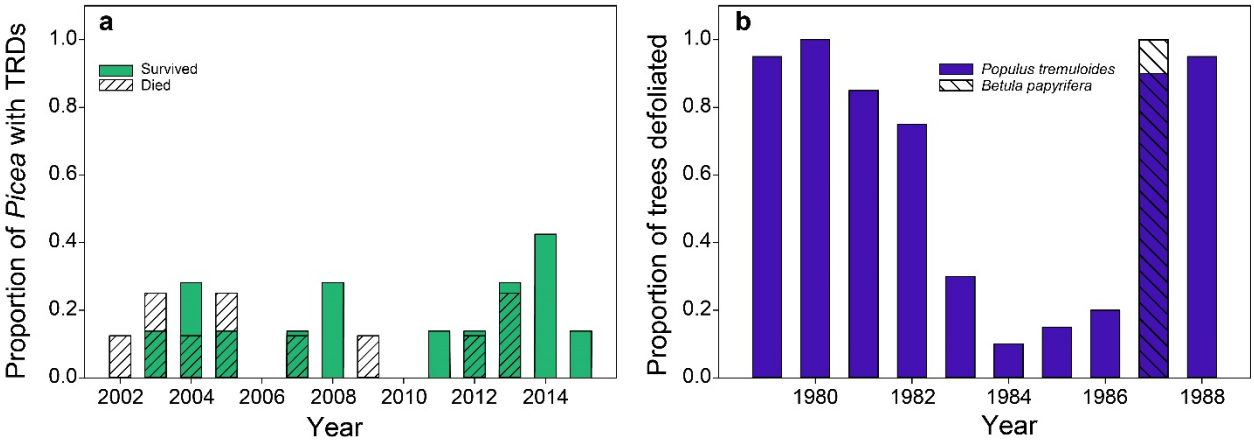

Figure S3.1 Proportion of tree cores with diagnostic features of insect attack at the GLR forest plot; Alberta, Canada. All years with diagnostic features on more than one tree-core are plotted. (**a**) The proportion of *Picea glauca* with a record of traumatic resin ducts (TRD). Trees alive in 2017 (n= 7) with TRD are plotted in green. Trees that were standing-dead (n=7) in 2017 are plotted as dashed bars. The greatest proportion of TRDs was found at 42% of tree-cores in 2014. The earliest TRD was detected in 2002; the latest in 2015. (**b**) The proportion of *Populus tremuloides* (n=20; filled bars) and *Betula papyrifera* (n=10; hatched bars) with distinctly white-colored rings, which are a sign of severe leaf defoliation in that year. Originally printed in the Appendix 1 of Birch et al. (2019).

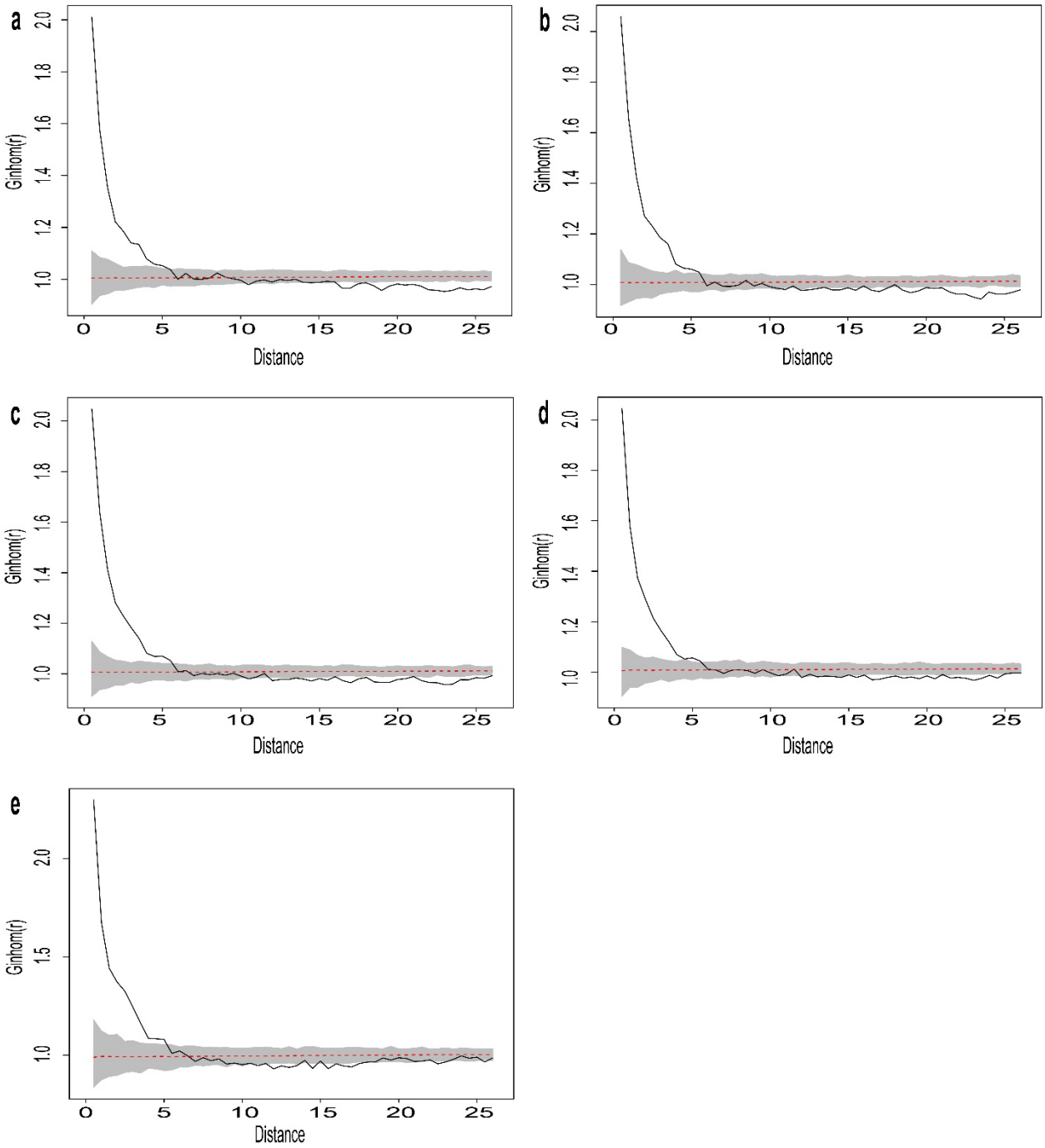

Figure S3.2 Spatial patterns of all stems pooled from the **a**) 1967, **b**) 1977, **c**) 1988, **d**) 1997, and **e**) 2017 censuses of the George LaRoi Forest Plot; AB, Canada. Values above (below) the dashed line indicate aggregation (dispersion) of stems.

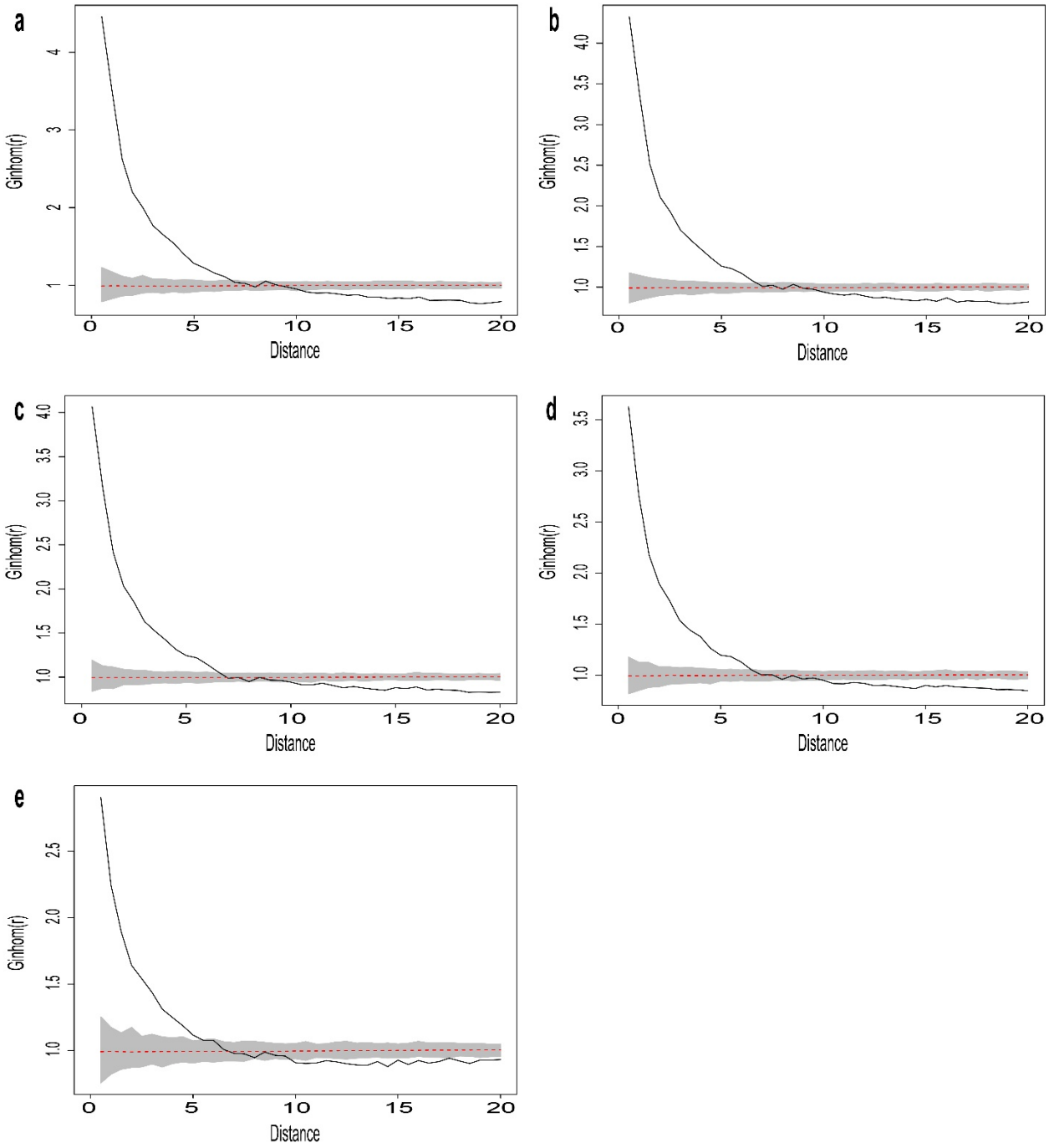

Figure S3.3 Spatial patterns of *Picea glauca* from the **a**) 1967, **b**) 1977, **c**) 1988, **d**) 1997, and **e**) 2017 censuses of the George LaRoi Forest Plot; AB, Canada. Values above (below) the dashed line indicate aggregation (dispersion) of stems.

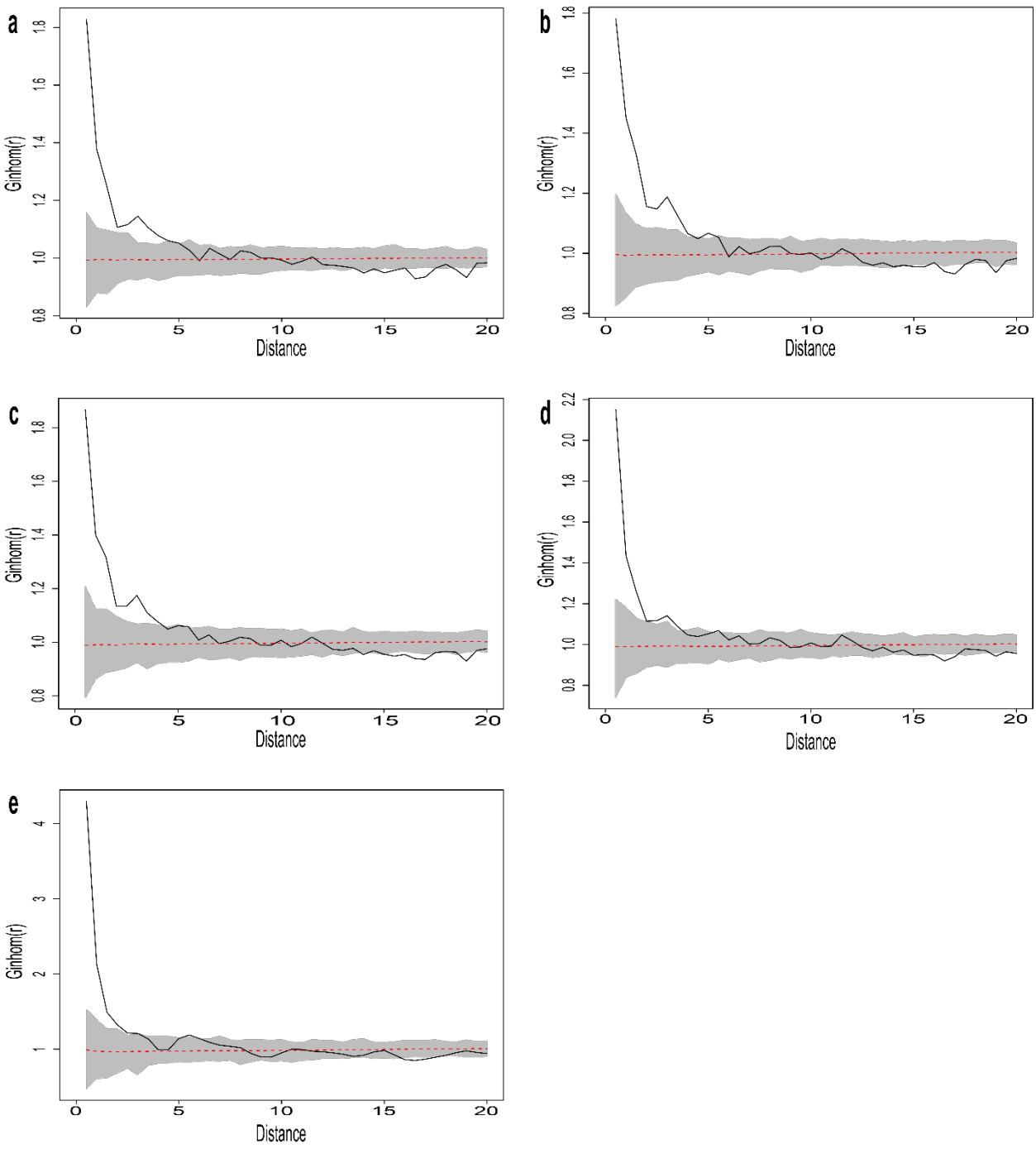

Figure S3.4 Spatial patterns of angiosperms (*Populus tremuloides* and *Betula papyrifera*) from the **a**) 1967, **b**)1977, **c**)1988, **d**)1997, and **e**) 2017 censuses of the George LaRoi Forest Plot; AB, Canada. Values above (below) the dashed line indicate aggregation (dispersion) of stems.

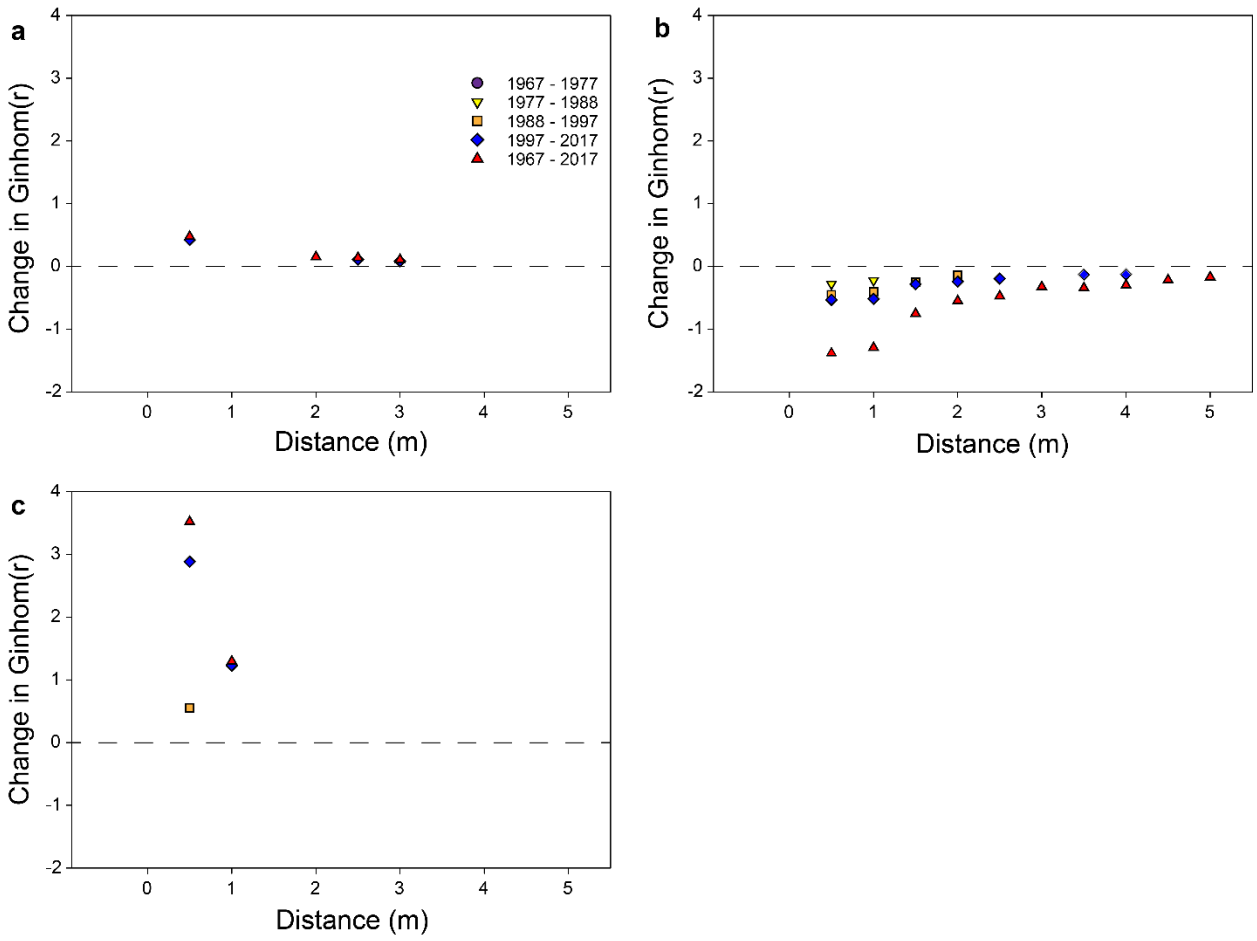

Figure S3.5 Significant changes in spatial patterns of all stems (Ginhom(r)) between census measurements within the George LaRoi Forest Plot; Alberta, Canada. Points > 0 (dashed line) represent aggregation of stems. Points < 0 represent dispersion of stems. The x-axis denotes the distance in meters, between points. Closed circles, open triangles, closed squares, open diamonds and closed triangles represent inter-census changes in stem patterns of 1967–1977, 1977–1988, 1988–1997, 1997–2017, and 1967–2017, respectively. **a**) The significant changes in all stems (pooled). **b**) The significant changes in *Picea glauca* stems. **c**) The significant changes in angiosperm (*Populus tremuloides* and *Betula papyrifera*) stems.

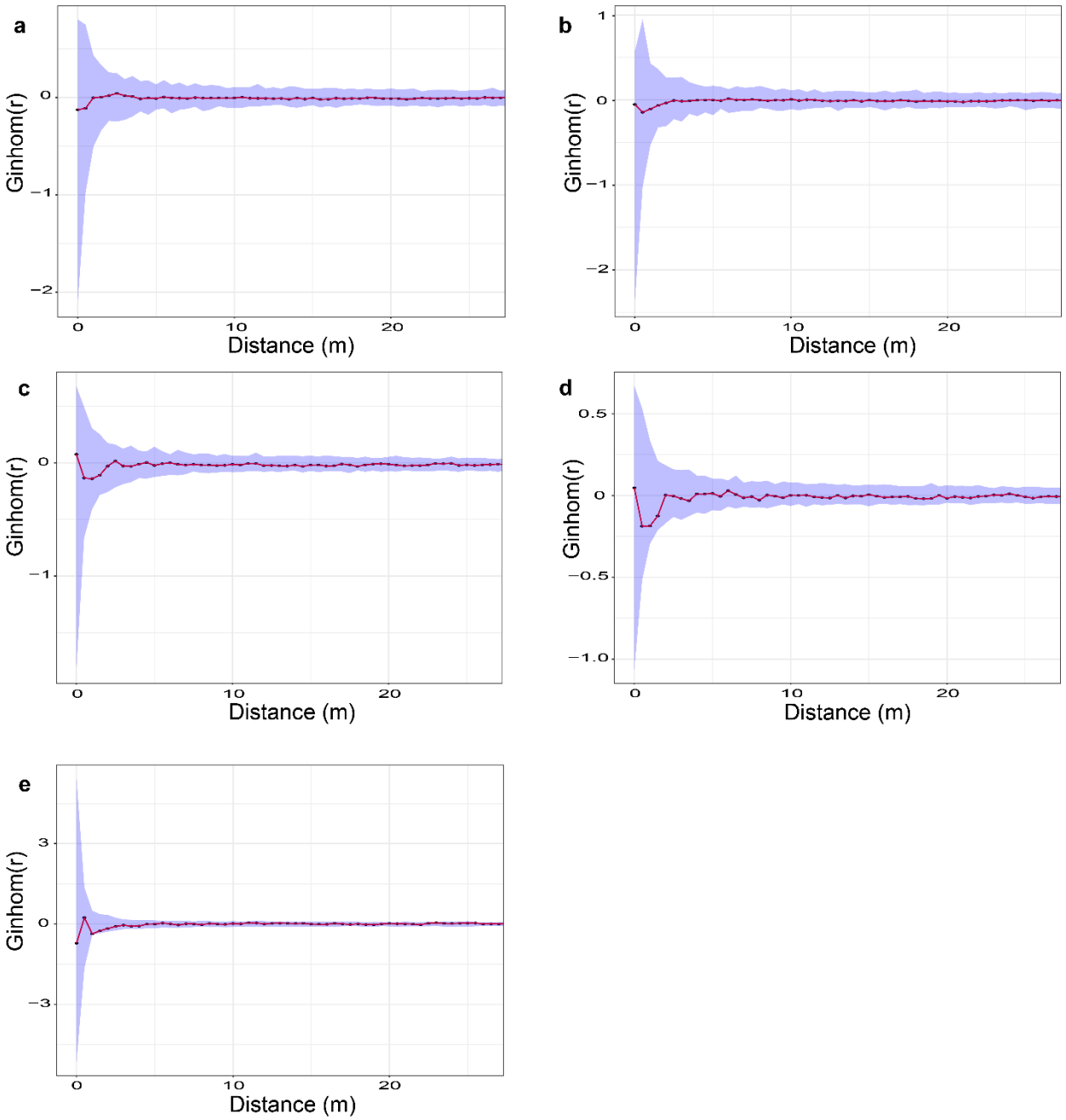

Figure S3.6 Change in spatial patterns due to negative density-dependence (NDD) for all stems, pooled from the 1967 **a**), 1977 **b**), 1988 **c**), 1997 **d)**, and 2017 **e**) censuses of the George LaRoi Forest Plot; AB, Canada. Values above (below) the dashed line indicate aggregation (dispersion) of stems due to NDD.

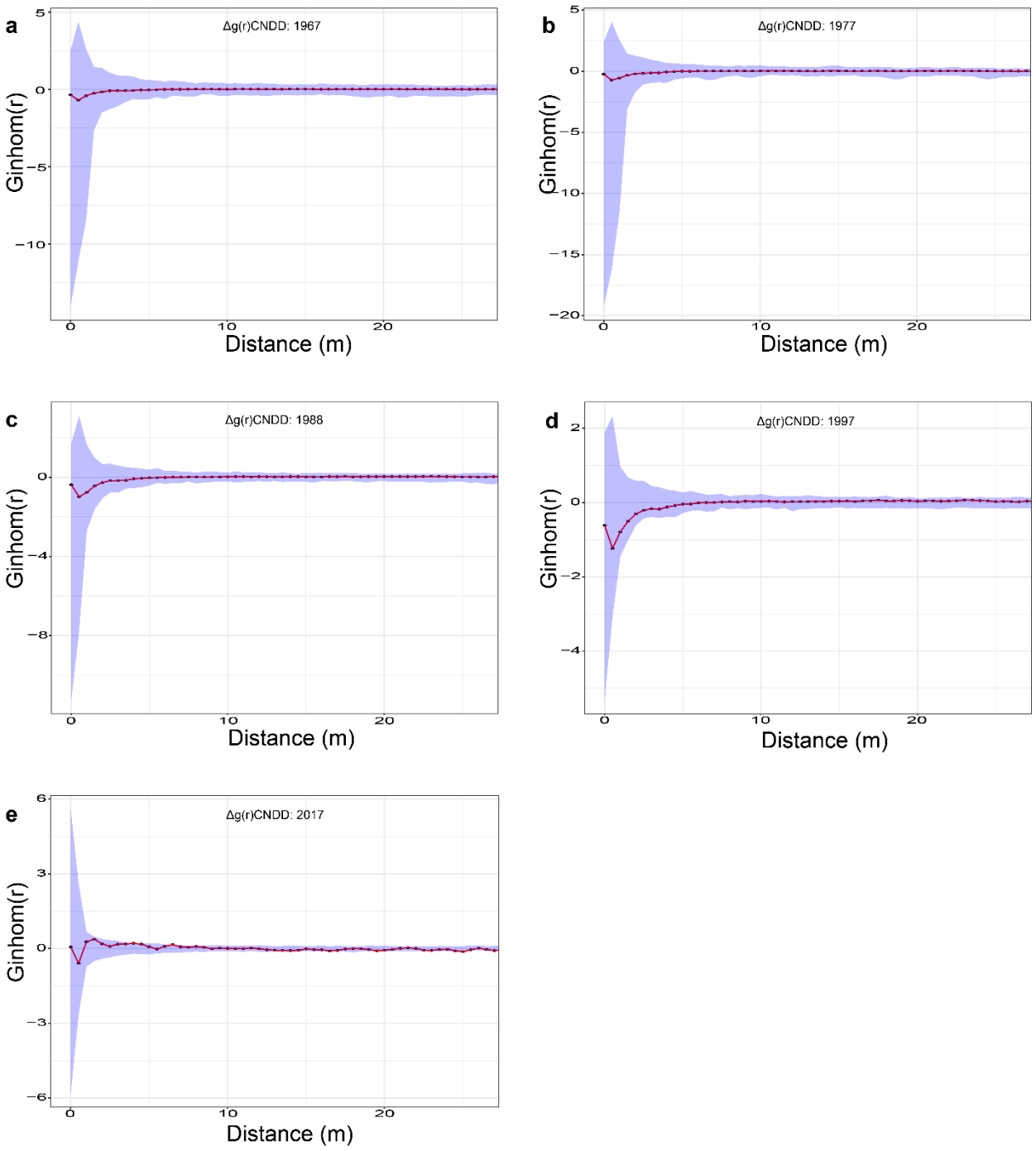

Figure S3.7 Change in spatial patterns due to conspecific negative density-dependence (CNDD) for *Picea glauca* stems from the 1967 **a**), 1977 **b**), 1988 **c**), 1997 **d**), and 2017 **e**) censuses of the George LaRoi Forest Plot; AB, Canada. Values above (below) the dashed line indicate aggregation (dispersion) of stems due to CNDD.

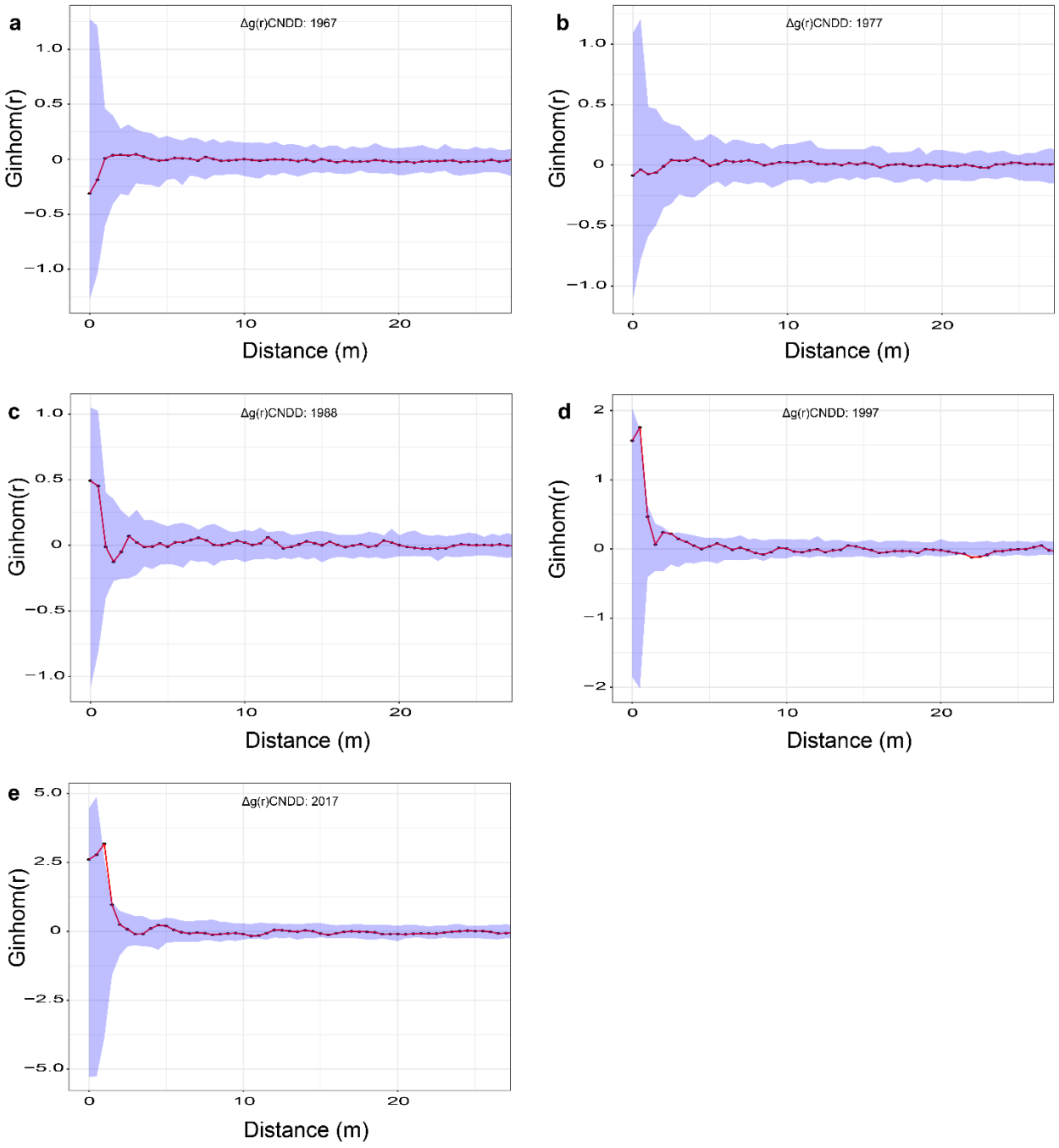

Figure S3.8 Change in spatial patterns due to conspecific negative density-dependence (CNDD) for angiosperm stems (*Populus tremuloides* and *Betula papyrifera*) from the 1967 **a**), 1977 **b**), 1988 **c**), 1997 **d**), and 2017 **e**) censuses of the George LaRoi Forest Plot; AB, Canada. Values above (below) the dashed line indicate aggregation (dispersion) of stems due to CNDD.

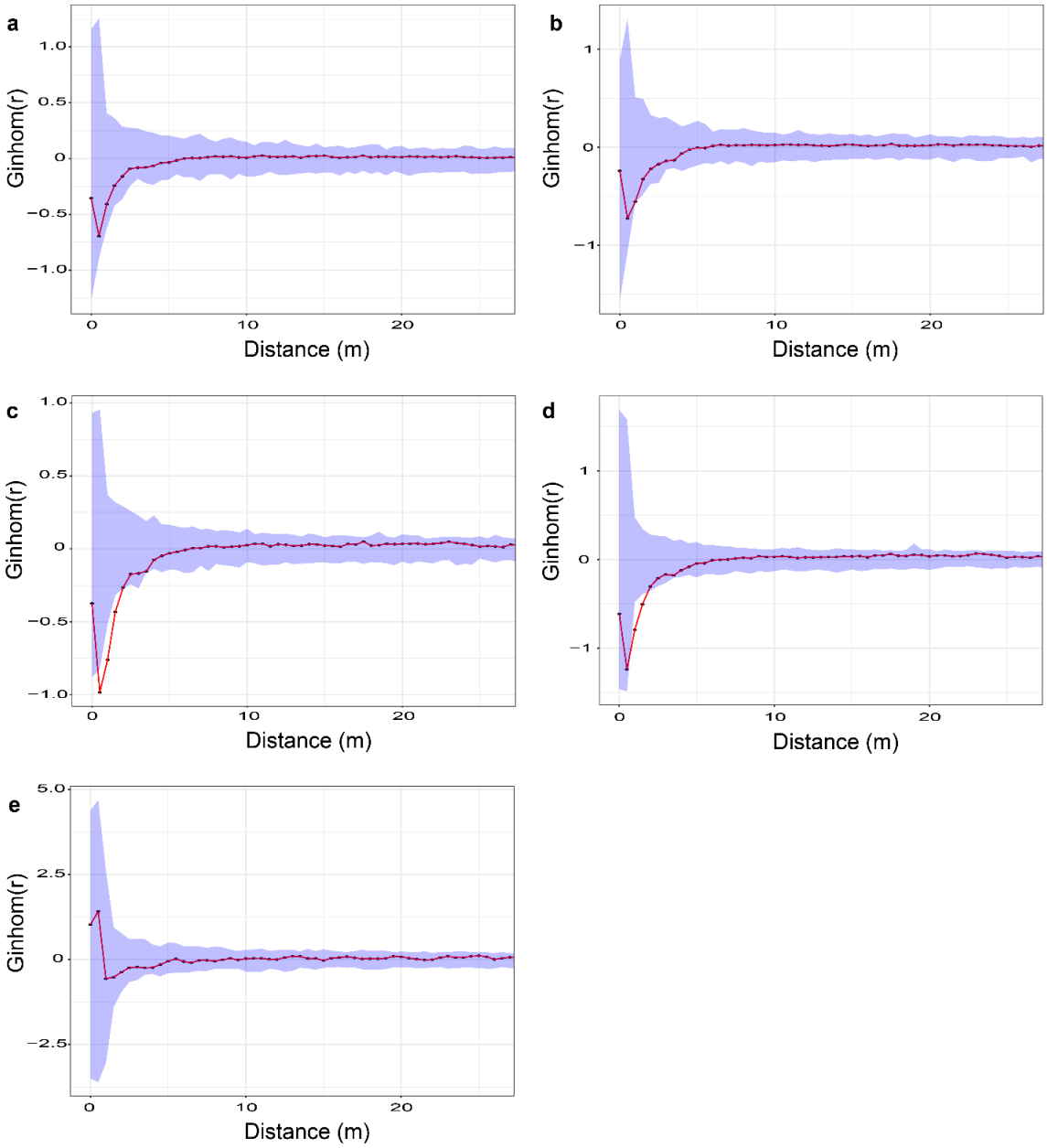

Figure S3.9 Change in spatial patterns due to heterospecific negative density-dependence (HNDD) experienced by *Picea glauca,* from angiosperms (*Populus tremuloides* and *Betula papyrifera*), over the 1967 **a**), 1977 **b**), 1988 **c**), 1997 **d**), and 2017 **e**) censuses of the George LaRoi Forest Plot; AB, Canada. Values above (below) the dashed line indicate aggregation (dispersion) of stems due to HNDD.

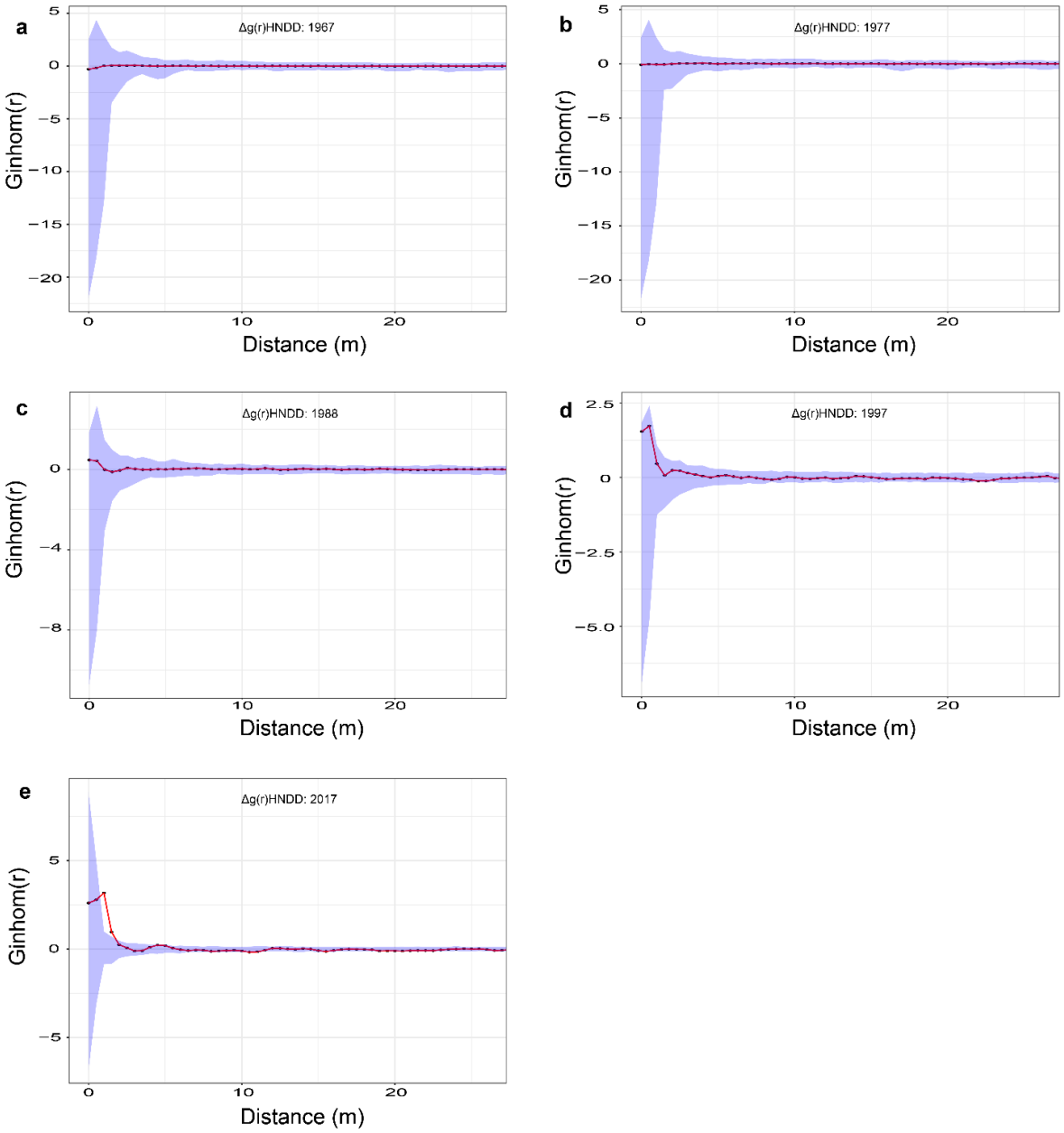

Figure S3.10 Change in spatial patterns due to heterospecific negative density-dependence (HNDD) experienced by angiosperms (*Populus tremuloides* and *Betula papyrifera*), from *Picea glauca*, over the 1967 **a**), 1977 **b**), 1988 **c**), 1997 **d**), and 2017 **e**) censuses of the George LaRoi Forest Plot; AB, Canada. Values above (below) the dashed line indicate aggregation (dispersion) of stems due to HNDD.

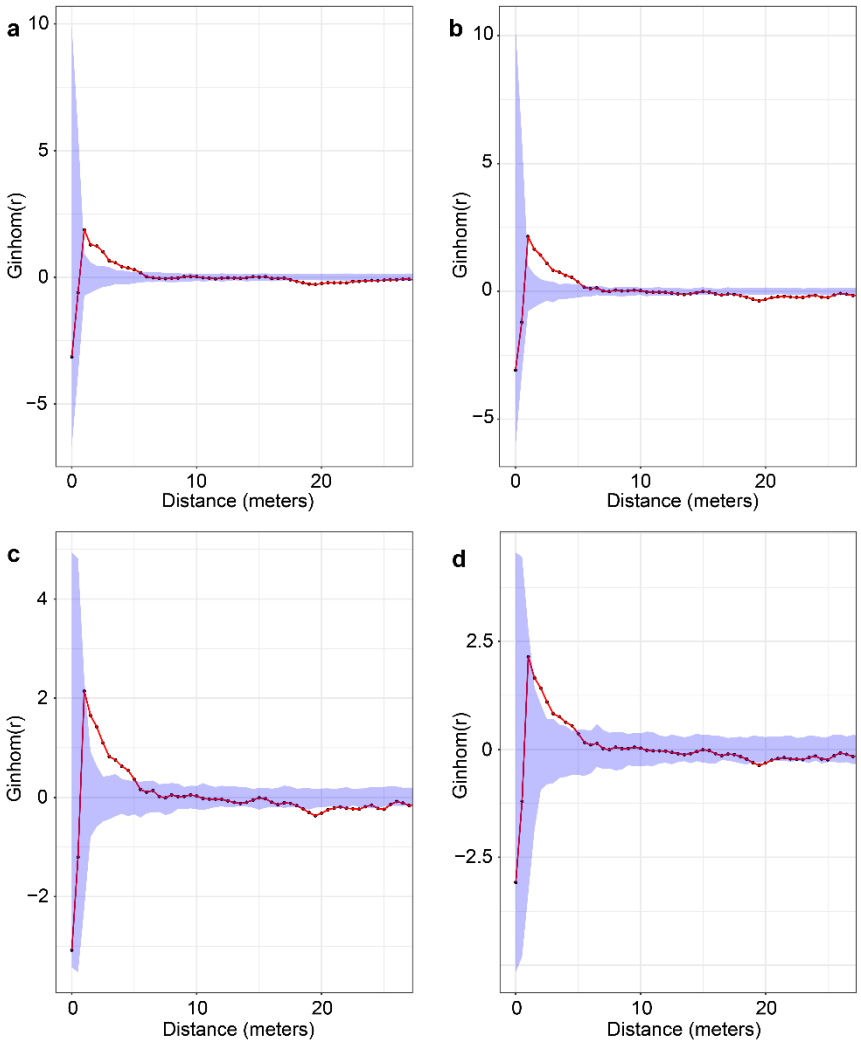

Figure S3.11 Spatial patterns of *Picea glauca* killed by *Dendroctonus rufipennis* within the GLR forest plot; Alberta, Canada. Values generated by the bivariate pair correlation function with Ginhom(r) above and below the confidence envelopes represent aggregation and dispersion of stems, respectively. Values within the confidence envelopes are indistinguishable from complete spatial randomness. *P. glauca* that died from beetle attack had significantly more crowded neighborhoods of living *P. glauca* **a**) and dead *P. glauca* **b**) at distances < 5.0 m, relative to living, non-attacked *P. glauca*. *P. glauca* that died from beetle attack had significantly more

crowded neighborhoods of living **c**) and dead **d**) angiosperms at distances < 5.0 m, relative to living, non-attacked *P. glauca*.

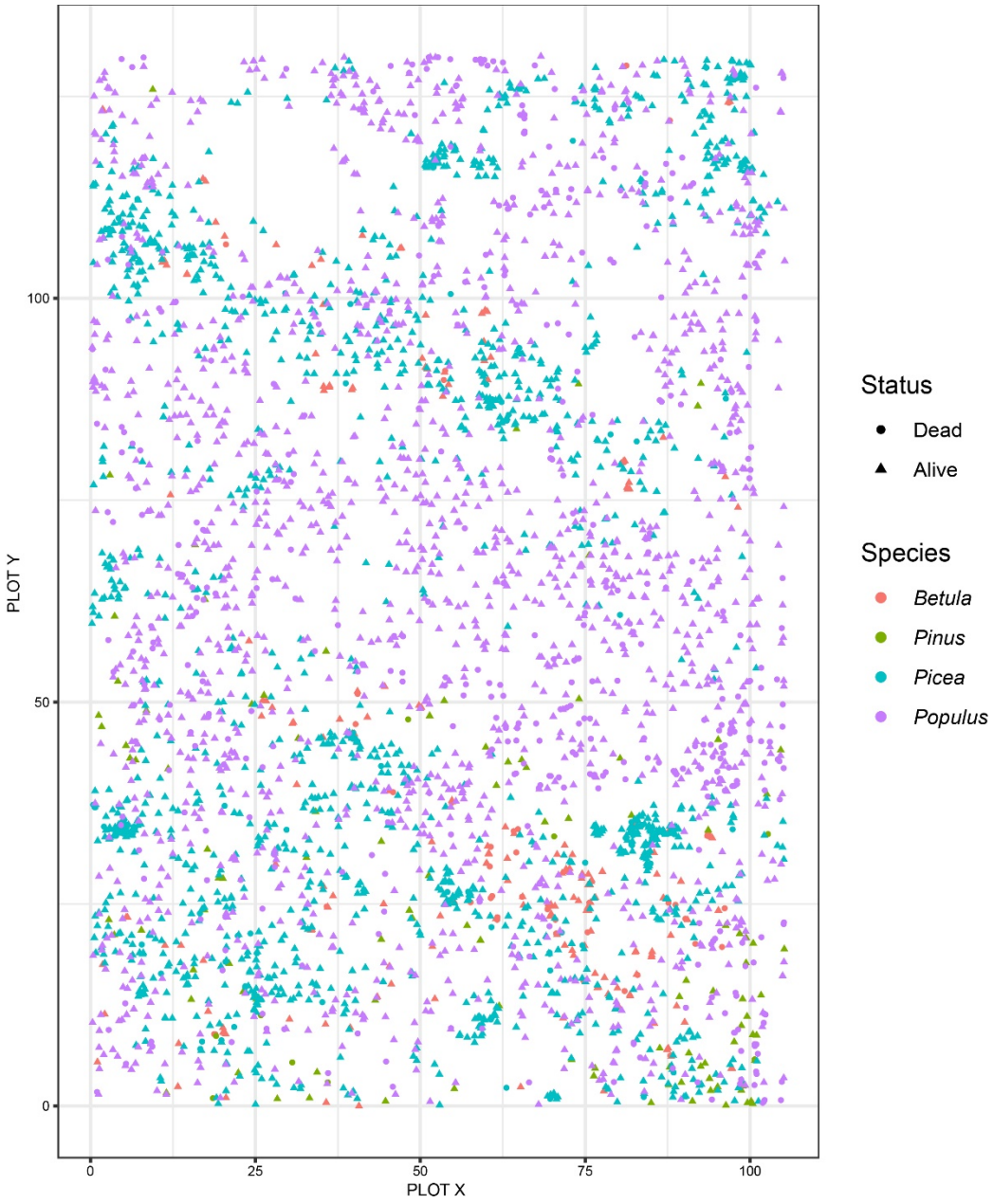

Figure S3.12 Pooled tree-stem map for the 1967 census of the George LaRoi Forest Plot; AB, Canada. The four-principle species within the plot (*Picea glauca, Populus tremuloides, Betula papyrifera,* and *Pinus banksiana*) are plotted with living stems (triangles) and dead stems (circles).

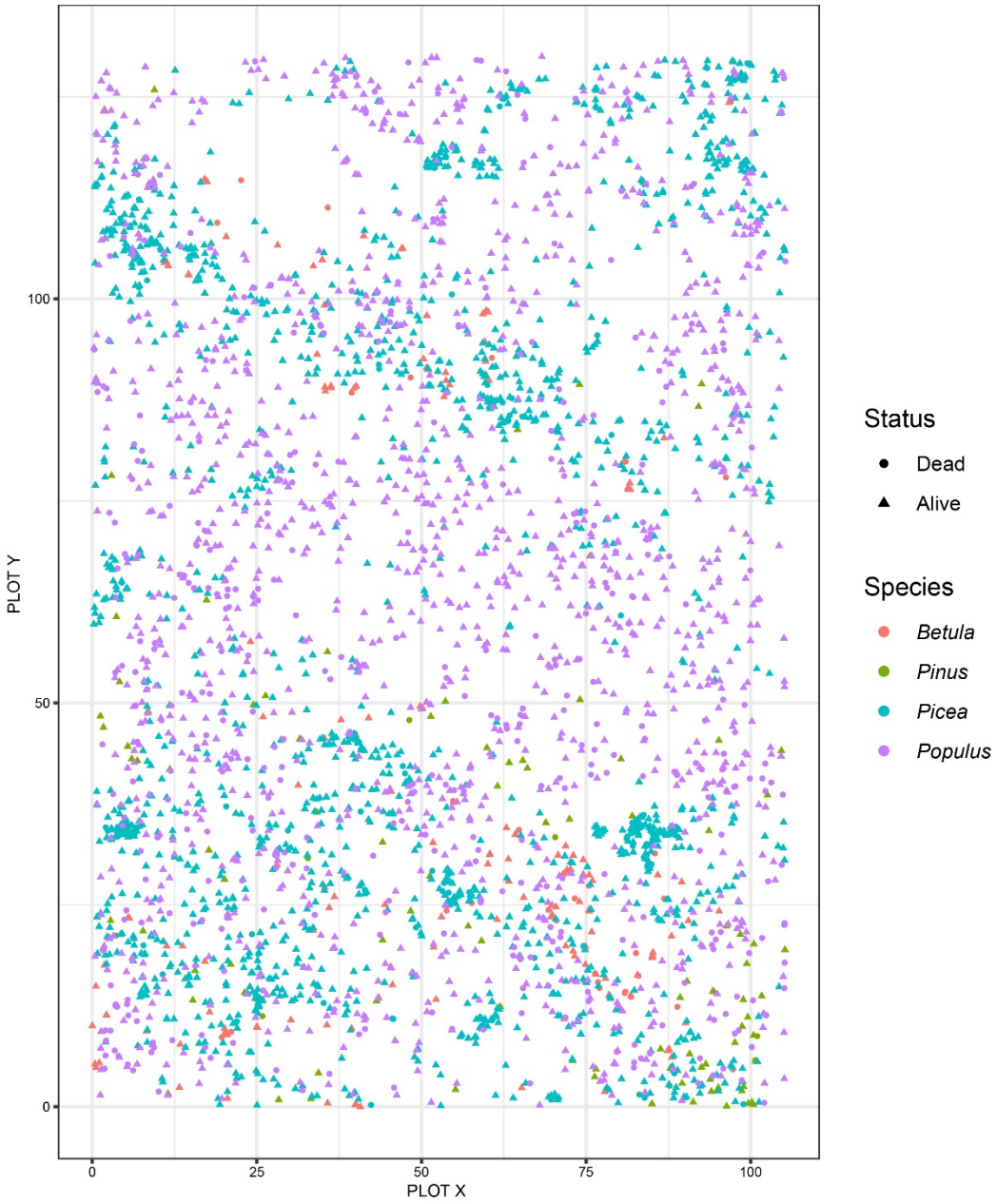

Figure S3.13 Pooled tree-stem map for the 1977 census of the George LaRoi Forest Plot; AB, Canada. The four principle species within the plot (*Picea glauca, Populus tremuloides, Betula papyrifera,* and *Pinus banksiana*) are plotted with living stems (triangles) and dead stems (circles).

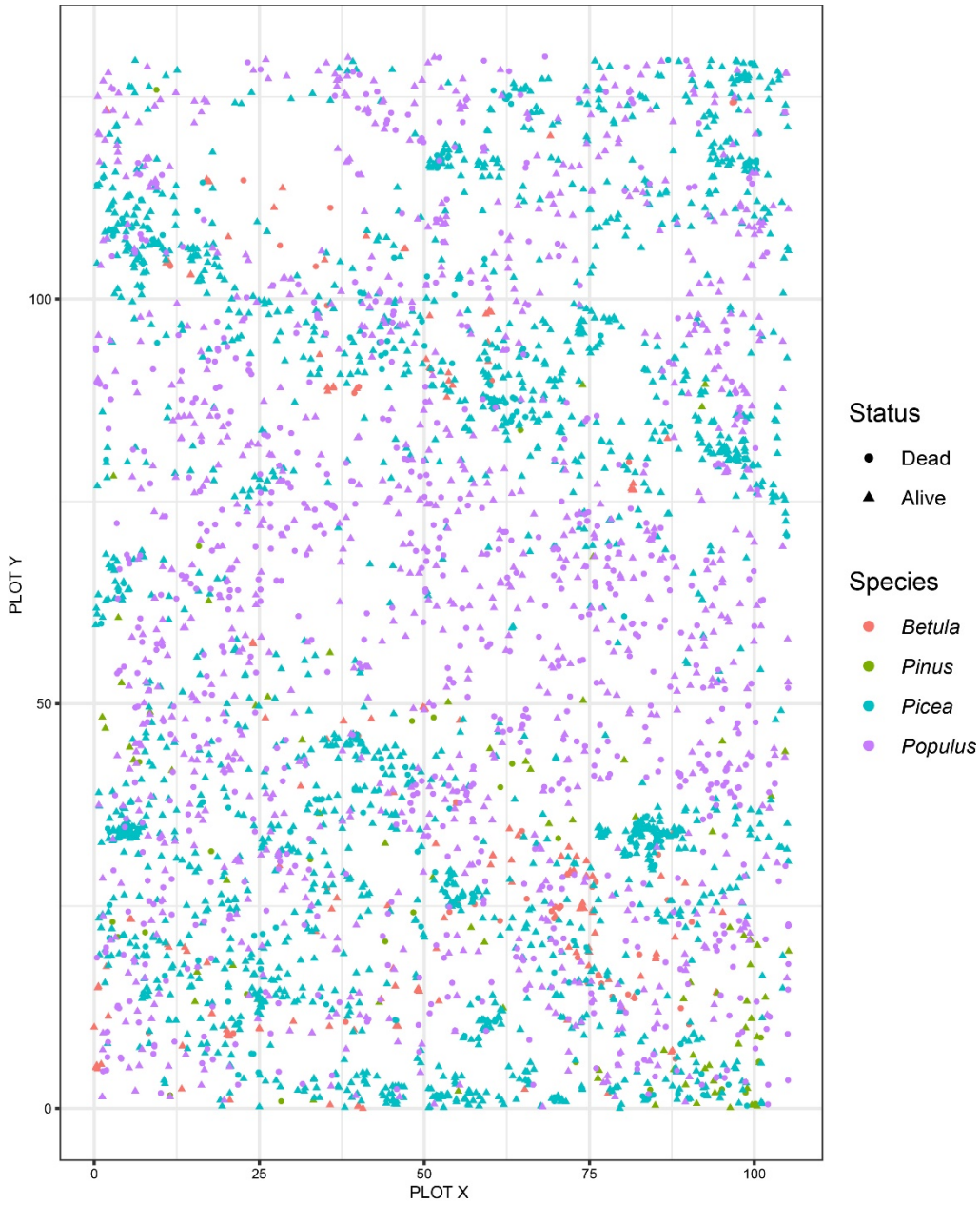

Figure S3.14 Pooled tree-stem map for the 1988 census of the George LaRoi Forest Plot; AB, Canada. The four principle species within the plot (*Picea glauca, Populus tremuloides, Betula papyrifera,* and *Pinus banksiana*) are plotted with living stems (triangles) and dead stems (circles).

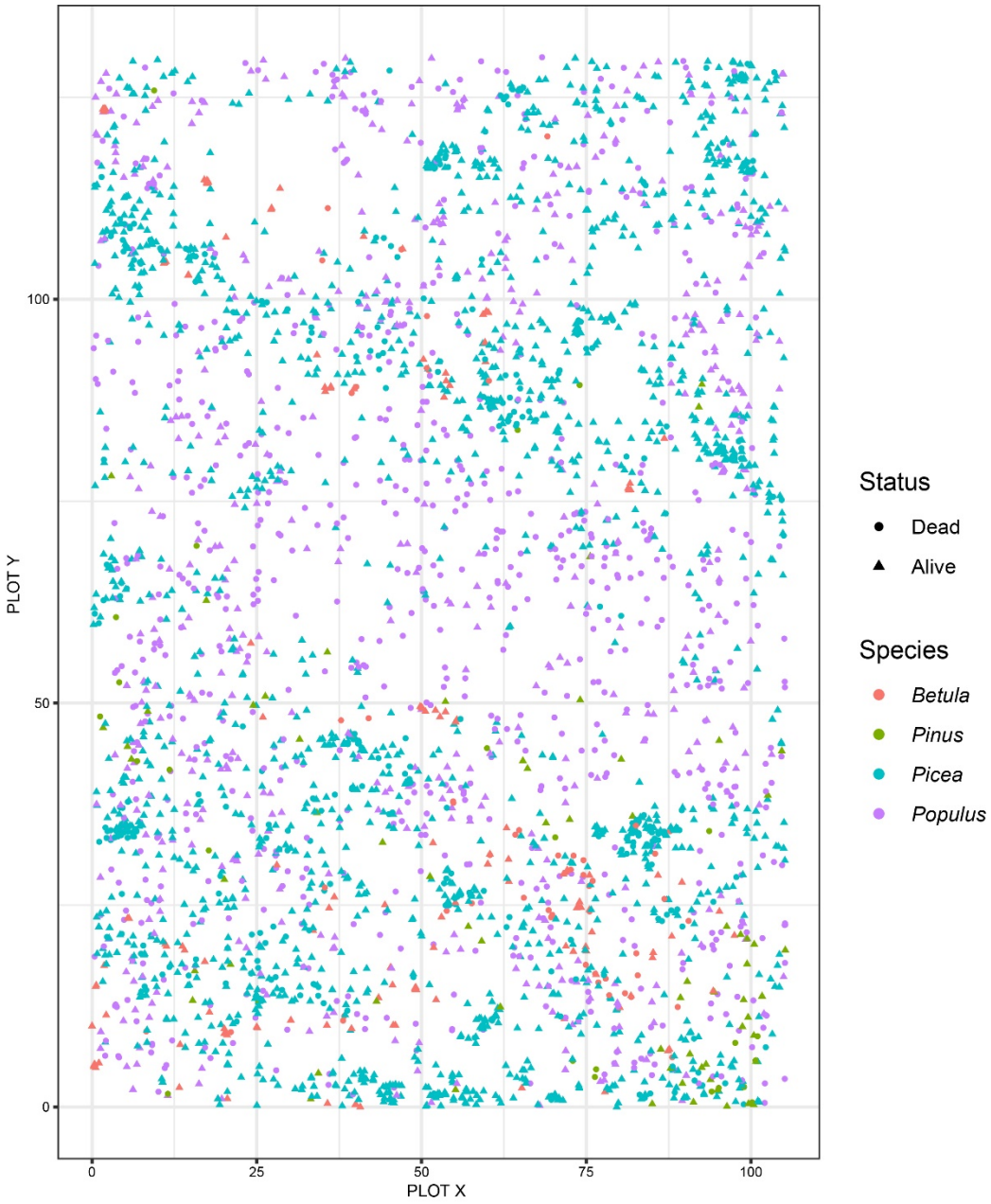

Figure S3.15 Pooled tree-stem map for the 1997 census of the George LaRoi Forest Plot; AB, Canada. The four principle species within the plot (*Picea glauca, Populus tremuloides, Betula papyrifera,* and *Pinus banksiana*) are plotted with living stems (triangles) and dead stems (circles).

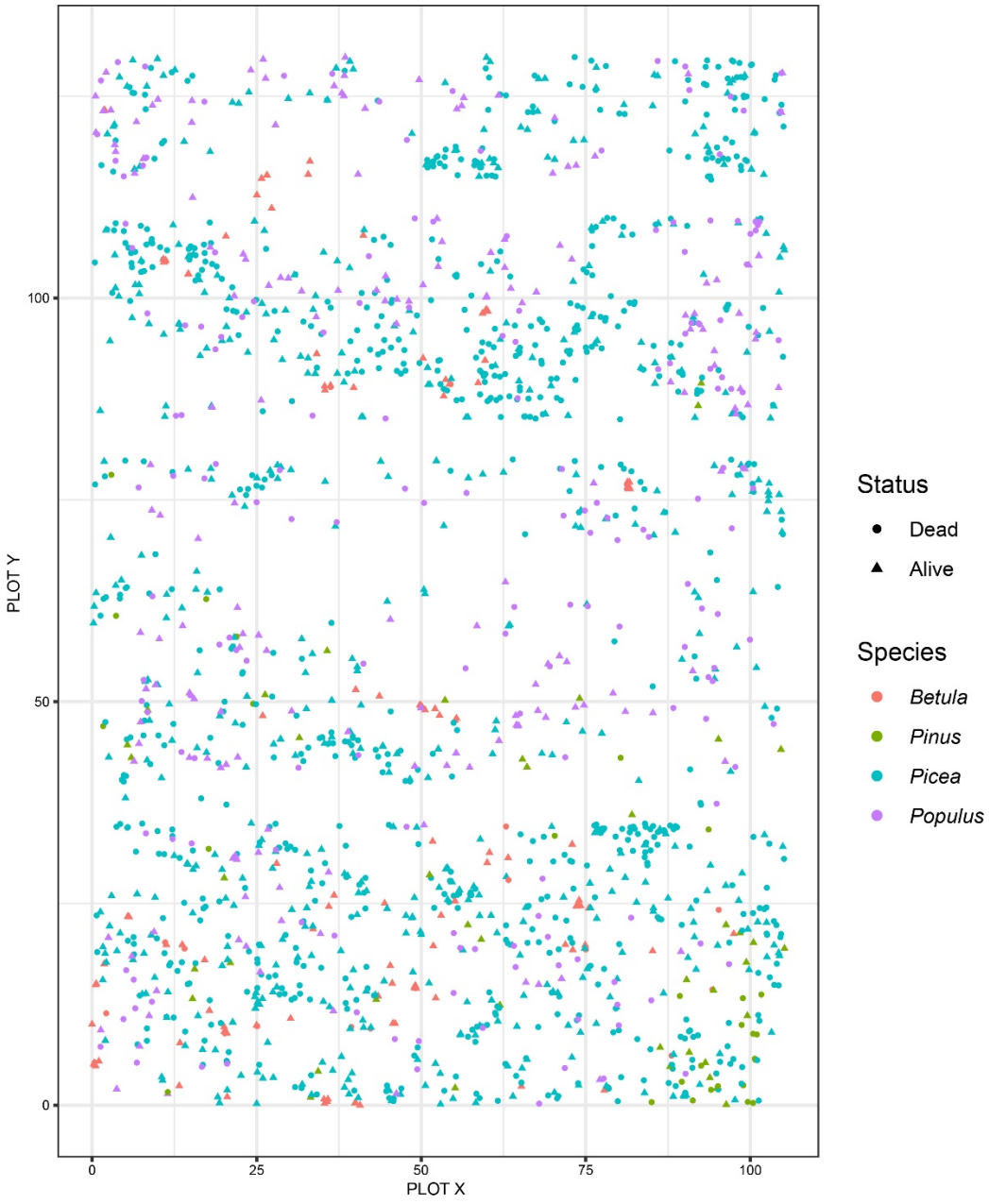

Figure S3.16 Pooled tree-stem map for the 2017 census of the George LaRoi Forest Plot; AB, Canada. The four principle species within the plot (*Picea glauca, Populus tremuloides, Betula papyrifera,* and *Pinus banksiana*) are plotted with living stems (triangles) and dead stems (circles).

References

Birch, J. D., J. A. Lutz, E. Hogg, S. W. Simard, R. Pelletier, G. H. LaRoi, and J. Karst. 2019. Decline of an ecotone forest: 50 years of demography in the southern boreal forest. *Ecosphere* 10:e02698.

Appendix 4.1

Seasonal climate analysis

To identify patterns of drought and tree-response to climate I conducted a seasonal climate analysis for the trees pooled across the six plots described in section '4.2 Methods'.

Methods

A full description of the methods used to sample and assemble tree-ring measurements into a chronology are described in section 4.2.3 'Sampling tree growth records and environmental variability'.

I used a *Pseudotsuga menziesii* var. *glauca* chronology and conducted Pearson correlation analysis between the chronology and the climate variables of interest using the R package, treeclim 2.0 (Zang and Biondi 2015). I detrended the raw chronology using a Friedman Super Smoother Spline in dplR 1.7.0 (Bunn et al. 2019). I used the SEASCORR procedure (Meko et al. 2011) on a pre-whitened chronology. Historical climate data spanned 1951–2016 (Environment and Climate Change Canada 2017). I tested for correlations over aggregated season lengths of 3, 6, 9, and 12 months. The primary variable that explained the most variation, precipitation, and the secondary variable that explained the most residual variation, mean maximum temperature, were selected for the final model (Fig. S4.1).

FIGURES

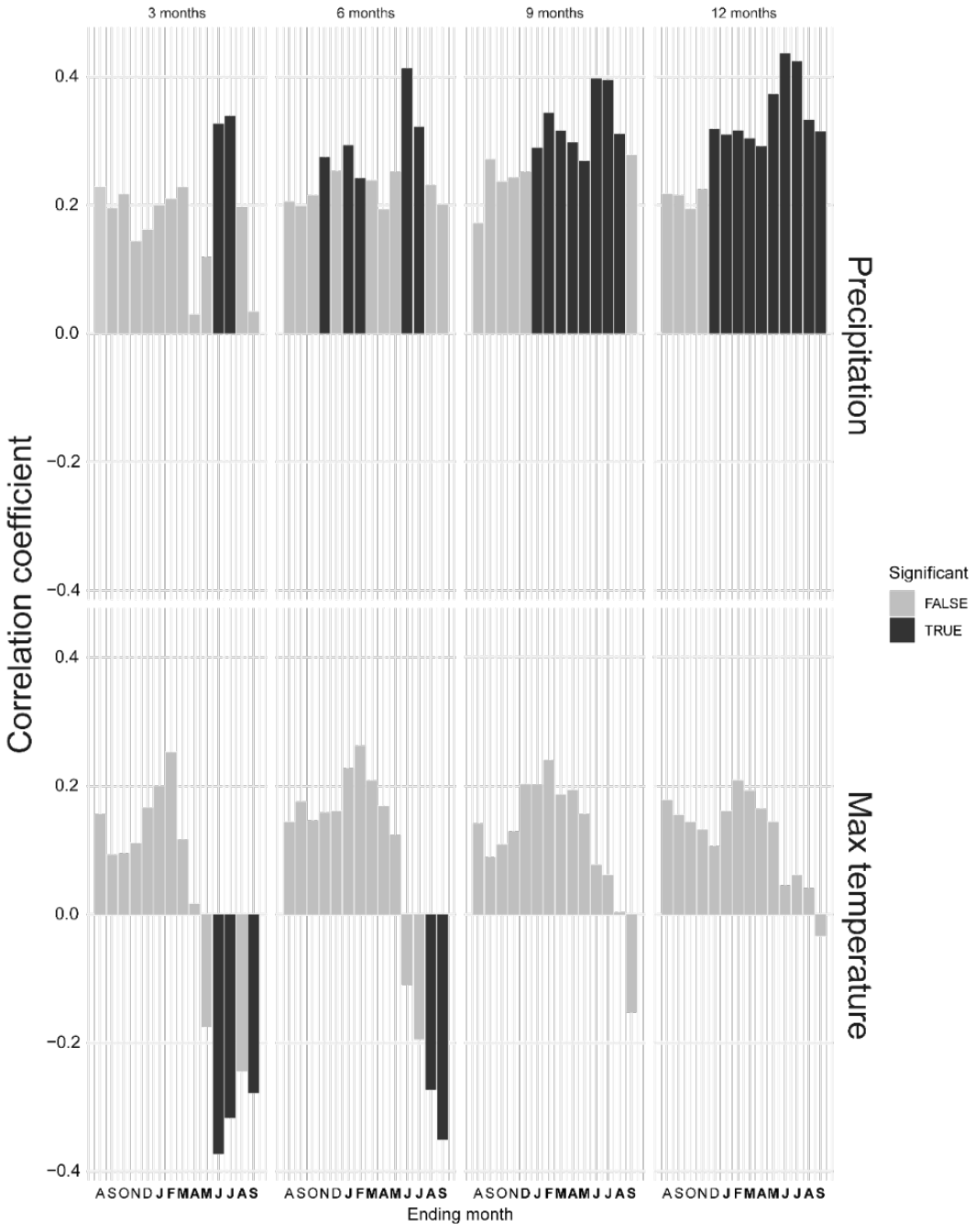

Figure S4.1 Pearson correlation coefficients for the primary (precipitation) and secondary (mean maximum temperature) variables, and *Pseudotsuga menziesii* var. *glauca* ring width at six pooled plots located north of Kamloops, British Columbia, Canada. The strength of correlation is

plotted on the y-axis with time, in months, on the x-axis. The x-axis spans from the previous year's August to the current year's September (months in the current year are bolded). Data is grouped by length of season lengths: 3, 6, 9 and 12 months. Significant correlations are colored black with non-significant correlations colored light grey.

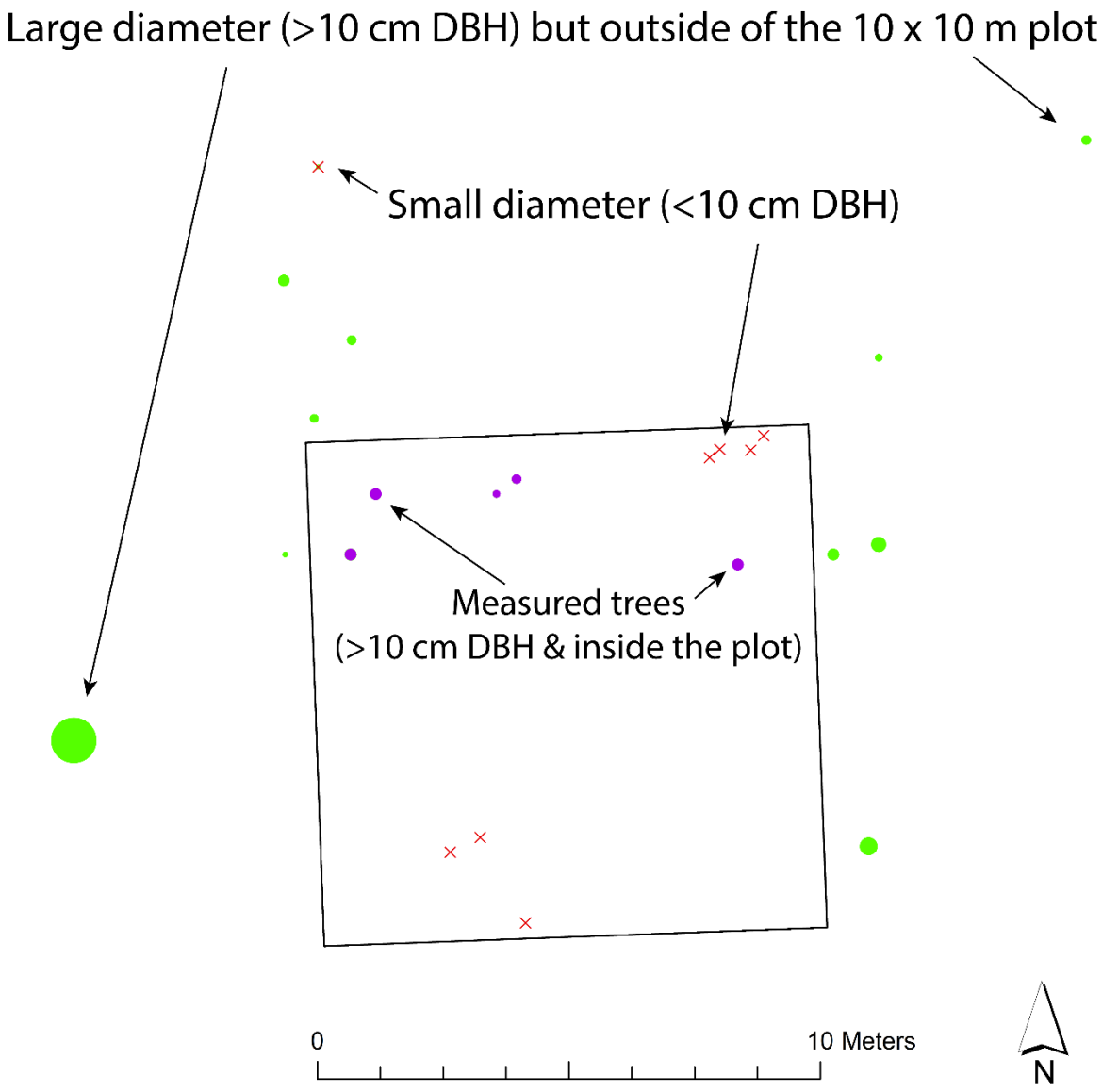

Figure S4.2 A map of the *Pseudotsuga menziesii* var. *glauca* located at one of six plots north of Kamloops, British Columba, Canada. Trees > 0 DBH are plotted proportionally to their actual size on the landscape. Only trees within the 10 × 10 m plot and ≥ 10 cm DBH (purple circles) were included within a model testing how ectomycorrhizal network topology influenced tree growth. Trees that were outside of the plot (green circles) or < 10 cm DBH (red crosses) were excluded from the model. The plots were established and described by Beiler et al. (2015).

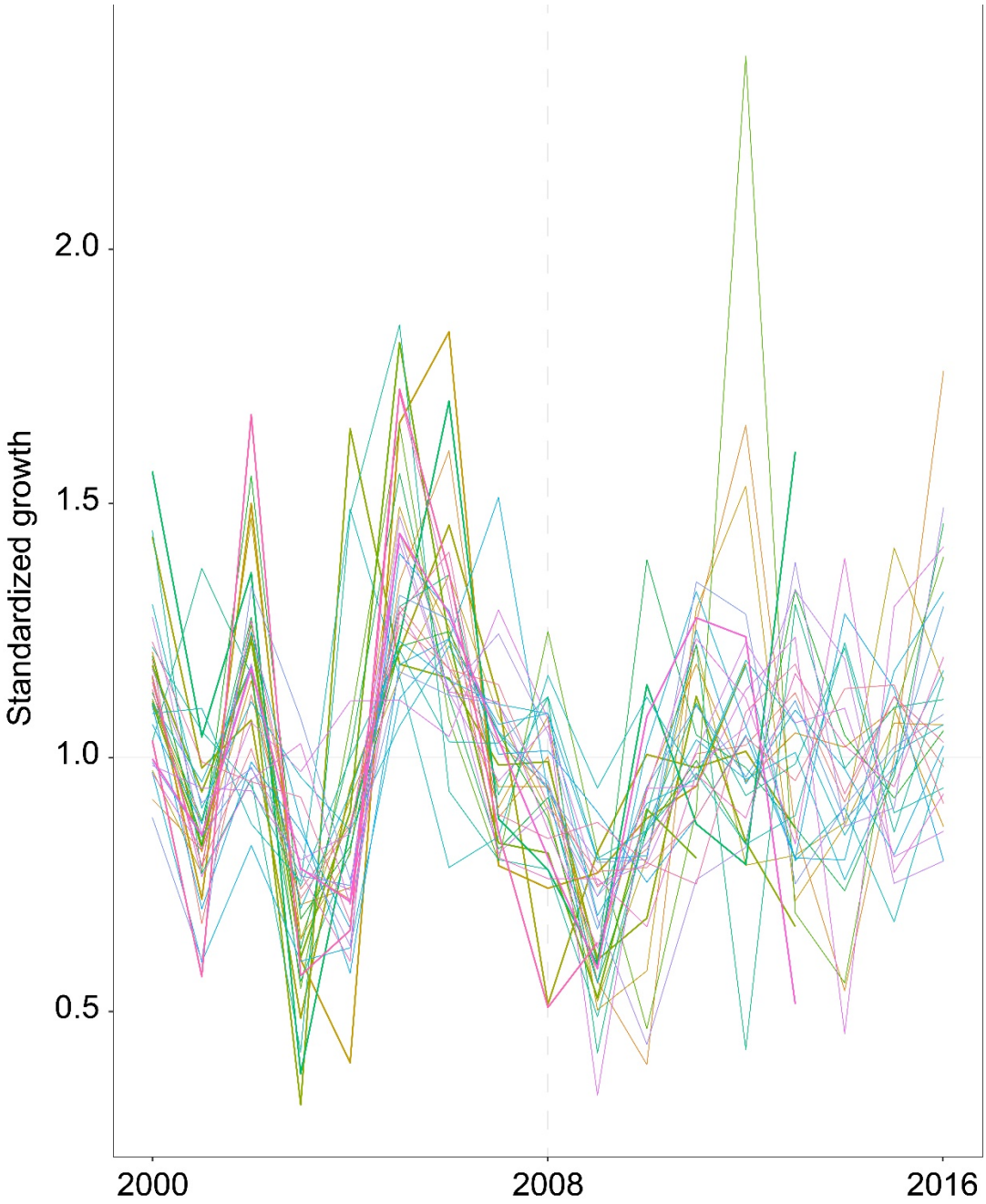

Figure S4.3 The standardized basal area increment 2000–2016 of *Pseudotsuga menziesii* var. *glauca* from six pooled plots located north of Kamloops, British Columbia, Canada. The moving average was calculated based on the preceding two years and following two years for each year 2000–2016. Values above (below) '1' indicate growth greater (lower) than the moving average. Each tree is plotted in a different color.

TABLES

Table S4.1 Ring width characteristics for *Pseudotsuga menziesii* var. *glauca* sampled within and around six forest plots located north of Kamloops, British Columba, Canada. Mean values are reported with standard deviations in parentheses. Variables are N = the number of measured ring series; Age = the mean age of the population; MRW = mean ring width for the entire core; MRW [2000–2016] = the mean ring width from the years 2000 through 2016; MRW [2008] = the mean ring width for the year 2008; IntrC = the inter-correlation value; GINI = the gini coefficient; and AR1 = the auto-regression value for the series.

Plot	N (cores)	Age	MRW (mm)	MRW [2000–2016] (mm)	MRW [2008] (mm)	IntrC	GINI	AR1
1	37	91.30 (2.50)	0.94 (0.32)	0.34 (0.22)	0.31 (0.18)	0.70 (0.09)	0.35 (0.01)	0.78 (0.09)
2	32	103.00 (2.70)	0.81 (0.63)	0.33 (0.18)	0.27 (0.08)	0.73 (0.07)	0.34 (0.00)	0.74 (0.10)
3	52	96.44 (3.13)	1.05 (0.70)	0.74 (0.55)	0.69 (0.35)	0.66 (0.14)	0.27 (0.00)	0.68 (0.12)
4	126	67.64 (1.39)	1.44 (1.01)	0.61 (0.38)	0.48 (0.22)	0.72 (0.14)	0.34 (0.00)	0.80 (0.08)

Plot	N (cores)	Age	MRW (mm)	MRW [2000–2016] (mm)	MRW [2008] (mm)	IntrC	GINI	AR1
5	54	74.36 (2.95)	1.72 (1.02)	0.81 (0.51)	0.64 (0.32)	0.72 (0.15)	0.30 (0.00)	0.79 (0.08)
6	118	65.72 (1.02)	1.60 (0.96)	0.91 (0.61)	0.77 (0.51)	0.71 (0.14)	0.27 (0.00)	0.76 (0.11)

References

Beiler, K. J., S. W. Simard, and D. M. Durall. 2015. Topology of tree–mycorrhizal fungus interaction networks in xeric and mesic Douglas-fir forests. *Journal of Ecology* 103:616-628.

Bunn, A., M. Korpela, F. Biondi, F. Campelo, P. Mérian, F. Qeadan, and C. Zang. 2019. dplR: Dendrochronology Program Library in R. R package version 1.7.0

Environment and Climate Change Canada (2017) Historical climate data: -- climate station 1163780– concatenated, 1951 to 2017. [Data set]. Accessed from https://climate.weather.gc.ca/historical_data/search_historic_data_e.html

Meko, D. M., R. Touchan, and K. J. Anchukaitis. 2011. Seascorr: A MATLAB program for identifying the seasonal climate signal in an annual tree-ring time series. *Computers & Geosciences* 37:1234-1241.

Zang, C., and F. Biondi. 2015. treeclim: an R package for the numerical calibration of proxy-climate relationships. *Ecography* 38:431-436.

Appendix 4.2

Plots and sampling

Six 10 × 10 m plots each separated by ≥ 150 m were selected within a multi-storied, old-growth *Pseudotsuga menziesii* var. *glauca* (Beissn.) Franco forest. Mesoslope position and the relative abundance of *Calamagrostis rubescens* Buckl. and *Pleurozium schreberi* Brid. served as indicators of soil moisture regime. Three relatively xeric plots (plots 1–3) had a greater proportion of *C. rubescens* in the understory, while mesic plots (plots 4–6) had a greater proportion of *P. schreberi* (Beiler et al. 2015).

In each plot, 200 person-hours were spent collecting *Rhizopogon* spp. mycorrhizas between May and June 2008. A dispersed, non-random sampling approach was used to maximize the probability of sampling roots from every tree in the plot. A visual search of the forest floor was conducted at four sampling points surrounding every tree within the plots, oriented in the four cardinal directions and at the inside edge of the crown dripline. When encountered, two or more *Rhizopogon* spp. tuberculate mycorrhizas were collected from each sampling location, placed in 2 ml polypropylene tubes, and frozen at -20°C for molecular analysis. To identify the origin of tree roots isolated from mycorrhiza samples, reference DNA was collected in the form of needle and/or cambium tissue from 646 trees in and surrounding plots. Trees surrounding plots were sampled if their height was greater than distance to plot, with height used as a proxy for potential rooting extent. Tree cambial tissue was placed immediately on dry ice and extracted within 24 hours of collection.

Molecular analysis and network modelling

A subsample of approximately 0.1 g tree needle or cambium tissue and fine-root tissue from within *Rhizopogon* spp. tuberculate mycorrhizas underwent molecular analysis. The work flow included DNA extraction, amplification of microsatellite loci in multiplex PCR reactions, and fragment analysis using a capillary sequencer (3130XL genetic analyzer, Applied Biosystems, Foster City, USA) with GeneMapper software (V4.0, Applied Biosystems; see Beiler et al. 2010, 2015). Tree DNA was genotyped at microsatellite loci *PmOSU*_1C3, *PmOSU*_1F9 and *PmOSU*_2D4 using primers developed by Slavov et al. (2004). *Rhizopogon* DNA was identified to species using the microsatellite loci *Rve2.10* and *Rve2.14*, and to genotype at microsatellite loci *Rv02*, *Rv15*, *Rv46*, *Rve1.21*, *Rv1.34*, *Rve2.44*, *Rve2.77* and *Rve3.21* (*R. vesiculosus*); and at loci *Rv02*, *Rv15*, *Rv46*, *Rv53*, *Rv1.34*, *Rve2.77* and *Rve3.21* (*R. vinicolor*) using primers developed by Kretzer et al. (2003). Two or more samples were considered to represent the same individual if they had identical multilocus genotypes based on the amplified microsatellite loci. The probability of identity for multilocus genotypes are reported in Beiler et al. (2015).

Mycorrhizal network architecture was modeled using Pajek version 2.04 (Batagelj and Mvar 2011, Ljubljana, Slovenia). Two trees were considered linked if they were colonized by the same fungal genet. Network measures were simplified by the exclusion of loops (a tree linked to itself through a single fungal genet) and multiple links between nodes (two or more trees linked through more than one genet). The spatial orientation of tree nodes was integrated with graph-theoretical measures for network analysis and was used to produce a spatially explicit model of network topology. The number of links a tree had to other trees (node degree i.e., degree centrality) and the number of networking trees in each plot are summarized in Table S1.

Summary of sampling and genotyping results

A total of 478 *R. vesiculosus* and 280 *R. vinicolor* mycorrhizas collected within the six 10 × 10 m plots were successfully genotyped to the targeted fungal and tree microsatellite DNA loci. These corresponded to 28 *R. vesiculosus* genets and 27 *R. vinicolor* genets (summarized by plot in Table S1). Among fungal genets represented by more than one mycorrhiza sample, only one was not found to be associated with multiple trees.

Among the 81 tree boles located within plot boundaries, 65 were found in association with *Rhizopogon* spp. mycorrhizas. An additional 101 tree genotypes associated with *Rhizopogon* spp. mycorrhizas inside 10 × 10 m plots were found to originate from tree boles located outside plot boundaries. Together, 166 tree genotypes were encountered as roots (i.e., *Rhizopogon* spp. mycorrhizas) inside the 10 × 10 m plots, 165 of which were connected in a mycorrhizal network.

Table S4.2.1. Attributes of mycorrhizal networks (MN) modelled with *Pseudotsuga menziesii* var. *glauca* trees (i.e., nodes), linked through common affiliation with *Rhizopogon vesiculosus* and *R. vinicolor* fungal genets (links) in 10 × 10 m plots as reported in Beiler *et al*. 2015. Numbers (No.) of trees linked includes all genotypes with roots encountered / connected in MNs within 10 × 10 m plot boundaries, regardless of source tree bole location.

	Xeric soil moisture regime			Mesic soil moisture regime		
	Plot 1	Plot 2	Plot 3	Plot 4	Plot 5	Plot 6
No. tree boles:	13	12	16	13	9	18
No. of trees linked in MN:	26	13	31	27	27	41
No. *R. vesiculosus* mycorrhizas sampled:	69	29	79	59	112	130
No. *R. vinicolor* mycorrhizas sampled:	7	39	48	53	12	121
No. *R. vesiculosus* genets in plot:	4	2	4	4	7	7
No. *R. vinicolor* genets in plot:	2	4	5	2	4	10
No. *R. vesiculosus* genets per tree:	0–2	0–2	0–2	0–4	0–2	0–4
Mean ± SD:	0.92 ± 0.64	0.50 ± 0.67	0.81 ± 0.66	1.15 ± 0.80	1.22 ± 1.30	1.33 ± 1.19
No. *R. vinicolor* genets per tree:	0–1	0–3	0–3	0–1	0–2	0–5
Mean ± SD:	0.15 ± 0.38	0.67 ± 0.98	0.75 ± 0.93	0.85 ± 0.69	0.56 ± 0.53	1.39 ± 1.29
Proportion of trees in 10 × 10 m colonized by *Rhizopogon spp.*:	0.846	0.500	0.875	0.846	0.778	0.889
Node degree range:	0–24	0–12	0–29	0–26	0–24	0–37
Mean node degree ± SD:	18.00 ± 8.49	6.95 ± 4.94	17.15 ± 8.92	17.52 ± 7.34	12.21 ± 7.03	20.19 ± 10.10

References

Batagelj, V., and A. Mrvar. 2011. PAJEK: Program for Analysis and Visualization of Large Networks. Version 2.02.

Beiler, K. J., D. M. Durall, S. W. Simard, S. A. Maxwell, and A. M. Kretzer. 2010. Architecture of the wood-wide web: *Rhizopogon* spp. genets link multiple Douglas-fir cohorts. *New Phytologist* 185:543-553.

Beiler, K. J., S. W. Simard, and D. M. Durall. 2015. Topology of tree–mycorrhizal fungus interaction networks in xeric and mesic Douglas-fir forests. *Journal of Ecology* 103:616-628.

Kretzer, A. M., S. Dunham, R. Molina, and J. W. Spatafora. 2003. Microsatellite markers reveal the below ground distribution of genets in two species of *Rhizopogon* forming tuberculate ectomycorrhizas on Douglas fir. *New Phytologist* 161:313-320.

Slavov, G., G. Howe, I. Yakovlev, K. Edwards, K. Krutovskii, G. Tuskan, J. E. Carlson, S. H. Strauss, and W. Adams. 2004. Highly variable SSR markers in Douglas-fir: mendelian inheritance and map locations. T*heoretical and Applied Genetics* 108:873-880.

Appendix 5.1

Methods

To reconstruct the climatic growth response of the *Pseudotsuga menziesii* var. *glauca* (interior Douglas-fir) I retrieved climate data for a period of at least 50 of the last 100 years. The closest representative climate stations for Cedar Breaks (station 1154) and Wellsville Mountains (station 332) did not have complete temperature or precipitation records pre-1980 (Natural Resources Conservation Service 2020). I retrieved regional climatic data covering 1895–2019 for southern Utah (division 04) and northern Utah (division 05) for climate-growth response analysis (Natural Climatic Data Center 2020). The climate station at Fort St. James, near John Prince, had monthly climate data from 1911–2006 while the Kamloops station had data covering 1951–2016 (Environment and Climate Change Canada 2017).

The site-specific chronologies were created using the cores from *Pseudotsuga* sampled for fungal communities (Fig. S5.1) as well as additional cores from trees that were not sampled for fungal communities. These additional samples were taken using the methods described in section 5.3.4 “Identification of tree age”. The addition of the extra samples resulted in a greater sample size of cores for John Prince (n=70), Kamloops (n=80), Wellsville Mountains (n=51), and Cedar Breaks (n=25). I measured the cores from each site and imported the raw ring measurements into dplR 1.7.0 (Bunn et al. 2019) for detrending. I used a Friedman Super Smoother Spline with a 0.5 rigidity to remove unwanted variation in each site’s chronology. I then used the detrended and pre-whitened chronologies from each site to conduct a Pearson correlation analysis between the chronology and local climate variables of interest using the R package, treeclim 2.0.3 (Zang and Biondi 2015). I used the SEASCORR procedure (Meko et al.

2011) on a pre-whitened chronology. Climate data covered 1895–2017 for the Utah chronologies and from 1950 to 2017 for the British Columbia studies.

I tested for correlations over combined season lengths of 3, 6, 9, and 12 months. I tested a combination of precipitation, mean maximum temperature, mean minimum temperature, and mean temperature as climatic variables. The primary variable that explained the most variation, precipitation, and the secondary variable that explained the most residual variation, mean maximum temperature, were selected for the final model (Fig. S5.1:S5.4).

TABLES

Table S5.1 The number of successfully amplified fungal communities on roots and soils collected around *Pseudotsuga menziesii* var. *glauca* at John Prince Research Forest (British Columbia, Canada), Kamloops (British Columbia, Canada), Wellsville Mountains National Wilderness (Utah, USA), and Cedar Breaks National Monument (Utah, USA).

Location	Roots	Soils	Total
John Prince	10	13	23
Kamloops	11	12	23
Wellsville Mountains	11	10	21
Cedar Breaks	10	9	19

Table S5.2 The number of sampled trees of *Pseudotsuga menziesii* var. *glauca* by soil texture classification at John Prince Research Forest (British Columbia, Canada), Kamloops (British Columbia, Canada), Wellsville Mountains National Wilderness (Utah, USA), and Cedar Breaks National Monument (Utah, USA).

	Location			
Soil classification	John Prince	Kamloops	Wellsville Mountains	Cedar Breaks
Clay	2			
Clay Loam	2			
Fine Sand			5	3
Loam	5	7		1
Loamy Fine Sand			3	4
Sandy Loam	1	3	1	2
Silt Loam	2	3	2	
Silty Clay Loam	1			

Table S5.3 The mean number of reads (standard deviations in parenthesis) after each step of data filtering for fungal communities in soil and on roots collected around *Pseudotsuga menziesii* var. *glauca*.

Input	Filtered	Denoised-Forward Reads	Denoised-Reverse Reads	Merged	Non-chimeric
45,180	22,076	21,384	21,369	18,671	17,819
8,666)	(4,852)	(4,737)	(4,752)	(4,370)	(4,078)

Table S5.4 The p-values reported from a pairwise permutational t-tests analysis of the distributions of the Beta nearest taxonomic index (βNTI) differ for roots and soils collected around *Pseudotsuga menziesii* var. g*lauca* at John Prince Research Forest (British Columbia, Canada), Kamloops (British Columbia, Canada), Wellsville Mountains National Wilderness (Utah, USA), and Cedar Breaks National Monument (Utah, USA).

	Cedar Breaks roots	Cedar Breaks soil	John Prince roots	John Prince soils	Kamloops roots	Kamloops soils	Wellsville soils
Cedar Breaks soil	0.900	-	-	-	-	-	-
John Prince roots	0.004	0.004	-	-	-	-	-
John Prince soils	0.443	0.338	0.002	-	-	-	-
Kamloops roots	0.002	0.002	0.002	0.002	-	-	-
Kamloops soils	0.002	0.002	0.007	0.002	0.002	-	-
Wellsville roots	0.002	0.002	0.002	0.002	0.002	0.002	-
Wellsville soils	0.002	0.002	0.002	0.002	0.011	0.002	0.002

Table S5.5 The output of a Chi-square analysis testing if the proportion of deterministic and stochastic assembly processes varied for fungal communities on roots and soils around *Pseudotsuga menziesii* var. *glauca* at John Prince Research Forest (British Columbia, Canada), Kamloops (British Columbia, Canada), Wellsville Mountains National Wilderness (Utah, USA), and Cedar Breaks National Monument (Utah, USA). Each cell contains its relative contribution (%) towards the final Chi-square score.

	Cedar Breaks		Wellsville		Kamloops		John Prince	
	Roots	Soil	Roots	Soil	Roots	Soil	Roots	Soil
Homogenizing selection	1.4	3.0	13.1	2.7	0.3	0.0	1.2	2.8
Drift	1.8	3.3	10.3	3.9	0.3	0.6	1.8	4.8
Dispersal-limitation	2.2	5.1	28.4	3.7	0.5	1.7	1.5	2.8
Homogenizing dispersal	0.0	0.0	0.0	0.0	0.6	0.5	0.0	0.1

Table S5.6 The number of post-rarefied fungal amplicon sequence variant (ASVs) found on roots and soils around *Pseudotsuga menziesii* var. *glauca* at John Prince Research Forest (British Columbia, Canada), Kamloops (British Columbia, Canada), Wellsville Mountains National Wilderness (Utah, USA), and Cedar Breaks National Monument (Utah, USA). ASVs found in both root and soil habitats are listed in the 'Overlap' column.

Site	Roots	Soils	Overlap	Total
John Prince	1190	1897	627	2460
Kamloops	1286	1779	580	2485
Wellsville Mountains	1134	1608	452	2290
Cedar Breaks	972	988	426	1534
Total	3887	5270	1877	7280

Table S5.7 The p-values from pairwise T-tests of the difference in Shannon's alpha diversity for fungal communities on roots and soils collected around *Pseudotsuga menziesii* var. *glauca* at John Prince Research Forest (British Columbia, Canada), Kamloops (British Columbia, Canada), Wellsville Mountains National Wilderness (Utah, USA), and Cedar Breaks National Monument (Utah, USA). A false discovery rate p-adjustment was used to correct for multiple testing.

	Cedar Breaks roots	Cedar Breaks soil	John Prince roots	John Prince soil	Kamloops roots	Kamloops soil	Wellsville roots
Cedar Breaks soil	0.47	-	-	-	-	-	-
John Prince roots	0.02	0.14	-	-	-	-	-
John Prince soil	0.00	0.00	0.03	-	-	-	-
Kamloops roots	0.07	0.39	0.49	0.00	-	-	-
Kamloops soil	0.00	0.00	0.16	0.47	0.03	-	-
Wellsville roots	0.54	0.81	0.05	0.00	0.20	0.00	-
Wellsville soil	0.00	0.00	0.02	0.81	0.00	0.39	0.00

Table S5.8 The outputs of two PERMANOVA analyses testing if soil and root fungal communities differ by site. Fungal communities were collected around *Pseudotsuga menziesii* var. *glauca* at John Prince Research Forest (JOHN; British Columbia, Canada), Kamloops (KAML; British Columbia, Canada), Wellsville Mountains National Wilderness (WELL; Utah, USA), and Cedar Breaks National Monument (CEBR: Utah, USA). Pairwise PERMANOVA were conducted to test for pairwise differences between roots or soils across sites.

Soil samples

	Df	SumsOfSqs	MeanSqs	F	R^2	Pr(>F)
Site	3	3.488	1.163	2.903	0.186	0.001
Residual	38	15.215	0.400		0.814	
Total	41	18.703			1.000	

Pairwise PERMANOVA p-values

	CEBR soil	JOHN soil	KAML soil
JOHN soil	0.001	-	-
KAML soil	0.001	0.001	-
WELL soil	0.001	0.001	0.001

Root samples

	Df	SumsOfSqs	MeanSqs	F	R^2	Pr(>F)
Site	3	3.488	1.163	2.903	0.186	0.001
Residual	38	15.215	0.400		0.814	
Total	41	18.703			1.000	

Pairwise PERMANOVA p-values

	CEBR roots	JOHN roots	KAML roots
JOHN roots	0.001	-	-
KAML roots	0.001	0.002	-
WELL roots	0.001	0.001	0.001

Table S5.9 The proportional read abundance (%) of fungal amplicon sequence variants for roots and soils collected around *Pseudotsuga menziesii* var. *glauca* at four sites in western North America. The sites are John Prince Research Forest (British Columbia, Canada), Kamloops (British Columbia, Canada), Wellsville Mountains National Wilderness (Utah, USA), and Cedar Breaks National Monument (Utah, USA).

		John Prince		Kamloops		Wellsville		Cedar Breaks	
		Root	Soil	Root	Soil	Root	Soil	Root	Soil
Ascomycota		61.3	57.5	58.9	61.3	61.3	57.9	54.3	57.6
	NA	23.2	24.4	33.4	33.1	42.5	42.7	20.9	23
	Pyronemataceae	0.7	0.2	2.2	1.1	2.1	2.5	23.9	27
	unidentified_29	9.6	7.1	4.7	8.9	1.9	3.9	4.1	3.1
	Vibrisseaceae	10.3	2.1	1.5	0.2	0.1	0.2	0.8	0.0
Basidiomycota		15.1	13.9	13.8	13.2	12.6	11.7	35.5	32.7
	Atheliaceae	2.7	1.8	0.5	0.8	2.6	0.0	9.0	4.0
	Inocybaceae	0.0	0.2	0.0	0.1	0.0	0.2	2.4	5.9
	Rhizopogonaceae	1.9	0.2	1.9	0.3	0.3	0.0	7.1	0.1
	Tricholomataceae	2.0	0.2	2.7	1.9	4.8	1.9	6.8	8.0

		John Prince		Kamloops		Wellsville		Cedar Breaks	
Mucoromycota		5.8	9.0	5.9	10.4	0.2	5.9	0.1	0.5
	Umbelopsidaceae	5.7	8.9	5.8	10.4	0.2	5.9	0.1	0.5
NA		14.4	16.3	14.9	11.3	23.7	19.1	8.2	7.3
Unidentified		2.8	2.6	4.9	3.3	1.8	4.1	1.6	1.7

Table S5.10 The proportional fungal sequence abundance by functional guild for roots and soils sampled around *Pseudotsuga menziesii* var. *glauca* at John Prince Research Forest (British Columbia, Canada), Kamloops (British Columbia, Canada), Wellsville Mountains National Wilderness (Utah, USA), and Cedar Breaks National Monument (Utah, USA). The 'Habitat' of each community is the substrate (roots or soils) by site.

Guild	Cedar Breaks		Wellsville		Kamloops		John Prince	
	Roots	Soils	Roots	Soils	Roots	Soils	Roots	Soils
Ectomycorrhizal	44.4	44.1	4.3	3.6	5.3	5.5	9.2	5.6
Ecto-mixed	13.5	14.4	5.0	2.5	5.2	4.5	4.7	8.2
Saprotrophic	2.7	2.7	7.7	9.5	10.7	15.7	10.3	14.6
Other guilds	2.3	0.9	7.7	4.2	16.4	10.8	20.8	11.5
Unknown	36.8	37.7	75.0	80.0	62.2	63.2	54.8	59.9

FIGURES

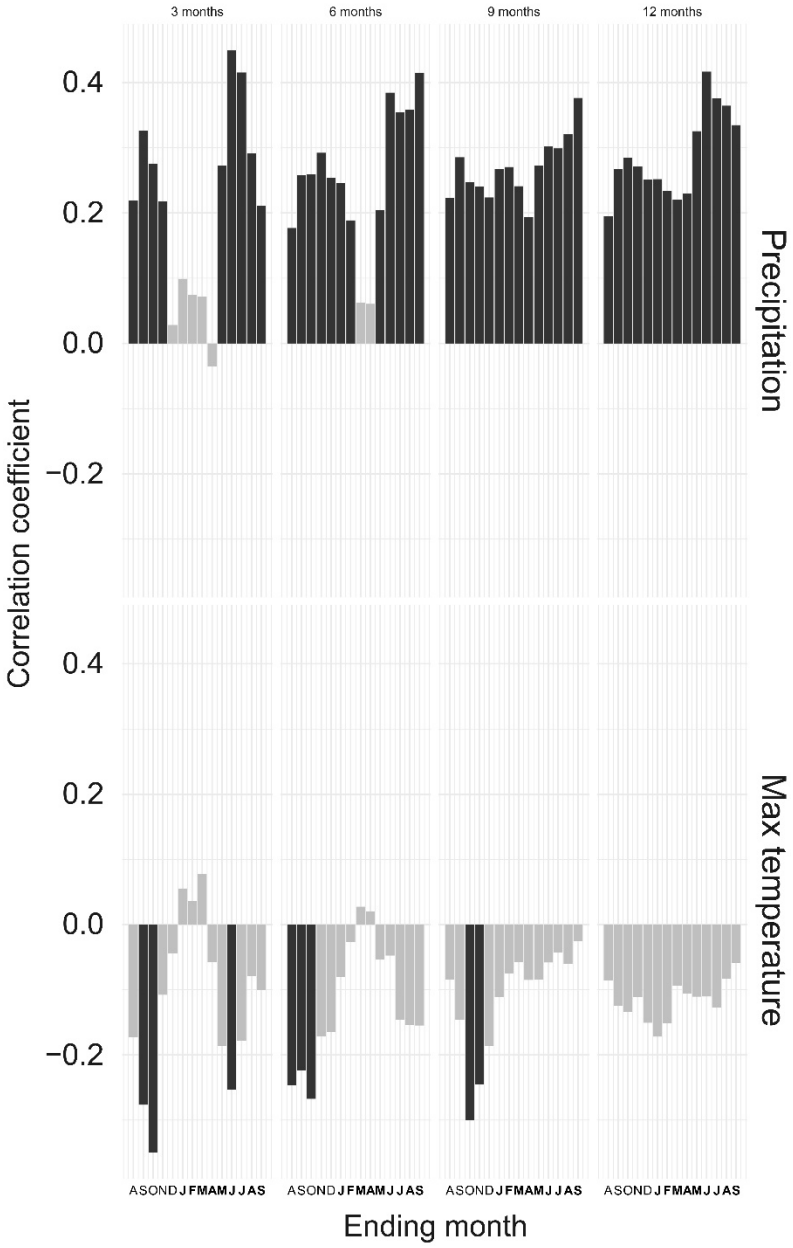

Figure S5.1 Pearson correlation coefficients for the primary (precipitation) and secondary (mean maximum temperature) variables, and *Pseudotsuga menziesii* var. *glauca* ring width from John Prince Research Forest, British Columbia, Canada. The strength of correlation is plotted on the y-axis with time, in months, on the x-axis. The x-axis spans from the previous year's August to

the current year's September (months in the current year are bolded). Data is grouped by length of season lengths: 3, 6, 9 and 12 months. Significant correlations are colored black with non-significant correlations colored light grey.

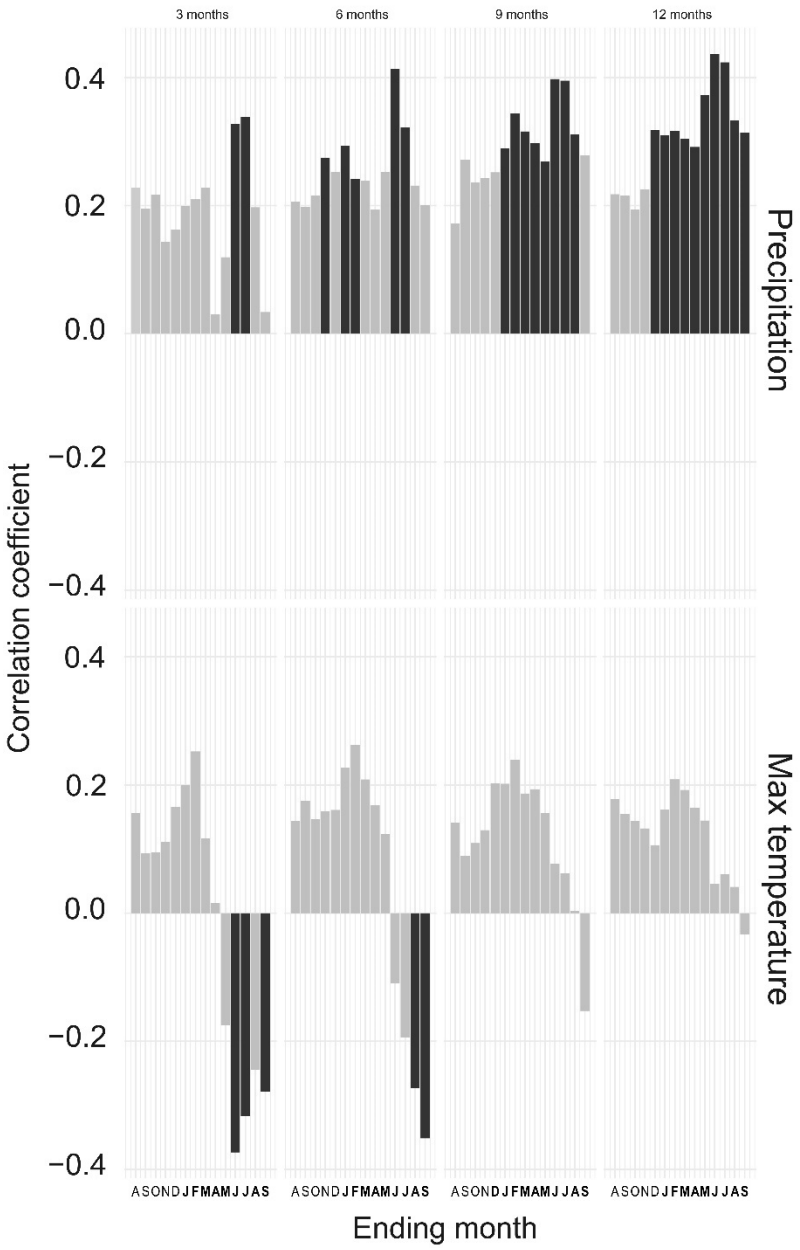

Figure S5.2 Pearson correlation coefficients for the primary (precipitation) and secondary (mean maximum temperature) variables, and *Pseudotsuga menziesii* var. *glauca* ring width from Kamloops, British Columbia, Canada. The strength of correlation is plotted on the y-axis with time, in months, on the x-axis. The x-axis spans from the previous year's August to the current year's September (months in the current year are bolded). Data is grouped by length of season

lengths: 3, 6, 9 and 12 months. Significant correlations are colored black with non-significant correlations colored light grey. This figure is reproduced from the analysis in Appendix 4.1.

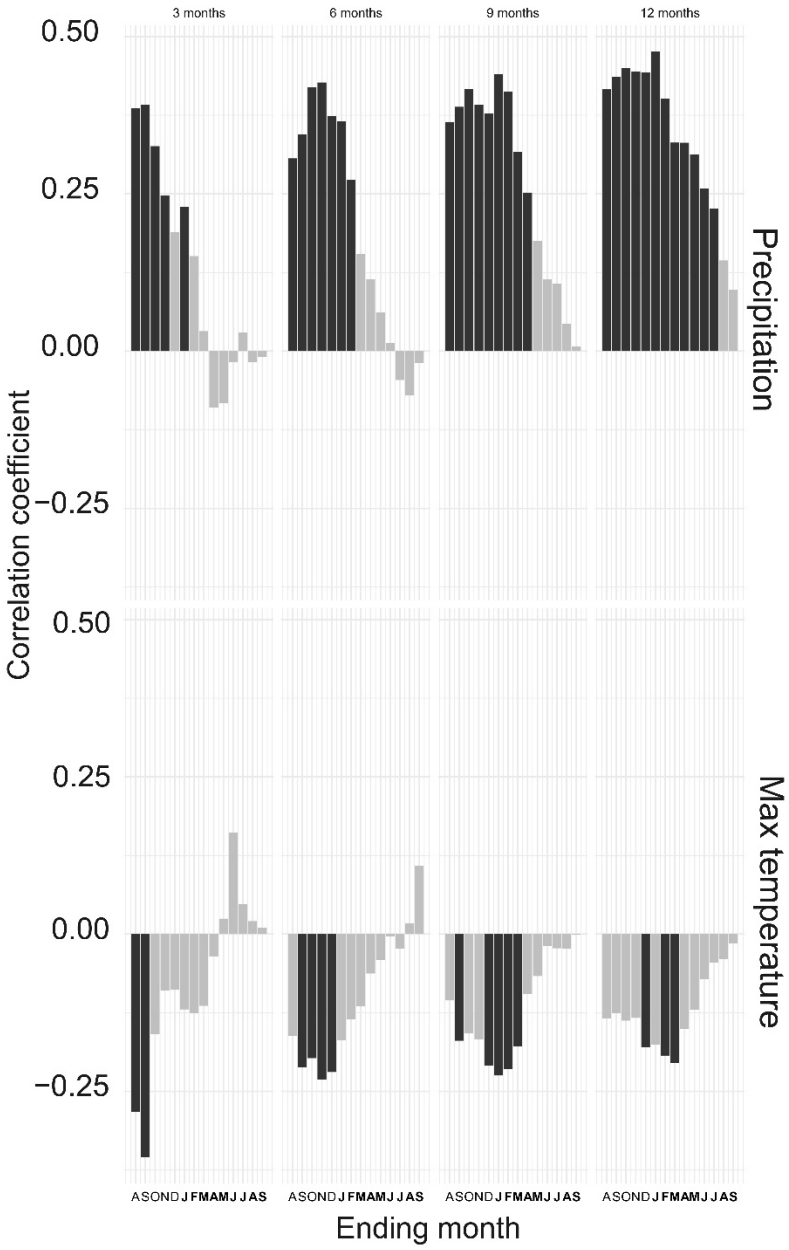

Figure S5.3 Pearson correlation coefficients for the primary (precipitation) and secondary (mean maximum temperature) variables, and *Pseudotsuga menziesii* var. *glauca* ring width from the Wellsville Mountain Wilderness, Utah, USA. The strength of correlation is plotted on the y-axis with time, in months, on the x-axis. The x-axis spans from the previous year's August to the current year's September (months in the current year are bolded). Data is grouped by length of

season lengths: 3, 6, 9 and 12 months. Significant correlations are colored black with non-significant correlations colored light grey.

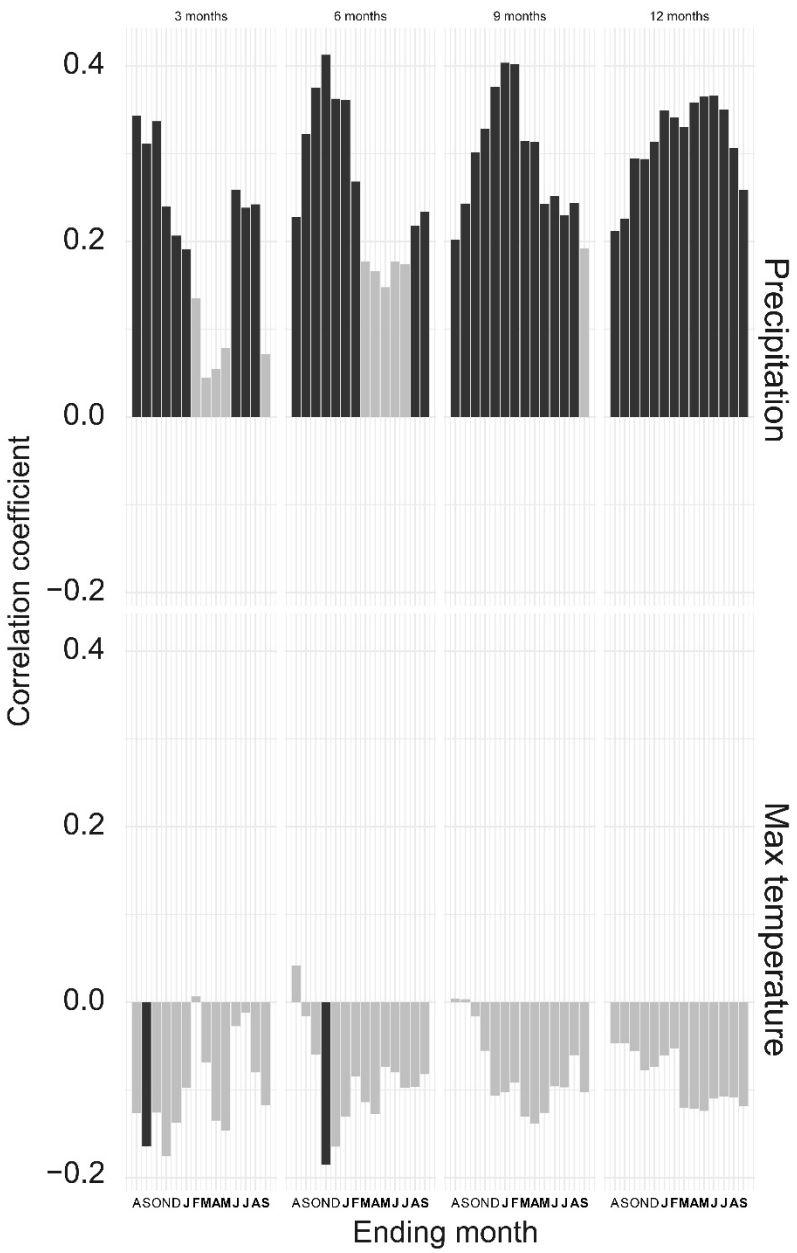

Figure S5.4 Pearson correlation coefficients for the primary (precipitation) and secondary (mean maximum temperature) variables, and *Pseudotsuga menziesii* ring var. *glauca* width from Cedar Breaks National Monument, Utah, USA. The strength of correlation is plotted on the y-axis with time, in months, on the x-axis. The x-axis spans from the previous year's August to the current

year's September (months in the current year are bolded). Data is grouped by length of season lengths: 3, 6, 9 and 12 months. Significant correlations are colored black with non-significant correlations colored light grey.

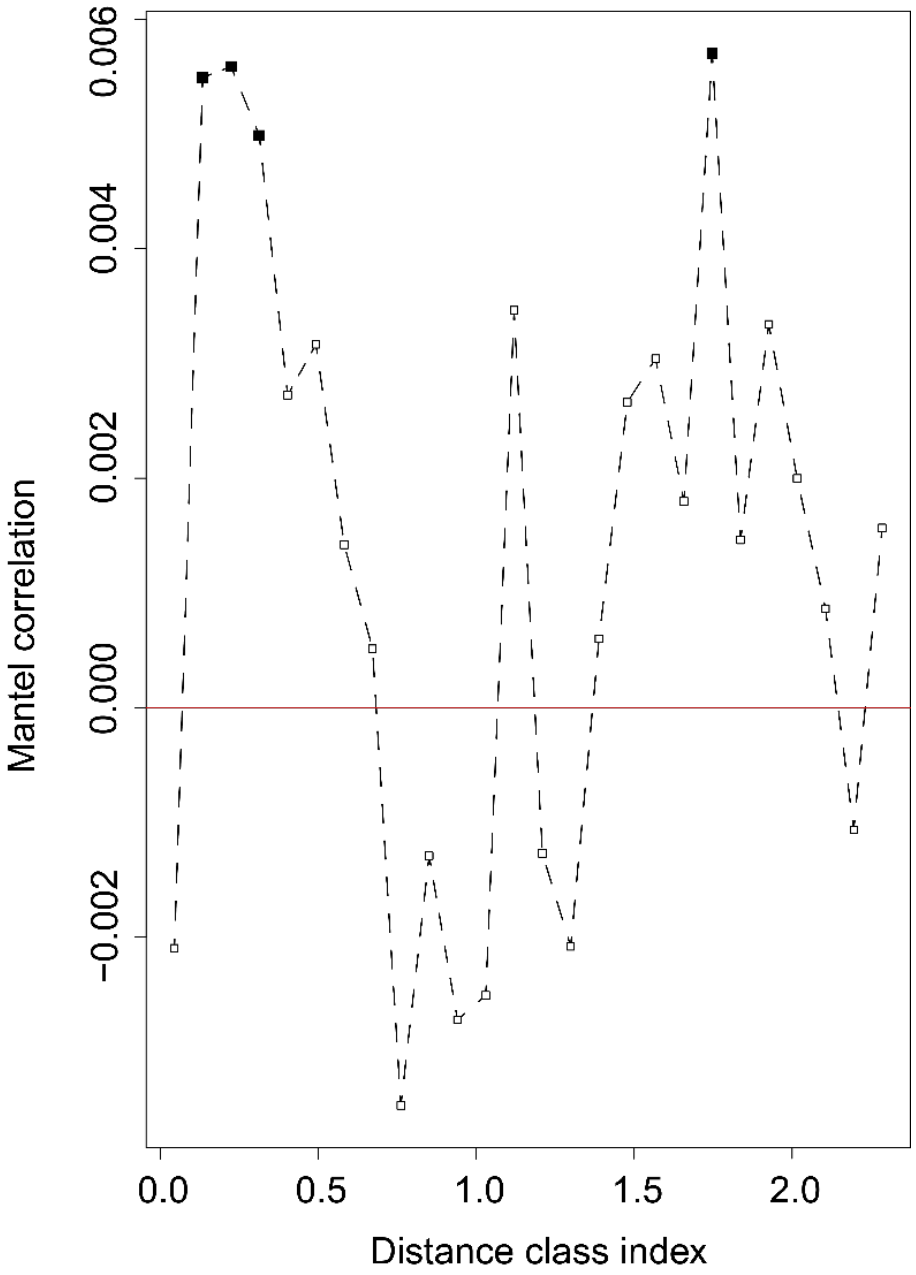

Figure S5.5 The mantel correlogram of the phylogenetic signal between fungal communities around *Pseudotsuga menziesii* var. *glauca*. Significant Pearson correlation coefficients ($p < 0.05$; bolded) indicate that fungal amplicon sequence variants (ASVs) have correlated environmental optima (niches) at a specific phylogenetic distance (relatedness; x-axis).

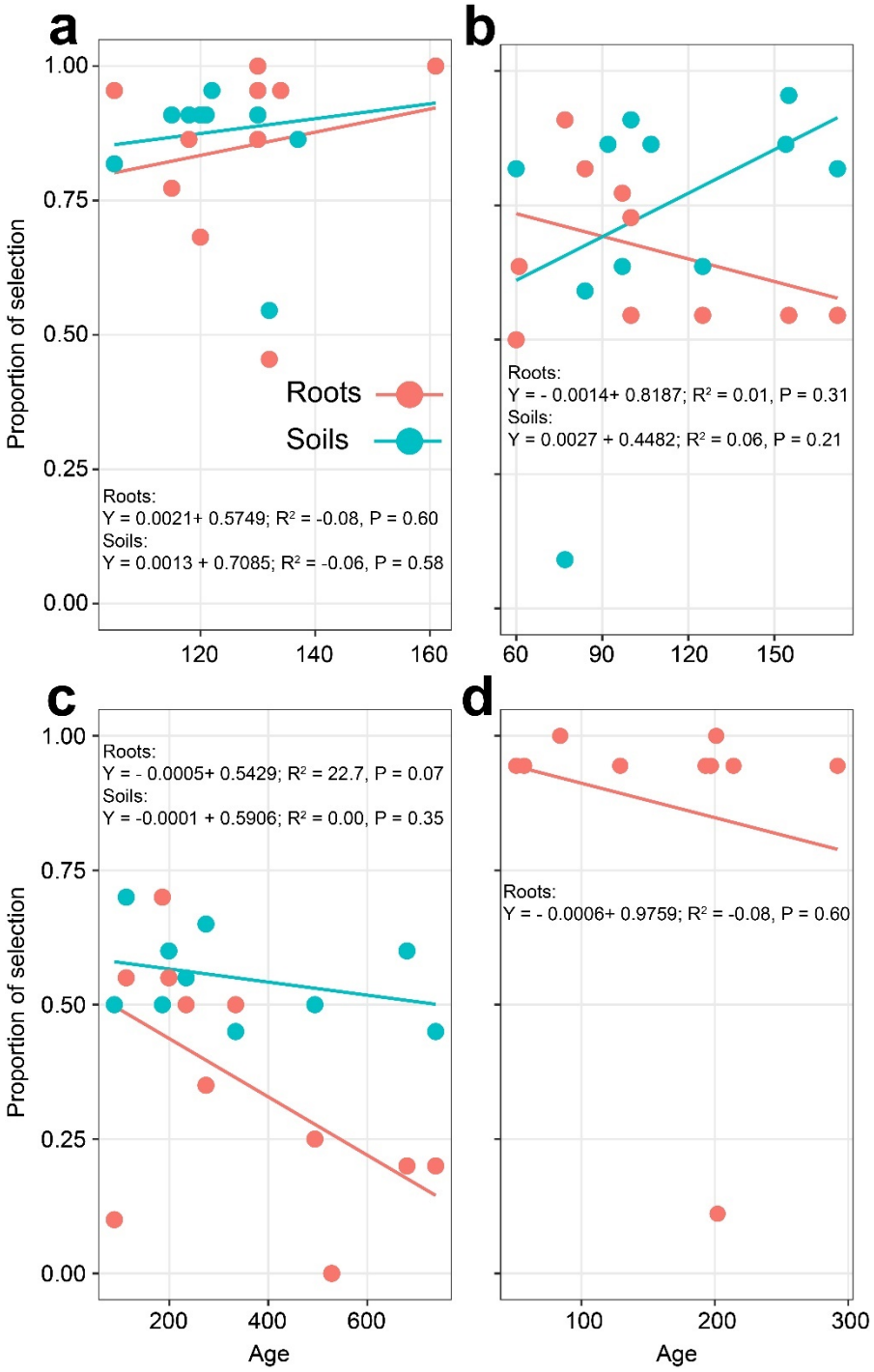

Figure S5.6 The linear relationships between the proportion of deterministic selection pressures and tree age for fungal communities found on roots and soil around *Pseudotsuga menziesii* var. glauca at (**a**) John Prince Research Forest (British Columbia, Canada), (**b**) Kamloops (British

Columbia, Canada), (**c**) Wellsville Mountains National Wilderness (Utah, USA), and (**d**) Cedar Breaks National Monument (Utah, USA).

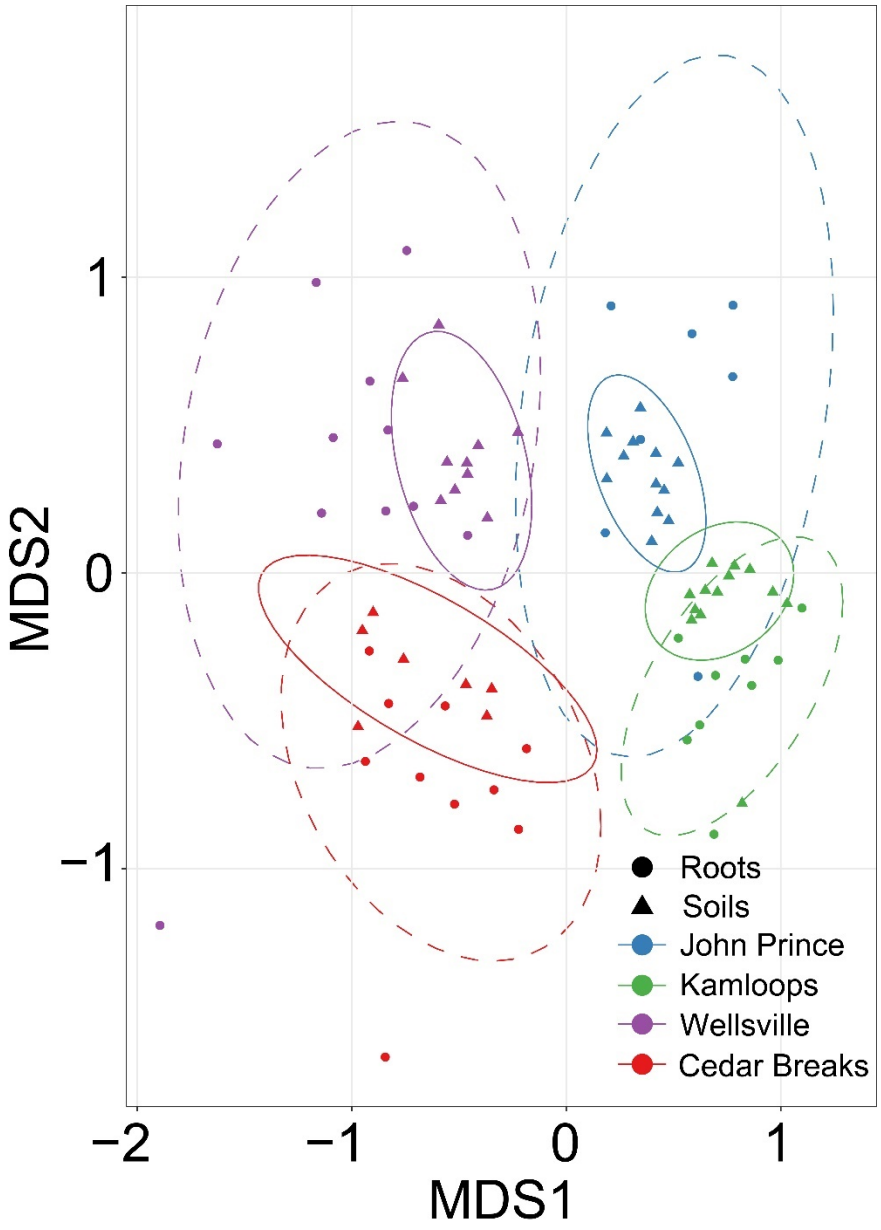

Figure S5.7 An ordination of fungal community composition found on roots and soil around *Pseudotsuga menziesii* var. glauca at John Prince Research Forest (British Columbia, Canada), Kamloops (British Columbia, Canada), Wellsville Mountains National Wilderness (Utah, USA), and Cedar Breaks National Monument (Utah, USA). Community dissimilarity was calculated using a Bray-Curtis dissimilarity metric and ordinated using 999 permutations. Ordination stress was 0.1628.

Image S5.1 The dispersed stands of *Pseudotsuga menziesii* var. *glauca* on the Wellsville Mountain National Wilderness, Utah, USA. Image taken facing north-east at approximately 2,800 m elevation.

REFERENCES

Bunn, A., M. Korpela, F. Biondi, F. Campelo, P. Mérian, F. Qeadan, and C. Zang. 2019. dplR: dendrochronology program library in R. R package version 1.7.0.

Environment and Climate Change Canada. (2017). Historical climate data: -- climate station 1163780 and 1092970 – concatenated, 1911 – 2016. [Data set]. Retrieved from https://climate.weather.gc.ca/historical_data/search_historic_data_e.html

Meko, D. M., R. Touchan, and K. J. Anchukaitis. 2011. Seascorr: A MATLAB program for identifying the seasonal climate signal in an annual tree-ring time series. *Computers & Geosciences* 37:1234-1241.

Natural Climatic Data Center. (2020). State divisional data. U.S. Department of Commerce. [Data set]. Accessed on Sept 25, 2020 from https://www7.ncdc.noaa.gov/CDO/CDODivisionalSelect.jsp#

Natural Resources Conservation Service. (2020). Utah SNOTEL climate records: -- climate station 332 and 1154. [Data set]. US Department of Agriculture.

Zang, C., and F. Biondi. 2015. treeclim: an R package for the numerical calibration of proxy-climate relationships. *Ecography* 38:431-436.

Appendix 6.1

Ethanol precipitation protocol

To improve amplification of rDNA I used an ethanol precipitation of DNA to help remove polymerase chain reaction (PCR) inhibitors that were likely present in extracted root and soil samples. In a 1.5 ml Eppendorf tube I added 1/10 volume of 3M sodium acetate, extracted DNA, and 2.5 volume of 100% ethanol that had been chilled at -20^{o} C. I mixed the solution and incubated in the freezer at -20^{o} C for 30 mins. The incubated samples were spun at full speed in a microcentrifuge at 4^{o} C for 15 mins. I then decanted the supernatant before adding 1 mL of 70% chilled ethanol. I mixed the solution and then placed the samples on a microcentrifuge, full speed, at 4^{o}C for 5 mins. I then decanted the supernatant and air-dried the samples before resuspending the pellet with nuclease free water to the original sample volume.

Kriging of soil nutrients

Spatial interpolation of soil nutrients by kriging

To assess if soil nutrients differed significantly between *Pinus flexilis* (limber pine) and *Pinus longaeva* (Great Basin bristlecone pine) I interpolated soil nutrient data via kriging. The soil was originally sampled in a semi-random grid across the Utah Forest Dynamics Plot (UFDP) following the sampling design of John et al. (2007). The soil nutrients were measured using the analytical methods detailed in Baldeck et al. (2013).

I used the gstat 2.0.6 package to interpolate each soil nutrient across the UFDP (Pebesma 2004). Nitrate, iron, calcium, and magnesium were transformed with a square-root

transformation prior to kriging to normalize the data across a 1 × 1 m grid between the measured points.

I used the 'powerTransform' function from the car 3.0-7 package (Fox and Wiesberg 2019) to identify the optimal transformation to normalize the variables (pH, phosphorous, ammonium, nitrate, calcium, iron, potassium, magnesium, manganese, effective cation exchange capacity, base saturation, and sodium). I excluded several variables that were still strongly non-normal after transformation (nitrate, base saturation). After normalizing the variables, I generated semi-variograms and assessed the degree of spatial autocorrelation for each variable to ensure that variables were autocorrelated over the distance between samples. I excluded sodium, aluminum, effective cation exchange capacity, and iron from the dataset due to weak spatial autocorrelation and high variance. I used the 'krige' function (Pebesma 2004) to interpolate the remaining nutrients and then back-transformed each nutrient to their original units (mg kg^{-1}). After exporting the interpolated nutrients from R, I used ArcMap 10.4. (ESRI, Redlands, CA) to extract the interpolated nutrient values that intercepted the center of each sampled tree's bole.

To test if soil nutrients differed between the tree species and fungal sample types (roots vs. soil) I used the 'vegdist' function from vegan 2.5-6 (Oksanen et al. 2019) to create a Mahalanobis distance matrix representing the dissimilarities in soil nutrients between each sampled tree. I used a metaMDS to visualize the differences between trees and a PERMANOVA to test if significant differences existed between the soil nutrients around the tree species (Appendix 5.1 Fig. S6.8; Table S6.8).

Table S6.1 The mean number of sequence reads (standard deviations in parenthesis) for soil and root samples taken from *Pinus flexilis* and *Pinus longaeva* at the Utah Forest Dynamics Plot, Cedar Breaks National Monument, Utah, USA. The columns represent the subsequent steps of sequence filtering and denoising from the initial reads to the final non-chimeric reads.

Species	Sample	Initial reads	Filtered	Forward denoised	Reverse denoised	Merged	Non-chimeric
P. flexilis	Roots	47062 (6459)	23074 (2945)	22672 (2945)	22647 (2980)	20008 (2898)	19159 (2818)
P. longaeva	Roots	51463 (6356)	26116 (3969)	25605 (3918)	25577 (3908)	23103 (3602)	22133 (3289)
P. flexilis	Soil	47983 (5105)	24462 (2841)	23935 (2821)	23925 (2816)	21850 (2660)	20918 (2638)
P. longaeva	Soil	48319 (5387)	24452 (2621)	23767 (2657)	23779 (2660)	21217 (2843)	20193 (2705)

Table S6.2 The number of successfully amplified root and soil samples from around *Pinus flexilis* and *Pinus longaeva* at the Utah Forest Dynamics Plot, Utah, USA. The presence of heartrot prevented the dating of the tree corresponding to one *P. longaeva* root sample.

	Pinus flexilis	*Pinus longaeva*	*Pinus flexilis*	*Pinus longaeva*
	Roots		Soil	
Samples with an accompanying tree age	9	6	9	9
Total sample number	9	7	9	9

Table S6.3 The number of rarefied fungal amplicon sequence variants (ASV) from roots and soils collected around *Pinus flexilis* and *Pinus longaeva* at the Utah Forest Dynamics Plot, Utah, USA.

Species	Roots	Soil	Total
P. flexilis	720	1262	1697
P. longaeva	736	1465	1863
Total	1257	2270	2898

Table S6.4 The output of a beta-dispersion test for the homogeneity of multivariate variance between fungal communities found on the roots and soils of Pinus flexilis and Pinus longaeva at the Utah Forest Dynamics Plot, Utah, USA.

	Df	SumofSqrs	MeanSqr	F statistic	# of Permutations	p-value
Sample type	1	0.024	0.024	10.373	999	0.002
Residuals	32	0.076	0.002			

Table S6.5 The output of two PERMANOVAs testing if fungal communities on roots and soils of *Pinus flexilis* varied with tree age. Communities distances were calculated with a Bray-Curtis distance metric and permuted 999 times.

Pinus flexilis roots

Roots	Df	SumsOfSqs	MeanSqs	F.Model	R2	Pr(>F)
Tree age	1	0.629	0.629	1.596	0.185	0.009
Residuals	7	2.761	0.394		0.814	
Total	8	3.391			1	

Pinus flexilis soils

	Df	SumsOfSqs	MeanSqs	F.Model	R2	Pr(>F)
Tree age	1	0.431	0.431	1.366	0.163	0.101
Residuals	7	2.210	0.315		0.836	
Total	8	2.641			1	

Table S6.6 The output of linear models testing the effects of tree age on Shannon's alpha diversity of fungal communities around *Pinus flexilis* roots and soils at the Utah Forest Dynamics Plot, Utah, USA.

Pinus flexilis roots

Coefficient	Estimate	Std. error	T value	Pr(>|t|)
Intercept	3.23	0.38	8.51	6.13E-05
Age	0.001	0.001	0.69	0.50

Pinus flexilis soils

Coefficient	Estimate	Std. error	T value	Pr(>|t|)
Intercept	4.60	0.28	16.14	8.51E-07
Age	0.001	0.001	-0.84	0.42

Table S6.7 The functional guilds of fungal amplicon sequence variants that were shared between the roots of *Pinus flexilis* and *Pinus longaeva* at the Utah Forest Dynamics Plot, Utah, USA.

Guild	Count
Bryophyte Parasite-Ectomycorrhizal-Ericoid Mycorrhizal-Undefined Saprotroph	1
Dung Saprotroph-Ectomycorrhizal-Litter Saprotroph-Undefined Saprotroph	1
Ectomycorrhizal	28
Ectomycorrhizal-Fungal Parasite	8
Ectomycorrhizal-Lichen Parasite-Lichenized-Plant Pathogen	5
Ectomycorrhizal-Orchid Mycorrhizal-Root Associated Biotroph	1
Ectomycorrhizal-Undefined Saprotroph	4
Endophyte-Lichen Parasite-Plant Pathogen-Undefined Saprotroph	1
Endophyte-Litter Saprotroph-Soil Saprotroph-Undefined Saprotroph	1
Ericoid Mycorrhizal	1
Fungal Parasite-Lichen Parasite	1
Fungal Parasite-Undefined Saprotroph	2
Plant Saprotroph-Wood Saprotroph	1
Undefined Saprotroph	4
Unknown guild	136
Wood Saprotroph	4

Table S6.8 The output of a PERMANOVA testing whether soil nutrients differed between sampled *Pinus flexilis* and *Pinus longaeva* at the Utah Forest Dynamics Plot, Utah, USA. Nutrients included: pH, ammonium, phosphorous, manganese, potassium, and calcium.

Variable	Df	SumsofSqs	MeanSqs	F.model	R^2	Pr(>F)
Tree species	1	10.92	10.92	1.86	0.05	0.07
Residuals	32	187.07	5.84			
Total	33	198				

Table S6.9 The approximate milliequivalent (mEq) values per 100g of soil for across the Utah Forest Dynamics Plot, Utah, USA. The mEq values were calculated by converting mg/kg of mEq.

Phosphorous	Ammonium	Nitrate	Aluminum	Calcium	Iron	Potassium	Magnesium	Manganese	Sodium
0.253	0.113	0.003	0.095	137.695	0.0198	4.974	21.248	0.102	0.290

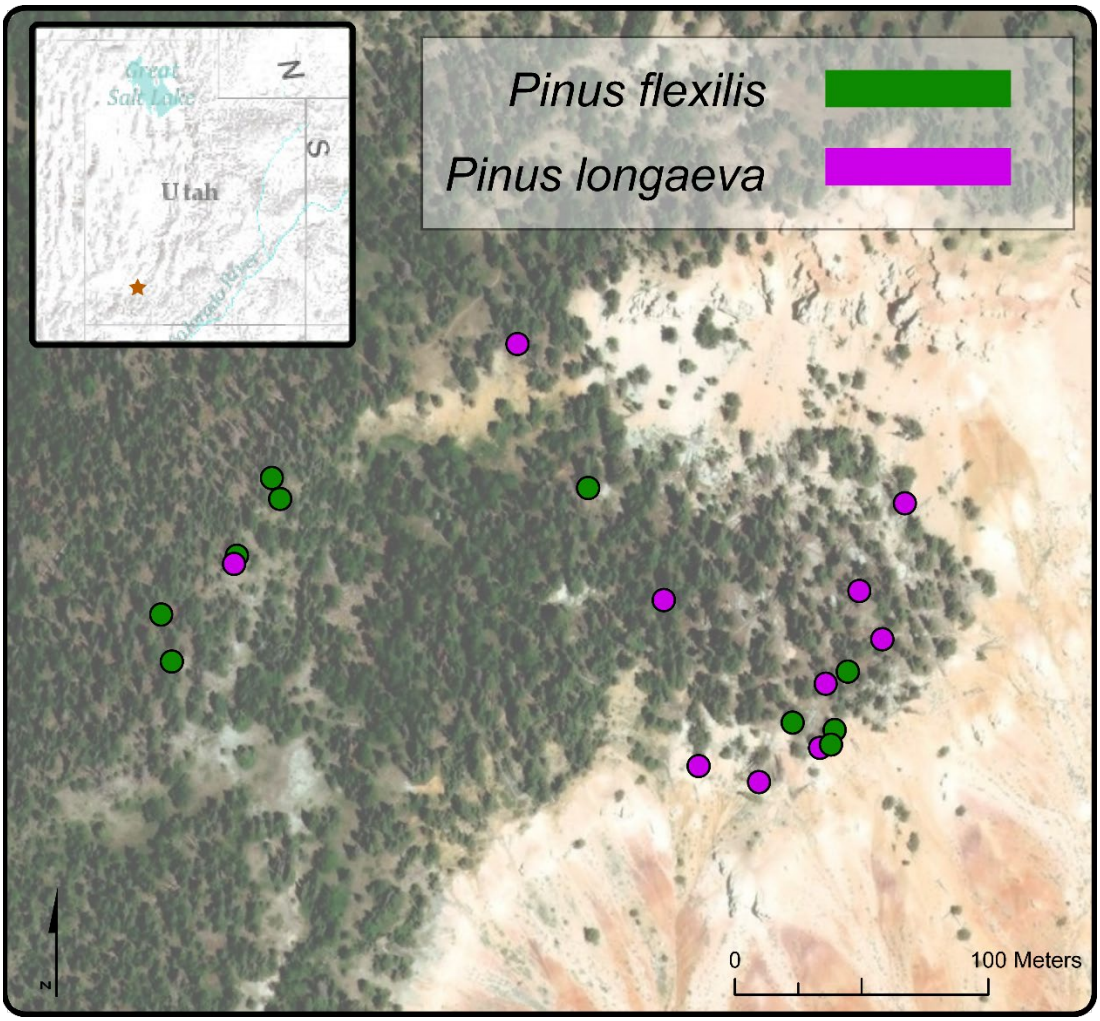

Figure S6.1 The location of each *Pinus flexilis* and *Pinus longaeva* sampled for roots and soil at the Utah Forest Dynamics Plot, Utah, USA. The Utah Forest Dynamics Plot is located within the boundaries of Cedar Breaks National Monument, Utah, USA.

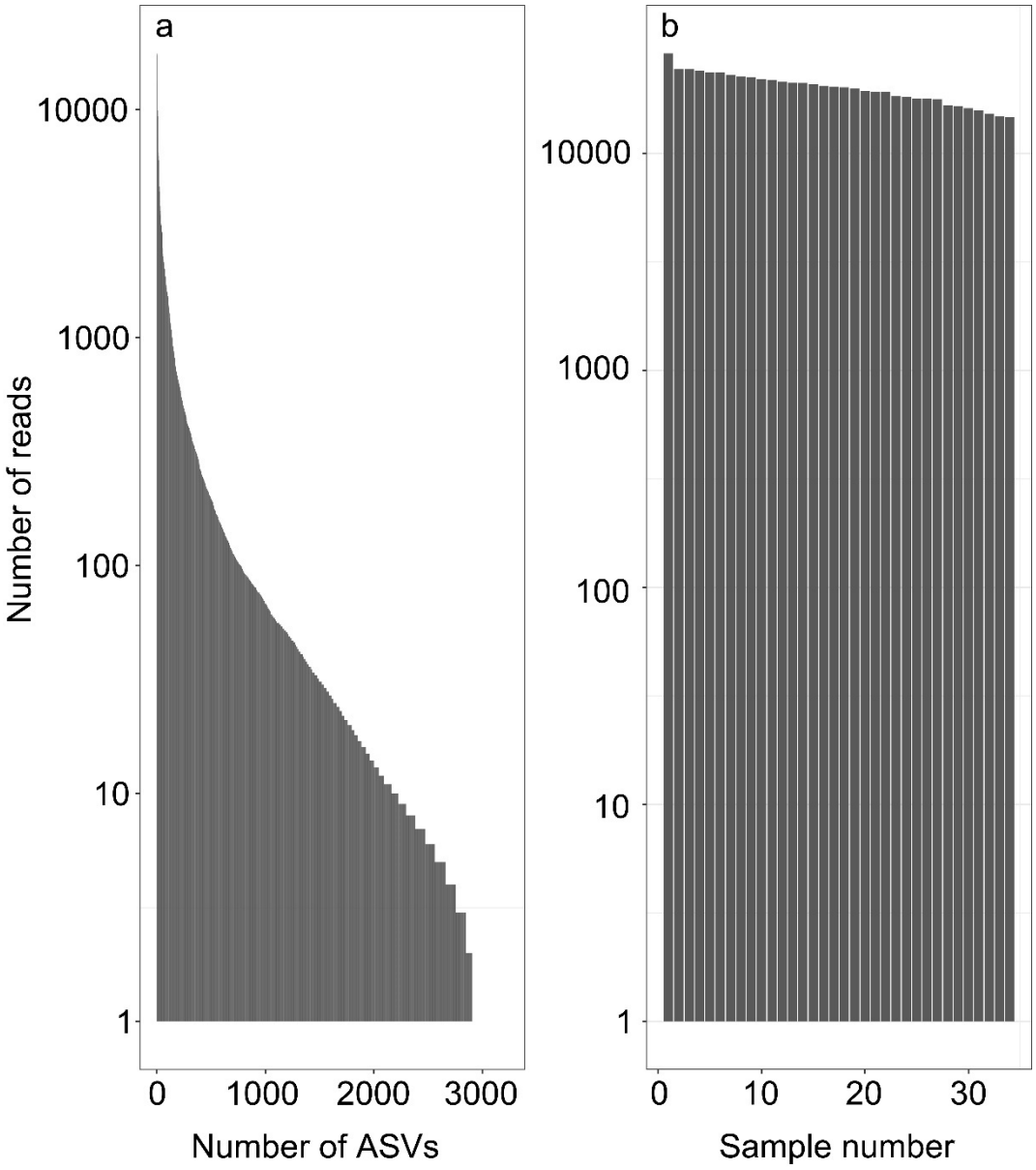

Figure S6.2 A rank-abundance curve of sequence reads for non-rarefied fungal amplicon sequence variants (ASV) from roots and soils surrounding *Pinus flexilis* and *Pinus longaeva* at the Utah Forest Dynamics Plot, Utah, USA. (a) The number of sequencing reads sorted by abundance-ranked ASV identity. (b) The number of sequence reads by sample.

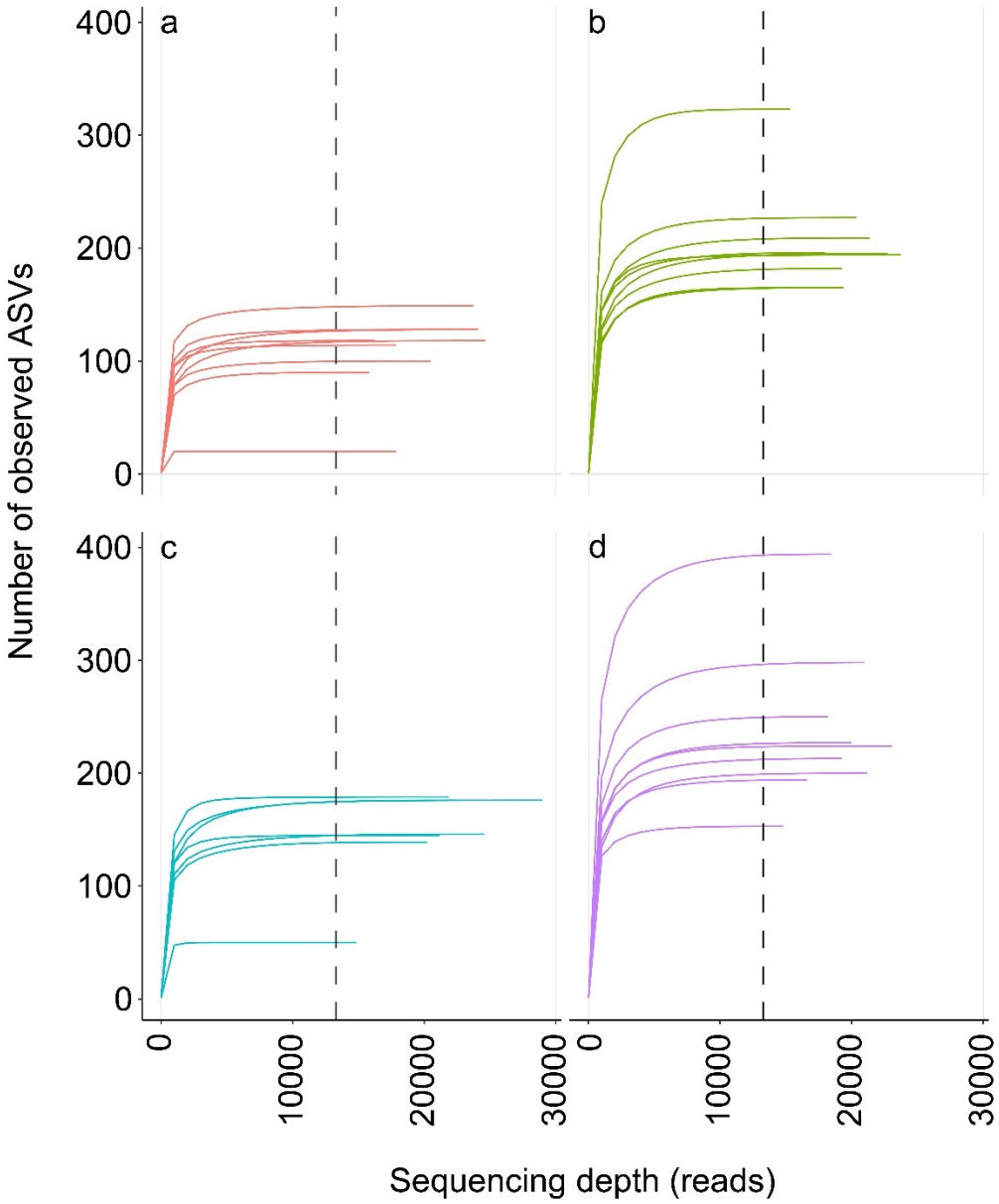

Figure S6.3 The number of fungal amplicon sequence variants (ASV) by the number of sequence reads from roots and soils around *Pinus flexilis* and *Pinus longaeva* at the Utah Forest Dynamics Plot, Utah, USA. The vertical dashed line marks the 13,286 read cutoff (90% of the minimum read count) used to rarify the sequence depth across *P. flexilis* roots (a), and soil (b), and *P. longaeva* roots (c) and soil (d).

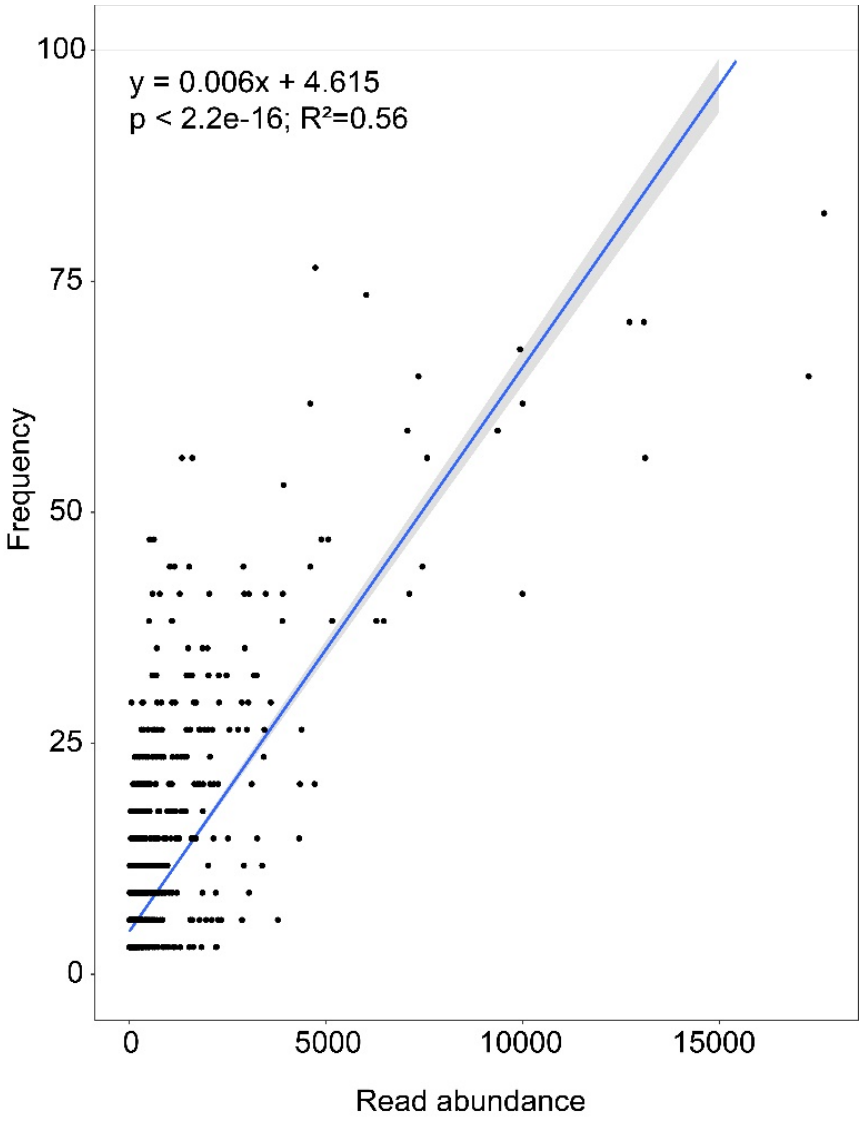

Figure S6.4 The non-rarefied sequence read abundance plotted against the frequency of fungal amplicon sequence variants (ASV) for root and soil samples taken from around *Pinus flexilis* and *Pinus longaeva* at the Utah Forest Dynamics Plot, Utah, USA. A linear model was used to plot the relationship for each sample type where shaded areas indicate 95% confidence intervals.

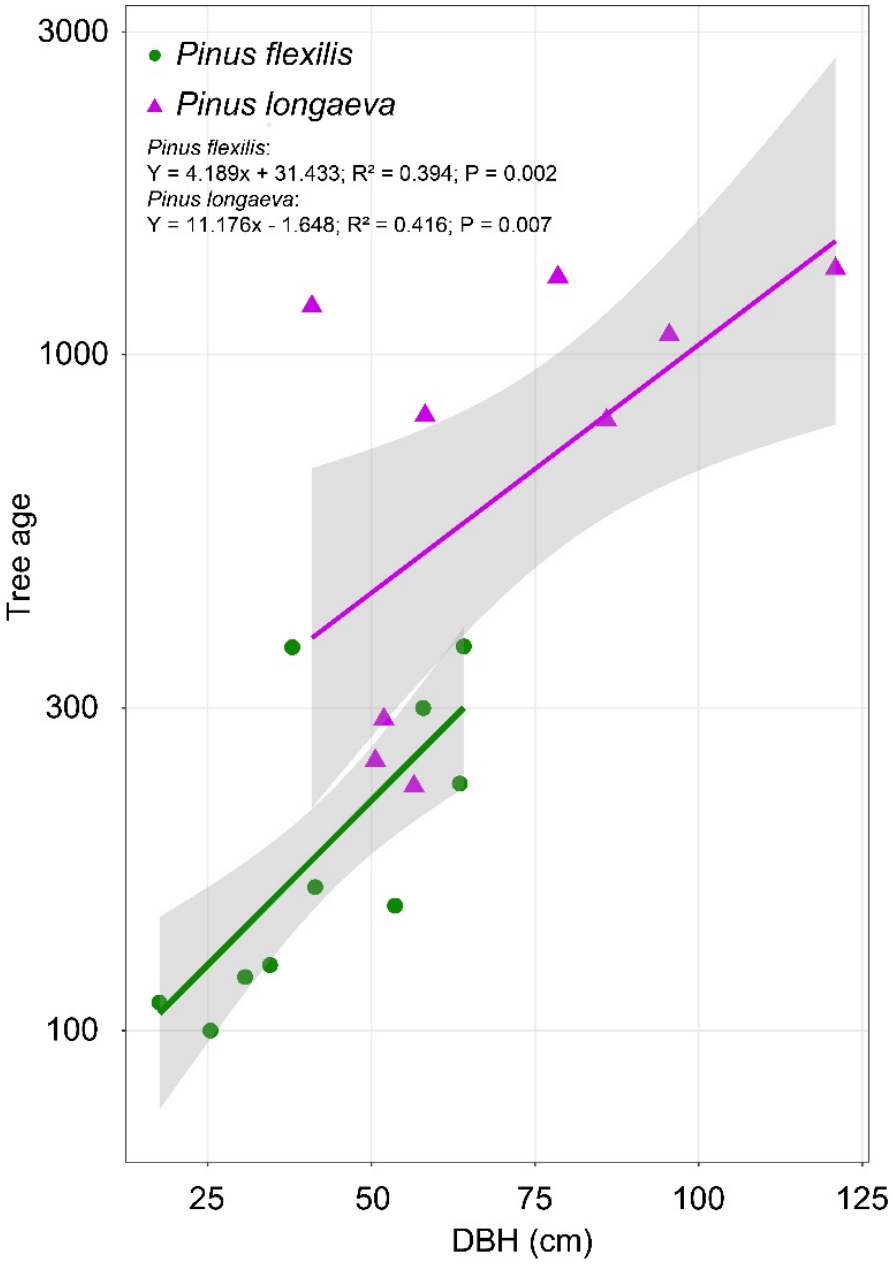

Figure S6.5 The distribution of tree age by diameter at breast height (DBH) for *Pinus flexilis* (circles) and *Pinus longaeva* (triangles) at the Utah Forest Dynamics Plot, Utah, USA. The y-axis is in log-scale. Equations are provided for the species-specific linear models. Shaded 95% confidence intervals are plotted for each linear model.

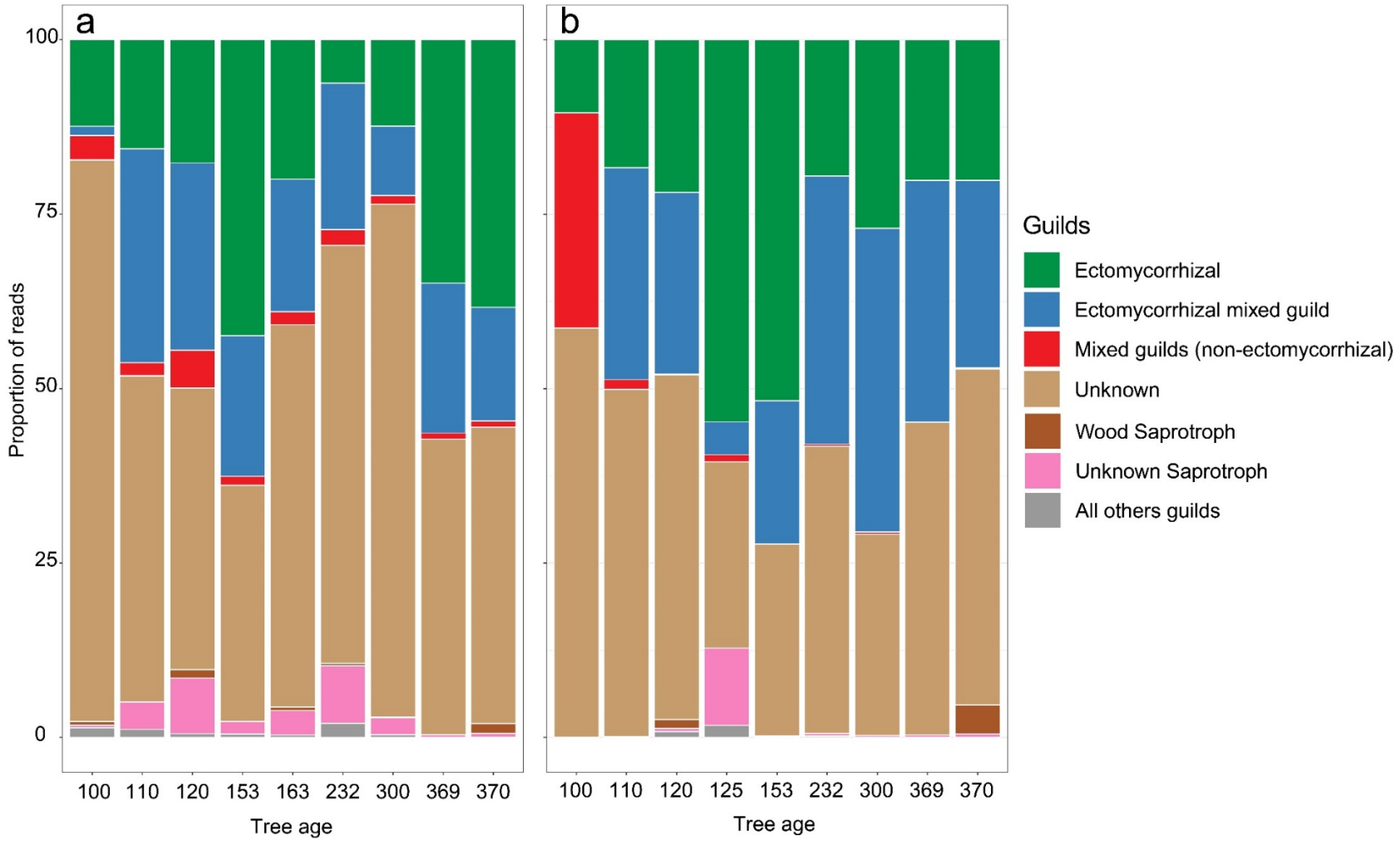

Figure S6.6 The proportional read abundance of the fungal functional guilds for *Pinus flexilis* soil (a) and roots (b) at the Utah Forest Dynamics Plot, Utah, USA. Fungal sequences were classified into functional guilds using the FUNGuild database (Nguyen et al. 2016). Classifications were sorted into categories where: ‘ Ectomycorrhizal’ consisted of sequences classified as ectomycorrhizal,

‘Ectomycorrhizal mixed guild’ consisted of multiple potential guilds including ectomycorrhizal, ‘Mixed guilds (non-ectomycorrhizal)’ which consisted of multiple potential guilds that did not include ectomycorrhizal guilds, ‘Unknown’ which consisted of sequences that did not receive a classification, ‘Wood saprotroph’ which consisted of all wood saprotrophs, ‘Unknown saprotrophs’ which consisted of saprotrophs with an unknown substrate, and ‘All other guilds’ which encompassed all other miscellaneous guilds including soil saprotrophs, pathogens, lichens, and others. There were no significant changes in the proportion of guilds with tree age.

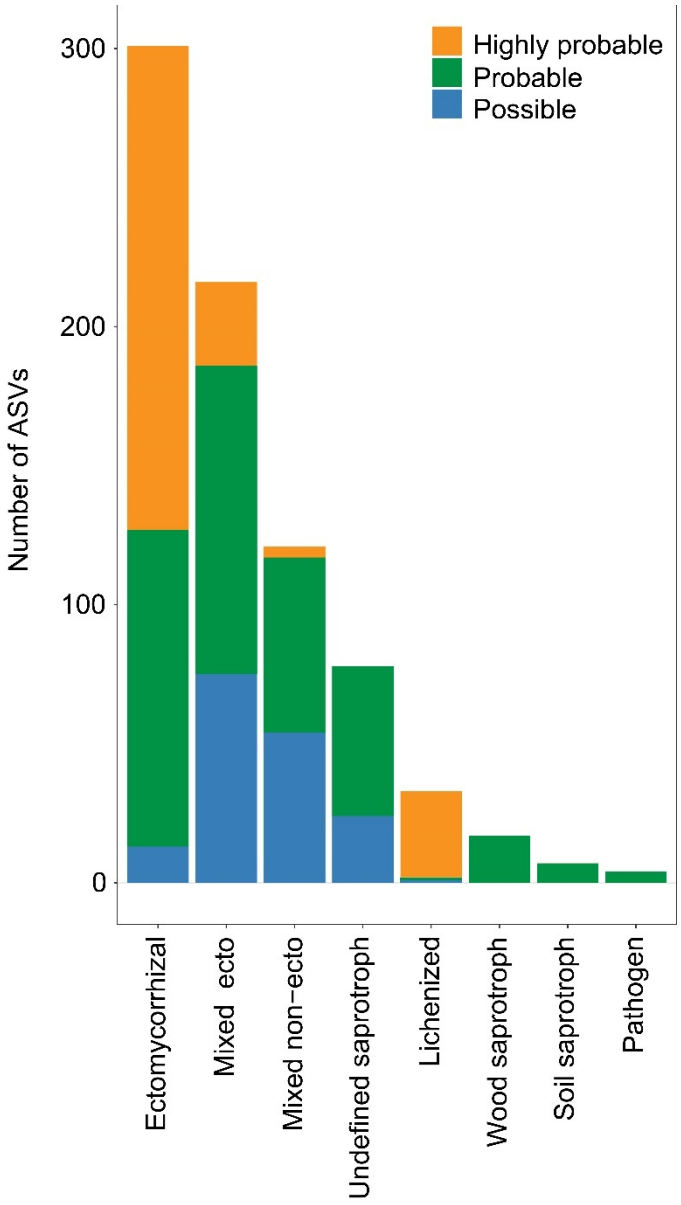

Figure S6.7 The distribution of functional guild classifications for fungal amplicon sequence variants (ASVs) from root and soil samples from around *Pinus flexilis* and *Pinus longaeva* at the Utah Forest Dynamics Plot, Utah, USA. The FUNGuild database was used to assign ecological guilds to ASVs (Nguyen et al. 2016). Fungal guild classifications are categorized as 'Highly Probable', 'Probable', or 'Possible' according to the strength of the evidence within the FUNGuild database. The majority of assigned ASVs were assigned to more than one potential

ecological guild and are plotted within the ‘Mixed’ category. For analysis I ignored ASVs with a ‘Possible’ classification. Of all sequenced ASVs, only 27.8% were assigned a classification by the FUNGuild database.

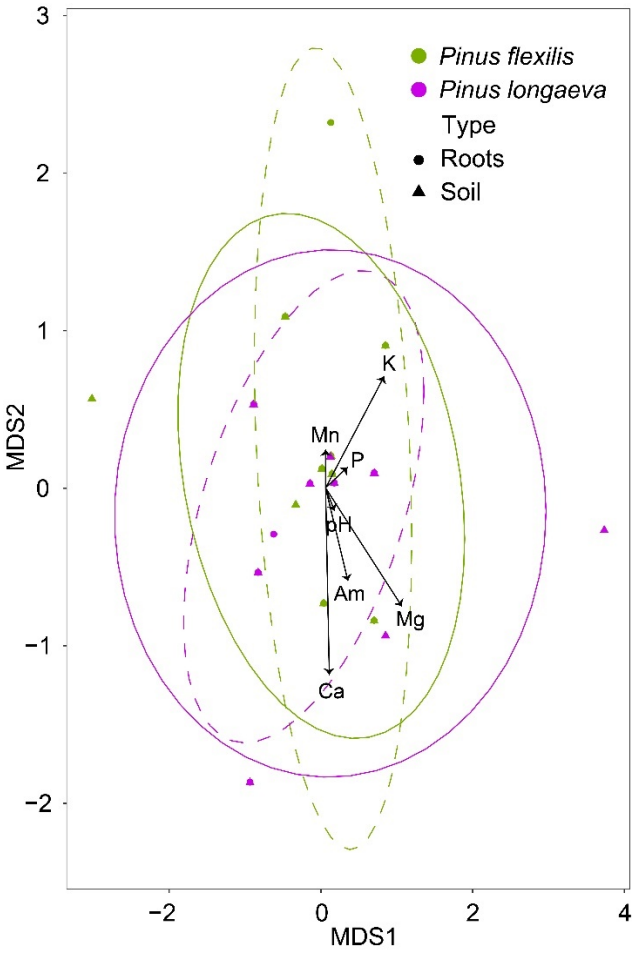

Figure S6.8 A meta nonmetric multidimensional scaling (NMDS) of soil nutrients interpolated at the locations of sampled *Pinus flexilis* and *Pinus longaeva* at the Utah Forest Dynamics Plot, Utah, USA. Soil nutrients included: pH, ammonium (Am), phosphorous (P), manganese (Mn), potassium (K), and calcium (Ca). Nutrients were measured in a semi-random grid and interpolated by kriging. Vectors and NMDS were calculated using 5000 permutations and the lowest stress permutation (0.15) chosen for plotting. Ellipses represent 95% confidence for the groups of soil (solid) and roots (dashed) for each pine species.

References

Baldeck, C. A., K. E. Harms, J. B. Yavitt, R. John, B. L. Turner, R. Valencia, H. Navarrete, S. J. Davies, G. B. Chuyong, and D. Kenfack. 2013. Soil resources and topography shape local tree community structure in tropical forests. *Proceedings of the Royal Society B: Biological Sciences* 280:20122532.

Fox, J., and S. Weisberg. 2018. An R companion to applied regression. Sage publications.

John, R., J. W. Dalling, K. E. Harms, J. B. Yavitt, R. F. Stallard, M. Mirabello, S. P. Hubbell, R. Valencia, H. Navarrete, and M. Vallejo. 2007. Soil nutrients influence spatial distributions of tropical tree species. *Proceedings of the National Academy of Sciences* 104:864-869.

Nguyen, N. H., Z. Song, S. T. Bates, S. Branco, L. Tedersoo, J. Menke, J. S. Schilling, and P. G. Kennedy. 2016. FUNGuild: an open annotation tool for parsing fungal community datasets by ecological guild. *Fungal Ecology* 20:241-248.

Oksanen, J., F. G. Blanchet, M. Friendly, R. Kindt, P. Legendre, D. McGlinn, P. R. Minchin, R. B. O'Hara, G. L. Simpson, P. Solymos, M. H. H. Stevens, E. Szoecs, and H. Wagner. 2018. vegan: Community ecology package. R package version 2.5-6.

Pebesma, E. J. 2004. Multivariable geostatistics in S: the gstat package. *Computers & Geosciences* 30:683-691.